EXPRESSION OF LIPID SIGNALLING MOLECULES IN EPITHELIAL AND LYMPHOID MALIGNANCIES

BY

MAIZATON ATMADINI ABDULLAH

A THESIS SUBMITTED TO

THE UNIVERSITY OF BIRMINGHAM

FOR THE DEGREE OF

DOCTOR OF PHILOSOPHY

School of Cancer Sciences

College of Medical and Dental Sciences

University of Birmingham

March 2014

ABSTRACT

Proteins which regulate the expression and activity of the small oncogenic lipids, LPA and S1P are important in the development and progression of cancers. This study set out to explore the expression of lipid signalling molecules in two types of lymphoid malignancies and a few epithelial malignancies and correlate their association with clinicopathological parameters. The expression of SPHK1, S1PR1, ABCC1 and ATX in epithelial malignancies were studied which included breast, bladder and lung cancer. It is shown that S1PR1 is a poor prognostic marker in breast cancer and ATX is a poor prognostic marker in both breast and lung cancers. The expression of lipid signalling proteins and mRNA showed that S1PR1 was commonly expressed in HL, while S1PR3 was expressed in all HL cases suggesting its role in lymphomagenesis. L591 Hodgkin lymphoma cells treated with anti-S1P, Sphingomab showed restoration of four B cell receptor genes namely BCL10, RAPGEF1, NFATC3 and MALT by gene expression microarray. Sphingomab also showed downregulation of S1PR3 and S1PR5 genes which may be a possible therapeutic target in cancer. The incidence of EBV^+ DLBCL in this series is 14/300 (4.7%). S1PR1 was commonly expressed in DLBCL and patients with S1PR1 expressing tumours were more likely to have more than one extranodal site involvement. EBV positivity, presence of B symptoms, bulky disease, BCL6 positivity and high IPI were found to be poor prognostic factors in DLBCL.

DEDICATION

This thesis is dedicated to my beloved father, the late Associate Professor Abdullah Tahir and my beloved mother Mariam Mohamad, who have inspired me in many ways to work hard and have strong faith in Allah the Almighty in order to succeed in life and the hereafter.

For my beloved husband Dr Esmady Esa and children,Muhammad Aiman, Muhammad Anas, Maisarah, Muhammad Amir and Madeehah for their enduring support and patience with my mood swings during my PhD years.

For my beloved parent inlaws for their continuous support and prayers. Thank you for always being there for us.

ACKNOWLEDGEMENTS

UNIVERSITI PUTRA MALAYSIA AND THE MALAYSIAN MINISTRY OF HIGHER EDUCATION FOR AWARDING A PHD SCHOLARSHIP. MY DEDICATED AND EVER ENCOURAGING SUPERVISOR PROFESSOR PAUL MURRAY FOR HIS GUIDANCE, COMPLEMENTARY SKILLS AND KNOWLEDGE THROUGHOUT THIS RESEARCH PERIOD. DR WILLIAM SIMMONS FOR HIS ABUNDANT ASSISTANCE IN PERFORMING IMMUNOHISTOCHEMITSRY OF SIX DIFFERENT ANTIBODIES ON 300 CASES OF DLBCL AND ON RETRIEVING LOADS OF CLINICAL DATA. PROFESSOR CIARAN WOODMAN AND DR WENBIN WEI FOR ASSISTING ME WITH THE MICROARRAY ANALYSIS. DR.CLAUDIA ROBERTS AND DR. STEFAN DOCJINOV FOR REVIEWING THE HISTOLOGY OF MY HODGKIN LYMPHOMA AND DLBCL SLIDES.

THE MURRAY AND WOODMAN GROUP WHO HAVE PROVIDED TECHNICAL ASSISTANCE AND GIVEN ME ENCOURAGEMENT IN TIMES OF DESPAIR, IN PARTICULAR JENNIFER ANDERTON AND KARL BAUMFORTH WHO FIRST TAUGHT ME WHAT MOLECULAR WORK IS ALL ABOUT, KAISHENG WEN FOR HIS EXCELLENT TECHNICAL ASSISTANCE IN IMMUNOHISTOCHEMISTRY AND IN SITU HYBRIDIZATION, MARTINA VOCKERODT AND CHRISTOTHEA CONSTANDINOU FOR THEIR CELL BIOLOGY EXPERTISE AND NICOLA RUTH FOR HER CONTRIBUTION TO MY RESEARCH PROJECT, SOUAD MESSAHEL, AFAF DIYAF, ZUMLA CADER,

MANJIT GILL, NAHEEMA GORDON AND SARAH LEONARD FOR LENDING ME THEIR EARS AND PROVIDING GOOD HUMOUR AND ENCOURAGEMENT. THANK YOU FOR THE WONDERFUL FRIENDSHIP AND FOR ALWAYS BEING THERE FOR ME.

ABBREVIATIONS

Ab	Antibody
ABCC1	ATP binding casette C1
ALL	Acute lymphoblastic leukaemia
AML	Acute myeloid leukaemia
ATX	Autotaxin
BARTs	BamHI-A rightwards transcripts
BL	Burkitt lymphoma
BSA	Bovine serum albumin
cHL	classical Hodgkin lymphoma
CRM	Chromosomal region maintenance
CTGF	Connective tissue growth factor
DAB	Diaminobenzidine
DEPC	Diethylpyrocarbonate
DLBCL	Diffuse large B- cell lymphoma
DNA	Deoxyribonucleic acid
EA	Early antigen
EBERs	Epstein-Barr virus encoded RNAs
EBNA	Epstein-Barr virus nuclear antigen
EBV	Epstein-Barr virus
ECL	Enhanced chemiluminescence
ECM	Extracellular matrix
EDG	Endothelial differentiation gene

EDTA	Ethylenediaminetetra-acetic acid
EGF	Epidermal growth factor
ER	Endoplasmic reticulum
FBS	Foetal bovine serum
FCS	Foetal calf serum
FFPE	Formalin fixed paraffin embedded
GAPDH	Glyceraldehyde-3-phosphate dehydrogenase
GCOS	GeneChip operating software
GPCR	G-protein coupled receptors
HDL	High density lipoprotein
H&E	Haematoxylin and eosin
HL	Hodgkin lymphoma
IF	Immunofluorescence
IGF	Insulin-like growth factor
Ig	Immunoglobulin
IHC	Immunohistochemistry
IM	Infectious mononucleosis
IPI	International prognostic index
ISH	i*n situ* hydridisation
JNK- c	Jun N-terminal kinase- c
LCL	Lymphoblastoid cell lines
LD	Lymphocyte depleted
LMP	Latent membrane protein

LP	Lymphocyte predominant
MALT	Mucosa associated lymphoid tissue
MAPK	Mitogen activated protein kinase
MC	Mixed cellularity
MDR	Multidrug resistance
MHC	Major histocompatability complex
MRP1	Multidrug resistant protein 1
NF-κB	Nuclear factor-kappa B
NHL	Non Hodgkin lymphoma
NLPHL	Nodular lymphocyte predominant Hodgkin lymphoma
NS	Nodular sclerosis
Ori-P	Plasmid origin of viral replication
PAF	Platelet-activating factor
PAGE	Polyacrylamide gel electrophoresis
PBS	Phosphate buffered saline
PCR	Polymerase chain reaction
PI3K	Phosphatidylinositol 3-kinase
PKC	Protein kinase- C
PLC	Phospholipase- C
PLD	Phospholipase- D
PMA	Phorbol 12-myristate 12-acetate
PMBL	Primary mediastinal B-cell lymphoma
PTLD	Post-transplant lymphoproliferative disease

Q-PCR	Quantitative polymerase chain reaction
RMA	Log scale robust multi-array analysis
RNA	Ribonucleic acid
RT	Reverse transcriptase
SD	Standard deviation
SDS	Sodium dodecyl sulphate
S1P	Sphingosine 1- phosphate
S1PR	Sphingosine 1- phosphate receptor
SPC	Sphingosylphosphorylcholine
SPHK	Sphingosine kinase
SGPL1	Sphingosine 1- phosphate lyase
S1PP	Sphingosine 1- phosphate phosphatases
TBS	Tris buffered saline
TGFβ1	Transforming growth factor beta 1
TMA	Tissue microarray
TNF	Tumour necrosis factor
VEGF	Vascular endothelial growth factor
WHO	World Health Organisation

Table of Contents

List of Figures

List of Tables

CHAPTER 1

INTRODUCTION

1.1 Introduction

In the Introduction (Chapter 1), I will discuss the three major areas of relevance to this study; sphingolipid metabolism, Hodgkin lymphoma and Diffuse Large B cell lymphoma (DLBCL), including EBV-positive DLBCL of the elderly. This will be followed by the Materials and Methods (Chapter 2) that will provide detailed information about the experimental procedures carried out during this investigation.

The remainder of this thesis consists of three studies. Chapter 3 describes the expression of SPHK1 and of other related lipid signalling molecules in three types of epithelial malignancies; breast, bladder and lung cancer. Chapter 4 investigates the expression of lipid signalling molecules in primary HL tissues and HL cell lines as well as the possible contribution of S1P signalling to the pathogenesis of HL. Chapter 4 also describes the gene expression profiling of the HL cell line L591, after treatment with anti- S1P antibody, Sphingomab. In Chapter 5, I estimated the incidence of EBV^+ DLBCL in a single centre in the UK and described the expression of lipid signalling molecules in DLBCL and their association with clinicopathological parameters including clinical outcome.

1.2 Sphingolipid metabolism

Lipids are long known to have important roles in cellular metabolism and membrane biology. However it is only in the last two decades that lipids have been recognised as cellular signalling molecules. The first observation which suggested that lipids could be involved in cell signalling was made by Hokin and Hokin in the 1950s. In their pioneering studies, pancreatic slices stimulated with acetylcholine resulted in the rapid turnover of inositol phospholipids. After a few dormant years, diacylglycerol (DAG) was implicated in regulating protein kinase C (PKC), and inositol 1,4,5-triphosphate (Ins (1,4,5)P_3) was found to regulate calcium release (Nishizuka 1992) leading to various cellular responses. This led to the idea that lipids could regulate cell signalling which subsequently ushered the era of bioactive lipids.

The concept of bioactive lipids implies any changes in lipid levels which results in functional consequences. The best studied bioactive lipids so far are ceramide, sphingosine (Sph) and sphingosine 1-phosphate (S1P). The precursor of these bioactive products is sphingomyelin (SM). The name Sphingosine, first described in the 1800s is derived from the word Sphinx, a Greek mythological character of a winged lion with a human face. The phosphorylation of sphingosine yields S1P.

1.3 Sphingolipid family

1.3.1 Ceramide and spingosine, precursors of S1P

Ceramide is formed from serine and palmitoyl CoA as well as by sphingomyelin hydrolysis.(Figure 1.1). Stress stimuli such as chemotherapeutic drug treatment and radiation increase its production. Ceramides modulate diverse signal transduction pathways and key regulatory enzyme activities including the mitogen activated protein kinases (MAPKs) p42/ 44, specific serine/ threonine kinases like protein kinase C (PKC), stress-activated protein kinases (JNKs), protein kinase B (PKB) and protein phosphatases, phospholipase A2 and phospholipase D (Simstein et al., 2003, Ogretmen & Hannun, 2004; Taha et al., 2006). Ceramide also mediates growth inhibition, apoptosis, modulation of telomerase activity and telomere length and senescence (Ogretmen & Hannun 2004). Ceramide is further metabolised by ceramidases to form the single fatty-chain, sphingosine (Baumruker & Prieschl, 2002). Sphingosine can then be phosphorylated by sphingosine kinases (SPHKs), to yield S1P (Van Brocklyn et al., 1998; Melendez, 2008; Spiegel, 1999). S1P is cleaved by S1P lyase (SGPL1) to hexadecenal and ethanolamine 1-phosphate or it can be converted back to sphingosine by S1P phosphatases. There are two main S1P phosphatases; S1P phosphatase 1 (SGPP1) and S1P phosphatase 2 (SGPP2). (Figure 1.1).

The sphingolipid metabolites are interconvertible and the dynamic ratio between S1P and ceramide determines cell fate, which gives rise to the sphingolipid biostat (Cuvillier et al., 1996). Conversion of sphingosine to S1P by Sphingosine kinase 1 (SPHK1) leads to enhanced cell growth and survival and suppression of apoptosis. In contrast, conversion of S1P to sphingosine and then to ceramide leads to cell death (Spiegel & Milstien, 2002).

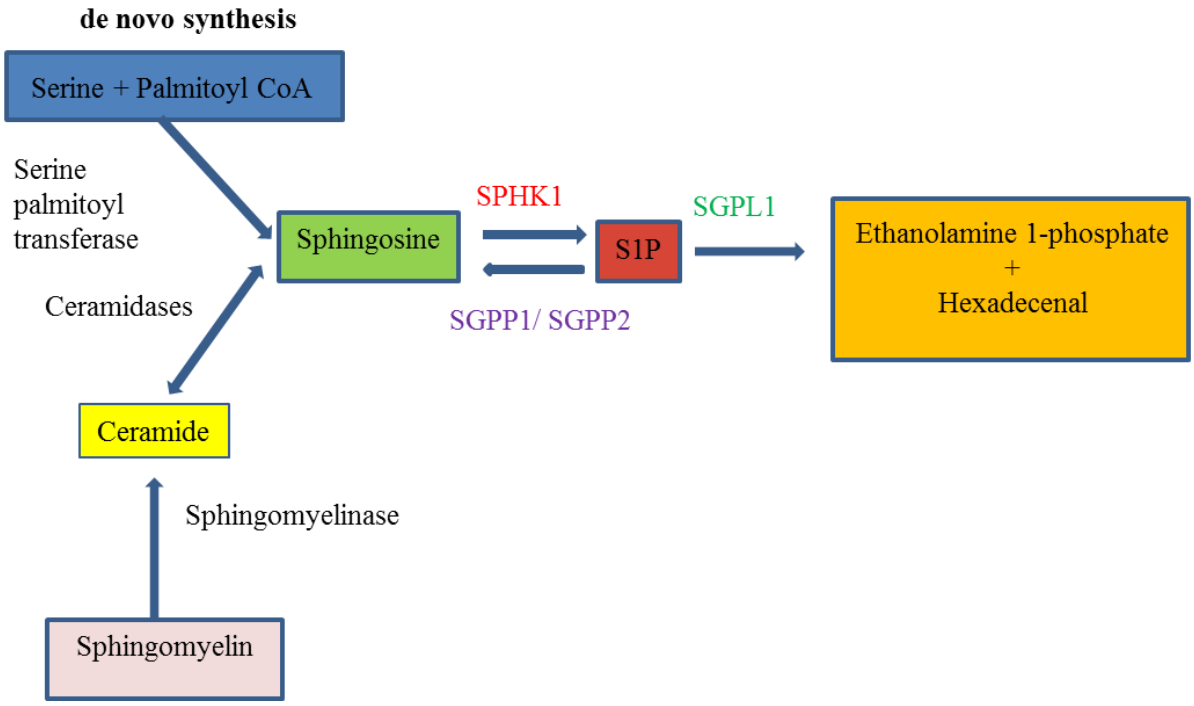

Figure 1.1: Pathways of sphingolipid metabolism. Sphingomyelin is hydrolysed by sphingomyelinase to form ceramide. Ceramide can be metabolized by ceramidases to form sphingosine which is then phosphorylated by SPHK1 to generate S1P. S1P is cleared by the S1P phosphatases; SGPP1/ SGPP2 or cleaved by S1P lyase (SGPL1) into ethanolamine 1-phosphate and hexadecenal. Sphingosine can also be formed de novo by the action of serine palmitoyl transferase on serine and palmitoyl CoA.

1.3.2 Sphingosine 1- phosphate

S1P regulates a large number of physiological and pathological processes including growth, survival, differentiation, cytoskeleton rearrangements, angiogenesis and vascular maturation (Anliker & Chun, 2004; Spiegel & Milstien, 2003; Takabe et al., 2008; Young & Van Brocklyn, 2006). S1P secreted from the cell binds to transmembrane hepta-helical G-protein coupled receptors (GPCRs), termed S1P receptors (S1PRs). In an autocrine manner, S1P promotes growth, survival, motility and metastasis and in a paracrine manner, it induces the production of endothelial adhesion molecules and promotes angiogenesis (Anelli et al.,2010), tumour-stromal interactions and lymphocyte trafficking (Chi 2011) S1PRs were formerly known as the endothelial differentiation gene receptors (EDGs). Five S1PRs have been identified ie S1PR1-S1PR5. Table 1.1 shows the cellular distributions of S1P receptor subtypes. Previously, it was believed that S1P acts as only an intracellular mediator. However in 1992, Igarashi's group found that S1P played a role as an extracellular mediator in controlling cell motility (Sadahira et al.,992). Independent of its cell surface receptors, S1P can act intracellularly by regulating calcium release (Van Brocklyn et al. 1998), cell growth, inflammatory responses (Melendez & Khaw 2002) and the suppression of apoptosis (Cuvillier et al., 1996). Intracellular S1P also modulates histone acetylation via histone deacetylases (HDACs) in breast cancer cells (Hait et al. 2009). From the observations that enzymes controlling sphingolipid metabolism (neutral sphingomyelinase and ceramidase) are present in the nucleus, it has been suggested that sphingolipids are also metabolised in the nucleus (Albi et al., 2008).

1.3.3 Cellular production of S1P

S1P is mainly produced by endothelial cells and platelets (Igarashi and Yatomi, 1998). However, epithelial cells, cerebellar granule cells, cerebellar astrocytes (Bassi et al., 2006), thrombocytes (Hänel et al., 2007), macrophages, mast cells and dendritic cells (Martino 2007; Goetzl & Tigyi 2004) can also produce S1P. Circulating erythrocytes do not produce S1P but are capable of storing and releasing it, protecting S1P from degradation. In plasma, S1P concentrations can reach a concentration of 0.2 to 0.9 μM where it is mostly bound to high density lipoproteins (HDLs). Levels in lymph fluid are about five-fold lower than in plasma. Tissue S1P levels are generally low, ranging from 0.5 to 0.75 pmol/mg (Edsall & Spiegel, 1999). The half life of S1P is less than 15 minutes (Venkataraman et al., 2008). Upon production in the cell following agonist-induced activation of SPHK1, S1P is transported to the extracellular space by ATP-binding cassette (ABC) transporters including ABCA1 (Sato et al., 2007), ABCC1 and ABCG2 (Takabe et al. 2010). ABCC1, also known as Multidrug Resistant Protein 1 (MRP1 or MDR), is one of the most extensively characterised ABC transporters and is involved in the export of S1P in activated mast cells (Mitra et al., 2006). Once in the extracellular space, S1P acts on cell surface S1PRs which interacts with various intracellular signaling systems leading to stimulation of Ras/MAPK, PKC, the small GTPase Rho pathways, stimulation of the PLC/Ca^{2+} mobilization and inhibition of adenylate cyclase (Moolenaar 1995; Meyer zu Heringdorf et al., 1998).

1.3.4 G protein coupling of S1PRs and pathways activated

Each S1PR subtype signals through a set of receptors which result in various downstream biological effects. Hence it is important to know which receptors are expressed in various organs to predict downstream effects following S1P stimulation. There are four major families of heterotrimeric G proteins; G_s, $G_{i/o}$, $G_{q/11}$, and $G_{12/13}$. Of these four, S1PRs couple to G_i, G_q, and $G_{12/13}$. Using GTPɣS binding assay, Width et al have shown that S1PR1 exclusively binds to G_i (Windh et al., 1999), while S1PR2 and S1PR3 have a broader coupling profile in which they binds to G_i, G_q, and $G_{12/13.}$ G protein coupling of each S1PRs and the pathways activated will be discussed further under the section 'S1P receptors' (1.3.5).

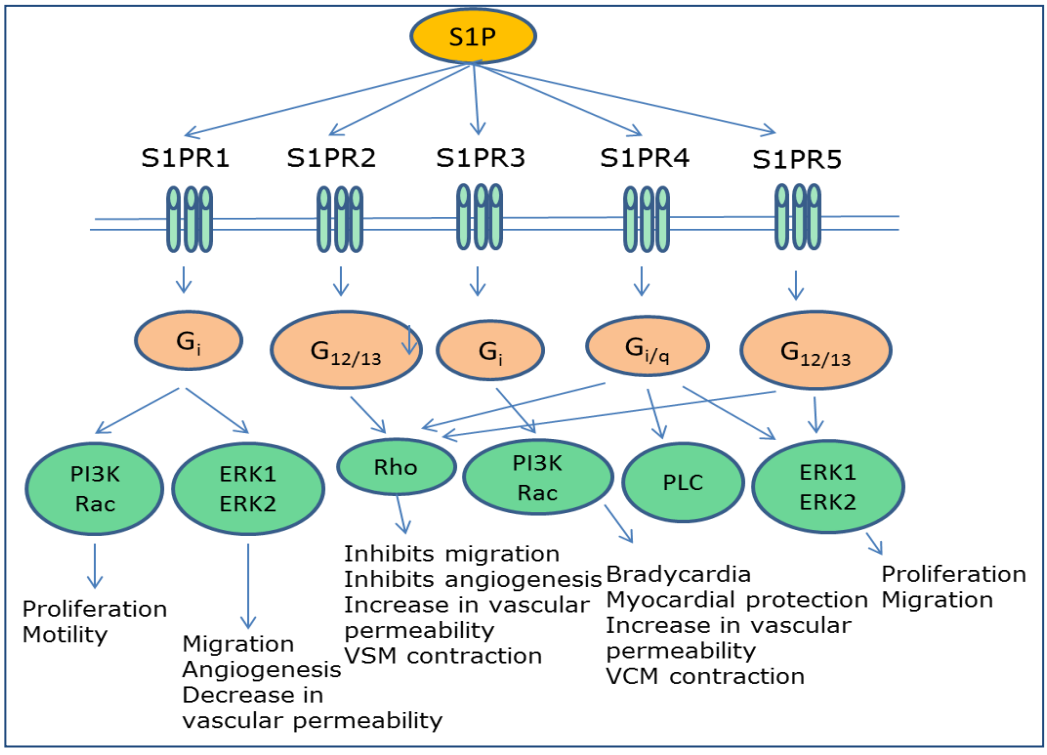

Figure 1.2:. The S1P receptors interact with several G protein families which result in subsequent downstream effects on second messenger and effector molecules.

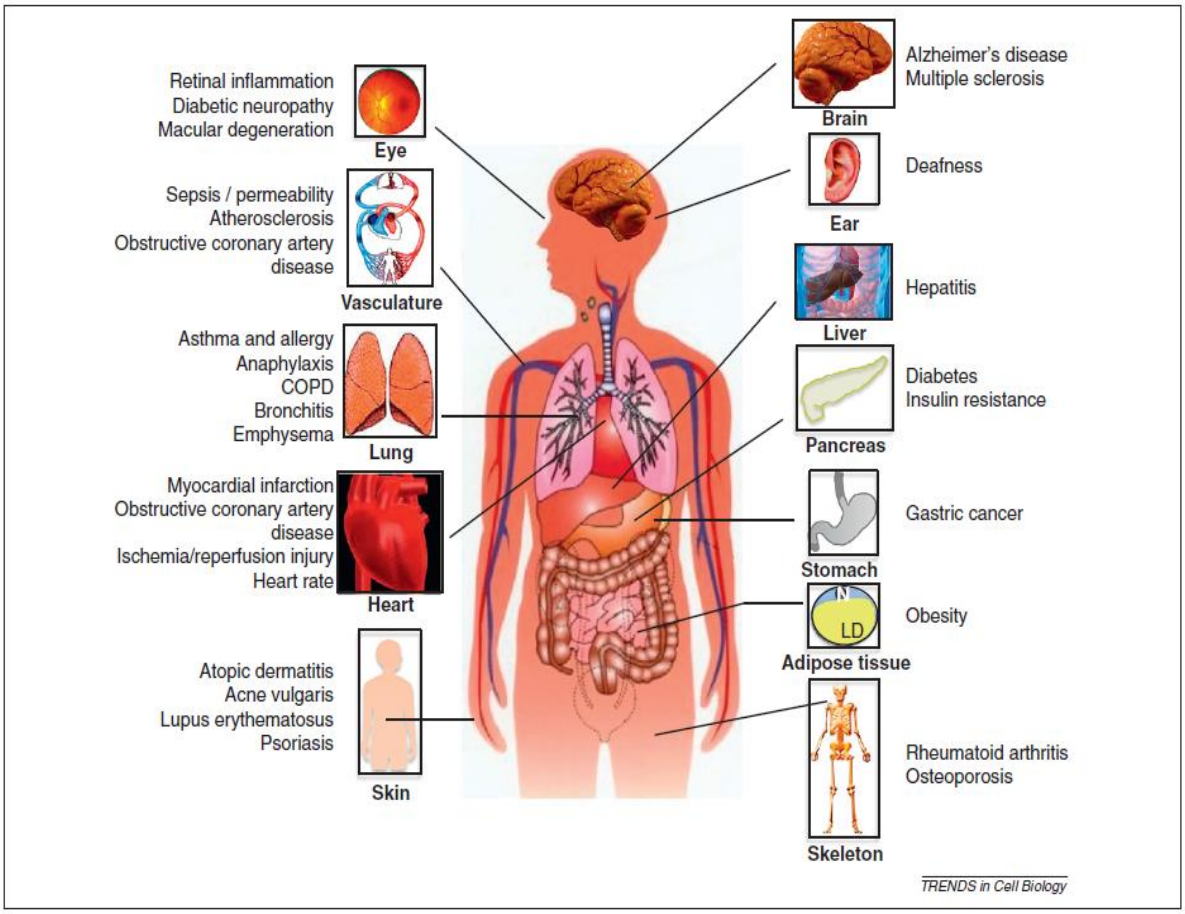

Figure 1.3: The pathobiology of S1P. S1P is implicated in various pathophysiological conditions affecting almost every organ. Only a few cancer types are shown here (taken from Maceyka et al., 2011).

1.3.5 S1P receptors

1.3.5.1 S1PR1

S1PR1 gene which is located on chromosome 1p21 was the first S1P receptor cloned from human endothelial cells and was thus named endothelial differentiation gene- 1 (EDG1)(Hla & Maciag., 1990). S1PR1 interacts exclusively with Gi and this interaction is inactivated by pertussis toxin. S1P/S1PR1 signalling leads to the activation of P13K, Rac, ERK1 and ERK2 (Young & Van Brocklyn, 2006)(Figure 1.3). S1PR1 is essential for blood vessel formation and vascular maturation. Disruption of S1PR1 in mice led to massive embryonic haemorrhage due to a defect in the recruitment of mural cells to vessel walls (Liu et al. 2000). S1PR1 is also involved in motility regulation in various cell types and in tumour cell invasiveness. Sadahira et al have shown that S1P/S1PR1 signalling inhibits the migration and invasion of B16 human melanoma cells and HT1080 human fibrosarcoma cells (Sadahira et al., 1992). S1PR1 also interacts with platelet derived growth factor (PDGF) signaling. PDGF has been shown to activate SPHK1 and increase the production of S1P. S1P interaction with S1PR1 leads to Rac activation and an increase in cell migration in human embryonal kidney (HEK) cells (Hobson et al., 2001). S1PR1 is also important for lymphocyte trafficking (Chiba et al., 2006) which will be discussed in more detail later under the section ‘S1P in immune cell signalling’ (1.4.2).

1.3.5.2 S1PR2

S1PR2 was isolated from rat vascular smooth muscle cells and rat brain (Okazaki et al.,1993). It is highly expressed in brain, heart, spleen and liver. S1PR2 binds to S1P with nanomolar affinity and is ubiquitously expressed throughout development and during adulthood (Takabe et al., 2008; Anliker & Jerold Chun 2004). By binding to G_i, Gq and $G_{12/13}$, S1PR2 activates ERK/MAP kinase via G_i coupling and activates Rho via $G_{12/13}$ coupling (Takabe et al., 2008; Anliker & Jerold Chun 2004). S1PR2 also activates p38 and Jun N-terminal kinase (JNK) MAP kinases (Gonda et al., 1999), phospholipase D (PLD) and NF-κB (Siehler et al., 2001). S1PR2 activation has been shown to inhibit cancer cell migration, invasion and metastasis (Lepley et al., 2005; Young, 2007). S1PR2 was recently shown to be expressed in normal germinal centre (GC) B cells in the mouse where it inhibited the chemotaxis of these cells towards follicular chemo-attractants and promoted their confinement to the GC (Green et al., 2011). S1PR2 deficient mice have been shown to develop diffuse large B cell lymphoma (Cattoretti et al., 2009).

1.3.5.3 S1PR3

S1PR3 was cloned from a human genomic library (Yamaguchi et al., 1996). Similar to S1PR2, S1PR3 couples to G_i, Gq and $G_{12/13,}$ activating similar pathways to S1PR2 (Windh et al., 1999). Mice deficient in both S1PR1 and S1PR3 showed more severe bleeding compared with those lacking only S1PR1. This indicates that S1PR3 could play a supportive role in the maintenance of vascular barrier homeostasis and vascular development (Kono et al., 2004).

S1PR3 is required for normal B-cell development (Donovan et al., 2010) and in the migration of dendritic cells (Spiegel & Milstien, 2011), ML-1 thyroid carcinoma cells (Bergelin et al. 2009) and gastric cancer cells (Yamashita et al., 2006). S1P/S1PR3 signaling is also involved in cholestasis-induced liver fibrosis. Therefore, it has been suggested that modulation of S1PR3 activity could be a new antifibrotic strategy (Li et al., 2009).

1.3.5.4 S1PR4

S1PR4 was cloned from *in vitro* differentiated human and murine dendritic cells (Gräler et al., 1998). S1PR4 couples to G_i and G_{12}, but not G_q. Through G_i coupling, S1P/S1PR4 signalling can activate PLC, ERK and the Rho family small GTPase, Cdc42. Wang et al have shown that S1P/S1PR4 signalling inhibits T cell proliferation but not T cell migration (Wang et al., 2005). S1PR4 can also suppress the generation of IL-2, IFN-α, and IL-4 from T cells while at the same time enhancing the secretion of IL-10 (Wang et al., 2005).

1.3.5.5 S1PR5

S1PR5 which was previously known as nrg-1, was cloned from a rat phaeochromocytoma (PC12) cell cDNA library (Glickman et al., 1999). In humans, S1PR5 expression is restricted to the brain and the skin. S1PR5 couples to G_i and G_{12}, but not G_q. G_i coupling leads to inhibition of cAMP accumulation in both Chinese hamster ovary (CHO) cells (H. Okamoto et al., 1998) and rat hepatoma R7777 cells (Im et al., 2000). S1PR5 plays a major role in the

regulation of natural killer (NK) cell activity and their egress from bone marrow and lymph node (Maghazachi 2003; Jenne et al., 2009). In the brain, S1PR5 regulates the retraction of glial processes and inhibits glial cell migration. In contrast to other S1PRs, S1PR5 causes a decrease in ERK 1/2 phosphorylation (Malek et al., 2001).

Table 1.1: S1PR subtype mRNA distribution and receptor subtype-specific actions in distinct cell types and tissues (adapted from Rosen et al., 2009)

Subtype	Distribution (mRNA)	Cellular functional expression and consequences
S1PR1	Brain, heart, spleen, liver, lung, thymus, kidney, skeletal muscle, lymphoid	Astrocyte: Migration B cell: blockade of egress, chemotaxis Cardiomyocyte: increased β-AR positive inotropy Endothelial cell: early vascular system development, adherens junction assembly, activated protein C-mediated increased barrier Pericyte: early vascular system development T cell: blockade of egress, chemotaxis, decreased late-stage maturation
S1PR2	Brain, heart, spleen, liver, lung, thymus, kidney, skeletal muscle	Cardiomyocyte: survival to ischaemia-reperfusion Epithelial hair cell (cochlea): integrity/ development Endothelial cell (retina): pathological angiogenesis Hepatocyte: proliferation/ matrix remodeling Mast cell: degranulation VSMC: decreased PDGF-induced migration
S1PR3	Brain, heart, spleen, liver, lung, thymus, kidney, testis, skeletal muscle	Cardiomyocyte: survival to ischaemia-reperfusion Dendritic cell: worsening experimental sepsis lethality/ inflammation/ coagulation
S1PR4	Lymphoid, lung	T-cell migration/ cytokine secretion
S1PR5	Brain, skin, spleen	NK cell: trafficking Oligodendrocyte: survival Oligodendrocyte progenitor cells: glial process retraction, inhibition of migration

1.3.6 S1P metabolizing enzymes

1.3.6.1 Sphingosine kinases

Cellular levels of S1P are low and are tightly regulated by the balance between its synthesis and degradation. Sphingosine kinases catalyse the phosphorylation of sphingosine to S1P. Two sphingosine kinase genes, SPHK1 and SPHK2, have been cloned (Kohama et al., 1998; Liu et al., 2000). These two kinases have different kinetic properties, developmental and tissue specific expression suggesting that they have distinct physiological functions. These kinases are ubiquitously distributed and are found at high concentration in erythrocytes (Pappu et al., 2007) and endothelium (Venkataraman et al., 2006). SPHK1, which predominantly localizes in the cytosol, phosphorylates sphingosine to S1P while SPHK2 can convert S1P back to sphingosine and then to ceramide (Maceyka et al., 2005). SPHK1 is activated by diverse stimuli such as growth factors which include epidermal growth factor (EGF), insulin-like growth factor-1 (IGF-1), hormones (estradiol) and the angiogenic factor; vascular endothelial growth factor (VEGF) (Alvarez et al., 2007). SPHK1 also upregulates NFκB in response to stress. In contrast to SPHK1, SPHK2 has a putative nuclear localization signal and it promotes apoptosis in lymphocytes (Don et al., 2007). A putative BH3-only domain has been defined in SPHK2, which may explain its proapoptotic functions (Liu et al., 2003). SPHK2 has been shown to inhibit DNA synthesis resulting in cell cycle arrest in various cell types (Igarashi et al., 2003). Recently, Weigert and co-workers suggested that SPHK2 may also play an important role in tumour progression. They showed that SPHK2-deficient MCF-7 breast tumour xenografts had markedly delayed growth as compared to controls (Weigert et al., 2009).

The levels of mRNA encoding SPHK1 are about 2-fold higher in tumours of the breast, colon, rectum, kidney, uterus,lung, ovary and stomach compared with normal adjacent tissue (French et al., 2003). The oncogenic role of SPHK1 was first demonstrated following its overexpression in mouse fibroblasts which resulted in H-Ras-mediated cellular transformation and tumour formation in nude mice (Xia et al., 2000). Enforced expression of SPHK1 in MCF7 breast cancer cells led to increased S1P levels and accentuation of oestrogen dependent cell growth and proliferation in soft agar and in nude mice (Nava, 2002). In contrast, loss of SPHK1 by siRNA inhibition resulted in cell cycle arrest and induction of apoptosis in MCF7 cells (Taha et al., 2006). Knockout of both SPHK1 and SPHK2 seized the synthesis of S1P leading to vascular and neural defects (Mizugishi et al., 2005).

1.3.6.2 Mechanisms of SPHK1 activation

SPHK1 activation involves three non-exclusive mechanisms: 1) phosphorylation, 2) translocation to the plasma membrane and 3) interaction with acidic phospholipids and/or other proteins (Pitson et al., 2003). To obtain full activation, all three mechanisms may be required. Upstream activators of SPHK1 include GPCRs, small GTPases, tyrosine kinase receptors, pro-inflammatory cytokines, FcgR1 and FcgR1 immunoglobulin receptors, calcium and protein kinase activators (M Maceyka 2002). Protein kinase- C (PKC) activation by phorbol 12-myristate 13-acetate (PMA) results in activation and translocation of SPHK1 to the plasma membrane which leads to the release of S1P to the extracellular medium (Johnson et al., 2002). Membrane translocation requires an ERK-dependent phosphorylation of SPHK1

at Ser225 (Pitson et al., 2003) which drives its oncogenic signalling (Pitson et al., 2005). Besides relocating to the plasma membrane, SPHK1 also traffics to the perinuclear and nuclear region (Kleuser et al., 2001). Two nuclear export sequences, NES1 and NES2 have been shown to mediate shuttling of SPHK1 from the nucleus to the cytosol (Inagaki 2003). Inhibition of the nuclear export receptor, CRM1 (chromosomal region maintenance 1) led to a marked nuclear accumulation of SPHK1 suggesting that the shuttling of SPHK1 between the cytoplasm and the nucleus is mediated by a CRM1-dependent pathway.

1.3.6.3 SPHK1 inhibitors

As the phosphorylation of sphingosine by SPHK1 is an established mechanism for the production of S1P, SPHK1 is a potential target of cancer therapeutics. Several SPHK1 inhibitors such as dimethylsphingosine (DMS), SK1-I (BML-248) and SK-II have been extensively used in vitro to block the production of S1P by tumour cells. DMS is an N-methylated metabolite of sphingosine. It inhibits both SPHK1 and SPHK2. It has been shown to inhibit the growth of gastric and lung cancer cells in athymic mice (Endo et al.,1991) and to decrease lung metastasis of melanoma cells in rodent models (Okoshi et al., 1991). SK1-I is a specific inhibitor of SPHK1. It was shown to reduce the survival and growth of human leukemia and Jurkat cells and to decrease the growth of acute myeloid leukaemia (AML) xenograft tumours (Paugh et al., 2008a). SK-II which is orally available showed significant suppression of mammary adenocarcinoma growth in mice (French et al., 2006). SPHK1 inhibition results in decreased signaling via Ras/mitogen-activated protein kinase (MAPK)

proliferation pathway and the phosphatidylinositol 3-kinase (PI3K)/Akt survival pathway which leads to inhibition of tumour activity (French et al., 2003b).

1.3.6.4 S1P phosphatases and S1P lyases

S1P phosphatases and S1P lyases (SGPL1) are the enzymes responsible for S1P catabolism. The two S1P phosphatases, SGPP1 and SGPP2, reversibly convert S1P back to sphingosine, thus controlling the cellular levels of S1P. S1P can also be converted to palmitaldehyde or phosphoethanolamine by SGPL1. Due to the presence of these enzymes, S1P elevation following SPHK1 activation is short lasting (Van Veldhoven and Mannaerts, 1991; Veldhoven and Mannaerts, 1994; Saba et al., 1997; Zhou and Saba, 1998; Mandala et al., 1998). Both SGPP1 and SGPP2 are located in the endoplasmic reticulum (ER) (Johnson et al., 2003). SGPP1 is expressed in most tissues with high levels found in the vascular tissues of placenta and kidney (Johnson et al., 2003) whereas SGPP2 is predominantly expressed in the heart and kidney (Ogawa et al.,2003). Loss of these phosphatases in yeast results in high S1P levels and renders cells more resistant to stress. In mammalian cells, overexpression of SGPP1 elevates ceramide levels and enhances apoptosis. siRNA knockdown of endogenous SGPP1 resulted in an increase in cellular S1P and a decrease in sphingosine (Johnson et al., 2003). Although SGPP2 shows similar activity, substrate specificity and localization to SGPP1, whether it has similar functions remains to be established (C. Ogawa et al., 2003).

SGPL1 activity has been reported to be located in the ER and human SGPL1 gene encodes a protein of 568 amino acids with a molecular weight of 63.5 kDa. SGPL1 expression has been

observed at variable levels in most mammalian tissues with high levels present in the liver, kidney and intestine. Lower levels are observed in muscle and brain. Inhibition of SGPL1 increases S1P levels and induces lymphopenia (Schwab et al., 2005). SGPL1 was also shown to be downregulated in human colonic cancer (Oskouian & Saba, 2007) and in metastatic lung adenocarcinoma (Ramaswamy et al., 2003). These findings indicate that SGPL1 and S1P phosphatases could potentially function as tumour suppressor genes (Oskouian et al., 2006).

1.4 Biological activities of S1P

1.4.1 S1P in cancer

Accumulating data on aberrant S1P signaling in various types of cancer has suggested that this signaling pathway may be involved in carcinogenesis. Among implicated cancers are those of the colon, prostate, breast, and head and neck. SPHK1 activation and the production of S1P promotes tumour growth, resistance to apoptosis, angiogenesis and metastasis (Pyne & Pyne, 2010). Elevated S1P levels were first identified in the ascitic fluid of ovarian cancer patients (Tilly & Kolesnick, 2002). The role of SPHK1/S1P in cancer is intricate and is influenced by many factors including the type of cells, receptors expressed and tumour micro-environment. Cells involved in maintaining tumour microenvironment include lymphocytes (cytotoxic T cells—CTL- and native killer—NK-), macrophages, dendritic cells, and neutrophils. Tumoral microenvironment is important in the regulation of tumour cell growth and metastasis. It also determines the tumour response to treatment The polyps of the $APC^{Min/+}$mouse model of intestinal tumorigenesis showed high levels of S1P and decreased SGPL1 activity and expression (Oskouian B & Saba J, 2007). S1P promotes cell growth and survival via extracellular signal-regulated kinase (ERK) activation in human glioblastoma cells (Kapitonov et al., 2009). In Wilms tumour, S1P was shown to have anti-proliferative effects by inducing the expression of connective tissue growth factor (CTGF) an effect mediated by S1PR2 (Mei-hong Li et al., 2009). In human prostate cancer PC3 cells, S1P induced autophagy through S1PR5 and inhibited rapamycin signalling (Chang et al., 2009). S1P also enhances the metastatic potential of tumour cells by promoting their motility and

invasion (Visentin et al., 2006). These findings demonstrate that S1P is generally a pro-tumour factor and may be a useful target in anti-cancer therapy.

1.4.2 S1P in immune cell signalling

FTY720 or Fingolimod is an S1P analogue developed to prevent skin allograft rejection and to treat autoimmune diseases such as multiple sclerosis and rheumatoid arthritis. The discovery of this novel immunosuppressive drug which induces lymphopenia has highlighted the significance of S1P in immune cells (Mandala et al., 2002). During normal lymphocyte recirculation system, B-cells from the lymphoid tissues and T-cells from the thymus migrate towards high S1P levels in the blood which is an S1PR1–dependent chemotactic process (Chiba et al., 2006). Upon phosphorylation of FTY720 by SPHK2, FTY720-P downregulates S1PR1 and inhibits the migration of lymphocytes to S1P. Hence FTY720-P inhibits lymphocytes egress from the lymphoid tissues and the thymus (Chiba et al., 2006) and increases the homing of lymphocytes in the circulation to the lymph nodes and Peyer's patches (Mandala et al., 2002). This leads to marked reduction of peripheral blood B and T lymphocytes upon FTY720 administration.

The S1P-S1PR1 axis also controls the trafficking of other immune cells including NK cells, dendritic cells, macrophages, mast cells and haematopoietic progenitor cells (Schwab & Cyster 2007).

1.4.3 S1P in inflammation

Extensive data shows that S1P is a pro-inflammatory molecule because it increases the production of cytokines and prostaglandins by immune effector cells (Kee et al., 2005). For example, during allergic reactions, the crosslinking of high affinity IgE receptors on mast cells upregulates SPHK1 and SPHK2 and increases the production of S1P (Olivera et al., 2007). S1P in turn enhances mast cell activation and degranulation, releasing histamine and other pro-inflammatory cytokines. Intraperitoneal administration of the SPHK1 inhibitor, DMS in a mouse model of asthma has been shown to decrease the infiltration of eosinophils and macrophages and also decreased the release of Th2 cell-mediated cytokines (Lai et al., 2008). Inhaled DMS and SK-I has also been shown to decrease airway hyper-responsiveness and inflammation in ovalbumin-sensitized mice (Nishiuma et al., 2008) which has led to potentially new directions for asthma therapy.

1.4.4 S1P in cardiovascular disease

Activation of S1PR1, S1PR2 and S1PR3 leads to distinct set of signalling pathways. S1P binds to these three receptors on vascular endothelial cells, vascular smooth muscle cells (VSMC) and cardiomyocytes (Takuwa et al., 2008). The S1P/ S1PR1 pathway plays a role in the promotion of vascular development in vivo (Argraves et al., 2004; Rosen & Goetzl, 2005) and decrease in vascular permeability (Takuwa et al., 2008). Via its action on S1PR1 and S1PR3, mediated by G_i, S1P stimulates the proliferation and migration of endothelial cells during angiogenesis (Paik et al.,2001)(Figure 1.2). In contrast to S1PR1, S1PR2 inhibits

VSMC migration and angiogenesis. S1P interaction with S1PR1 and S1PR3 induced migration of VSMC from the media to the intima following endothelial injury resulting in vascular occlusive lesions, hence inhibition of VSMC migration has potential for the treatment of vaso-occlusive diseases (Usui et al., 2004).

Chae et al. have demonstrated that S1PR1 is upregulated in lung cancer cells during angiogenesis and that S1PR1 is required for the angiogenic response of lung cancer in vivo (Chae et al., 2004). Stimulation of S1PR3 can also promote angiogenesis and vasculogenesis *in vitro* (Licht et al., 2003). S1P/ S1PR3 signalling is implicated in the constriction of VSMC giving rise to hypertensive effects, however in the vascular beds, S1P/ S1PR3 signalling leads to an endothelium-dependent dilatory effect which protects the heart from hypoxia (Takuwa et al., 2008).

Sachinidis et al have demonstrated that S1P activities are present in low density lipoproteins (LDL) (Sachinidis et al., 1999), and mildly oxidized LDL has also been shown to induce contraction of endothelial cells via a Rho-dependent pathway resulting in increased endothelial permeability (Essler et al., 1999). Oxidized LDL stimulates the production of S1P in the VSMC and induces the proliferation of VSMC (Augé et al., 1999). It is becoming clear that S1P is a mediator of atherosclerosis and that S1P is a robust predictor of both the occurrence and severity of coronary artery stenosis (Deutschman et al., 2003).

1.5 LPA signalling and Autotaxin

Lysophosphatidic acid (LPA) is a bioactive simple lipid closely related to S1P. It is composed of a single fatty acyl chain, a glycerol backbone and a free phosphate group (Wouter H Moolenaar 1995). LPA is primarily formed by hydrolysis of lysophosphatidylcholine (LPC) by the ectoenzyme ATX via its lysophospholipase D activity. LPA production also occurs within the hair follicles. LPA is secreted by activated cells particularly activated platelets in the plasma (Eichholtz et al., 1993). Similarly to S1P, LPA binds to specific cell-surface GPCRs and evokes its biological effects including enhancing tumour cell proliferation and migration, increasing cytokine production in inflammation and promoting survival of many cell types (Yanagida et al., 2013). There are at least six recognised LPA receptors, LPAR1-6 (Choi & Chun 2013). LPAR1 was discovered by Chun's group in 1996 (Hecht et al., 1996) followed by LPAR2 and LPAR3 (Chun et al., 2002). LPAR1 mRNA is elevated in most cancer cells (Hecht et al., 1996). LPAR2 and LPAR3 are highly expressed in ovarian cancer cells (Yu et al., 2008). LPA, mediated by ATX, promotes angiogenesis (Rivera-Lopez et al., 2008) and stimulates chemotaxis and proliferation of many cancer cell lines including breast cancer cells and human melanoma cells (Umezu-Goto et al., 2002). Therefore, ATX and LPA receptors are attractive targets for anti cancer drugs (Xu et al., 2009).

ATX, also known as an exo-nucleotide pyrophosphatase and phosphodiesterase (ENPP2) is a 125-kDa glycoprotein, originally identified from human melanoma A2058 cells (Stracke et al., 1992). It plays an important role in tumour progression and its mRNA is overexpressed in thyroid (Kehlen et al., 2004) and hepatocellular carcinoma (Wu et al., 2010), teratocarcinoma and neuroblastome cell lines (Yang et al., 1999). ATX mRNA was found in abundance in

human brain, placenta and small intestine (Fuss et al., 1997). Higher expression of ATX mRNA was observed in advanced stage of neuroblastoma compared to early stage of disease suggesting a role in tumour progression. ATX expression was also greater in poorly differentiated non small carcinoma of the lungs (Yang et al., 1999). In breast cancer and human melanoma cells, ATX was found to stimulate their motility (Gaetano et al., 2009). ATX and LPAR transgenic mice were shown to develop mammary tumours and mastitis (Liu et al., 2009a). Aberrant expression of ATX was found in breast cancer cells and was closely associated with their invasiveness (Yang et al., 2002). ATX-LPA signalling has also been shown to be important in ovarian cancer. High levels of LPA was observed in the ascitic fluid of ovarian cancer patients (Kita et al., 1997). Gene expression profiling of ovarian cancer cells treated with LPA showed that the LPA-signature-positive ovarian tumours had shorter progression free survival and were in advanced stage of disease (Murph et al., 2009). The inhibition of ATX has been shown to reduce the invasion and metastasis of human melanoma cells (Baker et al., 2006). A potent ATX inhibitor, PF-8380 has been reported to be able to reduce LPA levels by more than 95% in the plasma (Gierse et al., 2010).

1.6 S1P targeted therapies

Several pharmaceutical companies have established investigational programs to elucidate the potential of targeting S1P signaling for the treatment of cancer. A murine monoclonal antibody (mAb) or anti-S1P mAb (Sphingomab or LT1002) has been designed to neutralise extracellular S1P by molecular absorption (O'Brien et al., 2009). Anti-S1P mAb prevents S1P from binding to its receptors. S1P has been shown to act synergistically with basic fibroblastic

growth factor (bFGF) and vascular endothelial growth factor (VEGF) in stimulating angiogenesis (Licht et al., 2003b). Visentin et al have shown that systemic anti-S1P mAb treatment induced antiangiogenic and antiproliferative effects and substantially reduced tumour progression in mice. Mice implanted with VEGF or bFGF which were then injected with anti-S1P mAb showed marked reduction in tumour vasculature as compared to control groups (Visentin et al., 2006). Anti- S1P mAb also reduced the metastatic potential of tumour cells by reducing neovascularization in multiple tumour cell lines including breast carcinoma cells MDA MB-231 and MDA MB-468, the ovarian cancer cell line SKOV3 and A549 lung adenocarcinoma cells. Histopathological examination of A549 lung and SKOV ovarian tumours treated with anti-S1P mAb showed large areas of necrosis and extensive fibrosis when compared to the non-treated tumours. These data suggest that the anti-tumour effects of the anti-S1P mAb were not cancer type specific (Visentin et al., 2006) and has potential therapeutic use in humans.

The murine anti-S1P was humanised for clinical trials and is called Sonepcizumab or LT1009 (O'Brien et al., 2009). Sonepcizumab was formulated into two formulations: i) Asonep, the oncology formulation recently used in Phase 1 clinical trials and ii) Isonep, the ocular formulation used for treatment of age-related macular degeneration (Sabbadini 2011)

Some investigations have focused in modulating S1P receptor signalling using the S1P agonist, FTY720. FTY720 inhibited tumour development and angiogenesis in mice harboring human hepatocellular, bladder and lung cancers (Ho et al., 2005; Salinas et al., 2009). In ovarian cancer cells, FTY720 has been reported to induce necrosis and autophagy (Zhang et al., 2010). S1PR1 antagonism also inhibits angiogenesis. S1PR1 siRNA decreases

angiogenesis and reduces the growth of Lewis lung carcinoma *in vivo* (Recently, a novel class of orally bioavailable S1PR1 antagonists was described with potent anti-tumour effects in animal models (Ibrahim et al., 2012). However, targeting S1PRs may be complicated as not all S1PRs mediate tumourigenic responses, hence selectivity of receptor antagonism is crucial in determining the success of sphingolipid receptor-based therapeutics.

1.7 Hodgkin lymphoma

1.7.1 History

The discovery of Hodgkin lymphoma (HL) was attributed to Thomas Hodgkin (Hodgkin 1832). It was the first lymphoid neoplasm to be defined microscopically and is characterized by the presence of mononucleated Hodgkin cells and multinucleated Reed-Sternberg cells. These cells were first described by Dorothy Reed and Carl Sternberg in 1902 and 1898 respectively (Sternberg, 1898, Reed, 1902). Initially, HL was thought by Sternberg to be inflammatory in origin and related to tuberculosis, however Reed subsequently found that HL and tuberculosis were not related (Dawson 2003). In the 1970s, several cell lines were developed from pleural effusions, bone marrow and peripheral blood of patients with aggressive HL. Cytogenetic analysis revealed abnormal karyotypes and the aggressive nature of the disease was confirmed (Jaffe et al., 2008).

1.7.2 Classification of HL

HL is the 3rd commonest lymphoma after diffuse large B-cell lymphoma (DLBCL) and follicular lymphoma (FL). The first histological classification of HL was introduced by Jackson and Parker in 1947, which was then revised at Rye in 1966. In 1994, the Rye classification was incorporated into the Revised European-American Lymphoma (REAL) classification (Cartwright & Watkins 2004). Based on the REAL classification, the 2008 WHO Classification separated HL into classical HL (cHL) and nodular lymphocyte-predominant Hodgkin lymphoma (NLPHL). cHL which comprises 95% of all HL cases is further subdivided into four subtypes; nodular sclerosis (NS), mixed cellularity (MC), lymphocyte-depleted (LD) and lymphocyte-rich (LR) HL. This classification is based on the morphology and phenotype of the tumour cells and on the cellular infiltrate surrounding the tumour cells. cHL is characterised by the presence of Hodgkin and Reed-Sternberg (HRS) cells, while NLPHL is characterised by the presence of L&H—lymphocytic and histiocytic cells (Ralf Küppers 2009b). HRS cells as well as L&H cells account for only approximately 1% of the cells in the tissue. NSHL which comprises 60% of HL in the West is characterised by nodules containing HRS cells separated by extensive bands of fibrosis. MCHL accounts for 30% of HL cases in the West and exhibits a mixture of inflammatory cells including neutrophils, eosinophils, histiocytes and plasma cells. Fibrotic bands are not seen in this subtype.

1.7.3 Epidemiology of HL

The incidence of HL and its association with EBV varies considerably with age, gender, ethnicity and geographic location. The highest incidence of HL was reported among Caucasians, followed by African Americans and Hispanics. The lowest incidence was found among Orientals (Cartwright & Watkins 2004). The incidence of HL in the UK is about 0.6% of all cancers. 1,673 new cases of HL were diagnosed in the UK in 2007. Correa and O'Connor introduced three epidemiological patterns of HL which were related to the urbanization and economic status of a geographical region. Pattern I occurs in developing countries and shows a bimodal peak in children and elderly patients. Majority of patients in this pattern are of the mixed cellularity and lymphocyte depleted subtypes. Pattern III shows a first peak in young adults and the second peak in the older age groups and occurs in developed countries. Pattern II is intermediate between these two patterns and occurs in rural areas of developed countries. A significantly inverse relationship between rates of HL in children and young adults was observed; countries with high rates in children (aged 5–14 years) have low rates in young adults (aged 20–34 years), and vice versa (Correa & O'Conor 1971). In 1966, MacMahon suggested that an infectious agent might cause HL in young adults (Macmahon & June 1966). The risk of HL was suggested to be linked to social class background in childhood. Individuals from higher social class with better education and from a smaller family size and early birth order position have a higher risk of developing HL (Guttensohn & Cole., 1980). As the population moved to a higher living standard, the age of acquiring the primary EBV infection increases giving rise to a shift of incidence from children to young adult age group. In the USA and West Europe, the incidence of HL is higher among young adults as compared to children.

1.7.4 Biology of HL

In 1990, using the PCR technique and primers specific for target sequences of the IGH@ and T-cell receptor (TCR) loci on microdissected single HRS cells, these cells were confirmed to derive from mature B cells at a GC or post GC stage of differentiation (Küppers et al., 1994). This was based on the detection of clonally rearranged immunoglobulin V (IgV) heavy and light chain genes with many somatic mutations; somatic hypermutation of IgV genes occuring in antigen-activated B cells within GC (Küppers, 2009b). It is believed that HRS cells derive from crippled or non-functioning, pre-apoptotic germinal centre B cells (Kuppers & Rajewsky, 1998). Despite their origin from B cells, HRS cells have undergone reprogramming of gene expression and have lost most of their expression of the typical B-cell genes while at the same time acquiring expression of molecules of non B cells. Typically HRS cells express CD30, CD15, PAX5, NOTCH1, JUN, JUNB, STAT5A and STAT5B. They can also express T- cell markers, CD3 and CD4, the cytotoxic T cell marker, granzyme B and the dendritic markers, fascin and CCL17 (Ralf Küppers 2009c). However Tzankov et al found that the expression of T-cell markers is rare in HL comprising only 5% of HL cases and that less than 1% of cHL are of T-cell origin (Tzankov et al., 2005).

1.7.5 Epstein-Barr virus

EBV is a gammaherpes virus that results in infectious mononucleosis and which is associated with several malignancies including HL, Burkitt's lymphoma (BL), as well as some gastric cancers and nasopharyngeal carcinoma (NPC)(see Table 1.3). EBV has a large genome of 172 kb in length which has been entirely cloned and sequenced (Kutok & Wang 2006). The virus is composed of a toroid shaped protein core wrapped by linear double-stranded DNA which circularizes to form extrachromosomal episomes within the nuclei of infected cells (Figure 1.3). 95% of adults are infected with EBV and the infection persists for life. The virus gains entry into the main target, the naïve B-cell, by interaction of the viral envelope protein gp350/220 with CD21, the B-cell surface molecule. EBV can also infect epithelial cells, mesenchymal cells and T cells. EBV has two phases of its life cycle; the latent phase in which there is no viral replication and the replicative or lytic phase when infectious virus is produced, eventually killing the infected cells and releasing the virus particles (Rickinson & Kieff, 2001). In underdeveloped countries, EBV infection occurs in early childhood; while in developed countries, infection occurs most often in teens and young adults, one- third of cases manifesting clinically as acute infectious mononucleosis. In developed countries of low socioeconomic status, infection generally occurs in an intermediate age group, usually by the age of 15.

The immediate early genes expressed includes BZLF1 and BZRF1 which encode the Z and R proteins, respectively,which are responsible for the activation of the virus lytic cycle. In the latent phase, the virus persists as 1-100 episomes which rarely integrate into the human genome. During the latent phase, there is no production of infectious viruses. Latent genes expressed include six nuclear antigens; EBNA1, EBNA2, EBNA3A, EBNA3B, EBNA3C and

EBNA leader protein (LP), three membrane proteins; LMP1, LMP2A, and LMP2B; and two small nonpolyadenylated EBV-encoded small RNAs; EBER1 and EBER2, and the EBV encoded micro-RNAs encoded in *Bam*H1 region (BART).

Table 1.2: Patterns of latent infection gene expression in EBV infected cells.

Latency programme	**EBV genes expressed**	**Occurence**
0	EBERs, LMP2A (?)	Memory B cells in peripheral blood
I	EBERs, EBNA1	BL, primary effusion lymphoma
II	EBERs, EBNA1, LMP1, LMP2A	HL, NPC
III	EBERs, EBNA1, EBNA2, EBNA3, EBNA-LP, LMP1, LMP2A	PTLD, PCNSL

PCNSL= primary central nervous system lymphoma

The Epstein-Barr Virus

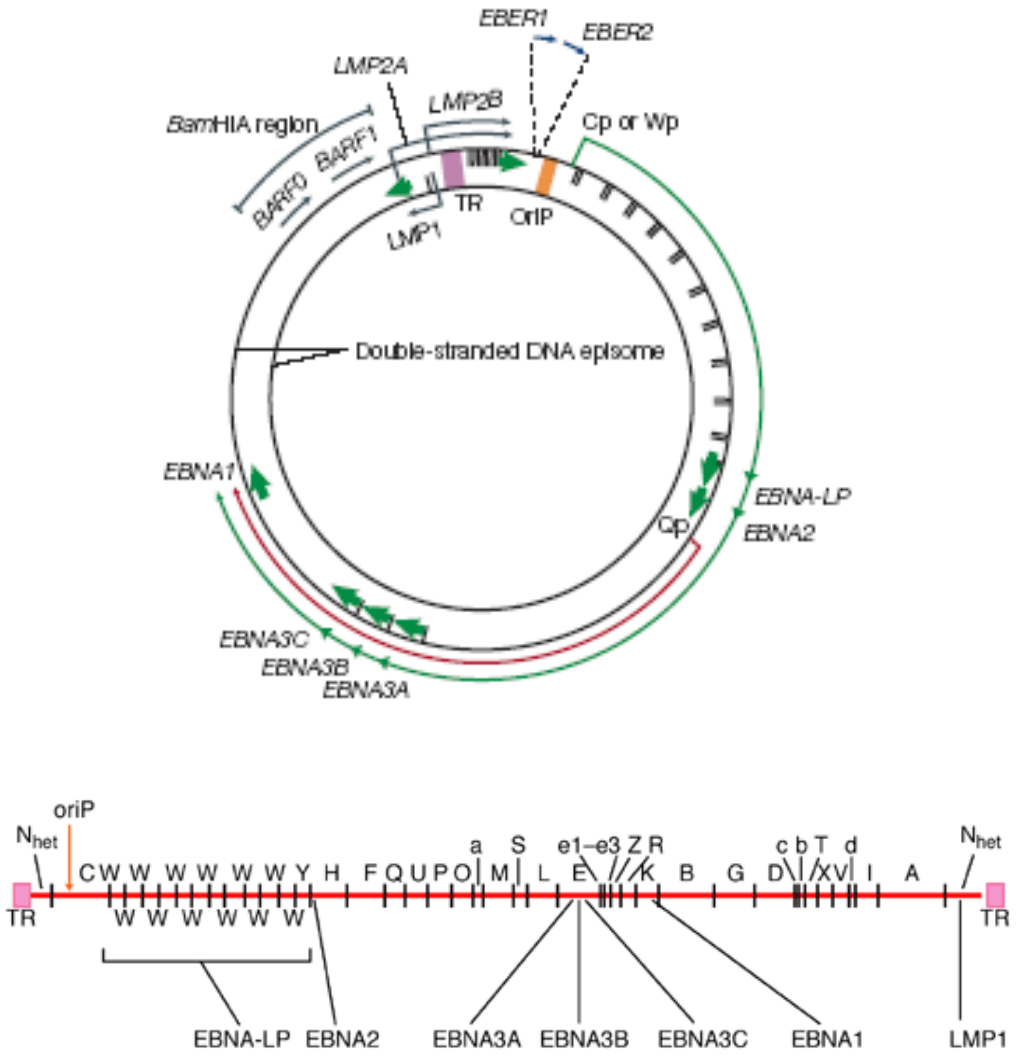

Figure 1.4: Map of EBV genome. EBV genome has five unique regions of DNA, punctuated by four internal repeat regions and capped on either end by a terminal repeat region (purple shaded region). The red and green arrows represent genes encoding the latent proteins (from Murray and Young 2002)

1.7.6 EBV gene expression in normal cells and in tumours

EBV can establish different latent states (i.e. infections not leading to replication of new virus particles) in normal and malignant B cells. EBV has growth- transforming property, in culture it infects resting primary B cells transforming them into lymphoblastoid cell lines (LCLs) (Henle W et al., 1967). EBV transformed LCLs express at least 6 nuclear antigens (EBNA1, EBNA2, EBNA3A, EBNA3B, EBNA3C and EBNA-LP) and three membrane proteins (LMP1, LMP2A and LMP2B). This pattern of gene expression is referred as Latency III. In this latency pattern, the EBNA transcripts are driven by one of two upstream promoters, Cp or Wp, in the BamHI C or W regions of the genome respectively. Latency II was originally identified in undifferentiated NPC and subsequently in EBV-associated gastric carcinomas, Hodgkin lymphomas and NK/T cell lymphomas (Rowe et al., 2009). This type of latency is characterized by expression of LMP1 and LMP2A/B in addition to Qp-driven EBNA1 but no expression of the other EBNAs. In gastric cancer, EBNA1 expression is associated with low LMP2. Even in a type of malignancy, the levels of LMP1 and LMP2 can be quite variable. For instance, LMP2A transcripts are consistently expressed in NPC but LMP1 transcripts are detected in only a proportion of cases (Khabir et al., 2005). In Latency I, EBNA1 transcripts are driven by the Qp promoter. In latency 0, no viral antigens are expressed. This is found in the memory B cells of asymptomatic EBV carriers. The EBERs are non-coding RNAs which are expressed at high copy number in all forms of latency, and which are useful for detecting EBV in tissues using *in situ* hybridization. Presence of EBV DNA in HL tissue was first demonstrated by Weiss and co-workers using the cloned *Bam*H1 W fragment of EBV as an *in situ* hybridization probe (Weiss et al., 1991).

1.7.7 Pathogenic role of EBV in Hodgkin lymphoma

EBV is found in HRS cells in approximately 40% of HL patients in developed countries and in a higher proportion in tumours from patients in developing countries. EBV is more frequently associated with mixed cellularity subtype and more often in males with HL (Anagnostopoulos et al., 1996). In AIDS patients with cHL, almost all cases are EBV positive. In paediatric HL in Central and South America, EBV association is almost 90% (Dolcetti et al., 2001; Kutok & Wang, 2006). Flavell et al. have shown a strong association between EBV positivity and South Asian ethnicity in paediatric HL patients from the UK (K. J. Flavell et al. 2001). EBV infection of B cells stimulates $CD8^+$ T cell response. These activated T cells give the appearance of atypical lymphocytes in the peripheral blood of infectious mononucleosis sufferers. Subsequently, EBV-specific T cell immunity develops, killing and reducing the number of infected B cells. In immunocompetent hosts, the infection is controlled and the virus enters a latent phase in a few infected B cells. In immunocompromised conditions, the cytotoxic T cell surveillance is decreased resulting in the development of EBV-associated diseases such as PTLD and OHL (Kutok & Wang 2006). The development of EBV-associated malignancies such as HL, BL, gastric carcinoma and NPC in non-immunosuppressed individuals might be a result of other co-factors besides persistent EBV infection. The first evidence that EBV is associated with HL was provided by the detection of raised antibody titres to EBV antigens in patients with HL when compared to patients with other lymphoproliferative diseases (McCormick et al., 1976).

Multiple signalling pathways have been shown to be activated in HRS cells including Janus kinase (Jak)-Stat and nuclear factor-κβ (NF-κβ). Activation of NF-κβ occurs through both

canonical and non-canonical pathways via signalling of members of Tnfr family such as CD40, CD30 and TAC1. NOTCH1 also contributes to the activation of NF-κβ in HRS cells (Cheng et al., 2001). Constitutive activation of NF-κβ may contribute to the development of HL by rescuing HRS cells from apoptosis.

EBNA1 which is expressed in all proliferating EBV-infected cells is very important in the replication and maintenance of the viral episome. This is achieved by sequence-specific binding of EBNA1 to the plasma origin of viral replication, OriP. The interaction results in a single replication of the EBV genome during S phase and subsequently segregation of replicated EBV genomes to progeny cells (Levitskaya et al., 1995). Latently infected B cells persistently expressing EBNA1 may evade elimination by the immune system (Levitskaya et al., 1997). EBV positive B cells expressing only EBNA1 are not recognized by cytotoxic T cells because EBNA1 is not presented by MHC class I molecules (Levitskaya et al., 1995). LMP1 is an oncogene expressed on the HRS cell membrane mimicking an active CD40 receptor, thereby inducing constitutive NF-κB activation. LMP1 transgenic mice has been shown to develop B-cell lymphomas (Kulwichit et al., 1998). LMP1 can also activate AP1, p38, PI3K and Jak–Stat signalling (Young & Murray, 2003). LMP1 and LMP2 contribute to the downregulation of B-cell phenotype in EBV-positive HRS cells (Vockerodt et al., 2008). LMP2A expression in EBV infected B-cells was associated with activated and proliferative state which could lead to the development of HL (Portis et al., 2003). Caldwell's group also found that LMP2A can mimic a B-cell receptor (BCR) and LMP2A expression in a transgenic mouse model led to the survival of BCR-deficient B-lineage cells (Caldwell et al., 1998). This

showed that the survival signals for B-cells that are normally mediated by the expression of BCR can be replaced by LMP2A.

Table 1.3: Epstein-Barr virus associated diseases

Lymphomas/lymphoproliferative diseases
Burkitt lymphoma
Classical Hodgkin lymphoma
Extranodal NK/ T cell lymphoma
Angioimmunoblastic T cell lymphoma
EBV-associated haemophagocytic lymphohistiocytosis (HLH)
AIDS-associated B-cell lymphomas: Plasmablastic lymphoma, PCNSL
PTLD
Lymphomatoid granulomatosis (LYG)
EBV+ DLBCL of the elderly
Primary effusion lymphoma (PEL)
Carcinomas
Nasopharyngeal carcinoma
Lymphoepithelioma-like carcinoma (salivary glands, liver, thymus, lungs, stomach)
Mesenchymal tumours
Follicular dendritic cell sarcoma
Smooth muscle tumours
Non malignant diseases
Infectious mononucleosis
Oral hairy leukoplakia
Chronic active EBV (CAEBV)

1.8 Diffuse large B- cell lymphoma

1.8.1 Introduction

Diffuse large B-cell lymphoma (DLBCL) is the commonest lymphoma accounting for nearly 40% of lymphoid neoplasms (Armitage et al., 1998). In the past it was known by many names which included reticulum cell sarcoma, diffuse histiocytic lymphoma followed by diffuse mixed lymphoma, diffuse large cell lymphoma, or immunoblastic lymphoma—terms from the Working Formulation. It was in the 1994 Revised European-American lymphoma (REAL) classification system that it was referred to as DLBCL. It is so named based on the diffuse effacement of normal lymph node or extranodal site architecture by malignant B cells. DLBCL is heterogeneous in morphological appearance (Table 1.5), immunophenotype, and biological behaviour. It may arise *de novo* or develop as a transformation from an underlying low-grade lymphoproliferative disease particularly follicular lymphoma. Less frequently, this transformation may occur in patients with chronic lymphocytic leukemia/ small lymphocytic lymphoma giving the eponym of Richter transformation. (Ghofrani et al., 2007; Tsimberidou & Keating, 2005). Patients in this category have poorer prognosis and poorer response to therapy.

The age range of DLBCL patients is broad with a median of 70 years old. Patients usually present with rapidly enlarging lymph nodes. Clinical outcome and response to chemotherapy also vary. For several decades, the CHOP (cyclophosphamide, doxorubicin, vincristine, and prednisone) chemotherapy regimen combined with field radiation was the mainstay of therapy. In 1997, the anti-CD20 monoclonal antibody, Rituximab was added into the

chemotherapy regime which resulted in markedly improved survival for DLBCL patients (Saini et al., 2011).

1.8.2 Microscopic pathology and differential diagnoses

DLBCL is characterised, in most cases, by effacement of normal lymph node architecture by sheets of large, atypical lymphoid cells. The cells may be divided by fine or broad bands of fibrosis. The 2008 WHO Classification of Tumours of Hematopoietic and Lymphoid Tissues is the most comprehensive classification system which includes morphological and clinical features, immunohistochemical, molecular, and genetic aspects of malignant lymphoid disorders (Nakamura S, Jaffe E 2008). Based on this classification, DLBCL is divided into centroblastic, immunoblastic, T-cell/ histiocyte-rich, and anaplastic, as well as the rarer entities, plasmablastic and anaplastic lymphoma kinase (ALK)–positive DLBCL (Table 1.4). The centroblastic variant which accounts for 80% of cases, is composed of cells resembling germinal centre centroblasts. The immunoblastic variant which accounts for 10% of cases comprises more than 90% immunoblasts. The microscopic description of each variant is given in Table 1.5. The plasmablastic variant of DLBCL may overlap with plasmablastic lymphoma showing CD79α and CD138 expression but typically lack EBER positivity. Plasmablastic lymphoma which typically presents in immunocompromised patients is negative for CD20 and is typically positive for CD138 and EBER.

The morphological differential diagnoses of DLBCL include carcinoma and malignant melanoma which also exhibit large malignant cells. Both of these malignancies are

distinguishable by immunohistochemical techniques with carcinoma being cytokeratin positive and melanoma being S100, HMB-45, and/or Melan A positive. Burkitt lymphoma, mediastinal large B-cell lymphoma, plasmablastic lymphoma, and plasmablastic myeloma are among haematological malignancies to be considered as differential diagnoses.

Another distinct clinicopathological entity having a similar immunophenotypic profile to systemic DLBCL is primary mediastinal large B-cell lymphoma (PMBL). It was listed as a separate entity in the 2000 WHO Classification of Hematopoietic and Lymphoid Tumour Tissue. Typically, it presents in young women with a mediastinal mass exhibiting distinctive clear-cell morphology and sclerosis and it can be distinguished immunohistochemically from DLBCL by the co-expression of c-Rel and TRAF1. 53% of PMBL exhibit c-Rel and TRAF1 expression while only 2% of DLBCLs are positive for these two proteins.

Table 1.4: The 2008 WHO Classification of Diffuse Large B cell lymphoma: variants, subgroups and subtypes/entities

Diffuse large B-cell lymphoma (DLBCL), not otherwise specified (NOS)
Common morphological variants
Centroblastic
Immunoblastic
Anaplastic
Rare morphological variants
Molecular subgroups
Germinal centre B cell-like (GCB)
Activated B cell- like (ABC)
Immunohistochemical subgroups
CD5-positive DLBCL
Germinal centre B cell-like (GCB)
Non Germinal centre B cell-like (Non GCB)
Diffuse large B-cell lymphoma subtypes
T cell/ histiocyte rich large B-cell lymphoma
Primary DLBCL of the CNS
Primary cutaneous DLBCL, leg type
EBV-positive DLBCL of the elderly
Other lymphomas of large B cells
Primary mediastinal (thymic) large B- cell lymphoma
Intravascular large B-cell lymphoma
DLBCL associated with chronic inflammation
Lymphomatoid granulomatosis
ALK-positive LBCL
Plasmablastic lymphoma
Large B cell ymphoma arising in HHV-8-associated multicentric Castleman disease
Primary effusion lymphoma
Borderline cases
B-cell lymphoma, unclassifiable, with features intermediate between diffuse large B-cell lymphoma and Burkitt lymphoma
B-cell lymphoma, unclassifiable, with features intermediate between diffuse large B-cell lymphoma and classical Hodgkin lymphoma

Table 1.5: Microscopic features of DLBCL variants

DLBCL variants	Microscopic features
Centroblastic	Exhibits vesicular nuclei with smooth chromatin, multiple small nucleoli, and scant cytoplasm. Occasionally, polylobated nuclei are present.
Immunoblastic	Shows single, prominent, centrally located nucleolus and has slightly more cytoplasm.
T-cell/ histiocyte-rich	Composed primarily of non-neoplastic small T cells with variable numbers of admixed histiocytes. The large, malignant B cells represent fewer than 10% of all cells.
Anaplastic	Characterised by very large, often cohesive cells with extensive pleomorphism of the nuclei.
Plasmablastic	Morphologically resembles the immunoblastic variant but may also show eccentric nuclear placement with more eosinophilic cytoplasm

*from Gatter & Pezzella, 2010.

1.8.3 Molecular classification of DLBCL

Using DNA microarray, Alizadeh et al found two molecularly distinct forms of DLBCL showing gene expression patterns of different stages of B cell differentiation. One group expressed genes characteristic of germinal centre B cells (GCB-like DLBCL) and the other, genes normally induced during the *in vitro* activation of peripheral blood B cells; referred to as activated B- cell-like (ABC) DLBCL. Based on this gene expression profiling, DLBCL is now divided into two prognostically significant subtypes (Alizadeh et al. 2000). Although patients with GCB subtype have been shown to have better survival than those with the ABC subtype, all patients are still treated in a similar way as studies have so far failed to show superiority of specific regimens for each subtype. In terms of prognosis, there was no correlation found between these two subgroups of DLBCL and the different morphological variants listed in Table 1.5 (Rosenwald et al., 2002). In 2000, Hans and co-workers developed a reproducible immunohistochemical algorithm using CD10, BCL6 and MUM1 which showed approximately 80% concordance with the gene expression profiling (GEP) classification of DLBCL (Hans et al., 2004). Nine years later Choi et al. proposed a new algorithm using GCET1, CD10, BCL6, MUM1, and FOXP1 which showed a higher (93%) concordance with GEP classification (W. W. L. Choi et al. 2009). Both algorithms are shown in Figure 1.5. Clinical characteristics of both GCB and ABC subtypes are listed in Table 1.6. BCL2 gene rearrangement as t(14;18)(q32;q21) was found to occur almost exclusively in the GCB subtype (Sharon LB et al. 2003; Jardin et al. 2006). GCB DLBCL cases mostly show centroblastic monomorphic morphology while the ABC DLBCL subtype mostly show immunoblastic and centroblastic polymorphic features (Rosenwald et al., 2002).

New algorithm

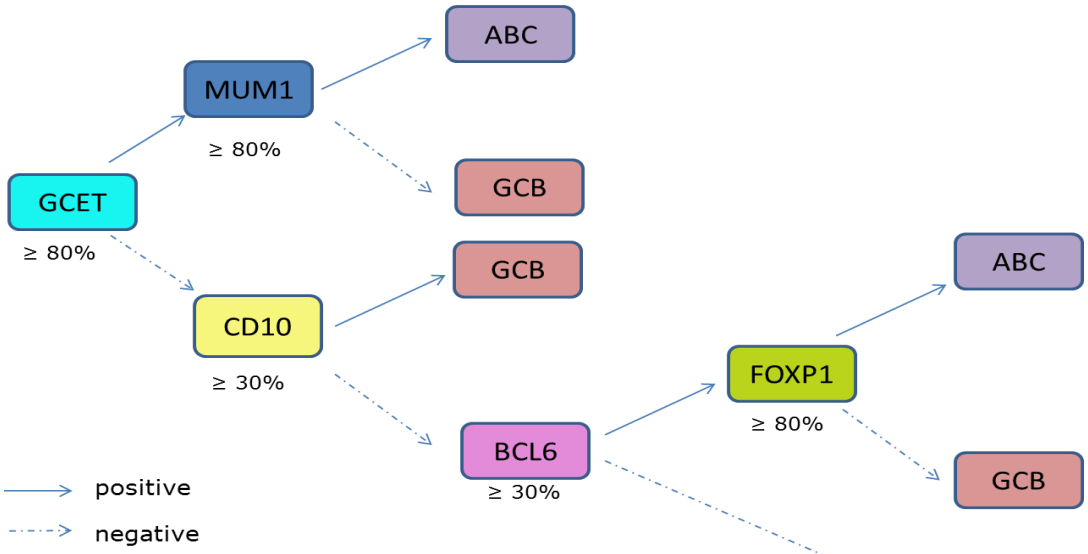

Hans algorithm

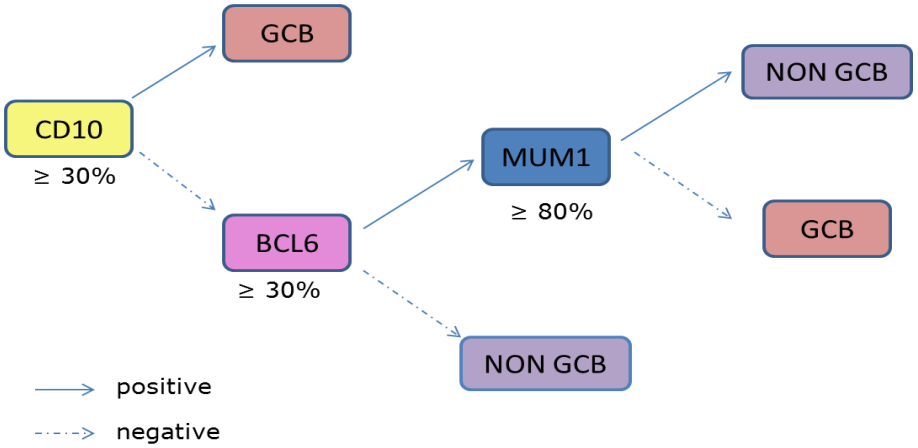

Figure 1.5: Decision tree for subtyping of DLBCL cases according to the A) New algorithm and B) Hans algorithm (adapted from Choi et al., 2009).

Table 1.6: Characteristics of GCB and ABC DLBCL

	GCB DLBCL	**ABC DLBCL**
Postulated normal counterpart	Germinal center B cell	Post-germinal center B-cell
Clinical outcome (5 year OS)	59%	30%
Oncogenic mechanism	REL amplification BCL2 translocation	Constitutive activation of NF-kB
Chromosomal alterations	Gain 12q12 t(14;18)	Trisomy 3 (FOXP1?) Gain 3q Gain 18q21–q22 (BCL2) Deletion 6q21–q22 (BLIMP1)

Abbreviations: ABC, activated B-cell; DLBCL, diffuse large B-cell lymphoma; GCB, germinal centre; NF-kB, nuclear factor kappa B: OS, overall survival. (Adapted from De Paepe & De Wolf-Peeters 2007)

1.8.4 Risk stratification of DLBCL patients

The International Prognostic Index (IPI) has been shown to be one of the best predictors of outcome. This model was developed to predict the outcome of patients with aggressive NHL based on their pre-treatment clinical characteristics (Shipp et al., 1993). The IPI categorised patients into prognostic groups based on the anatomic stage, ECOG performance status, the number of extranodal sites, serum lactate dehydrogenase (LDH) level, and age at diagnosis. For full index IPI, one point/ factor is allotted for the prognostic factors (Table 1.7). Based on the sum of the points allotted, patients are then assigned to one of four risk groups having different five year survival rates: The age- adjusted IPI is used to compare patients within an age group (i.e. 60 or younger, or over 60) and includes only 3 prognostic factors (Table 1.8).

Table 1.7: The Full International Prognostic Index

Prognostic factor	Risk category and factor	5 year survival
Age older than 60 years	Low risk, factor 0 or 1	73%
Performance status of 2 or higher	Low-intermediate risk, factor 2	51%
LDH level greater than 1x normal	High-intermediate risk factor 3	43%
Extranodal sites of 2 or more	High risk, factor 4 or 5	26%
Stage III or IV		

Table 1.8: The Age-adjusted International Prognostic Index

Prognostic factor	Risk category and factor	5 year survival
Performance status higher than 1	Low risk, factor 0	83%
LDH level greater than 1x normal	Low-intermediate risk, factor 1	69%
Stage III or IV	High-intermediate risk, factor 2	46%
	High risk, factor 3	32%

Table 1.9: ECOG performance status (from Oken et al., 1982)

Grade	ECOG
0	Fully active, able to carry on all pre-disease performance without restriction.
1	Restricted in physically strenuous activity but ambulatory and able to to carry out work of a light or sedentary nature eg., light house work, office work.
2	Ambulatory and capable of all selfcare but unable to carry out any work activities. Up and about more than 50% of waking hours.
3	Capable of only limited selfcare, confined to bed or chair more than 50% of waking hours.
4	Completely disabled. Cannot carry on any selfcare. Totally confined to bed or chair.
5	Dead

1.9 EBV-positive diffuse large B- cell lymphoma of the elderly

1.9.1 Introduction

"EBV-positive diffuse large B cell lymphoma of the elderly (EBV^+ DLBCL-E)" is a new entity included in the 2008 WHO Classification of Tumours of Hematopoietic and Lymphoid Tissues. It is defined as an EBV^+ DLBCL of patients older than 50 years, without any known underlying immunosuppression or prior lymphoma. The median age is 71 with a slight male predominance. Male to female ratio is 1.4:1 (Nakamura & Jaffe, 2008). The clinical course of this entity is usually aggressive with a median survival of 2 years and an overall 5- year survival of 25% (Oyama et al., 2007; Park et al., 2007). Although patients can present with lymphadenopathy, 70% of the cases show extranodal disease involving the skin, lung or gastrointestinal tract with associated moderate to severe clinical B symptoms. Age-related EBV^+ DLBCL was first described by Oyama et al. who performed a clinicopathological evaluation on 22 Japanese patients aged more than 60 years old without predisposing immunodeficiency. This entity is believed to be related to immunosenescence or immunological deterioration due to the aging process (Oyama et al. 2003). Subsequently Oyama et al evaluated the presence of EBV by EBER *in situ* hybridization in 1792 DLBCL cases and found 156 (8.7%) of EBV^+ cases without any predisposing immunodeficiency. Age-related DLBCL shows an EBV latency type 2 or 3 pattern and is associated with a poorer prognosis compared to age-matched EBV-negative DLBCL (Oyama et al. 2007). Most data to present has been obtained from Asian patients (Japan and Korea) with a prevalence of 8 to 11.4% (Kuze et al., 2000; Park et al., 2007), however the prevalence of this disease in the

Western population is much lower indicating a possible ethnic or geographic predisposition. In 2009, Gibson and Hsi found five cases of EBV^+ DLBCL-E in the United States from 2000 to 2007 and the clinical outcome of all these patients was poor despite multi-agent chemotherapy (Gibson & Hsi 2009). In addition, the authors also analysed 90 cases of DLBCL aged 60 and above and found that none of these patients was EBER positive. This suggests that the prevalence of this DLBCL subtype is very low in the United States as compared to Asian population. Hoeller et al. analysed 258 DLBCL cases from central Europe and found 8 (3.1%) patients who fit the criteria for EBV^+ DLBCL-E (Hoeller et al., 2010). Hofscheier et al. performed a comparison between Mexican and German cohort in parallel and found that the prevalence of EBV^+ DLBCL-E in Germany was 2% as compared to 7% in the Mexican population. (Hofscheier et al. 2011)

1.9.2 Histology and immunophenotype of EBV^+ DLBCL of the elderly

Two histological subtypes of EBV^+ DLBCL have been delineated (Asano et al., 2009). The commoner subtype is the polymorphous subtype which exhibits a broad range of malignant B-cells of varying maturation including centroblasts, immunoblasts, plasmablasts admixed with small lymphocytes, plasma cells, histiocytes, and epithelioid cells. HRS-like cells can also be present (Shimoyama et al. 2008). The second subtype is the monomorphic subtype which is composed of sheets of large transformed B-cells. It was later shown that both subtypes are actually different points in the disease progression and do not indicate any clinical importance (Oyama et al. 2007). Asano et al. observed that a significant proportion of

EBV^+ lymphoproliferative disease (LPD) have large areas of geographical necrosis (Asano et al. 2009). Gibson and Hsi also suggested a few pathological features other than necrosis that provide clues for EBV association which include polymorphic infiltrate, plasmacytic morphology, angioinvasion, and a non-germinal centre B-cell or the ABC immunophenotype (Gibson & Hsi 2009).

The neoplastic immunoblasts show positivity for EBER, CD20/CD79α and PAX-5, with variable expression of CD30, LMP-1 and EBNA-2. CD15, CD10 and BCL6 are usually negative. Expression of Ki-67 is high in the neoplastic cells. Differential diagnoses include EBV^+ B-cell LPD, cHL and EBV^-DLBCL. Presence of abundant HRS-like cells may pose a problem in differentiating this tumour from EBV^+ cHL presenting in elderly patients. Although the HRS–like cells in EBV^+ DLBCL of the elderly are occasionally CD30-positive, the typical inflammatory infiltrate of HL is absent and the HRS–like cells are strongly positive for CD20 or CD79α and CD45 and are negative for CD15, thus excluding the diagnosis of cHL. OCT2 and BOB1 positivity are also useful in supporting the diagnosis of EBV^+ DLBCL-E (Adam et al., 2011).

Docjinov et al. observed that age related EBV^+ B-cell LPD in the Western population encompasses a wide range of both reactive and neoplastic conditions which includes EBV-associated reactive hyperplasia, polymorphic extranodal LPD, polymorphic nodal LPD and DLBCL (Dojcinov et al. 2011). Similar authors have also identified a new subset of patients with localised extranodal disease manifesting as EBV mucocutaneous ulcer (EBVMCU) which has a good prognosis and high rate of spontaneous remission. This disease is characterized by a well circumscribed superficial ulcer containing abundant HRS-like cells,

prominent apoptosis with a rim of reactive T lymphocytes at the base of the ulcer. EBVMCUs usually occur in patients with iatrogenic suppression eg by methotrexate, cyclosporine A or Azathioprine. Withdrawal of the causative agent leads to spontaneous remission of the ulcer. Differentiating benign from malignant EBV^+ LPD can be difficult, hence clonality study might be useful. EBV associated RH lacks clonal IG rearrangements while clonal B-cell population is found in polymorphic nodal LPD and DLBCL. T-cell clonality would suggest the diagnosis of angioimmunoblastic T-cell lymphoma, a tumour containing abundant EBV^+ B cells. The authors also suggested that routine EBER testing to be done in patients older than 50 years suspected to have an aggressive B-cell lymphoma and those with atypical nodal, mucosal or cutaneous B-cell LPDs (Dojcinov et al. 2011).

CHAPTER 2

MATERIALS AND METHODS

2.1 Collection and preparation of clinical samples and cell lines

2.1.1 Collection of tissue biopsy specimens

Ethical approval for the work within this thesis was provided from the West Midlands Research Ethics Committee (REC 08/H1210/142). All formalin-fixed paraffin-embedded tissue biopsy specimens were obtained from various sources as described below.

Paraffin blocks of breast cancer, bladder cancer and DLBCL cases were from the Department of Pathology, Queen Elizabeth Hospital. Bladder cancer paraffin blocks were courtesy of Dr. Rik Bryan from Urology Department, Queen Elizabeth Hospital. Lung tissue microarray sections were courtesy of Maria Janikova and Dr Jozef Skarda from the Department of Pathology and Laboratory of Molecular Pathology, Faculty of Medicine and Dentistry, Palacky University, Olomouc, Czech Republic. Formalin-fixed paraffin-embedded tissues were obtained from archive of lung carcinomas derived from patients operated in the period between 1996 to 2000.

2.1.2 Tissue sectioning

Tissue sectioning was performed with a model AS325 microtome (Thermo Electron Corporation, Basingstoke, UK) to cut 3-4 micrometer (μm) sections from paraffin-embedded tissues. Gloves were worn at all times. Before cutting tissues for EBER ISH, the microtome blade (Surgipath Europe Ltd., Peterborough, UK) and cutting area was cleaned and sterilised with absolute alcohol between each tissue block to avoid cross-contamination. Tissue sections

were harvested from water bath containing distilled water at 50^{o} C and placed onto RNase-free adhesive-coated slides and incubated in a 60^{o} C incubator for 1 hour to adhere tissue sections onto the slides. All tissue sections were stored at room temperature in RNase-free conditions until further use in immunohistochemistry or *in situ* hybridisation. Sectioning was performed by Kaisheng Wen and Souad Messahel.

2.1.3 Preparation of deoxyribonuclease (DNase)/ribonuclease (RNase)-free equipment

All glassware was washed, dried and covered in aluminium foil. For DNase/RNase-free conditions, glassware was baked in a dry oven at 240^{o} C for a minimum of 4 hours. All microscope slides used for histology sections were placed in 25-place slide racks (VWR International Ltd., Poole, United Kingdom (UK), wrapped in aluminium foil and baked at 250^{o} C for a minimum of 4 hours. Filter pipette tips were bought as certified DNase/RNase-free (Starlab UK, Ltd., Milton Keynes, UK). All Gilson micropipettes (Anachem Ltd., Luton, UK) were wiped with absolute alcohol and exposed to ultraviolet (UV) light for 1 hour before use. DNase/RNase-free sterile water was obtained Sigma-Aldrich Company Ltd., Gillingham, UK.

2.1.4 Haematoxylin and eosin staining

Haematoxylin and eosin staining of tissue sections from each patient were performed to allow assessment of tissue samples before immunohistochemical staining or *in situ* hybridization. Tissue sections on adhesive-coated slides were dewaxed through Histoclear (Fisher Scientific UK Ltd., Loughborough, UK) for 10 minutes and then through ethanol (Sigma-Aldrich Company Ltd., Gillingham, UK) for 10 minutes, and washed under running tap water. Slides were then immersed in Mayer's haematoxylin (VWR International Ltd., Poole, UK) for 2 minutes before washing thoroughly in tap water. Scott's tap water (Surgipath Europe Ltd., Peterborough, UK) was then used to 'blue' the haematoxylin for 2 minutes and washed again in tap water. The slides were immersed in eosin (VWR International Ltd., Poole, UK) for 2 minutes before rinsing with tap water. Tissue sections were then dehydrated through ethanol twice, each time for 5 minutes and then through histoclear twice, each time for 5 minutes. Sections were mounted using coverslips with a drop of DPX (both Surgipath Europe Ltd., Peterborough, UK) and dried flat overnight.

2.2 Immunohistochemistry

2.2.1 Principles of immunohistochemistry

Immunohistochemistry is the process of detecting antigens or proteins in cells of a tissue section by application of antibodies which bind specifically to the cells. It is widely used in diagnostic surgical pathology for typing of tumours. To allow visualization of the antigen-antibody (Ag-Ab) reaction, labels or reporter molecules are attached to the primary,

secondary, or tertiary Abs. There are a variety of labels including enzymes, fluorescent dyes, biotin, colloidal gold and metals. The commonest type of label is an enzyme which can include peroxidase, alkaline phosphatase or glucose oxidase. In the presence of a specific substrate and a chromogen, enzymes will produce a coloured precipitate at the site of the Ag-Ab reaction. Detection systems can be classified as direct and indirect methods. The direct method is a one step process in which primary Ab is conjugated with a reporter molecule. This method is quick but is less sensitive in detecting most Ags in routinely processed tissues. The indirect method, which has higher sensitivity, involves a two-step model. The first layer of Ab is unlabelled, but the second layer, raised against the primary Ab, is labelled. There are multiple methods including the avidin-biotin complex (ABC), labelled streptavidin-biotin (LSAB), peroxidase-antiperoxidase (PAP), polymeric labelling two-step method and tyramine amplification method (Ramos-Vara 2005).

2.2.2 Preparation of cultured cells for immunohistochemistry

Adhesive-coated slides were placed on Cytoclips™ (Thermo Electron) followed by filter cards and Cytofunnel® disposable sample chambers instructions and were inserted into the Shandon Cytospin centrifuge (Thermo Electron). 2 x 10^6 cells were harvested and re-suspended in 1 ml PBS and fixed in 100 µl 10% formalin. 100 µl of fixed cells were transferred into the Cytofunnels®. Cells were adhered to slides by centrifugation in the Cytospin at 1000 rpm for 5 minutes. Cytospinned cells were air dried and stored at room temperature.

2.2.3 Preparation of tissue biopsy sections for immunohistochemistry

Sectioned paraffin-embedded tissue biopsies were placed in 25-place microscope slide racks and immersed in Histoclear (Fisher Scientific UK Ltd., Loughborough, UK) for 10 minutes to dewax. Slides were then placed in a staining jar (Surgipath Europe Ltd., Peterborough, UK) filled with ethanol for 10 minutes to rehydrate the tissue and then rinsed under running tap water for 5 minutes before proceeding to immunohistochemistry.

2.2.4 Immunohistochemistry protocol

2.2.4.1 Blocking of endogenous peroxidase activity and antigen retrieval

To reduce background staining, endogenous peroxidase activity was blocked by 10-minute incubation in 3% hydrogen peroxide in methanol (both Sigma-Aldrich Company Ltd., Gillingham, UK .Slides were then rinsed thoroughly in running tap water. Antigen retrieval was performed by microwaving the slides in citric acid buffer at pH 6.0 in a standard 750 watt (W) microwave oven. Citrate buffer was heated at high power for 10 minutes, the slides were immersed and heated at medium power for 10 minutes and low power for 10 minutes. Citric acid buffer was prepared by dissolving 0.25 g citric acid (VWR International Ltd., Poole, UK) and 1.26 sodium citrate in 800 ml distilled water; pH was adjusted to 6.0 using concentrated NaOH. Distilled water was then added to make 1000 ml citrate buffer solution. After microwaving, slides were allowed to cool in the citric acid buffer at room temperature for 30 minutes before washing under running tap water for 5 minutes.

2.2.4.2 Detection of antigen

Slides were placed in a metal microscope slide staining tray (Richardsons of Leicester Ltd., Leicester, UK). The area of the slide around the cells/ tissue was carefully dried with a tissue and a ring of wax applied using a PAP pen (Cambridge BioScience Ltd., Cambridge, UK). Slides were conditioned in 1X TBS for 2 minutes, then blocked with 5X casein blocking solution (Vector laboratories) for 10 minutes followed by incubation with appropriately

diluted primary antibody in PBS overnight at 4ºC in humidified covered slide trays to minimize evaporation. For negative controls, primary antibody was replaced with nonimmune serum of the same IgG subclass. On the next day, samples were washed in TBST for 5 minutes. Secondary antibody (DakoChemate envision) was added to each tissue section for 30 minutes and then washed again in TBST for 5 minutes.

2.2.4.3 Visualization and counterstaining

Visualization was performed using diaminobenzidine (DAB) (Vector laboratories). 20 µl of DAB was added to 1 ml of substrate solution. 100 µl of this DAB substrate solution was applied to each tissue section for 5 minutes. The substrate was converted to an insoluble brown product by the antigen-bound peroxidases. Slides were rinsed with TBST, counterstained with Mayer's haematoxylin for 2 minutes and washed under running tap water Slides were then dehydrated through ethanol and Histoclear for 10 minutes each before being mounted with coverslips with a drop of DPX mounting medium. Slides were dried flat overnight before microscopic analysis.

Table 2.1: Primary antibodies for immunohistochemical staining

Primary antibody	Species	Dilution	Supplier
SPHK1 (AP7237c)	Rabbit	1: 50	Abgent
S1PR1 (sc-25489)	Rabbit	1: 200	Santa Cruz
S1PR2 (13488)	Rabbit	1: 50	Sigma
S1PR3 (LS-A 1031)	Rabbit	1: 400	MBL International Corp.
S1PR4 (LS-B513/ 20935)	Rabbit	1: 150	Lifespan Biosciences
ABCC1 (M9067)	Mouse	1: 3000	Sigma
ATX	Rabbit	1:300	University of Cambridge
LMP1 (M0897)	Mouse	1: 50	Dako
EBNA2 (PE2)	Mouse	1: 50	Dako
CD10	Mouse	1:400	Novocastra
BCL6 (M7211)	Mouse	1:50	Dako
MUM1 (M7259)	Mouse	1:400	Dako

2.2.4.4 Scoring system for immunohistochemical staining

Scoring for all epithelial and lymphoid malignancies was based on the DAKO HercepTest™ scoring system which considers staining intensity and percentage of positive tumour cells as detailed out in Table 2.3.

Table 2.2: The DAKO HercepTest™ scoring system used in this study

Score	Protein expression	Staining pattern
0	negative	No reactivity or positivity in less than 10% of tumour cells
1	negative	Faint/barely perceptible positivity in ≥ 10% of tumour cells
2	positive	Weak to moderate staining in ≥ 10% of tumour cells
3	positive	Strong staining in ≥ 10% of tumour cells

2.3 EBER *in situ* hybridisation protocol

2.3.1 Section pre-treatment and digestion

Sections were dewaxed in two washes of Histoclear for 5 minutes, rehydrated in two washes of absolute ethanol and 95% ethanol for 5 minutes, rinsed with two washes of distilled water for 5 minutes, and then digested with 100 µl proteinase K (Sigma-Aldrich Company Ltd., Gillingham, UK) in 50 mM Tris/HCI buffer pH 7.6 for 30 minutes at 37 °C. Slides were rinsed in TBS for 5 minutes and sections were dehydrated in two washes of 95% ethanol and absolute ethanol for 5 minutes each before being air dried. A ring of wax was applied encircling the tissue using PAP pen.

2.3.2 Hybridisation

50 µl 1:7 dilution of Leica Novocastra^{TM} Fluorescein-conjugated probe solution (NCL-EBV-K) was pipetted onto the tissue and a plastic coverslip was placed on the top-slowly spreading the probe mixture evenly over the tissue section without trapping air bubbles . Slides were incubated in the oven at 55º C for 1 hour and a half. The plastic coverslips.were then removed and slides were washed in TBST for 5 minutes.

2.3.3 Detection

Prior to detection, slides were blocked for 10 minutes with rabbit serum diluted 1:5 in TBS, 3% w/v BSA, 0.1% v/v Triton X-100. The blocking solution was then tipped off and detection was performed by 30 minute incubation with 50 ul rabbit F(ab') anti-FITC/AP (Vial A, Vector Labs) diluted 1:200 in TBS, 3% w/v BSA, 0.1% v/v Triton X-100. Slides were washed with TBST for 2 x 3 minutes. 100 µl of enzyme substrate (Vial B) 1:50 in 100 mM Tris/HCI, 50 mM MgCI2, 100 mM NaCI pH 9.0 mixed with 1 µl of inhibitor (levamisole) (Vial C) to each ml of diluted enzyme substrate was pipetted onto the slides. Slides were incubated at room temperature in the dark overnight. Slides were washed with TBST, counterstained in fast red for 6 minutes and mounted with DPX. Slides were dried flat overnight before microscopic analysis of EBER.

2.4 Tissue culture

2.4.1 Collection and general culture of cell lines

The HL-derived cell lines used in this study are listed in Table 2.4 below. All cell lines were cultured in a humidified incubator at 37^{o} C in 5% carbon dioxide (CO_2) in normal growth media which was RPMI-1640 supplemented with 10% fetal calf serum (FCS), 2 mM glutamine (all Invitrogen Ltd., Paisley, UK) and 0.5% penicillin-streptomycin solution (Sigma-Aldrich Company Ltd., Gillingham, UK). Cell lines were subcultured twice a week in 50 cm^2 flasks.

2.4.2 Cryopreservation of cells

1 x 10^7 cells were pelleted by centrifugation at 1000 rpm in a 5810R Eppendorf centrifuge for 5 minutes and re-suspended in 1 ml freezing solution (RPMI-1640 supplemented with 40% v/v FCS and 10% v/v dimethylsulphoxide (DMSO; Sigma). Cells were then transferred to cryopreservation vials and placed in a freezing container at -80ºC freezer. A day later, cells were moved to liquid nitrogen freezer at -180ºC for long-term storage.

Table 2.3: HL cell lines used

Cell lines	Origin	Growth media
L591	EBV-positive HL cell line, from the pleural effusion of a nodular sclerosis female HL patient (Diehl et al., 1992).	RPMI 1640, 2mM glutamine, 10% FCS, 1%, pen/strep. 37ºC in 5% CO2
L1236	EBV-negative cell line from the peripheral blood of an advanced HL patient (Wolf et al., 1996). The HRS cell origin of L1236 cells has been confirmed by the finding of identical Ig gene rearrangement sequences in L1236 cells and HRS cells of the same patient's bone marrow (Kanzler et al., 1996).	RPMI 1640, 2mM glutamine, 10% FCS, 1%, pen/strep. 37ºC in 5% CO2
L540	EBV-negative HL cell line derived from the pleural effusion of an HL patient. Genomic analysis of the cell line has revealed monoclonal rearrangements of T-cell receptor beta and gamma loci and germ line configuration of Ig genes, suggesting a T-cell origin (Falk et al., 1987; Drexler et al., 1988).	RPMI 1640, 2mM glutamine, 10% FCS, 1%, pen/strep. 37ºC in 5% CO2
KMH2	EBV-negative cell line originally established from the pleural effusion of a mixed cellularity HL patient (Kamesaki et al., 1986)	RPMI 1640, 2mM glutamine, 10% FCS, 1%, pen/strep. 37ºC in 5% CO2
L428	EBV-negative cell line established from the pleural effusion of an HL patient (Schaadt et al., 1980).	RPMI 1640, 2mM glutamine, 10% FCS, 1%, pen/strep. 37ºC in 5% CO2
HDLM2	EBV-negative cell line established from the pleural effusion of an HL patient (Schaadt et al., 1980).	RPMI 1640, 2mM glutamine, 10% FCS, 1%, pen/strep.

2.4 3 Recovery of cells from nitrogen storage

Cells were thawed quickly at 37ºC to minimize exposure to DMSO and transferred to a 15 ml falcon tube. Warmed RPMI with supplements was added gradually to the cells to dilute the DMSO. Cells were then pelleted by centrifugation at 1000 rpm in a 5810R Eppendorf centrifuge for 5 minutes, re-suspended in 10 ml medium and transferred to a 25 cm^3 flask and incubated at 37ºC.

2.4.4 Determination of cell number in culture

Disposable Glasstic™ slides (Hycor Biomedical Ltd., Edinburgh, UK) were used for counting cells in culture. 100 µl of cell suspension was aspirated from culture and mixed with 100 µl of Trypan blue. 20 µl of this mixture was aspirated and pipetted into the Glasstic™ slide well. Using an inverted light microscope, all viable cells (bright spherical cells) contained within four diagonal zones of the Glasstic™ grid were counted. This number was divided by four to obtain an average count of cell number per zone. This average value was then multiplied by 10^4 to obtain the number of cells per ml of culture medium.

2.4.5 Treatment of L591 cells with Sphingomab

Prior to plating, cells were washed twice with Optimem and re-suspended in 14 ml Optimem. 1 ml of solution containing 2.5x 10^6 cells were plated in each well in a 48 well plate. The experiment was set up in triplicate at 2 time points; 2 hours and 12 hours. Sphingomab antibody (LT1002, LPath) concentration was 12.0 mg/ ml. To make a 3 mg/ ml working stock, a 4 fold dilution was made. 601. 7 µl PBS was added to 198.4 µl Sphingomab stock to achieve 800 µl antibody working solution. 250 µl antibody solution was added to each well. For control wells, 250 µl PBS was added. Cells were incubated at 37ºC for 2 and 12 hours. Cells were aspirated and spun down at 400 *g* for 5 minutes and RNA was harvested using QIAGEN RNeasy™ mini kit as described in section 2.7.1.2. RNA was stored at -80C for gene expression microarray as described in section 2.8.

2.5 Transfection of plasmid DNA into mammalian cells

Transfection was done using Cell Line Optimization Nucleofector® Kit (Amaxa). Prior to the day of transfection, cells were plated in 1 ml of culture media in a 12 well plate in a humidified 37ºC/5% CO2 incubator. An aliquot of cells were aspirated to determine the cell density. After centrifugation, cells were re-suspended in 1 ml nucleofector solution. Nucleofector solution was prepared by mixing 0.2 ml supplement to 0.9 ml Nucleofector solution. One nucleofection sample required 1x10^6 to 5x10^6 cells, 100 µl nucleofector solution and 2µg pmaxGFP. 100 µl sample was carefully transferred into an amaxa certified cuvette, avoiding air bubbles and closed with the blue cap. The appropriate nucleofactor

programme was selected and the cuvette inserted into the cuvette holder. The programme. was started and once 'ok' was displayed, the cuvette was immediately removed from the holder to avoid cell damage. 500 µl of pre-warmed culture media was added to the cuvette and the mixture was transferred to a 12 well plate and incubated at 37ºC. Sample was ready for analysis of gene expression.

2.6 Reverse transcriptase polymerase chain reaction (RT-PCR)

2.6.1 RNA extraction from cultured cells

2.6.1.1 Cell lysis

5×10^6 cells were pelleted by centrifugation at room temperature for 5 minutes at 400 *g* and the supernatant discarded. RNA was extracted using QIAGEN RNeasy™ mini kit (QIAGEN Ltd., West Sussex, UK). Lysis buffer was prepared by adding 1 µl of β-mercaptoethanol to every 100 µl of Buffer RLT. Cells were lysed using 350 µl of this lysis buffer and incubated at room temperature for 5 minutes.

2.6.1.2 RNA extraction

Total RNA was isolated from cells using the QIAGEN RNeasy™ mini kit according to the manufacturer's protocol. Cell lysates were mixed with 350 µl of 70% ethanol diluted in DNase/RNase-free water and transferred to spin columns placed in collection tubes. Columns were then centrifuged at 8000 *g* for 15 seconds. The flow-through was discarded and 700 µl Buffer RW was pipetted into spin columns before being centrifuged again at 8000 *g* for 15 seconds. The flow-through was discarded and columns were transferred to fresh collection tubes. 500 µl of Buffer RPE was pipetted into spin columns before being centrifuged at 8000 *g* for 15 seconds. Flow-through was discarded and another 500 µl Buffer RPE was added. Columns were centrifuged at 8000 *g* for 2 minutes. Flow-through and collection tubes were discarded and columns were centrifuged with the lids open for 1 minute at 16000 *g* to completely dry the membrane in the columns. Columns were transferred to fresh centrifuge tubes and RNA was eluted in 30 µl of DEPC water by centrifugation for 1 minute at 8000 *g*.

2.6.1.3 Determination of RNA concentration

The RNA concentration of each sample was measured on a NanoDrop ND-1000 Spectrophotometer: To initialize the NanoDrop, 2 µl of DNase/RNase-free water was applied to the sample well. The sample well was wiped clean with tissue, 1 µl RNase-free water (from RNeasy™ kit) was applied and used as a blank measurement. Again the sample well was wiped clean and 1 µl of eluted RNA was used to obtain the concentration and quality (ratio

260/280) of RNA for each sample. The sample well was wiped clean before applying a new sample of RNA.

2.6.2 cDNA synthesis

Complementary (c) DNA was synthesized using Qiagen reverse transcriptase kit. 1 µg RNA from each sample was pipetted into sterile 0.2 ml PCR tubes and 2 µl 7x gDNA wipeout buffer was added. The volume was made up to 14 µl using DNase/RNase-free water. A negative control (no RNA) was set up in parallel, consisting of DNase/RNase-free water and 2 µl 7x gDNA wipeout buffer only. The tubes were preheated for 2 minutes at 42ºC. In the mean time, a Reverse Transcriptase (RT)-reaction master mix consisting of the following components was prepared per reaction. 4 µl 5x Quantiscript RT buffer, 1 µl RT primer mix and 1 µl quantiscript reverse transcriptase. This master mix was added to each preheated tubes and mixed well. Using an Eppendorf Thermal Cycler, c-DNA was synthesized at 42^{o} C for 30 minutes, and at 95ºC for 3 minutes to inactivate quantiscript reverse transcriptase. cDNA was stored at -20^{o} C until required.

2.6.3 TaqMan quantitative polymerase chain reaction (Q-PCR)

Real time PCR amplifies and simultaneously quantifies a targeted DNA molecule against a known standard. The quantity of PCR product is directly proportional to the amount of nucleic acid template. Each well of a RT-Q-PCR reaction comprised 20 µl reaction volume

including 5 µl of input cDNA. A PCR-reaction master mix consisting of the following components was prepared per reaction: 10 µl of 2x Taqman Univesal PCR Mastermix, 1 ul of commercial primers/probe (Applied Biosystems), 1 ul reference gene (GAPDH) and 3 ul of DNA/RNAse free water. 15 ul of master mix was pipetted into each well in a 96 well plate followed by 5 ul of cDNA. Each reaction was assayed in triplicates. For control wells, cDNA was replaced by 5 ul of DNA/RNAse free water. The 96 well plate was sealed with an adhesive cover and spun at 900g for 1 minute and then placed in the 7500 Real-Time PCR System (Applied Biosystems) for thermocycling and fluorescence detection. Initial heating was at 95ºC for 10 minutes to activate the polymerase enzyme, followed by 40 cycles of denaturation at 95ºC for 15 seconds and primer annealing and extension at 60ºC for 60 seconds. Data was analysed using 7500 system software v1.4.0 (Applied Biosystems) and Excel (Microsoft 2010). The average Ct value was calculated for both target and reference gene and the dCt (Ct_{target}-Ct_{GAPDH}) was obtained. The ddCt (dCttarget-dCtcontrol) was determined and the relative fold change of gene expression in HL cell lines was calculated using the formula 2^-ddCt.

Table 2.4: Taqman primer and probe mixes

Gene	ABI Q-PCR Primer/Probe Reference Number
SPHK1	Hs 00184211_m1
S1PR1	Hs 00173499_m1
S1PR2	Hs 01055393_m1
S1PR3	Hs 00245464_s1
S1PR4	Hs 02330084_s1
S1PR5	Hs 00924881_m1
REL	Hs 00968440_m1
TOP2B	Hs 00172259_m1
CCDC88A	Hs 01559767_m1
BDP1	Hs 01055393_m1
RPL 35	Hs 00855441_gH
HAT1	Hs 00186320_m1
GAPDH	4310884E

2.7 Microarray expression analysis

2.7.1 Introduction to microarray expression analysis

DNA microarray measures the expression of large numbers of genes simultaneously. In this study, the Affymetrix GeneChip® Whole Transcript (WT) Sense Target (ST) Labeling Assay was used. This array was designed to generate amplified and biotinylated sense-strand DNA targets from the entire expressed genome. using1 µg Total RNA Labeling Protocol. It started with the reduction of a ribosomal RNA (rRNA) where the 28S and 18S rRNA population is reduced from the total RNA (Figure 2.3). Subsequently, double-stranded cDNA is synthesized which then acts as a template producing copies of antisense cRNA by the action of T7 RNA polymerase. Second cycle of single stranded cDNA is synthesized following reverse transcription of the cRNA. During this process, dUTP is incorporated into the DNA followed by addition of uracil DNA glycosylase (UDG) and apurinic/apyrimidinic endonuclease 1 (APE 1) which breaks the DNA strand. DNA is labeled by terminal deoxynucleotidyl transferase (TdT) with the Affymetrix® proprietary DNA Labeling Reagent that is covalently linked to biotin. Sufficient target is then generated for hybridization to a single array. The hybridisation of target sequences to oligonucleotide probes is detected by staining with a streptavidin-phycoerythrin conjugate and measuring the light emitted at 570 nm. The signal produced is proportional to the amount of bound target at each location on the array and reflects the transcript levels present in the original target population. A series of control genes are used to allow normalization and scaling between each array so that differences in signal intensities can be compared.

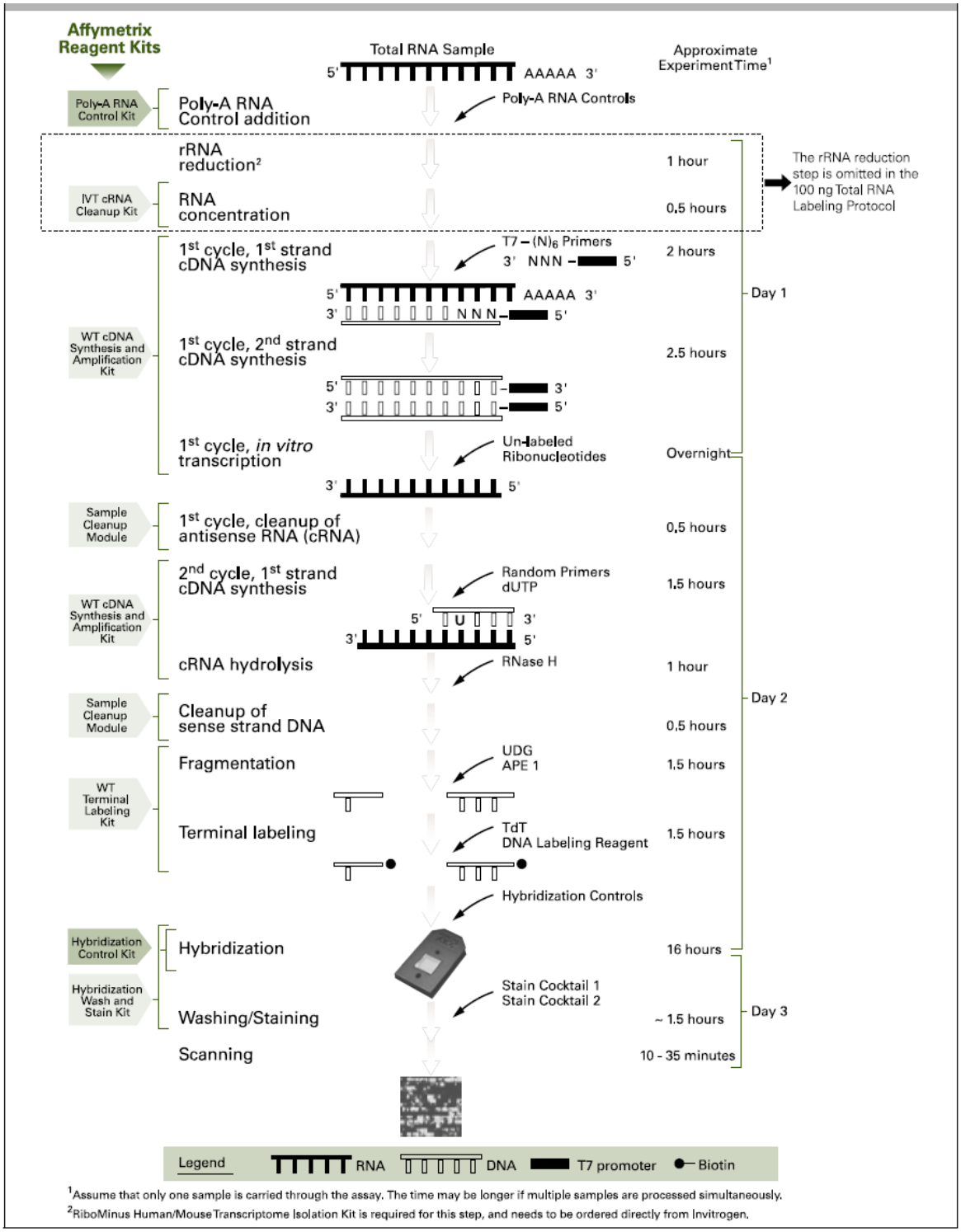

Figure 2.1 GeneChip® Whole Transcript Sense Target Labeling Assay (from www.affymetrix.com)

2.7.2 rRNA Reduction and Preparation of Total RNA with Diluted Poly-A RNA

Total RNA was extracted from the cells (Section 2.7.1.1 and 2.7.1.2) and prepared for hybridization to the arrays using GeneChip® Poly-A RNA Control Kit (Affymetrix). Three series of dilution was made by adding Poly-A Control Dilution Buffer to Poly-A RNA Control Stock. The Third Dilution was added to 1 µg of total RNA to make up the Total RNA/ Poly-A RNA Controls Mix. 5.2 µl Total RNA/Poly-A Controls Mix, 0.8 µl RiboMinus Probe (100 pmol/µL) and 30 µl Hybridization buffer with betaine was mixed, spun and incubated at 70°C for 5 minutes in a thermal cycler. The hybridized sample was added to the magnetic beads and incubated at 37ºC for 10 minutes, and spun again to obtain the rRNA-probe pellet. The supernatant was pipetted into a 1.5 ml non-stick RNAse free tube on ice. The beads were re-suspended again in hybridization buffer with betaine and incubated at 50ºC for 5 minutes. The supernatant was added to the previous supernatant containing rRNA-reduced total RNA/Ploy-A RNA control mix. Sample was cleaned up using GeneChip IVT cRNA cleanup kit. The quality of the concentrated RNA sample was then determined by running the Eukaryotic Total RNA Nano Assay in the bioanalyzer. On average, > 100 ng of rRNA-reduced sample may be recovered from 1 µg of total RNA starting material.

2.7.3 First-strand cDNA synthesis

10 µg RNA was reverse transcribed to first-strand cDNA by adding 5 µL of the First-Cycle, First-Strand MasterMix to the tube containing concentrated rRNA and spun down. The

reaction was incubated at 25°C for 10 minutes, 42°C for 60 minutes,70°C for 10 minutes and cooled at 4°C for 2 minutes and continued to the First-Cycle, Second-Strand cDNA synthesis

2.7.4 Second-strand cDNA synthesis

An RNase H-mediated second-strand cDNA synthesis reaction was performed using 10 µl of a master mix containing; 4 µl $MgCl_2$, 0.4 µl 10 mM dNTP Mix, 0.6 µl DNA Polymerase I, 0.2 µl RNase H and DNA/RNAse free water added to each of the first strand reaction tubes and incubated at 16ºC for 2 hours.and at 75ºC for 10 minutes with heated lid. Sample was cooled down for 2 minutes at 4ºC.

2.7.5 First cycle, cRNA synthesis and cleanup

The GeneChip® WT cDNA Amplification Kit and the GeneChip® Sample Cleanup Module were used for this procedure. IVT Master Mix (containing 5 µl 10x IVT Buffer, 20 µl IVT NTP Mix, 5 µl IVT Enzyme Mix) was added to each sample and incubated at 37ºC for 16 hours. Sample was cleaned up using cRNA Cleanup Spin Columns. The eluted cRNA concentration was measured using the NanoDrop ND-1000.

2.7.6 Second cycle, first strand cDNA synthesis

cRNA sample was mixed with 1.5 µl random primers and 8 µl RNAse free water and incubated at 70ºC for minutes, 25ºC for 5 minutes and 4ºC for 2 minutes. Second cycle, first strand cDNA synthesis Master Mix was added and the sample was incubated at 25ºC for 10 minutes, 42 ºC for 90 minutes, 70 ºC for 10 minutes and 4 ºC for at least 2 minutes.

2.7.7 Hydrolysis of cRNA and cleanup of single-stranded DNA

1 µL of RNase H was added to each sample and incubated at 37°C for 45 minutes,95°C for 5 minutes and 4°C for 2 minutes. Sample was cleaned up using cDNA Cleanup Spin Columns from the GeneChip® Sample Cleanup Module according to the manufacturer's protocol.

2.7.8 Fragmentation and labelling of single stranded DNA

Fragmentation Master Mix was prepared and added into the sample and incubated at 37°C for 60 minutes, 93°C for 2 minutes, 4°C for at least 2 minutes GeneChip® WT Terminal Labeling Kit was used for labelling of fragmented single stranded DNA. Labelling reaction was added to the sample and incubated at 37°C for 60 minutes, 70°C for 10 minutes and 4°C for at least 2 minutes.

2.7.9 Hybridization, washing, staining and scanning

Hybridization cocktail (containing fragmented and labeled DNA target, control oligonucleotide B2, 20X eukaryotic hybridization controls, 2X hybridization mix, DMSO and nuclease free water) was prepared and heated at 99°C for 5 minutes, cooled to 45°C for 5 minutes, and centrifuged at maximum speed for 1 minute. Sample was injected into the GeneChip® ST array through one of the septa and placed in 45°C hybridization oven, at 60 rpm, and incubated for 16 hours. The array was removed from the oven and the hybridization cocktail was aspirated through the septa and the array probe was filled with Wash Buffer A for 10 cycles at 30ºC and then with Wash Buffer B for 4 cycles at 50ºC. The probe array was stained for 300 seconds with Stain Cocktail 1 at 35°C and then washed with Wash Buffer A at 30°C. Staining was repeated for 300 seconds with Stain Cocktail 2 at 35°C and for 300 seconds with Stain Cocktail 1 at 35°C followed by a final 15 cycle wash with Wash Buffer A at 35°C. The probe array was then filled with array holding buffer and scanned on the GeneChip Scanner 3000.

2.7.10 Data analysis using R and Microsoft Excel software packages.

The analysis of these arrays was performed with the help of Dr. Wenbin Wei and Prof Ciaran Woodman. Images of the microarrays were analysed using Affymetrix microarray Suite 5.0. Probe level quantile normalization and robust multiarray analysis on the raw CEL files were performed using the Affymetrix Bioconductor package (http://www.bioconductor.org) Differentially expressed genes were identified using GeneSpring GX software Version12.5.

2.8 Statistical Package

Statistical Package for the Social Sciences 21.0 (SPSS 21.0) was used for all statistical analysis. Associations between clinical parameters and S1P signaling molecule expression were assessed by chi-square tests. Survival probabilities were calculated using Kaplan–Meier method. Differences between the curves were evaluated with log–rank test. Overall survival time was defined as the period between the time of diagnosis and the time of death. Disease-free survival time was defined as the period between the time of complete remission and the time of death or relapse. Survival times of patients who were still alive were censored with the last follow-up date. Logistic regression models and Cox regression analysis were used to assess the independent effects of co-variables on survival.

CHAPTER 3

EXPRESSION OF LIPID SIGNALLING MOLECULES IN HODGKIN LYMPHOMA AND GENE EXPRESSION MICROARRAY OF L591 CELLS TREATED WITH SPHINGOMAB

3.1 Introduction

Although cHL is largely a curable disease, about 10% of patients do not respond to chemotherapy. The widely accepted standard chemotherapy regime consists of doxorubicin (Adriamycin), bleomycin, vinblastin and dacarbazine (ABVD) with or without consolidation radiotherapy. Patients who relapse may require salvage chemotherapy and stem cell transplantation. Novel prognostic biomarkers are still being investigated to improve survival rates of cHL patients which include CD20, BCL2, MAL and Ki67 (Huang et al. 2007; Sup et al. 2005; Hsi et al. 2006; Morente et al. 1997).

Upregulation of SPHK1 protein and mRNA was observed in cases of Non Hodgkin lymphoma and correlates with increasing clinical grade (Bayerl et al. 2008) suggesting SPHK1 as a possible target for therapeutic intervention in these patients. ABCC1 overexpression has been shown to confer resistance to multidrug treatment in cHL patients. ABCC1 overexpression is also associated with refractory disease and poorer failure-free survival in cHL patients (Greaves et al. 2012).

The aims of this study are to:

i) examine the expression of SPHK1, S1PR1, S1PR3, ABCC1 and ATX in HL cell lines and primary HL tissue samples and correlate their expression with clinicopathological variables.

ii) determine if a humanised monoclonal antibody against S1P, Sphingomab could reverse the B cell receptor phenotypes in L591 cells.

3.2 Antibody specificity testing

Similarly to SPHK1 and S1PR1 antibodies, I also established the specificity of S1PR3 antibodies prior to performing immunohistochemistry on the HL cases. DG75 BL cell lines transfected with S1PR3 plasmids or with an empty vector were fixed in formaldehyde, cytospun and stained to confirm antibody specificity. Immunocytochemistry demonstrated that S1PR3 was strongly expressed in transfected cells compared to cells with empty vector (Figure 3.1).

Figure 3.1: Cells transfected with plasmids expressing SPHK1 and S1PR1 were immunostained with respective antibodies.

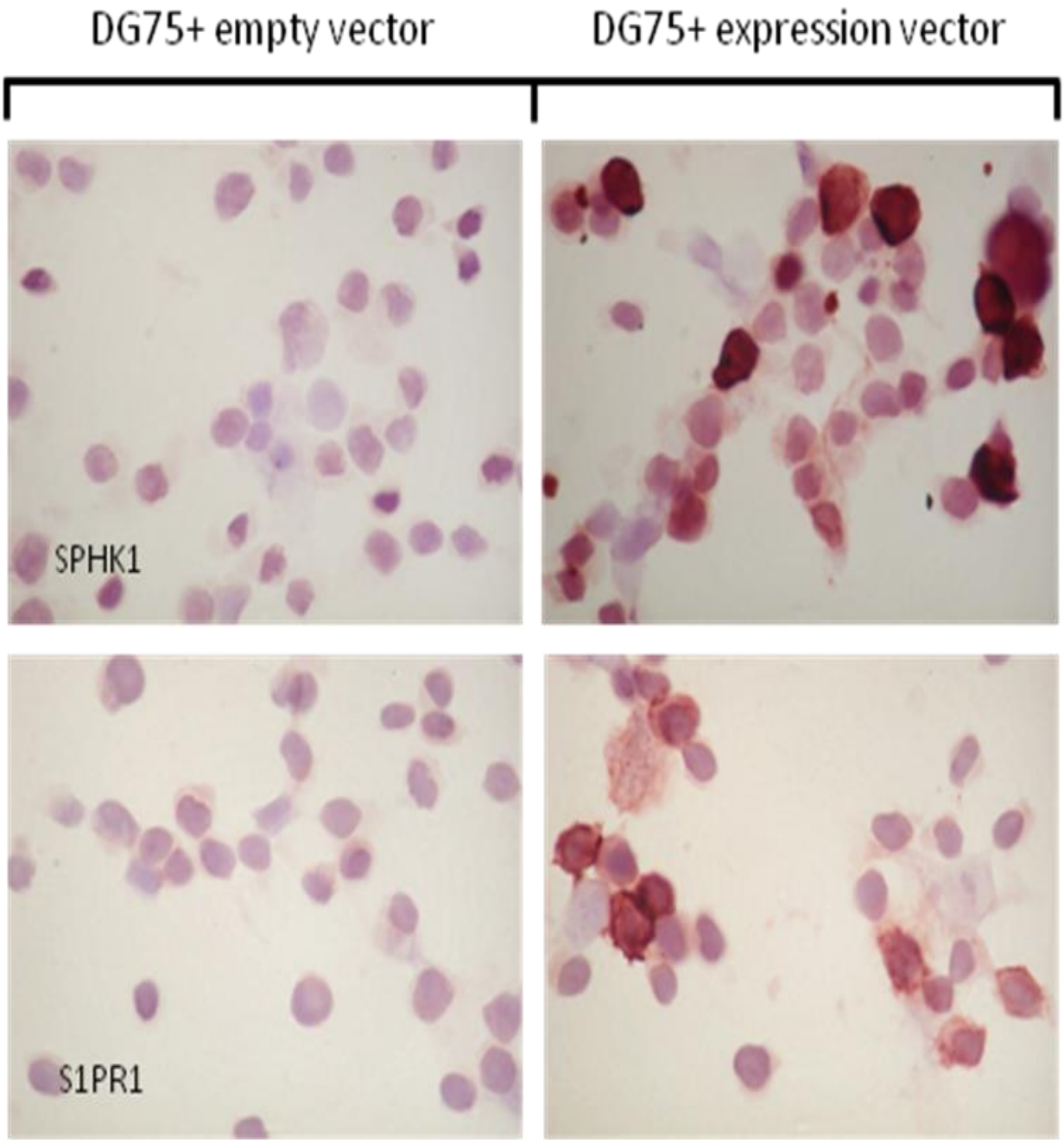
DG75+ empty vector
DG75+ expression vector
SPHK1
S1PR1

A

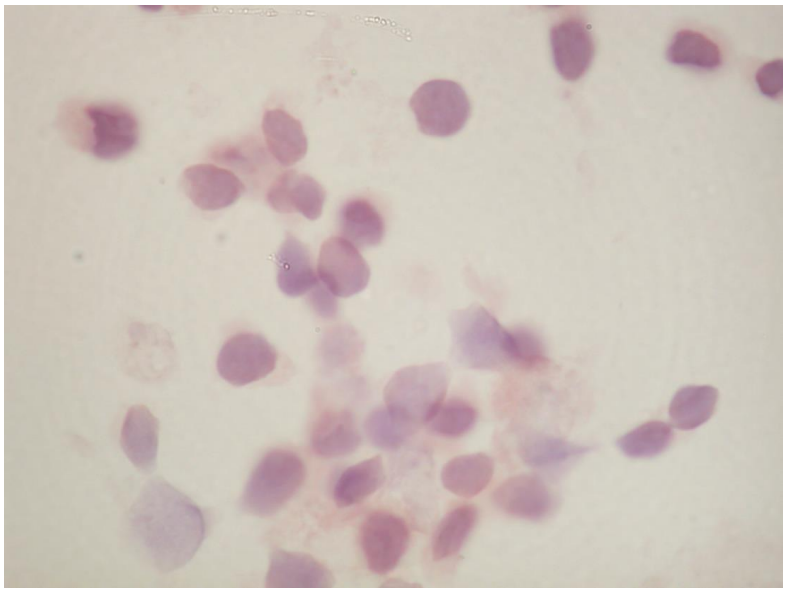

B

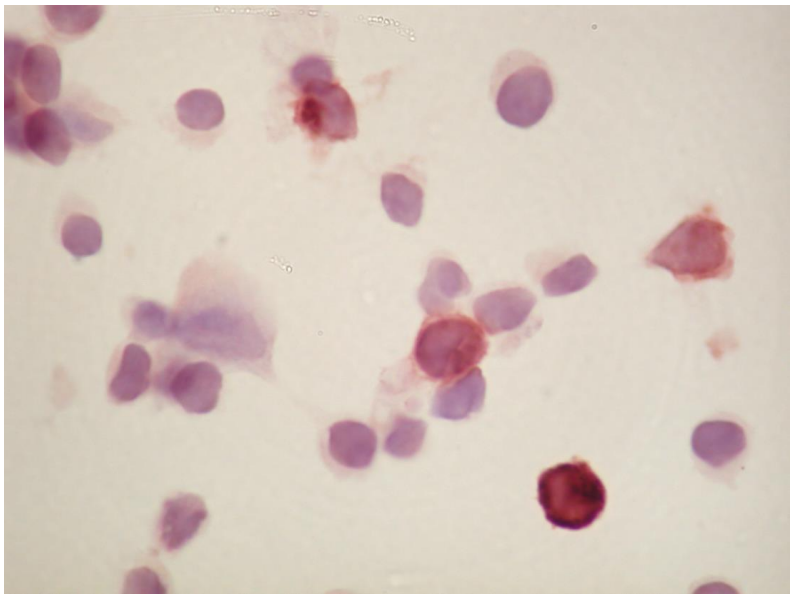

Figure 3.2: Cells transfected with plasmid expressing S1PR3 were immunostained with respective antibody.A) DG75 BL cells with empty vector, B) DG75 BL cells with S1PR3 vector

3.3 Re-analysis of expression of lipid signalling molecules on 'Brune' array

The re-analysis of a published dataset (18; GEO database no GSE12453) revealed that the expression of SPHK1 was increased in micro-dissected HRS cells compared to normal centrocytes, the presumed progenitors of HRS cells (Table 3.1,Figure 3.3) S1PR1 was expressed in HRS cells but was not significantly changed compared to centrocytes (Table 3.2, Figure 3.3). The expression of S1PR3 was significantly increased in micro-dissected HRS cells compared to centrocytes.

Table 3.1: Expression of SPHK1 in primary HRS cells compared with normal centrocytes

Gene	Gene expression in HRS cells compared with centrocytes (mean fold change)	Number of present calls in HRS cells (n=12)	Number of present calls in centrocytes (n=5)
SPHK1	+2.56	10	0

Table 3.2: Expression of S1P receptors in primary HRS cells compared with normal centrocytes

Gene	Gene expression in HRS cells compared with centrocytes	Number of present calls in HRS cells (n=12)	Number of present calls in centrocytes (n=5)
S1PR1	No significant change	6	2
S1PR2	-3.37	10	5
S1PR3	+2.75	5	0
S1PR4	+1.79	3	1
S1PR5	No significant change	0	0

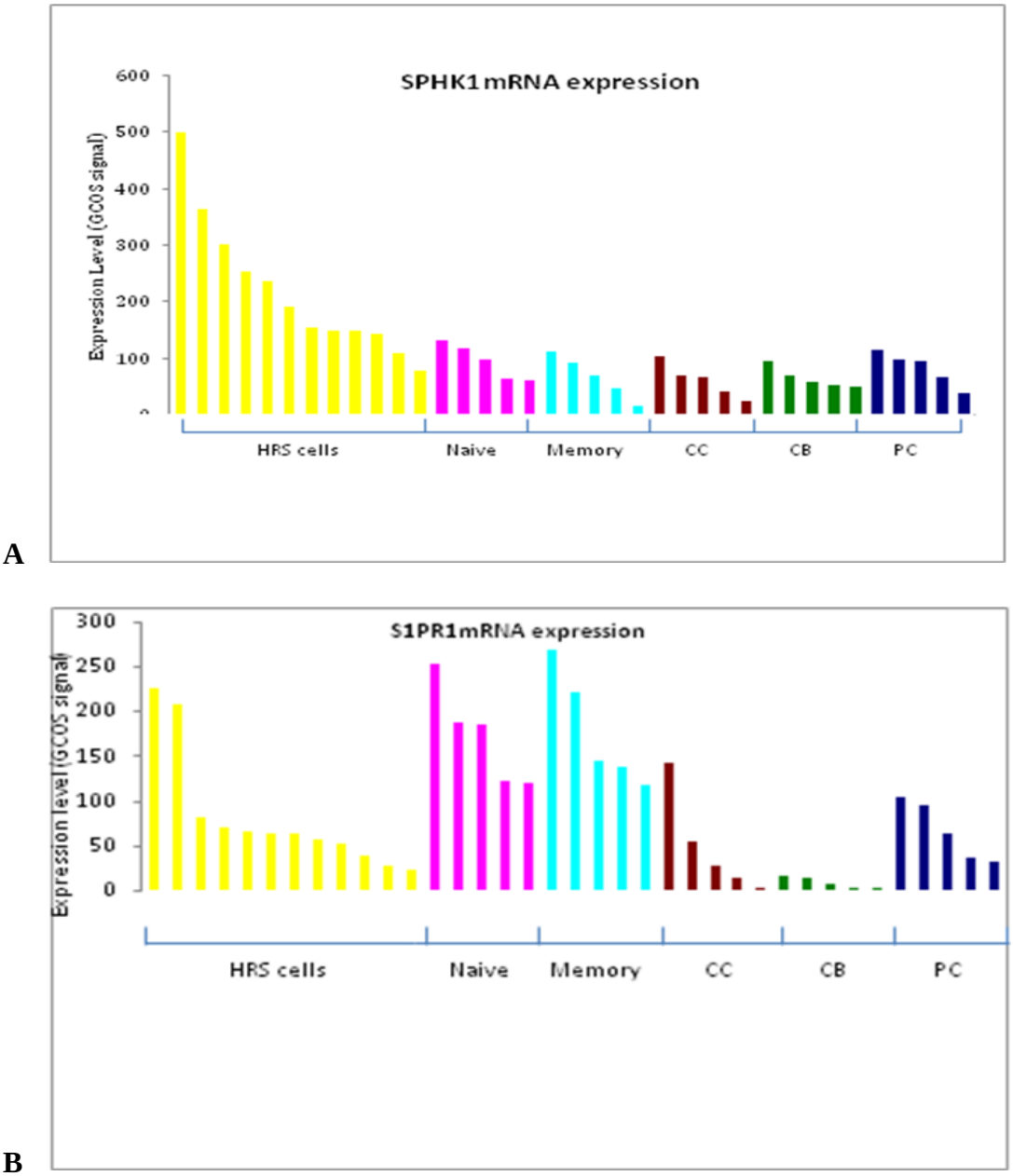

Figure 3.3: Differential expression of A) SPHK1 and B) S1PR1 receptor in primary HRS cells and different B cell subsets. Re-analysis of a published dataset (18; GEO database no GSE12453) revealed that the expression of SPHK1 was increased and that of S1PR1 was not significantly changed compared to centrocytes (CC).

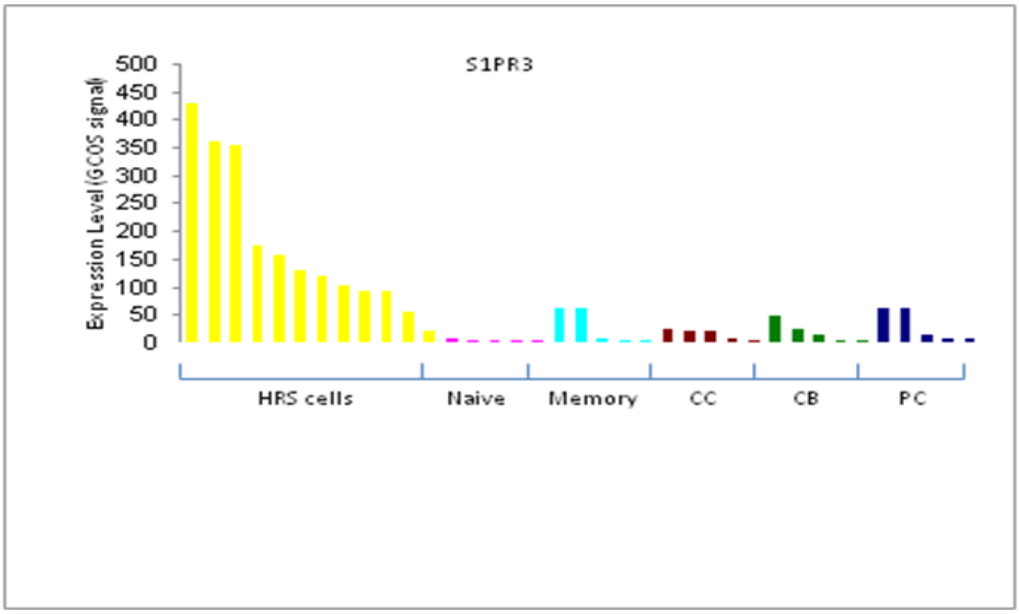

Figure 3.4: Differential expression of S1PR3 in primary HRS cells and different B cell subsets. Re-analysis of a published dataset (18; GEO database no GSE12453) revealed that when compared to centrocytes (CC), the expression of S1PR3 was increased in HRS cells.

3.4 Expression of lipid signalling molecules in normal lymphoid tissue

Along with staining on primary HL tissue, immunohistochemical staining using antibodies to SPHK1, S1PR1, S1PR3, ABCC1 and ATX were performed on normal lymphoid tissue. SPHK1 was detectable in the germinal centre B cells of reactive tonsils (Figure 3.6). The follicular mantle cells were negative for SPHK1. Fibroblasts, macrophages, plasma cells and endothelial cells lining the blood vessels were positive for SPHK1 and served as internal positive control. S1PR1 was strongly expressed in the mantle zone surrounding the germinal centres. Germinal centre cells were negative for S1PR1. Positive staining was observed in the endothelium of blood vessels. S1PR3 was expressed in the germinal centres of normal lymphoid tissue, but showing weaker intensity to that found in HRS cells. Endothelium of blood vessels showed strong positivity for S1PR3. ABCC1 was negative in the **g**erminal centre cells but show strong positivity in the endothelium of blood vessels. ATX was expressed in the germinal centre cells and in the endothelial cells of blood vessels (Figure 3.9).

3.5 Expression of lipid signalling molecules in primary HL tissue

61 cases of HL were obtained from the Pathology Department, Queen Elizabeth Hospital, Birmingham. Histopathological review to confirm the diagnosis and subtype of HL was performed by Dr Claudia Roberts, Consultant Haematopathologist from the same department. Paraffin sections from each case were stained with antibodies to SPHK1, S1PR1, S1PR3, ABCC1 and ATX. LMP1 staining was also performed to determine the EBV status of these patients. Staining was scored according to the criteria set out in Section 2.2.4.4. The clinical characteristics of these HL cases are shown in Table 3.3. The expression of lipid signalling

proteins in HL is summarised in Figure 3.5. Immunohistochemistry showed that SPHK1 was expressed in HRS cells in 25/61 (41%) cases. SPHK1 was localised to the cytoplasm of HRS cells (Figure 3.6). S1PR1 was strongly expressed in HRS cells in 48/61 cases (78.7%) and was localised to the cell membrane of HRS cells (Figure 3.7). Strong S1PR3 expression in HRS cells was observed in all samples of HL (100%) and was localised to the cytoplasm of these cells (Figure 3.8). ABCC1 was expressed in HRS cells in 44/61 cases (72.1%). Staining was observed in the cytoplasm of HRS cells. ATX was expressed in the cytoplasm of HRS cells in 69% of cases (Figure 3.9).

Table 3.3: Clinical characteristics of 61 HL cases

Characteristic	All patients (%)
Age	
15-34 years	25 (41.0)
35-44 years	10 (16.4)
≥ 45 years	26 (42.6)
Gender	
Male	37 (60.7)
Female	24 (39.3)
Disease subtype	
Nodular sclerosis	34 (55.7)
Mixed cellularity	27 (44.3)
Lymphocyte predominant	0 (0.0)
Lymphocyte depleted	0 (0.0)
EBV status	
Positive	24 (39.3)
Negative	37 (60.7)
Stage	
I-II, limited	31 (59.6)
III-IV, advanced	21 (40.4)
Treatment	
chemotherapy only	30 (49.2)
radiotherapy only	9 (14.8)
chemotherapy and radiotherapy	10 (16.4)
palliative	2 (3.3)

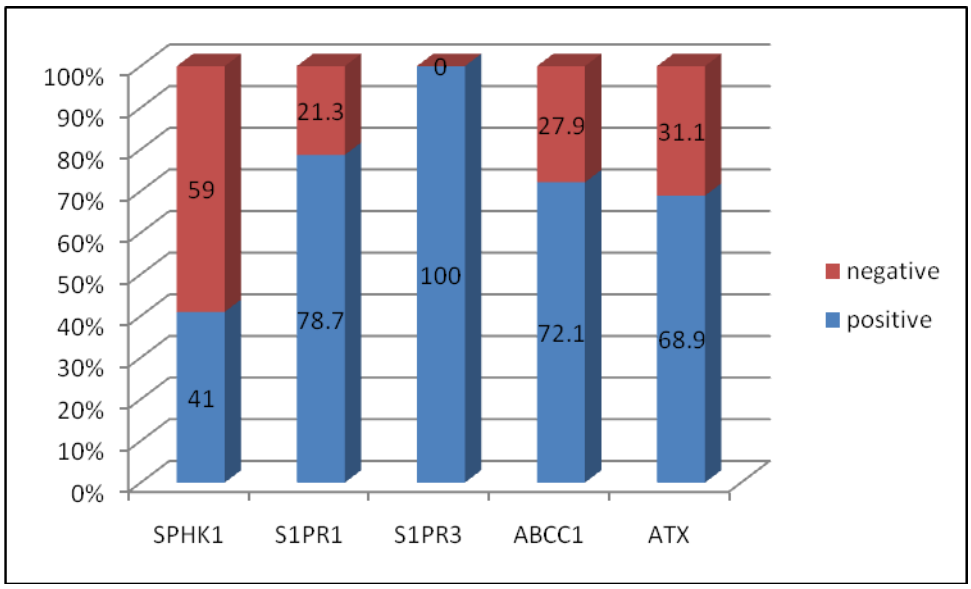

Figure 3.5: Summary of expression of lipid signalling molecules in Hodgkin lymphoma

A

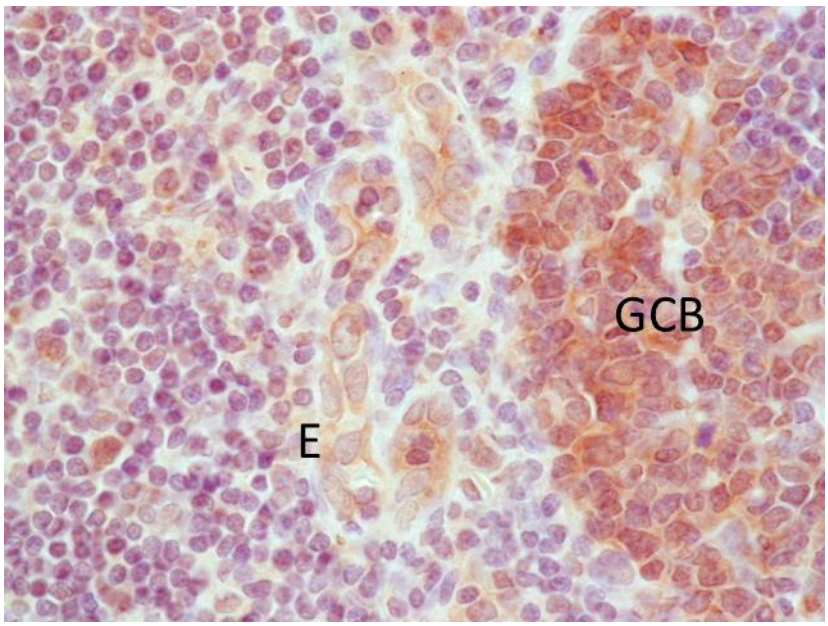

B

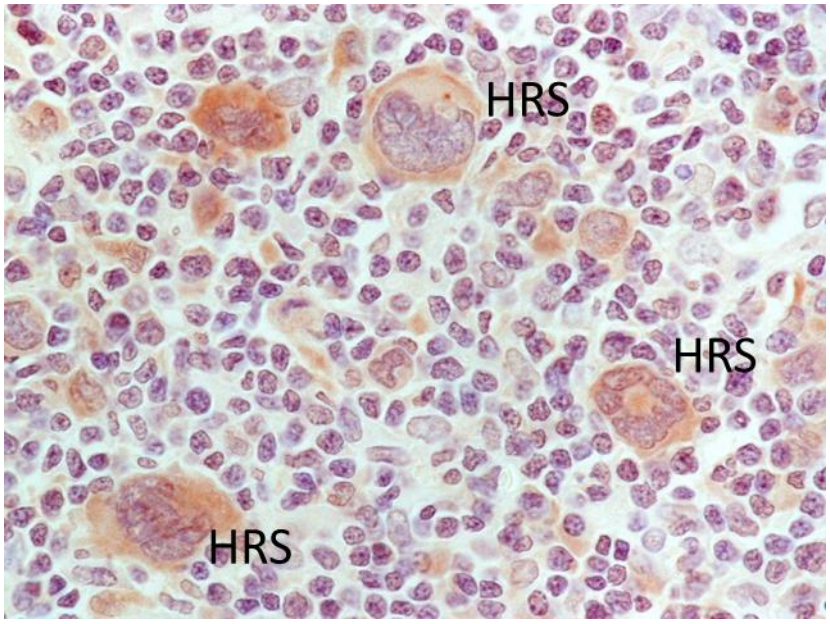

Figure 3.6: SPHK1 expression in reactive tonsil and HL tissue. A) SPHK1 was expressed in the GCB cells and endothelial lining of blood vessels (E). B) SPHK1 was expressed in the cytoplasm of HRS.

A 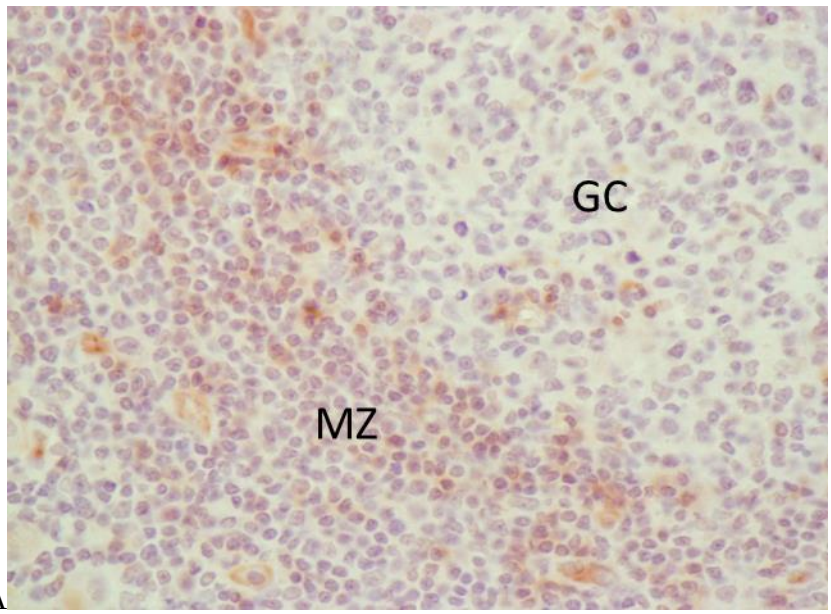

B 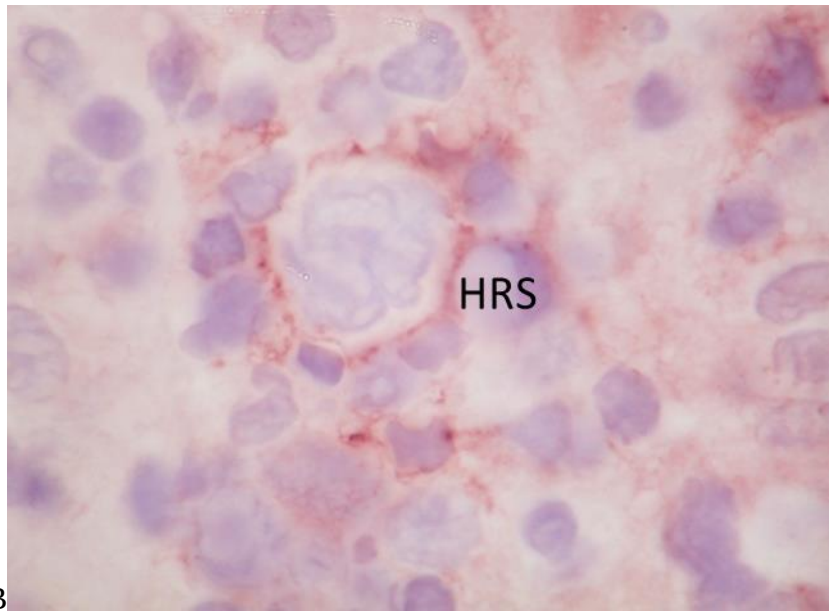

Figure 3.7: S1PR1 expression in reactive tonsil and in HL tissue A) S1PR1 was expressed in the mantle zone (MZ) surrounding germinal centres (GC) of reactive tonsil (x200) B) S1PR1 was expressed in the cell membrane of HRS cell of HL (x600).

A

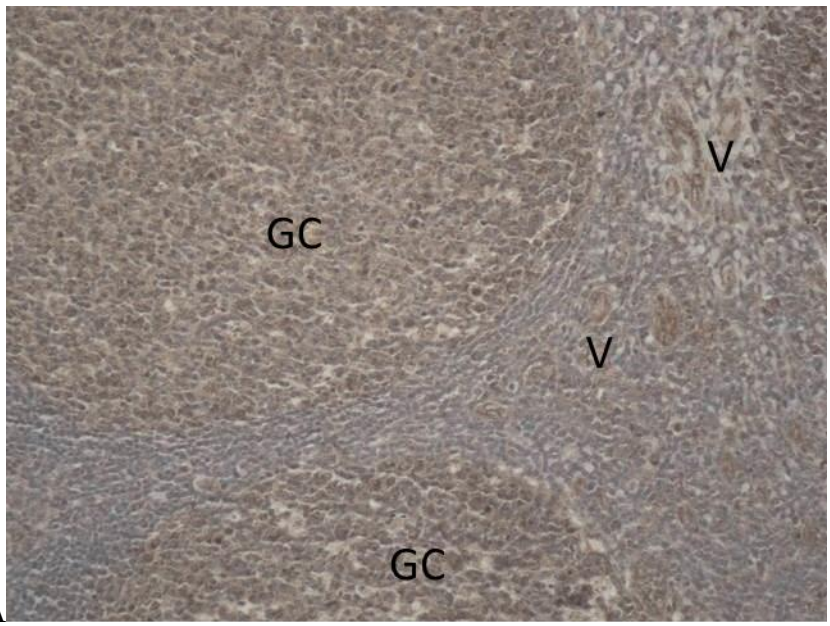

B

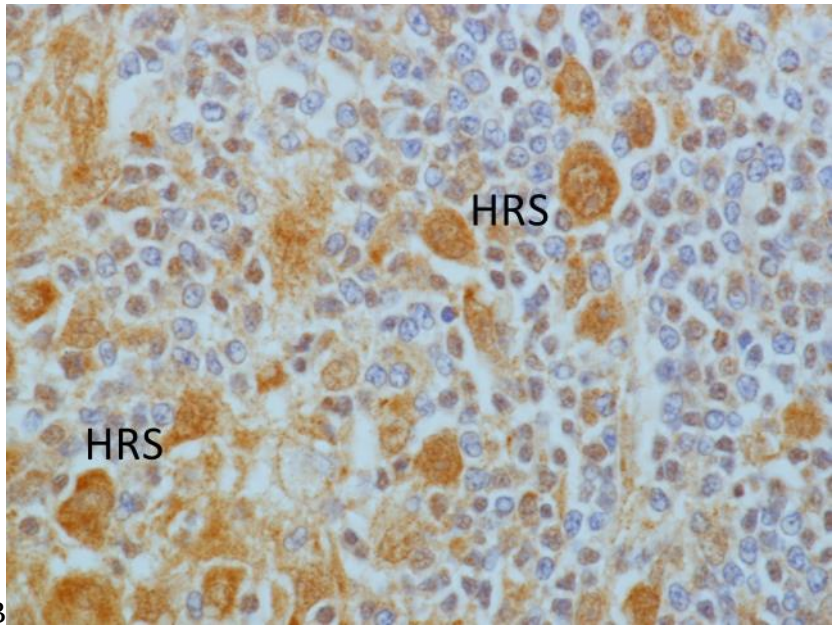

Figure 3.8: S1PR3 expression in reactive tonsil and HL tissue. A) S1PR3 was expressed in the germinal centre of lymphoid follicles (GC) and blood vessels (V) B) Strong S1PR3 expression was seen in the cytoplasm of HRS cells (x 400).

A

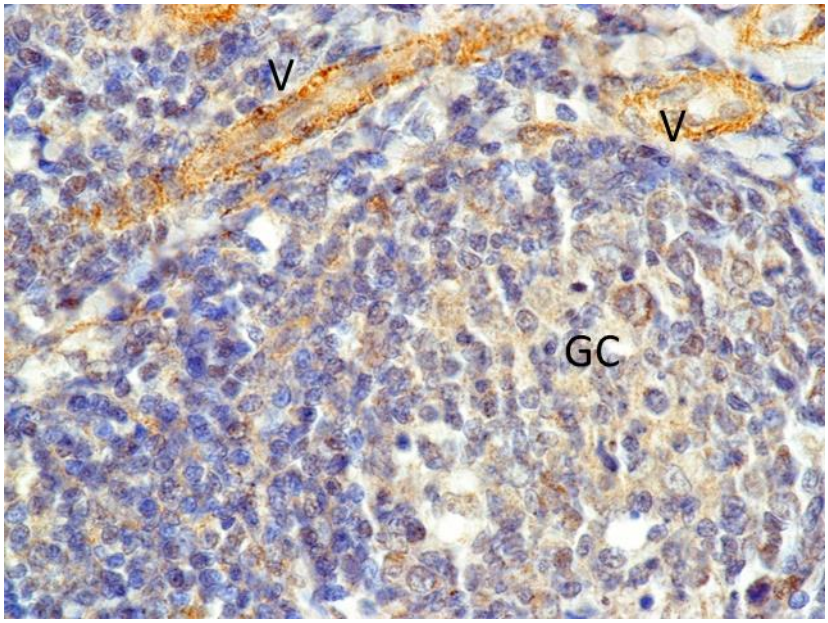

B

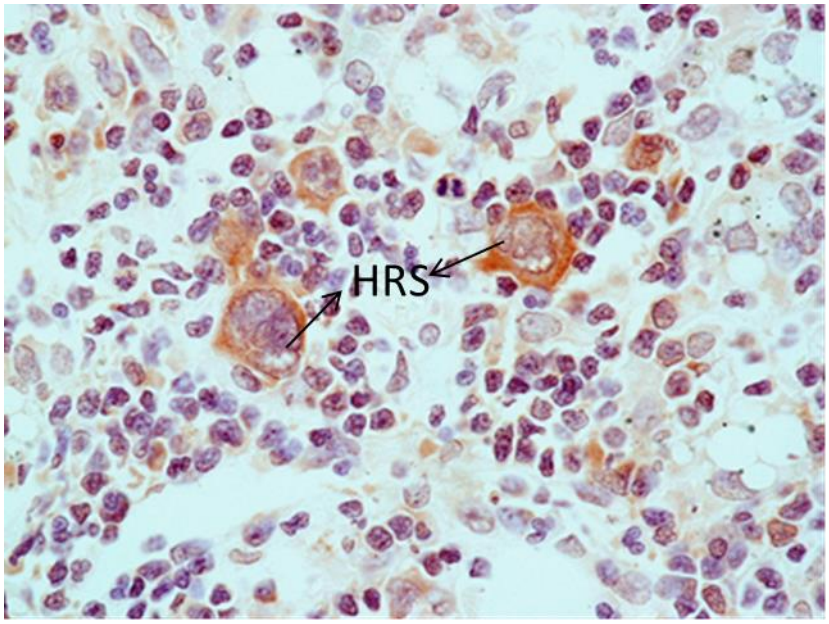

Figure 3.9: Expression of ATX in reactive tonsil and HL tissue. A) ATX was weakly expressed in the germinal centre cells (GC) of reactive tonsil and was strongly expressed in the endothelial cells of blood vessels (V). B) ATX was strongly expressed in the cytoplasm of HRS cells of HL (x600).

3.5.1 Expression of lipid signalling molecules in HL and their relationship with clinicopathological parameters

Tables 3.4-3.8 summarises the expression of each lipid signalling molecules in HL in relation to clinicopathological parameters. I found that EBV positivity was not significantly associated with any clinicopathological parameter (Table 3.4). More patients expressing SPHK1 and ATX were treated with chemotherapy only (p=0.024 and p=0.041 respectively)(Table 3.5 and Table 3.8). S1PR1 expression was associated with lower stage disease (p=0.035)(Table 3.6).

Table 3.4: Clinical characteristics of 61 cases of HL by EBV positivity

Characteristic	All patients (%)	EBV+	EBV-	$\chi 2$ value	p value
Age					
15-34 years	25 (41.0)	10 (41.7)	15 (42.1)	0.724	0.697[#]
35-44 years	10 (16.4)	5 (20.8)	5 (13.2)		
≥ 45 years	26 (42.6)	9 (37.5)	17 (44.7)		
Gender					
Male	37 (60.7)	15 (62.5)	22 (57.9)	0.056	0.812[#]
Female	24 (39.3)	9 (37.5)	15 (42.1)		
Disease subtype					
Nodular sclerosis	34 (55.7)	14 (58.3)	20 (55.3)	0.108	0.742[#]
Mixed cellularity	27 (44.3)	10 (41.7)	17 (44.7)		
Lymphocyte predominant	0 (0.0)	0 (0.0)	0 (0.0)		
Lymphocyte depleted	0 (0.0)	0 (0.0)	0 (0.0)		
Stage					
I-II, limited	31 (59.6)	15 (62.5)	16 (42.1)	1.162	0.281[#]
III-IV, advanced	21 (40.4)	7 (29.2)	14 (39.5)		
Treatment					
chemotherapy only	30 (58.8)	13 (61.9)	17 (56.7)	4.806	0.187[#]
radiotherapy only	9 (17.6)	4 (19.0)	5 (16.7)		
chemotherapy & radiotherapy	10 (19.6)	2 (9.5)	8 (26.7)		
palliative	2 (3.9)	2 (9.5)	0 (0.0)		

[#]Chi square test, *Fisher's exact test

Table 3.5: Expression of SPHK1 in 61 cases of HL by clinicopathological variables

Characteristic	All patients (%)	SPHK1 +	SPHK1 -	χ2 value	p value
Age					
15-34 years	25 (41.0)	10 (37.0)	15 (44.1)	0.605	0.739#
35-44 years	10 (16.4)	4 (14.8)	6 (17.6)		
≥ 45 years	26 (42.6)	13 (48.1)	13 (38.2)		
Gender					
Male	37 (60.7)	15 (55.6)	22 (64.7)	0.528	0.467#
Female	24 (39.3)	12 (44.4)	12 (35.3)		
Disease subtype					
Nodular sclerosis	34 (55.7)	16 (59.3)	18 (52.9)	0.244	0.622#
Mixed cellularity	27 (44.3)	11 (40.7)	16 (47.1)		
Lymphocyte predominant	0 (0.0)	0 (0.0)	0 (0.0)		
Lymphocyte depleted	0 (0.0)	0 (0.0)	0 (0.0)		
EBV status					
Positive	24 (39.3)	13 (48.1)	11 (32.3)	1.513	0.210#
Negative	37 (60.7)	14 (51.9)	23 (67.6)		
Stage					
I-II, limited	31 (50.8)	13 (48.1)	18 (52.9)	0.550	0.458#
III-IV, advanced	21 (34.4)	11 (40.7)	10 (29.4)		
Treatment					
chemotherapy only	30 (58.8)	17 (73.9)	13 (46.4)	8.359	**0.024***
radiotherapy only	9 (17.6)	5 (21.7)	4 (14.3)		
chemotherapy & radiotherapy	10 (19.6)	1 (4.3)	9 (32.1)		
palliative	2 (3.9)	0 (0.0)	2 (7.1)		

#Chi square test, *Fisher's exact test

Table 3.6: Expression of S1PR1 in 61 cases of HL by clinicopathological variables

Characteristic	All patients (%)	S1PR1+	S1PR1-	$\chi 2$ value	p value
Age					
15-34 years	25 (41.0)	19 (39.6)	6 (46.2)	0.185	0.916[#]
35-44 years	10 (16.4)	8 (16.7)	2 (15.4)		
≥ 45 years	26 (42.6)	21 (43.8)	5 (38.5)		
Gender					
Male	37 (60.7)	30 (62.5)	7 (53.8)	0.321	0.571[#]
Female	24 (39.3)	18 (37.5)	6 (46.2)		
Disease subtype					
Nodular sclerosis	34 (55.7)	27 (56.2)	7 (53.8)	0.024	0.877[#]
Mixed cellularity	27 (44.3)	21 (43.8)	6 (46.2)		
Lymphocyte predominant	0 (0.0)	0 (0.0)	0 (0.0)		
Lymphocyte depleted	0 (0.0)	0 (0.0)	0 (0.0)		
EBV status					
Positive	24 (39.3)	21 (43.8)	3 (23.1)	1.832	0.176[#]
Negative	37 (60.7)	27 (56.2)	10 (76.9)		
Stage					
I-II, limited	31 (59.6)	28 (66.7)	3 (30.0)	4.424	**0.035***
III-IV, advanced	21 (40.4)	14 (33.3)	7 (70.0)		
Treatment					
chemotherapy only	30 (58.8)	25 (61.0)	5 (50.0)	6.094	0.075*
radiotherapy only	9 (17.6)	9 (22.0)	0 (0.0)		
chemotherapy & radiotherapy	10 (19.6)	6 (14.6)	4 (40.0)		
palliative	2 (3.9)	1 (2.4)	1 (10.0)		

[#]Chi square test, *Fisher's exact test

Table 3.7: Expression of ABCC1 in 61 cases of HL by clinicopathological variables

Characteristic	All patients (%)	ABCC1+	ABCC1-	$\chi 2$ value	p value
Age					
15-34 years	25 (41.0)	15 (34.1)	10 (58.8)	3.716	0.156#
35-44 years	10 (16.4)	9 (20.5)	1 (5.9)		
≥ 45 years	26 (42.6)	20 (45.5)	6(35.3)		
Gender					
Male	37 (60.7)	27 (61.4)	10 (58.8)	0.033	0.856#
Female	24 (39.3)	17 (38.6)	7 (41.2)		
Disease subtype					
Nodular sclerosis	34 (55.7)	24 (54.5)	10 (58.8)	0.091	0.763#
Mixed cellularity	27 (44.3)	20 (45.5)	7 (41.2)		
Lymphocyte predominant	0 (0.0)	0 (0.0)	0 (0.0)		
Lymphocyte depleted	0 (0.0)	0 (0.0)	0 (0.0)		
EBV status					
Positive	24 (39.3)	17 (38.6)	7 (41.2)	0.033	0.856#
Negative	37 (60.7)	27 (61.4)	10 (58.8)		
Stage					
I-II, limited	31 (50.8)	23 (60.5)	8 (57.1)	0.049	0.825#
III-IV, advanced	21 (34.4)	15 (39.5)	6 (42.9)		
Treatment					
chemotherapy only	30 (58.8)	23 (62.2)	7 (50.0)	2.140	0.549*
radiotherapy only	9 (17.6)	7 (18.9)	2 (14.3)		
chemotherapy and radiotherapy	10 (19.6)	6 (16.2)	4 (28.6)		
palliative	2 (3.9)	1 (2.7)	1 (7.1)		

#Chi square test, *Fisher's exact test

Table 3.8: Expression of ATX in 45 cases of HL by clinicopathological variables

Characteristic	All patients (%)	ATX+	ATX-	$\chi 2$ value	p value
Age					
15-34 years	19 (42.2)	12 (38.7)	7 (50.0)	0.646	0.724#
35-44 years	9 (20.0)	7 (22.6)	2 (14.3)		
≥ 45 years	17 (37.8)	12 (38.7)	5 (35.7)		
Gender					
Male	26 (57.8)	16 (51.6)	10 (71.4)	1.552	0.213#
Female	19 (42.2)	15 (48.4)	4 (28.6)		
Disease subtype					
Nodular sclerosis	25 (55.6)	18 (58.1)	7 (50.0)	0.254	0.614#
Mixed cellularity	20 (44.4)	13 (41.9)	7 (50.0)		
Lymphocyte predominant	0 (0.0)	0 (0.0)	0 (0.0)		
Lymphocyte depleted	0 (0.0)	0 (0.0)	0 (0.0)		
EBV status					
Positive	19 (42.2)	15 (48.4)	4 (28.6)	1.552	0.213#
Negative	26 (57.8)	16 (51.6)	10 (71.4)		
Stage					
I-II, limited	24 (60.0)	15 (51.7)	9 (81.8)	3.009	0.088*
III-IV, advanced	16 (40.0)	14 (48.3)	2 (18.2)		
Treatment					
chemotherapy only	21 (53.8)	17 (60.7)	4 (36.4)	8.273	**0.041***
radiotherapy only	9 (23.1)	7 (25.0)	2 (18.2)		
chemotherapy & radiotherapy	7 (17.9)	2 (7.1)	5 (45.5)		
palliative	2 (5.1)	2 (7.1)	0 (0.0)		

#Chi square test, *Fisher's exact test

3.5.1 Co-expression of lipid signalling molecules in HL

I used chi square and Fisher's exact tests to determine if there was any evidence of co-expression of lipid signalling molecules in HL. As shown in Table 3.9, this analysis revealed that tumours which were positive for SPHK1 (52%) were also positive for S1PR1 ($p = 0.018$). No other significant co-expression was observed. These data might suggest that S1P signaling mediated through S1PR1 regulates SPHK1 expression or vice versa. Figure 3.10 illustrates my hypothesis ie. tumours are more likely to be S1PR1 positive if they also express SPHK1, in other words S1PR1 increases the expression of SPHK1 in HL.

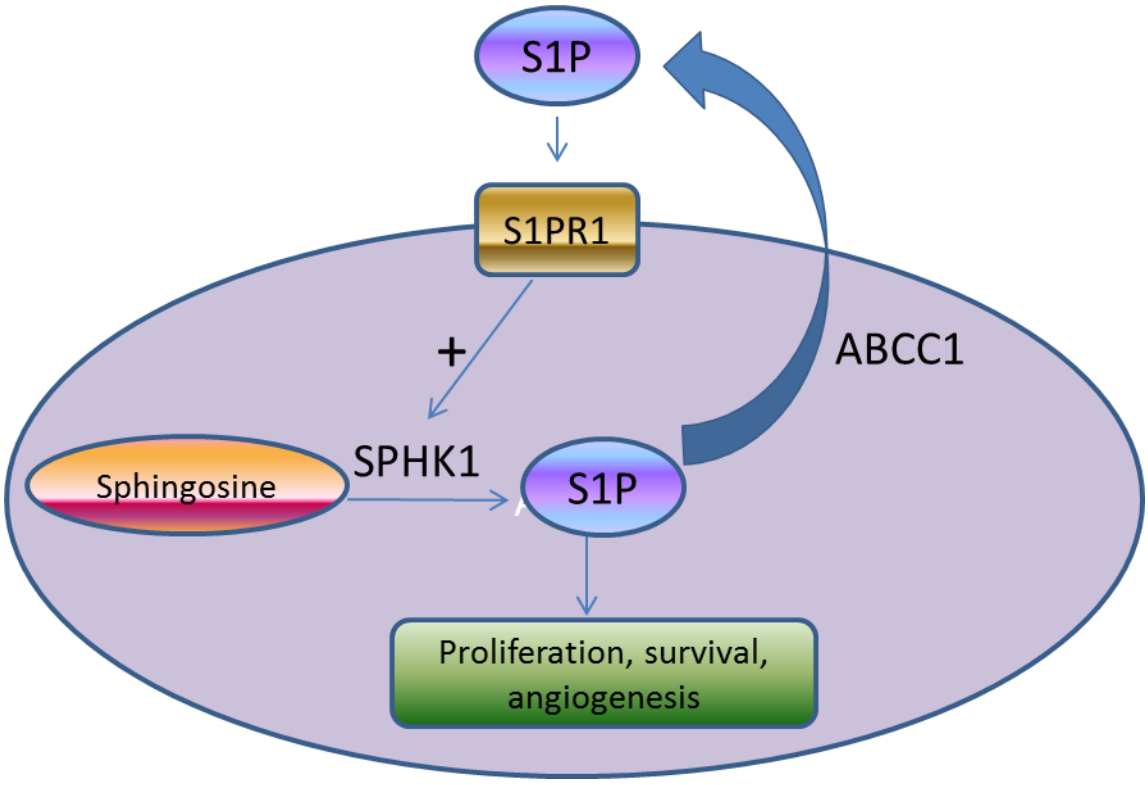

Figure 3.10 showing the suggested hypothesis that overexpression of S1PR1 increases the expression of SPHK1 in HL.

Table 3.9: Co expression of lipid signalling molecules in HL.

Lipid signalling molecule	**Associated lipid signalling molecule (%)**		**χ2 value**	**p value**
	S1PR1+	S1PR1-		
SPHK1 +	25 (52.1)	2 (15.4)	5.584	**0.018**[#]
SPHK1 -	23 (47.9)	11 (84.6)		
	ATX+	ATX-		
SPHK1 +	1 (25.0)	26 (45.6)	0.296	0.586[#]
SPHK1 -	3 (75.0)	31 (54.4)		
	ABCC1+	ABCC1-		
SPHK1 +	21 (47.7)	6 (35.3)	0.768	0.381[#]
SPHK1 -	23 (52.3)	11 (64.7)		
	ABCC1+	ABCC1-		
S1PR1+	33 (75.0)	15 (88.2)	1.260	0.319*
S1PR1-	11 (25.0)	2 (11.8)		
	ATX+	ATX-		
S1PR1+	26 (83.9)	10 (71.4)	0.912	0.428*
S1PR1-	5 (16.1)	4 (28.6)		
	ATX+	ATX-		
ABCC1+	25 (80.6)	8 (57.1)	2.724	0.099[#]
ABCC1-	6 (19.4)	6 (42.9)		

[#]Chi square test, *Fisher's exact test

3.6 Profiling the mRNA expression of S1P signalling molecules in HL cell lines

After examining the expression of lipid signalling molecules at the protein level by immunohistochemistry, I next wanted to investigate which of HL cell lines were representative of the primary tumours. Therefore, I profiled the expression of these lipid signalling molecules at the mRNA level by RT Q-PCR. All data was normalised to GAPDH transcript level.

I found that SPHK1 mRNA was upregulated in HL cell lines compared to tonsils and BL cell lines (Figure 3.11). EBV negative L540 cells exhibit the highest SPHK1 mRNA level followed by EBV negative L428 cells, L1236 and EBV positive L591 cells.

Compared to GCB cells, S1PR1 mRNA levels were elevated in EBV positive L591 cells and in EBV negative L428 and HDLM2 cells (Figure 3.12) S1PR3 was only expressed at high levels in L428 cells (Figure 3.13).

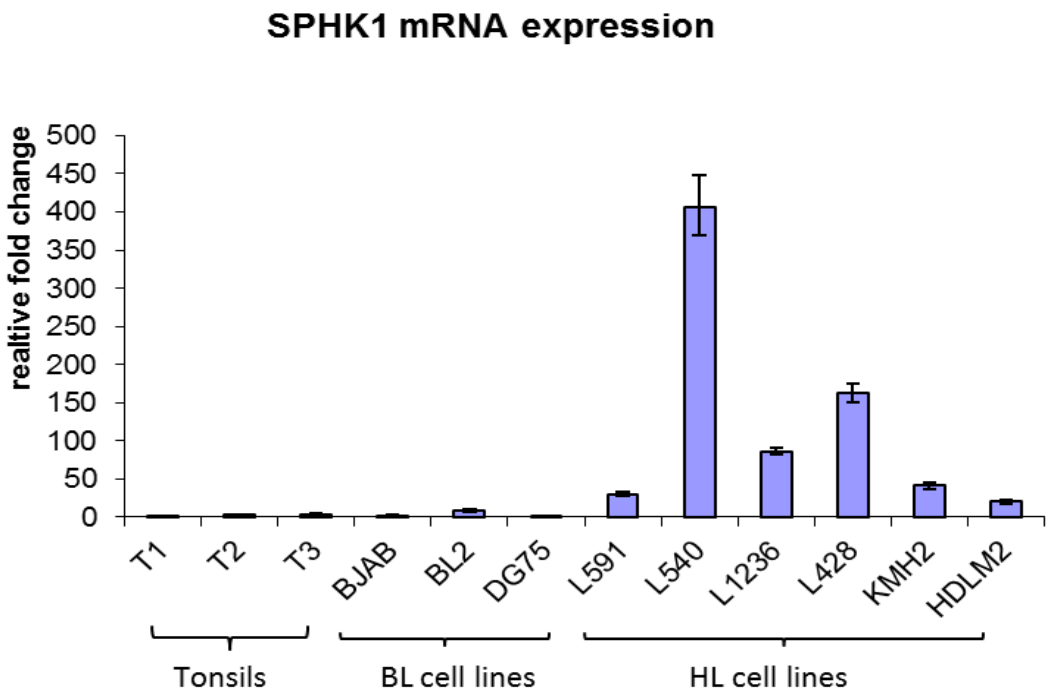

Figure 3.11: Expression of SPHK1 in tonsils, BL and HL cell lines by RT Q-PCR. SPHK1 mRNA was upregulated in HL cell lines compared to GCB cells and BL cell lines. All data is normalised to GAPDH transcript levels. Data is expressed relative to GC B cells of Tonsil 1, assigned as value of 1 (Data by Nicola Ruth).

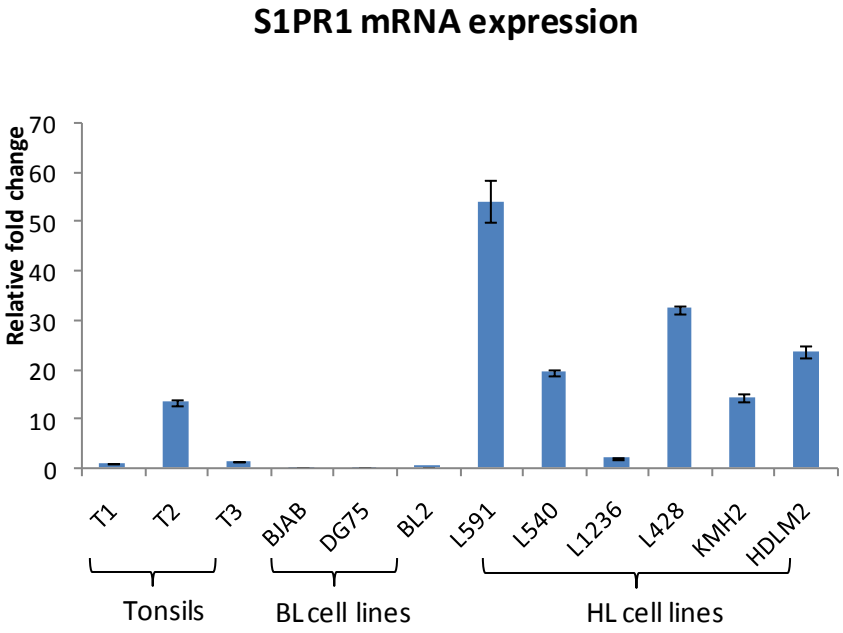

Figure 3.12: Expression of S1PR1 in tonsils, BL and HL cell lines by RT Q-PCR. S1PR1 was markedly elevated in L591 cells and was expressed in other HL cell lines. All data is normalised to GAPDH transcript levels. Data is expressed relative to GC B cells of Tonsil 1, assigned as value of 1 (Data by Nicola Ruth).

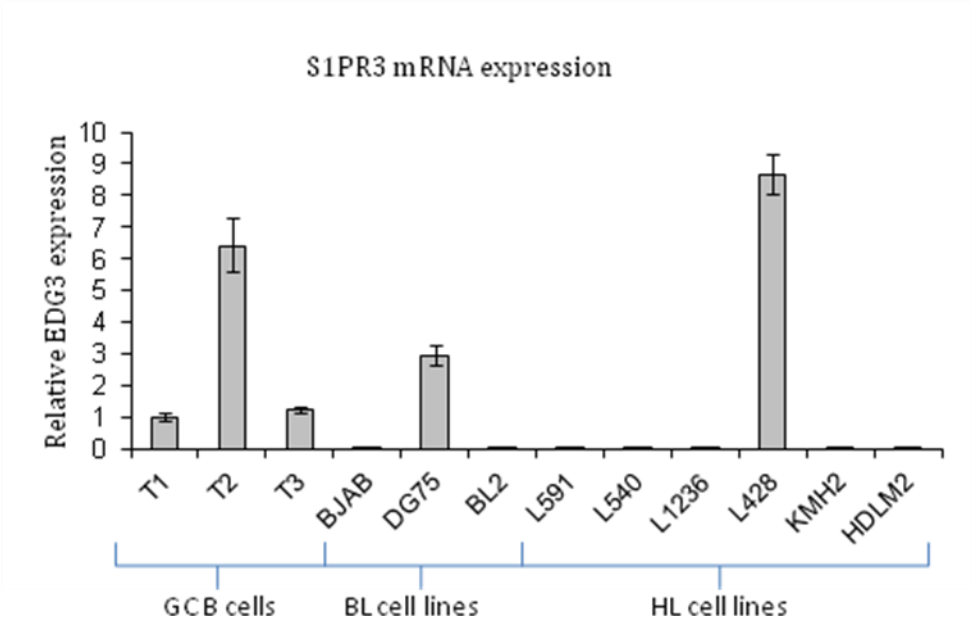

Figure 3.13: Expression of S1PR3 in tonsils, BL and HL cell lines by RT Q-PCR. Expression of S1PR3 was increased in tonsils and was markedly increased in L428 HL cell line. All data is normalised to GAPDH transcript levels. Data is expressed relative to GC B cells of Tonsil 1, assigned as value of 1 (Data by Nicola Ruth).

3.7 Gene expression profiling after treatment of HL derived cell line, L591 with Sphingomab

The objective of this experiment is to profile the genes upregulated and downregulated by Sphingomab and show whether the B-cell phenotype is restored in the HL cell line. I treated L591 cells with Sphingomab, a human monoclonal Ab which binds to S1P and prevents its interaction with its receptors. I then extracted the RNA from these cells at 2 and 12 hours time points. Gene expression profiling was performed using GeneChip Whole Transcript Sense Target Labelling Assay as described in section 2.7. Microarray data was then analysed using Genespring GX version 12.5 as described in section 2.8.

3.7.1 Quality control of samples

Quality control of each sample was determined using Principal Component Analysis (PCA). Figure 3.14 shows PCA of 2 hour and 12 hour samples in triplicates. The samples were coded into two different colours, blue are the control samples, red are the treated samples. For 2 hour samples, the plot seem to be quite scattered from each other but are still in the same plane. The plot of 12 hour samples seem to show better distribution compared to 2 hour samples.

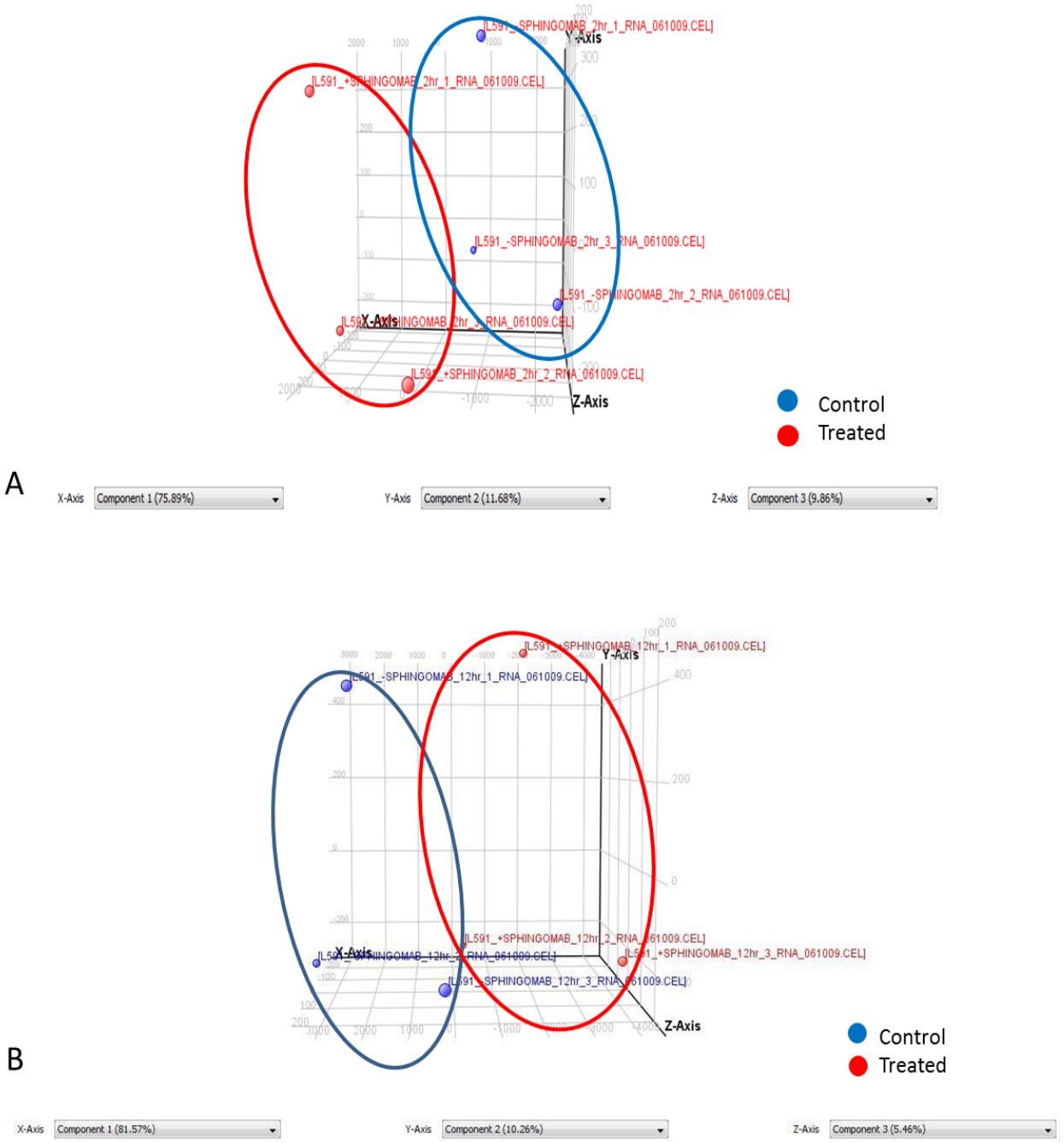

Figure 3.14: Principal component analysis of 2 hour samples (A) and 12 hour sample (B).

3.7.2 Selection of differentially expressed genes:

A gene was considered to be differentially expressed if the fold-change was more than 1.2 and the p value was < 0.05. When the fold change was set at 2 and 1.5, no genes were differentially expressed, therefore a fold change of 1.2 was used. For 2 hour samples, 841 genes were obtained and when fold change was set at 1.2, 94 genes were expressed in which 15 genes were upregulated and 79 genes were downregulated (Table 3.10). As for 12 hour samples, 1301 genes were obtained and after fold change of 1.2 was set, 237 genes were differentially expressed, of which 27 genes were upregulated and 207 genes were downregulated (Table 3.11). Figure 3.15 shows hierarchical clustering of 2 hour and 12 hour samples and Figure 3.16 and Figure 3.17 show gene expression profiles for 2 hour and 12 hour samples respectively. The list of top 20 genes (lower p values) upregulated and downregulated by Sphingomab are detailed in Table 3.10-3.13. Table 3.14 showed the list of eight B-cell receptor signaling genes which were differentially expressed following treatment with Sphingomab ($p < 0.005$). However the fold change of these genes range from -1.07 to 1.02. Figure 3.18 shows the B cell receptor pathway and these eight genes are highlighted yellow. The summary of the roles of these eight B cell receptor signaling genes are shown in Table 3.15. Two S1P signaling genes were expressed in this array ie S1PR3 was found to be downregulated by Sphingomab at 12 hours and S1PR5 was downregulated at 2 hours (these genes are highlighted in the tables in the Appendix).

A

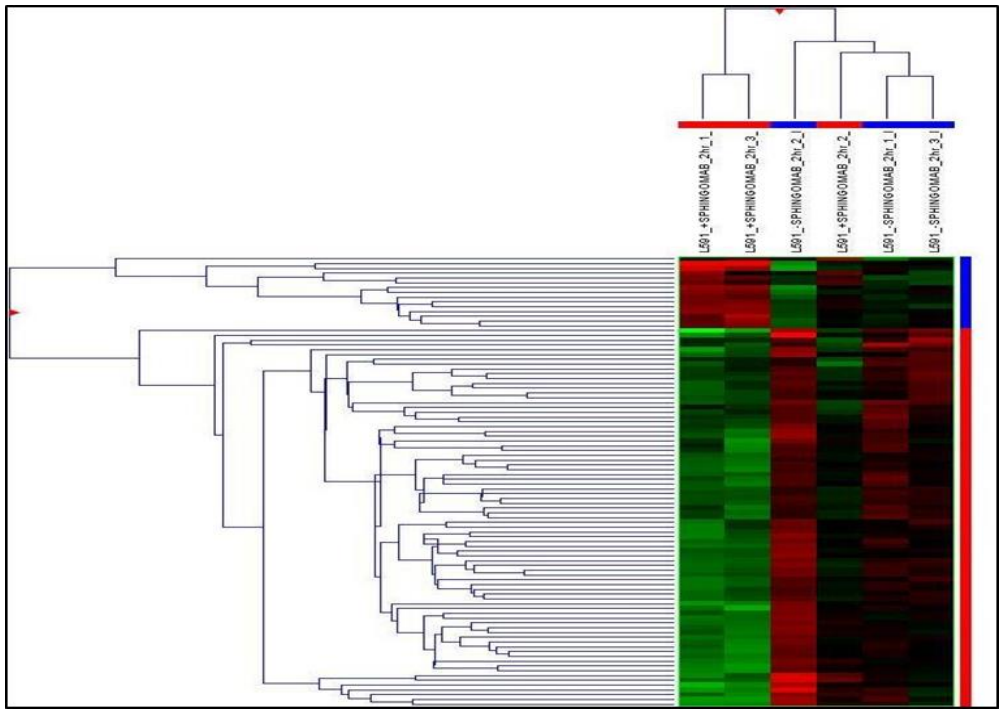

B

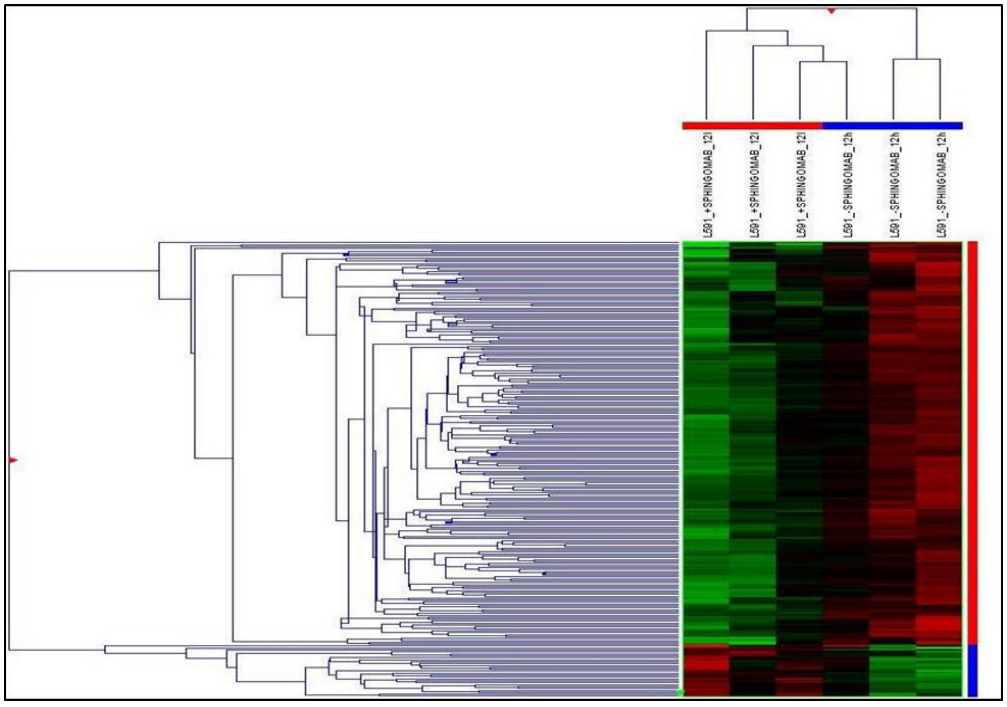

Figure 3.15 Hierarchical clustering of 2 hour samples (A) and 12 hour samples (B) after treatment with Sphingomab. Relative expression of each gene is shown in red indicating upregulation and green indicating downregulation. The horizontal lines indicate each gene.

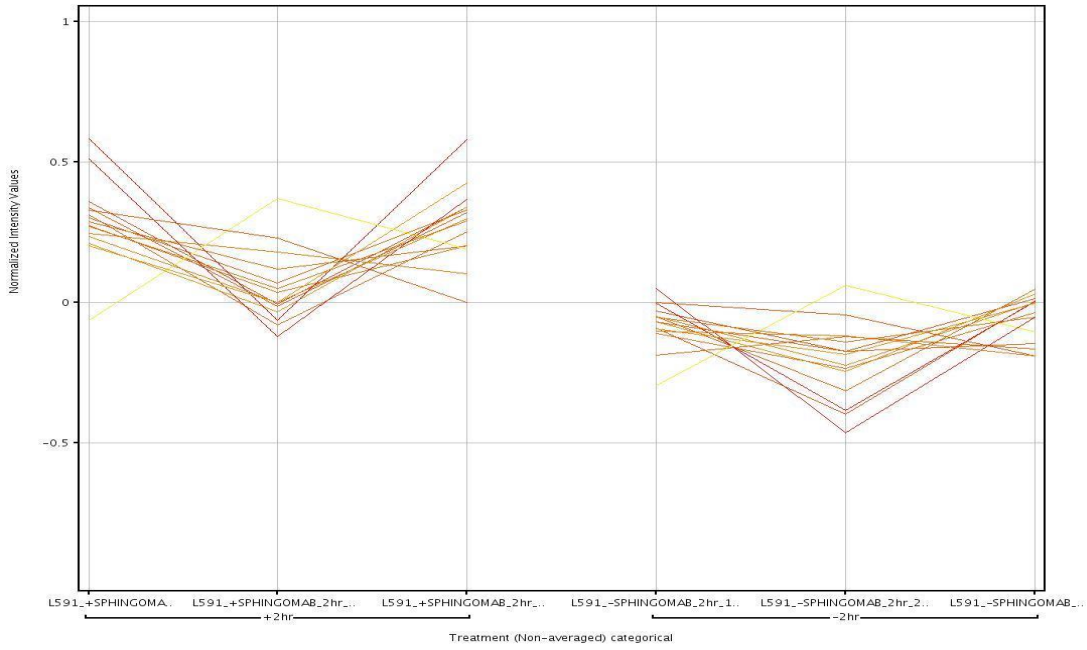

A

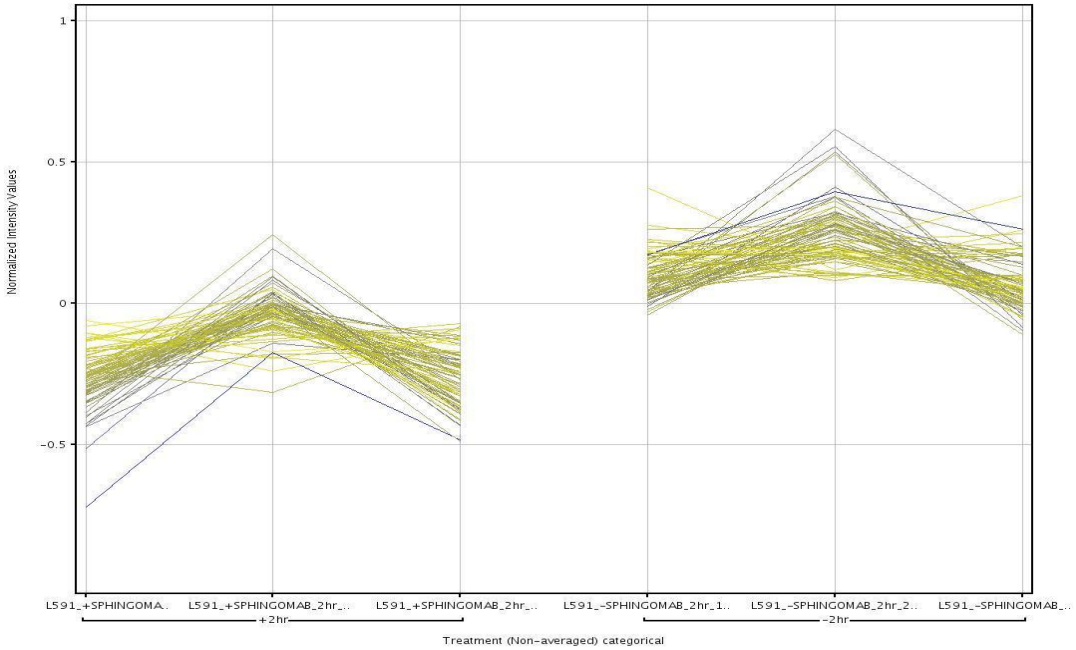

B

Figure 3.16 Gene expression profile of 2 hour samples. A) 15 genes were upregulated and B) 79 genes were downregulated by Sphingomab (control samples are on the left and treated samples are on the right of each diagram).

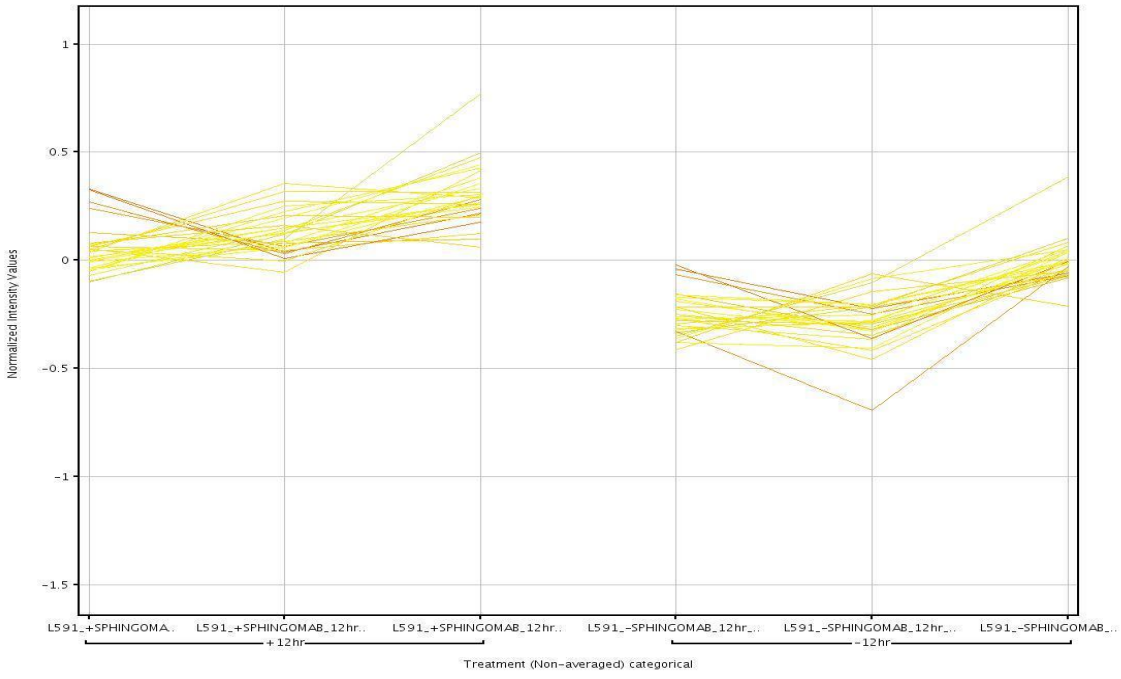

A

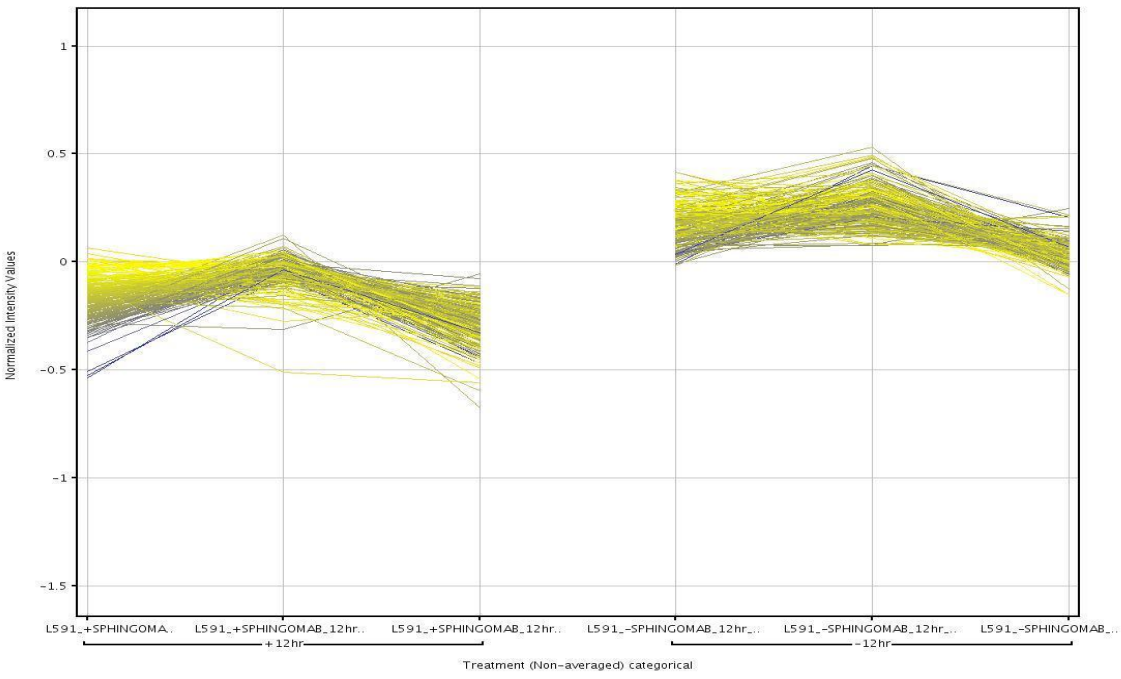

B

Figure 3.17 Gene expression profile of 12 hour samples. A) 23 genes were upregulated and B) 207 genes were downregulated by Sphingomab (control samples are on the left and treated samples are on the right of each diagram).

Table 3.10 List of all 15 genes upregulated by Sphingomab at 2 hours post treatment (fold change > 1.2, p value < 0.05).

Transcript ID	Gene symbol	Gene description	p value	Fold change
3737677	LOC100129503	uncharacterised	0.003402	1.242232
3755316	MLLT6|LOC100129395	myeloid/lymphoid or mixed-lineage leukemia (trithorax homolog, Drosophila); translocated to, 6 | NS5ATP13TP1	0.006773	1.212979
3249043	REEP3	receptor accessory protein 3	0.00698	1.325794
3716048	TAOK1	TAO kinase 1	0.007025	1.205202
2409069	CCDC23	coiled-coil domain containing 23	0.007082	1.311701
2464484	FAM36A|NCRNA00201	family with sequence similarity 36, member A | non-protein coding RNA 201	0.011231	1.203204
2717481	AFAP1-AS	AFAP1 antisense RNA (non-protein coding) | actin filament associated protein 1	0.020966	1.227855
3645764	OR1F1	olfactory receptor, family 1, subfamily F, member 1	0.023378	1.201179
2514441	PPIG	peptidylprolyl isomerase G (cyclophilin G)	0.025828	1.218231
2783473	C4orf3	chromosome 4 open reading frame 3	0.029463	1.409258
2418339	LRRIQ3	leucine-rich repeats and IQ motif containing 3	0.031467	1.201805
2766262	TLR6	toll-like receptor 6	0.033284	1.285438
2620150	ZNF660|ZNF197	zinc finger protein 660 | zinc finger protein 197	0.033869	1.284663
2383524	ZNF678	zinc finger protein 678	0.045883	1.212393
3625674	RFX7	regulatory factor X, 7	0.049481	1.23359

Table 3.11 List of top 20 out of 79 genes downregulated by Sphingomab at 2 hours post treatment

Transcript ID	Gene symbol	Gene description	p value	Fold change
2902609	C6orf25	chromosome 6 open reading frame 25	3.28E-04	1.224931
2445876	NCRNA00083	non-protein coding RNA 83	0.001321	1.212823
3596263	FOXB1	forkhead box B1	0.001523	1.213903
2472054	GDF7	growth differentiation factor 7	0.001704	1.294686
3349948	REXO2	REX2, RNA exonuclease 2 homolog (S. cerevisiae)	0.002165	1.284174
3673880	C16orf81	chromosome 16 open reading frame 81	0.002187	1.255238
2532626	C2orf82	chromosome 2 open reading frame 82	0.003264	1.315103
3339722	P2RY2	purinergic receptor P2Y, G-protein coupled, 2	0.004045	1.20298
2948810	PSORS1C2	psoriasis susceptibility 1 candidate 2	0.004198	1.225966
2641479	GP9	glycoprotein IX (platelet)	0.004377	1.22743
3272706	VENTX	VENT homeobox homolog (Xenopus laevis)	0.004462	1.263463
3744127	HES7	hairy and enhancer of split 7 (Drosophila)	0.004808	1.245594
3745287	MYH1|MYH2|MYH8	myosin, heavy chain 1, skeletal muscle, adult | myosin, heavy chain 2, skeletal muscle, adult | myosin, heavy chain 8, skeletal muscle, perinatal	0.005257	1.228423
3023964	CPA1	carboxypeptidase A1 (pancreatic)	0.00529	1.205926
3474418	PXN	paxillin	0.005522	1.280956
3380126	FGF19	fibroblast growth factor 19	0.005533	1.232402
3579114	BCL11B	B-cell CLL/lymphoma 11B (zinc finger protein)	0.006832	1.260329
3404823	PRH2	proline-rich protein HaeIII subfamily 2	0.007001	1.22648
3204285	CCL19	chemokine (C-C motif) ligand 19	0.007718	1.253403
3273110	DUX4L4|DUX4L7|DUX4L2 |DUX4L3|DUX4L5|DUX4L6	double homeobox 4 like 4 | double homeobox 4 like 7 | double homeobox 4 like 2 | double homeobox 4 like 3 | double homeobox 4 like 5 | double homeobox 4 like 6	0.008839	1.339572

Table 3.12 List of all 23 genes upregulated by Sphingomab at 12 hours post treatment

Transcript ID	Gene symbol	Gene description	p value	Fold change
3951190	C2orf27A|DUXAP10|FLJ39632	chromosome 2 open reading frame 27A | double homeobox A pseudogene 10 | hypothetical LOC642477	0.006769	1.231519
3929664	TMEM50B	transmembrane protein 50B	0.037376	1.202532
3873086	DEFB129	defensin, beta 129	0.005991	1.348438
3843399	ZNF134|ZNF211	zinc finger protein 134 | zinc finger protein 211	0.029627	1.287905
3826504	ZNF431|ZNF714	zinc finger protein 431 | zinc finger protein 714	0.028561	1.265593
3811086	PIGN	phosphatidylinositol glycan anchor biosynthesis, class N	0.044249	1.237523
3764872	PTRH2	peptidyl-tRNA hydrolase 2	0.035615	1.231048
3760268	ARL17A|ARL17B|LOC100294341	ADP-ribosylation factor-like 17A | ADP-ribosylation factor-like 17B | ADP-ribosylation factor-like protein 17-like	0.020879	1.236461
3727510	STXBP4	syntaxin binding protein 4	0.0138	1.296312
3722286	RUNDC1	RUN domain containing 1	0.046301	1.458222
3666282	ZFP90	zinc finger protein 90 homolog (mouse)	0.045151	1.224183
3561110	RALGAPA1	Ral GTPase activating protein, alpha subunit 1 (catalytic)	0.047613	1.217444
3547375	GPR65	G protein-coupled receptor 65	0.040823	1.281755
3526425	PCID2	PCI domain containing 2	0.030258	1.295463
3489212	FNDC3A	fibronectin type III domain containing 3A	0.038012	1.221823
3425134	TMTC3	transmembrane and tetratricopeptide repeat containing 3	0.041587	1.279973
3392996	SIK3	SIK family kinase 3	0.019756	1.309694
3382596	PRKRIR	protein-kinase, interferon-inducible double stranded RNA dependent inhibitor, repressor of (P58 repressor)	0.041219	1.301903
3352485	TMEM136	transmembrane protein 136	0.04574	1.220377
3249043	REEP3	receptor accessory protein 3	0.02051	1.250174
3182984	NIPSNAP3B|LOC286367	nipsnap homolog 3B (C. elegans) | FP944	0.047097	1.211697
3150663	TAF2	TAF2 RNA polymerase II	0.048844	1.237538
3136178	PLAG1	pleiomorphic adenoma gene 1	1.86E-05	1.240392
2349848	PRMT6	protein arginine methyltransferase 6	0.011779	1.232427

Table 3.13 List of top 20 out of 207 genes downregulated by Sphingomab at 12 hours post treatment

Transcript ID	Gene symbol	Gene description	p value	Fold change
3002183	POM121L12	POM121 membrane glycoprotein-like 12	1.42E-05	1.25003
4032271	GOLGA2P2Y| GOLGA2P3Y|CSPG4P5	golgin A2 pseudogene 2, Y-linked | golgin A2 pseudogene 3, Y-linked | chondroitin sulfate proteoglycan 4 pseudogene 5	1.27E-04	1.202986
3726537	EPN3	epsin 3	1.33E-04	1.21147
3259959	C10orf62	chromosome 10 open reading frame 62	6.05E-04	1.253822
3332964	C11orf66	chromosome 11 open reading frame 66	6.97E-04	1.277711
3704928	SPATA2L	spermatogenesis associated 2-like	0.001033	1.2394
4010183	SPIN3	spindlin family, member 3	0.001286	1.245429
2576608	C2orf27B|C2orf27A|C9orf172	chromosome 2 open reading frame 27B | chromosome 2 open reading frame 27A | chromosome 9 open reading frame 172	0.001336	1.209652
3233182	NET1	neuroepithelial cell transforming 1	0.001428	1.421568
2352338	FAM19A3	family with sequence similarity 19 (chemokine (C-C motif)-like), member A3	0.001693	1.213123
3706113	HIC1	hypermethylated in cancer 1	0.001701	1.202551
3662093	MT3	metallothionein 3	0.001709	1.330172
3934573	KRTAP10-1|KRTAP10-11	keratin associated protein 10-1 | keratin associated protein 10-11	0.002112	1.214363
3858993	CEBPA	CCAAT/enhancer binding protein (C/EBP), alpha	0.002587	1.25142
3227070	PTGES	prostaglandin E synthase	0.002637	1.201343
3713278	FLJ35934		0.002705	1.257513
3031399	ZNF775|LOC728743	zinc finger protein 775 | similar to GLI-Kruppel family member HKR1	0.002811	1.231678
3707950	FAM64A	family with sequence similarity 64, member A	0.002832	1.297886
3483046	GSX1	GS homeobox 1	0.003022	1.235101
3590275	CHAC1	ChaC, cation transport regulator homolog 1 (E. coli)	0.003309513	1.2028043

Table 3.14 List of B cell receptor signaling genes expressed after treatment with Sphingomab

Transcript ID	Gene symbol	Expression	p value	Fold change
2420808	BCL10	up	6.07E-04	1.0468156
3227696	RAPGEF1	up	0.033392854	1.0243601
3666033	NFATC3	up	0.005136701	1.0350204
3790259	MALT1	up	0.017520413	1.0423235
2436985	SHC1	down	0.026881663	-1.0422614
2438207	MEF2D	down	0.016683191	-1.0548377
2505529	PTPN18	down	0.009659263	-1.0770031
2881300	CAMK2A	down	0.001493649	-1.064041

Table 3.15 Summary of the roles of B cell receptor signaling genes

Gene	Summary
BCL10	Translocates in mucosa-associated lymphoid tissue (MALT) lymphoma and is an apoptosis-associated gene via the activation of NF-κB signaling (Zhu et al., 2013).
RAPGEF1	Binds to GTP to regulate proliferation, differentiation and apoptosis. Hypomethylation is frequent in gastrointestinal and gynecological cancers (Samuelsson et al., 2011).
NFATC3	Targets of immune receptor signals in B lymphocytes leading to a rapid rise of intracellular calcium and controlling proliferation and survival (Rudolph et al., 2014).
MALT1	Involved in the pathogenesis of mucosa-associated lymphoid tissue (MALT) lymphoma via the activation of NF-κB. Has anti-apoptotic effect and regulates the subcellular location of BCL10 (Hosokawa 2005).
SHC1	Regulates the transfer of mitogenic signals in cells, to participate in p53-dependent apoptosis under oxidative stress, regulates lifespan, and drug resistance in mammalian cells (Kashkin et al., 2013).
MEF2D	Mediates response to mitogenic signals and survival of neurons and T-lymphocytes and contributes to the pathogenesis of acute lymphoblastic lymphoma (ALL) (Prima et al., 2005).
PTPN18	Regulates cell growth, differentiation, mitotic cycle, and oncogenic transformation. Involved in leukaemogenesis via bcr-abl signaling (Rubhi et al., 2011).
CAMK2A	Involved in cell survival, apoptosis, cytoskeletal re-organization and learning and memory. Plays an important role in the growth of osteosarcoma (Yuan et al., 2007).

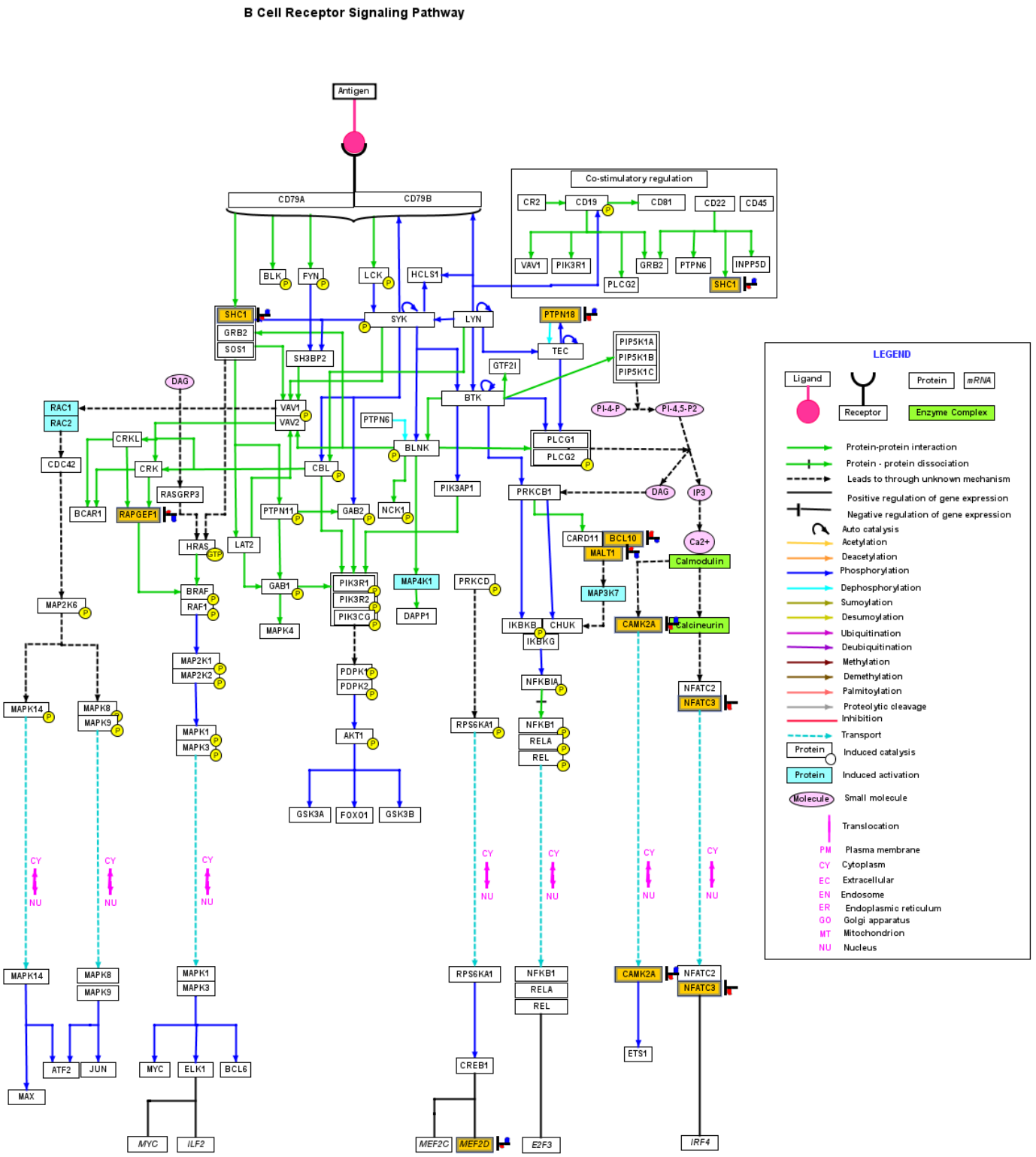
B Cell Receptor Signaling Pathway
Antigen
CD79A
CD79B
Co-stimulatory regulation
CR2
CD19
CD81
CD22
CD45
VAV1
PIK3R1
GRB2
PTPN6
INPP5D
PLCG2
SHC1
BLK
FYN
LCK
HCLS1
SYK
LYN
PTPN18
TEC
PIP5K1A
PIP5K1B
PIP5K1C
GTF2I
BTK
SH3BP2
GRB2
SOS1
DAG
RAC1
RAC2
VAV1
VAV2
PTPN6
BLNK
PLCG1
PLCG2
PI-4-P
PI-4,5-P2
CRKL
CRK
CDC42
CBL
PIK3AP1
PRKCB1
DAG
IP3
BCAR1
RAPGEF1
RASGRP3
PTPN11
GAB2
NCK1
CARD11
BCL10
MALT1
Ca2+
Calmodulin
HRAS
LAT2
BRAF
RAF1
GAB1
PIK3R1
PIK3R2
PIK3CG
MAP4K1
PRKCD
MAP3K7
IKBKB
CHUK
IKBKG
CAMK2A
Calcineurin
MAP2K6
MAPK4
DAPP1
MAP2K1
MAP2K2
PDPK1
PDPK2
NFKBIA
NFATC2
NFATC3
MAPK14
MAPK8
MAPK9
MAPK1
MAPK3
AKT1
RPS6KA1
NFKB1
RELA
REL
GSK3A
FOXO1
GSK3B
CY
NU
ATF2
JUN
MAX
MYC
ELK1
BCL6
ILF2
CREB1
MEF2C
MEF2D
E2F3
ETS1
IRF4
LEGEND
Ligand
Receptor
Protein
mRNA
Enzyme Complex
Protein-protein interaction
Protein - protein dissociation
Leads to through unknown mechanism
Positive regulation of gene expression
Negative regulation of gene expression
Auto catalysis
Acetylation
Deacetylation
Phosphorylation
Dephosphorylation
Sumoylation
Desumoylation
Ubiquitination
Deubiquitination
Methylation
Demethylation
Palmitoylation
Proteolytic cleavage
Inhibition
Transport
Induced catalysis
Induced activation
Small molecule
Translocation
PM Plasma membrane
CY Cytoplasm
EC Extracellular
EN Endosome
ER Endoplasmic reticulum
GO Golgi apparatus
MT Mitochondrion
NU Nucleus

3.8 Discussion

I found that SPHK1 was overexpressed in HRS cells in 27/61 (44 %) of HL cases. Bayerl et al reported that SPHK1 protein and mRNA was significantly higher in NHL as compared to lymph nodes with reactive hyperplasia (Bayerl et al. 2008). Increases in SPHK1 protein and mRNA have also been reported in several human malignancies such as breast, brain, colon, ovary, stomach, kidney, uterus, prostate and small intestine (French et al., 2003a). High levels of SPHK1 is associated with increased proliferation and resistance to chemotherapy. Preliminary studies in situ and in animal models indicate that SPHK1 inhibitors prevent cancer cell proliferation and tumour growth. As pro-mitogenic S1P formation is catalysed by SPHK1, blockade of SPHK1 is thought to be a promising target in cancer treatment (Ader et al., 2009). Importantly, down-regulation of SPHK1 leads to increased cytotoxicity of chemotherapeutic drugs and chemosensitivity restoration of multidrug resistance HL60 AML cells (Bonhoure et al., 2006).

S1PR1 was commonly expressed in HRS cells in 48/61 (79%) of cases and S1PR1 expression was significantly associated with SPHK1 expression. Significantly enhanced expression of S1PR1 was observed in HRS cells and the staining pattern exhibited strong association with S1PR1 mRNA expression by RT Q-PCR. Amongst all types of lymphomas, S1PR1 expression has only been reported in classical mantle cell lymphoma. A study by Nishimura et al showed that S1PR1 was expressed in all cases of mantle cell lymphoma suggesting that S1PR1 could be useful in reaching a histological diagnosis of mantle cell lymphoma (Nishimura et al., 2010).

S1PR3 was strongly expressed in all 61 HL cases, however the mRNA levels were only increased in L428 cell lines. This discrepancy could be explained that the protein and mRNA expression was not a case by case basis. There are novel S1PR3 antagonists, and inhibition of these receptors with these compound may inhibit cancer cell growth.

In a previous study, ABCC1 was found to be expressed in 20% of HL patients and was associated with failure to respond to chemotherapy (Greaves et al. 2012). In this study, I found that ABCC1 protein was expressed in 78% of HL cases exhibiting moderate to strong staining pattern. This difference in the percentage of cases expressing ABCC1 might be attributed to the different antibodies used.

ATX was the only lipid signalling molecule which showed significant association with OS. Baumforth et al have shown that high ATX expression in HRS cells was found in EBV positive HL cases and that ATX upregulation led to increased growth and survival of HL cells. Downregulation of ATX led to reduced cell growth and viability (Baumforth et al. 2008). These findings suggest that ATX could a promising target for therapeutic intervention.

Gene expression microarrays have emerged as powerful tool in molecular biology and offer high throughput analysis of gene expression on a large genomic scale. The initial microarray analysis was using SAM analysis (data not shown here) which found a different list of genes. Using SAM analysis, only one B cell receptor gene named SOS1 was differentially expressed. Therefore I have re-analysed this array using GeneSpring software as shown in this chapter. GeneSpring analysis showed that eight B cell receptor genes were expressed at after treatment with Sphingomab. Sphingomab seemed to upregulate the expression of BCL10, RAPGEF1, NFATC3 and MALT1 which suggests that Sphingomab could possibly

restore the B cell phenotype in HL. However the low fold change observed, could be contributed by technical errors. There are many steps which could lead to errors in microarray experiments, from sample preparation to data analysis. The quality of RNA is of utmost importance. DNA contamination, RNA degradation and traces of phenols could contribute to poor labelling and quality of signals. During data visualization and interpretation, raw images are captured using a laser imaging system, analysed and filtered. Statistical methods are then applied for interpretation.

BCL10 was identified by its translocation in a case of MALT lymphoma. It forms a complex with MALT1 gene and activates NF-κB signaling. BCL10 is mutated in multiple types of malignant tumour cell lines including colon cancer, mesothelioma, germ cell tumour, follicular lymphoma, Sezary syndrome and T-ALL (Willis et al., 1999). MALT1 is mucosa associated lymphoid tissue lymphoma translocation gene 1 and is involved in the nuclear export of BCL10. Chromosomal aberration of MALT1 is recurrent in low-grade mucosa-associated lymphoid tissue (MALT lymphoma) which is a slow growing indolent lymphoma. RAPGEF1 is Rap guanine nucleotide exchange factor 1 which belongs to the adaptor-type Src homology (SH)2-containing molecules. It is involved in signal transmission from the cell surface to the nucleus (Samuelsson et al., 2011). NFATC3 is a member of the nuclear factors of activated T cells DNA-binding transcription complex. It regulates gene expression in T cells and immature thymocytes (Rudolph et al., 2014).

Considering that this array is working, it could shed some light on the molecular mechanism of HL. Perhaps the four B cell receptor genes upregulated by Sphingomab could be evaluated further to determine their significance in the pathogenesis of HL.

CHAPTER 4

ANALYSIS OF EBV STATUS AND EXPRESSION OF LIPID SIGNALLING MOLECULES IN A COHORT OF DIFFUSE LARGE B CELL LYMPHOMAS FROM THE UNITED KINGDOM

4.1 Introduction

In 2007, Park et al studied the impact of EBV status on the clinical outcome of 380 DLBCL patients aged ≥ 18 years in Korea. 34 cases (9.0%) were identified to be EBV^+. In this series, EBV^+ status was significantly associated with age > 60 years, more advanced stage, more than one extranodal involvement, higher IPI, presence of B symptoms, poorer outcome to clinical treatment and poorer overall survival and progression-free survival (Park et al. 2007). The non-GCB DLBCL showed poorer overall survival compared to the GCB DLBCL. In 2008, Cho et al. identified 29/387 (7.5%) EBV^+ DLBCL among Korean patients. A study in Peru reported a prevalence of 14.1% of EBV^+ DLBCL-E. These cases were associated with non GCB subtype, advanced stage, high IPI score and short overall survival (Beltran et al. 2011).

In contrast to a relatively high incidence of EBV^+ DLBCL in the Asian countries, Hoeller et al reported an EBV positivity in only 3.1% of EBV^+ DLBCL of the elderly (EBV^+ DLBCL-E) in European populations (Hoeller et al., 2010). The majority of these cases showed EBV latency II (62.5%) and latency III (25.0%). A markedly worse survival rate of 5.5 months was observed for latency III patients with diseases, compared to 103 months in other DLBCL patients aged > 50 years. A recent Turkish study showed a prevalence of 5.3% for EBV^+ DLBCL and 3.5% for EBV^+ DLBCL-E (Uner et al. 2011). Little is known about the incidence and the clinicopathological characteristics of EBV^+ DLBCL in the UK. The prognostic implications of EBV in DLBCL has also not been widely studied in this population.

4.2 Aim of study

The aims of this study were to:

i) estimate the incidence of EBV^+ DLBCL including EBV^+ DLBCL-E in the UK.

i) determine the clinicopathological characteristics of EBV^+ DLBCL and EBV^+ DLBCL-E in these populations.

ii) determine the impact of EBV on the clinical outcome of DLBCL patients

iii) classify the EBV^+ tumours according to their pattern of EBV gene expression.

iv) determine the expression and prognostic significance of lipid signalling molecules (SPHK1, S1PR1, ABCC1 and ATX) in EBV^+ DLBCL compared to the EBV^- DLBCL.

4.3 Case selection

A list of DLBCL cases was obtained using an electronic search of histopathological reports from the Pathology Department of the Queen Elizabeth Hospital, Birmingham searching on 'High grade lymphomas' and 'DLBCL' over a 15 year period from 1996 to 2010. Reports from 550 patients were retrieved. Sufficient paraffin material was available in 300/550 cases. All 300 cases were subjected to EBER *in situ* hybridization to detect EBV according to the methods described in section 2.3. Known EBV^+ HL cases were included as positive controls. Cases were recorded as 'EBV-positive' if > 10% of tumour cells were positive. Cases in which non-malignant cells were EBER-positive were recorded as negative. Immunohistochemistry for LMP1 and EBNA2 were performed to classify cases into one of

three EBV latency types. EBV^+ DLBCL-E were selected using the following criteria; age > 50 years, no history of immunosuppression including immunodeficiency, transplantation, autoimmune disease or prior lymphoma. All cases were also stained for CD10, BCL6 and MUM1 for subtyping. Based on the Hans algorithm, cases were recorded as the GCB subtype if CD10 alone was positive or if both CD10 and BCL6 were positive. If both CD10 and BCL6 were negative, cases were categorised as the Non-GCB subtype. If BCL6 was positive and CD10 negative, MUM1 expression was used; if MUM1 was negative, the case was assigned to the GCB group and if MUM1 was positive, the case was categorised into the Non-GCB subtype. Immunohistochemistry was also performed for SPHK1, S1PR1, ABCC1 and ATX.

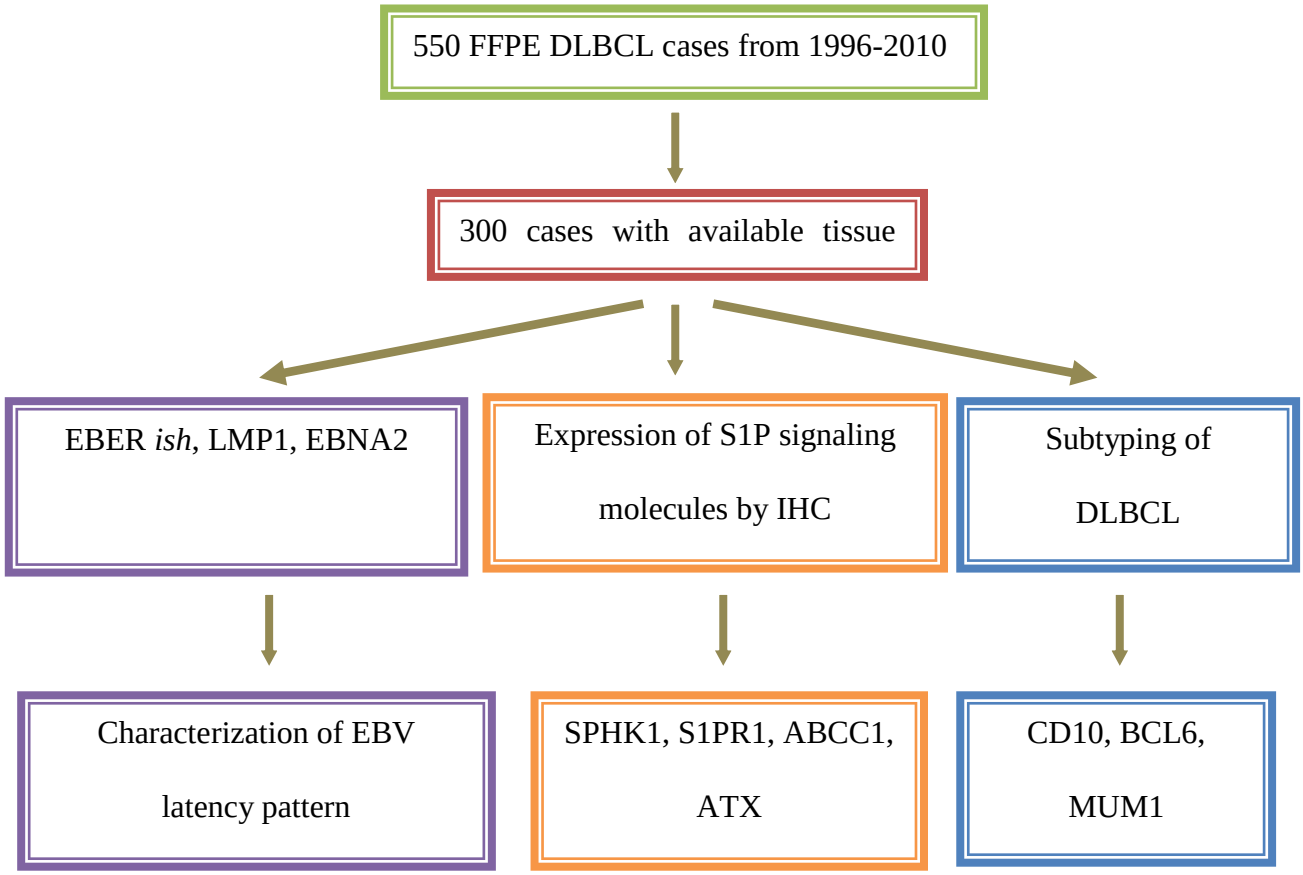

Figure 4.1: Flow chart for the characterization of DLBCL patients.

4.4 Analysis of clinical data

Clinical data for each patient was retrieved, noting the age, gender, site of specimen, disease subtype, number of extranodal sites involved, ECOG performance status, presence or absence of B symptoms, LDH level, Ann Arbor stage of disease, type of treatment, response to treatment, survival (dead or alive) and survival time. Based on the negative prognostic factors at the time of diagnosis ie age > 60 years, stage III/IV disease, elevated LDH level, ECOG performance status ≥2 and more than one extranodal involvement, patients were categorised into four outcome groups (low, low to intermediate , high to intermediate and high risk groups) in standard IPI and 3 outcome groups (very good, good and poor) in R-IPI. The median follow up time was 26 months (range 0-193 months). Overall survival time was measured from the date of initial diagnosis to the date of death or until date of last known follow up. Event free survival time was calculated from the date of diagnosis to the date of first relapse after treatment.

4.5 Statistical methods

Statistical analysis was performed on all patient data to ascertain which variables influenced the outcomes in terms of survival. Cox proportional analysis and logistic regression analysis were used to identify factors which influenced survival. Chi square ($\chi 2$) test was used to evaluate the association between categorical variables. *Univariate analysis*: Survival curves were calculated using the Kaplan-Meier method. Patients who were alive at last contact were censored in the overall survival analysis. Differences between the curves were analysed using the log-rank test. *Multivariate analysis:* A Cox stepwise proportional hazard model was used

to identify any factors that might be of independent significance in influencing survival. Variables included in the maximum models were age, gender, histological subtype (GCB or non-GCB), clinical stage of disease, type of therapy, presence or absence of B symptoms, LDH level, ECOG performance status, number of extranodal sites involved, standard and revised IPI scores. Statistical Package for the Social Sciences 21.0 (SPSS 21.0) was used for all statistical analysis.

4.6 Results

4.6.1 Clinical characteristics of 300 DLBCL patients

300 patients with DLBCL were analysed including 171 (57.0%) with nodal disease and 123 (41.0%) with extranodal disease (22 gastrointestinal, 15 ear/nose/throat/oral cavity, 16 central nervous system, 6 genital, 11 mediastinal, and 19 skin, 3 breast, 7 thyroid, 4 bladder, 2 ocular adnexa, etc). 6 patients (2.0%) had both nodal and extranodal involvement.

171 (57.0%) patients were male and 129 (43.0%) were female. The mean age of male patients was 63 years (median: 65 years; range: 25 – 96 years) and the mean age for female patients was 68 years (median: 71 years; range: 24 - 93 years).

254 patients (8 EBV^+ and 246 EBV^-) were aged ≥ 50 years. 67 (22.3%) patients presented with stage 1 disease, 97 (32.3%) with stage 2, 65 (21.7%) with stage 3, and 71 (23.7%) with stage 4. International Prognostic Index data were available for 298 patients; 33 (11.0%) presented with an index of 0, 94 (31.5%) with an index of 1, 92 (30.4%) with an index of 2, 63 (21.1%) with an index of 3,14 (4.7%) and 2 (0.7%) with an index of 5.

Most patients received chemotherapy with R-CHOP (54.9%) and those who received combination of chemotherapy and radiotherapy was 21.9% of total patients. Radiotherapy alone was given in 2.4% of cases and 16.0% of patients received palliative treatment. Complete remission was achieved in 66.7% of cases, 9.0% achieved partial remission, 15.7% had progressive disease and 4.7% had stable disease (Table 4.2). The mean follow-up time was 43 months (median: 27 months; range: 0 - 193 months). Of the 157 patients who died, the cause of death was known in 124 patients, of which 57 died of disease, 4 died of

complications of fungal infection and septicaemia and 63 died of unrelated causes including secondary malignancies and cardiovascular diseases. The median survival for the patients who died was 7 months. 141 (47.3%) patients were alive at last contact. The clinical characteristics of all DLBCL patients are summarised in Table 4.1.

Table 4.1: Clinical characteristics of DLBCL patients

Clinical characteristic	All patients
Sex	
Male	171 (57.0)
Female	129 (43.0)
Age group	
< 60 years	99 (33.0%)
≥ 60 years	201 (67.0%)
ECOG PS	
≤1	66 (75.0%)
>1	22 (25.0%)
B-symptoms	
Present	155 (51.7%)
Absent	145 (48.3%)
LDH level (n=297)	
Low (≤ 450 U/I)	153(51.5%)
High (> 450 U/I)	144(48.5%)
Ann Arbor stage	
1/II	164 (54.7%)
III/IV	136 (45.3%)
Subtype	
GCB	132 (44.0%)
Non GCB	168 (56.0%)
Site of involvement	
Nodal	171 (57.0%)
Extranodal	123 (41.0%)
Both	6 (2.0%)
Extranodal involvement	
≤ 1 site	270 (90.6%)
> 1 site	29 (9.4%)
Standard IPI (n=298)	
Low	127 (42.6%)
Low to intermediate	92 (30.9%)
Intermediate to high	63 (21.1%)
High	16 (5.4%)
Revised IPI (n=298)	
Very good	31 (10.3%)
Good	188 (62.7%)
Poor	81 (27.0%)

Table 4.2: Management, treatment response and clinical outcome of 300 DLBCL patients

Clinical characteristic	All patients
Management (n=288)	
Chemotherapy	158 (54.9%)
Radiotherapy	7 (2.4%)
Chemotherapy & radiotherapy	63 (21.9%)
Surgery	14 (4.9%)
Palliative	46 (16.0%)
Treatment response (n=288)	
Complete remission	200 (66.7%)
Partial remission	27 (9.0%)
Stable disease	14 (4.7%)
Progressive disease	47(15.7%)
Clinical outcome (n=124)	
Died of disease	57 (46.0%)
Died of complications	4 (3.2%)
Died of unrelated cause	63 (50.8%)

A

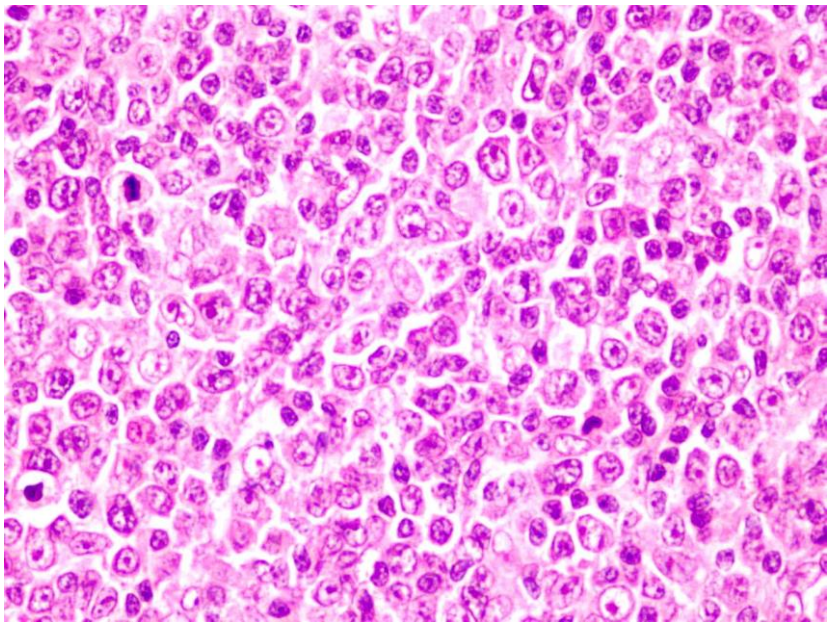

B

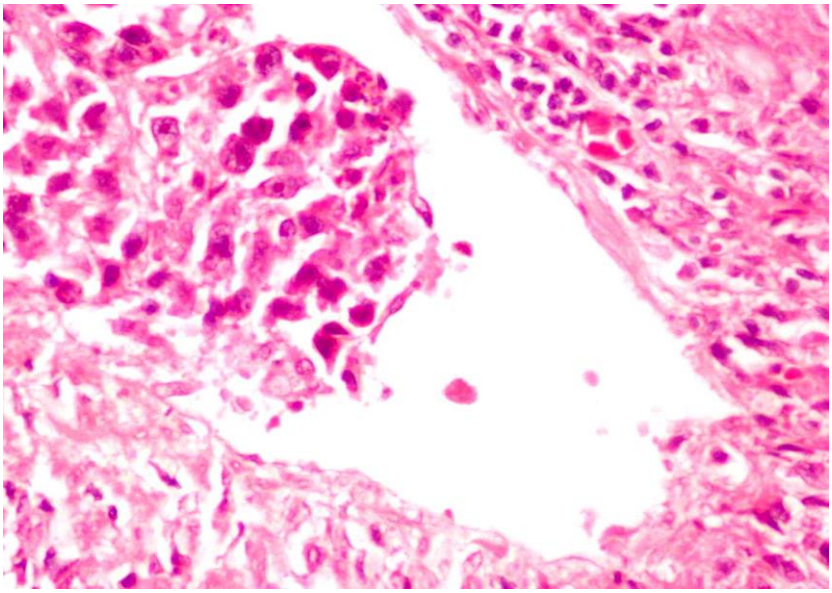

Figure 4.2: Histological findings of an EBV+ DLBCL. A) centroblastic morphology (x 400) B) angioinvasion (x 400).

A

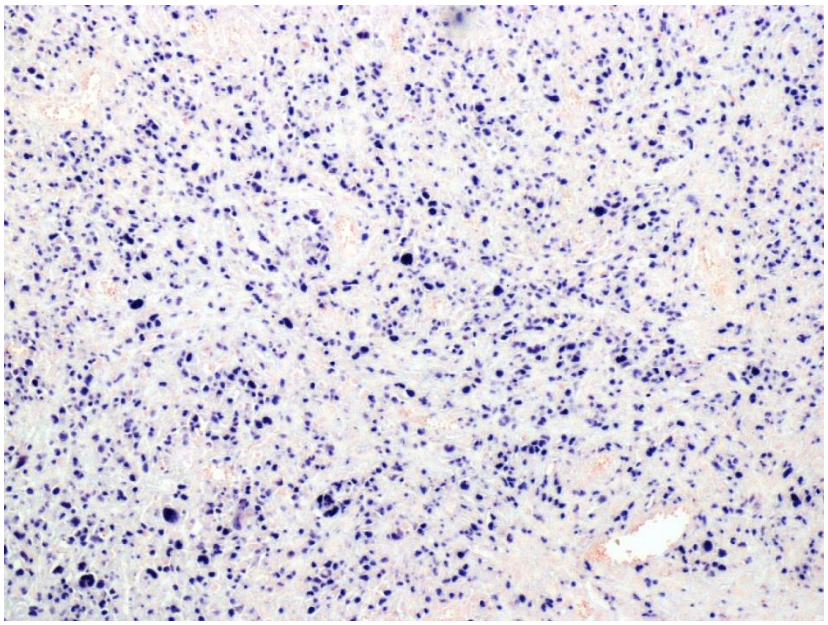

B

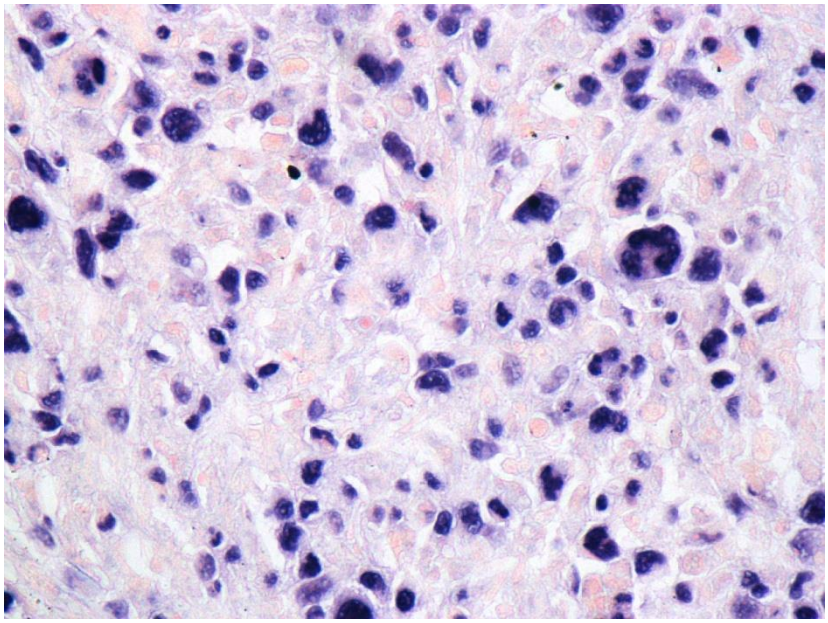

Figure 4.3: EBER positivity in EBV$^+$ DLBCL A) Nuclear positivity of EBER (x 200), B) Nuclear positivity of EBER (x400).

A

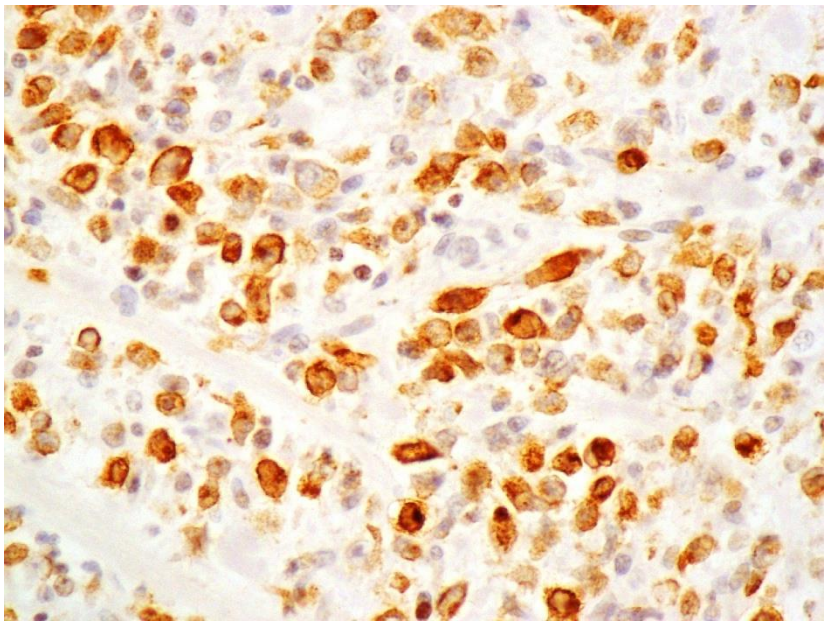

B

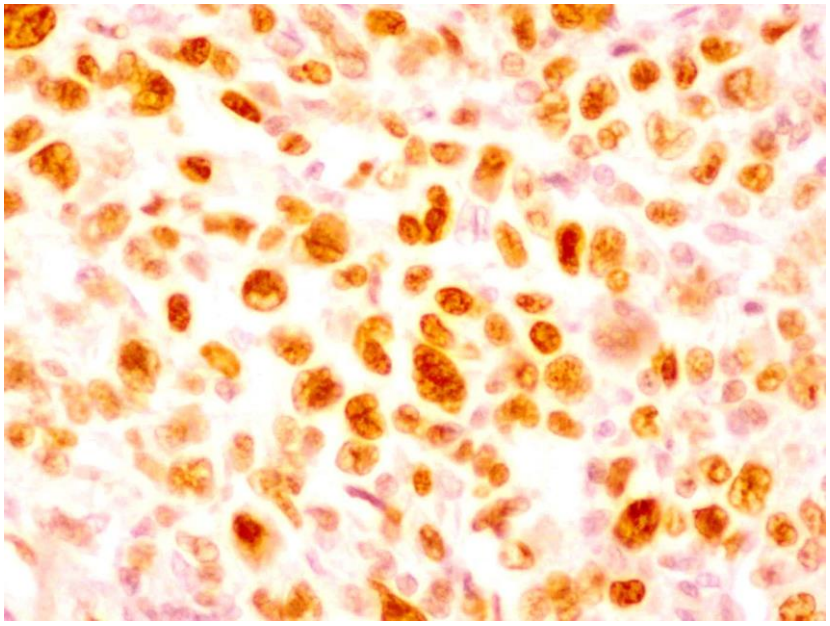

Figure 4.4 A) LMP1 positivity in EBV$^+$ DLBCL (x 400) B) EBNA2 positivity in EBV$^+$ DLBCL (x 400).

4.7 Clinical relevance of CD10, BCL6 and MUM1 expression in DLBCL

4.7.1 Expression of CD10, BCL6 and MUM1 in DLBCL

DLBCL can be stratified into GCB and non-GCB subtype based on the immunohistochemical profile of CD10, BCL6 and MUM1. Subgrouping of DLBCL patients into these two groups allows prediction of the clinical outcome of patients. In this section, I used immunohistochemistry to separate DLBCL into GCB and non-GCB subtypes based on their expression of CD10, BCL6 and MUM1. Figure 4.5 showed the proportion of patients whose tumours expressed CD10, BCL6 and MUM1.

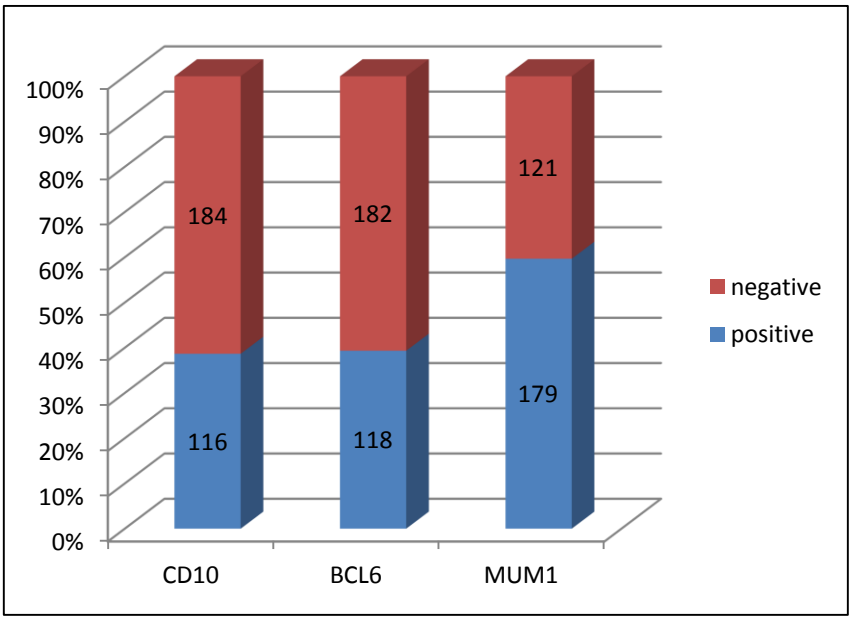

Figure 4.5: Expression of CD10, BCL6 and MUM1 in all DLBCL patients.

4.7.2 Co-expression of CD10, BCL6 and MUM1 in DLBCL

Co-expression of CD10 and BCL6 was observed in 52 (44.1%) cases. MUM1 expression showed a significant inverse association with the expression of CD10 and BCL6 ($p < 0.001$); 90% of tumours expressing MUM1 were negative for CD10 and 81% of tumours expressing CD10 were negative for MUM1 (Table 4.3). The expression of MUM1 and BCL6 also showed an inverse association; 52.9% of tumours expressing BCL6 were negative for MUM1 and 69.8% of tumours expressing MUM1 were negative for BCL6 (Table 4.3). Table 4.4 shows that all EBV^+ DLBCL patients were CD10 negative (p=0.002) and MUM1 positive (p=0.002). Patients whose tumours expressed BCL6 had longer overall survival (p=0.001) and event free survival (p=0.002)(Figure 4.6). Patients whose tumours expressed MUM1 had shorter event free survival rate (p=0.05)(Figure 4.7). CD10 expression showed no significant association with overall and event free survival.

Table 4.3: Co- expression of markers in DLBCL

Markers	Associated markers		χ2 value	p value
	BCL6+	**BCL6-**		
CD10+	52 (44.1%)	64 (35.2%)	2.393	0.122[#]
CD10-	66 (55.9%)	118 (64.8%)		
	MUM1+	**MUM1-**		
CD10+	18 (10.1%)	98 (81.0%)	153.85	**< 0.01**[#]
CD10-	161 (89.9%)	23 (19.0%)		
	MUM1+	**MUM1-**		
BCL6+	54 (30.2%)	64 (52.9%)	15.62	**< 0.01**[#]
BCL6-	125 (69.8%)	57 (47.1%)		

[#] chi square test

Table 4.4: Expression of CD10, BCL6 and MUM1 by EBV positivity

Markers	EBV+	EBV-	x2 value	p value
$CD10^{+}$	0 (0.0%)	116 (40.6%)	9.258	**0.002**[#]
$CD10^{-}$	14 (100.0%)	170 (59.4%)		
$BCL6^{+}$	6 (42.9%)	112 (39.2%)	0.076	0.782[#]
$BCL6^{-}$	8 (57.1%)	174 (60.8%)		
MUM1+	14 (100.0%)	165 (57.7%)	9.927	**0.002**[#]
MUM1-	0 (0.0%)	121 (42.3%)		

[#] chi square test

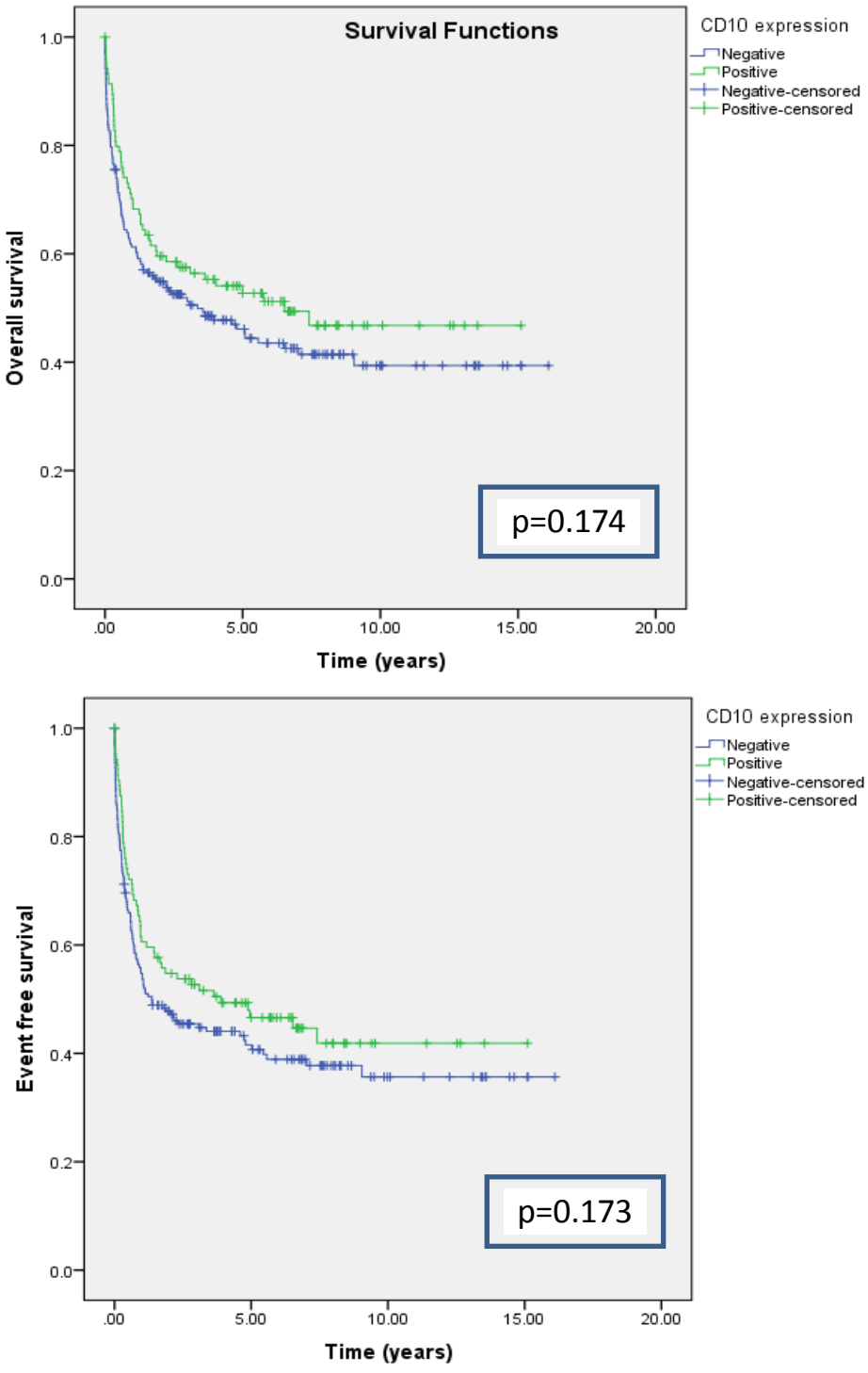

Figure 4.6: Kaplan Meier overall and event free survival curves for DLBCL patients expressing CD10.

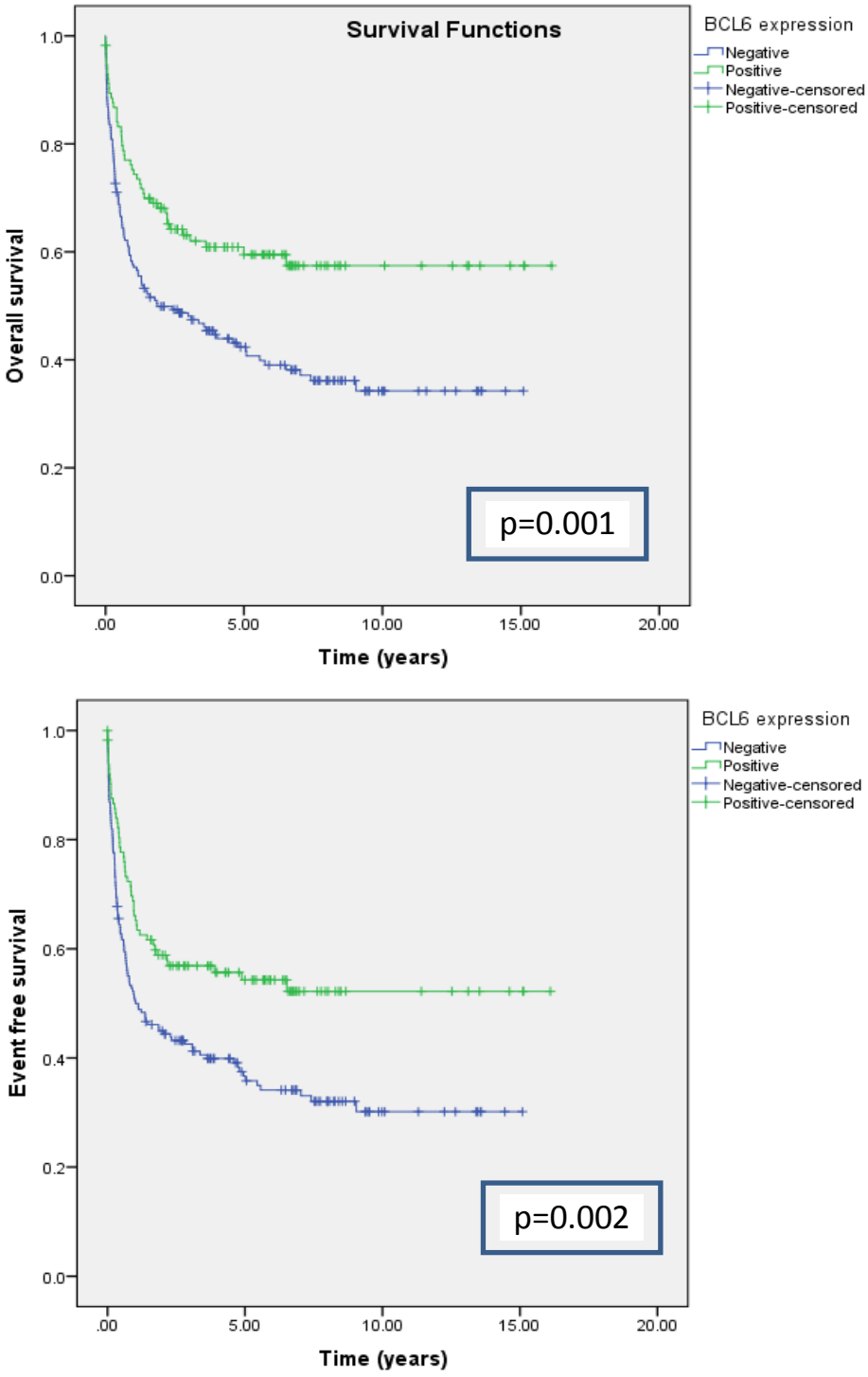

Figure 4.7: The Kaplan Meier overall and event free survival curves for DLBCL patients expressing BCL6.

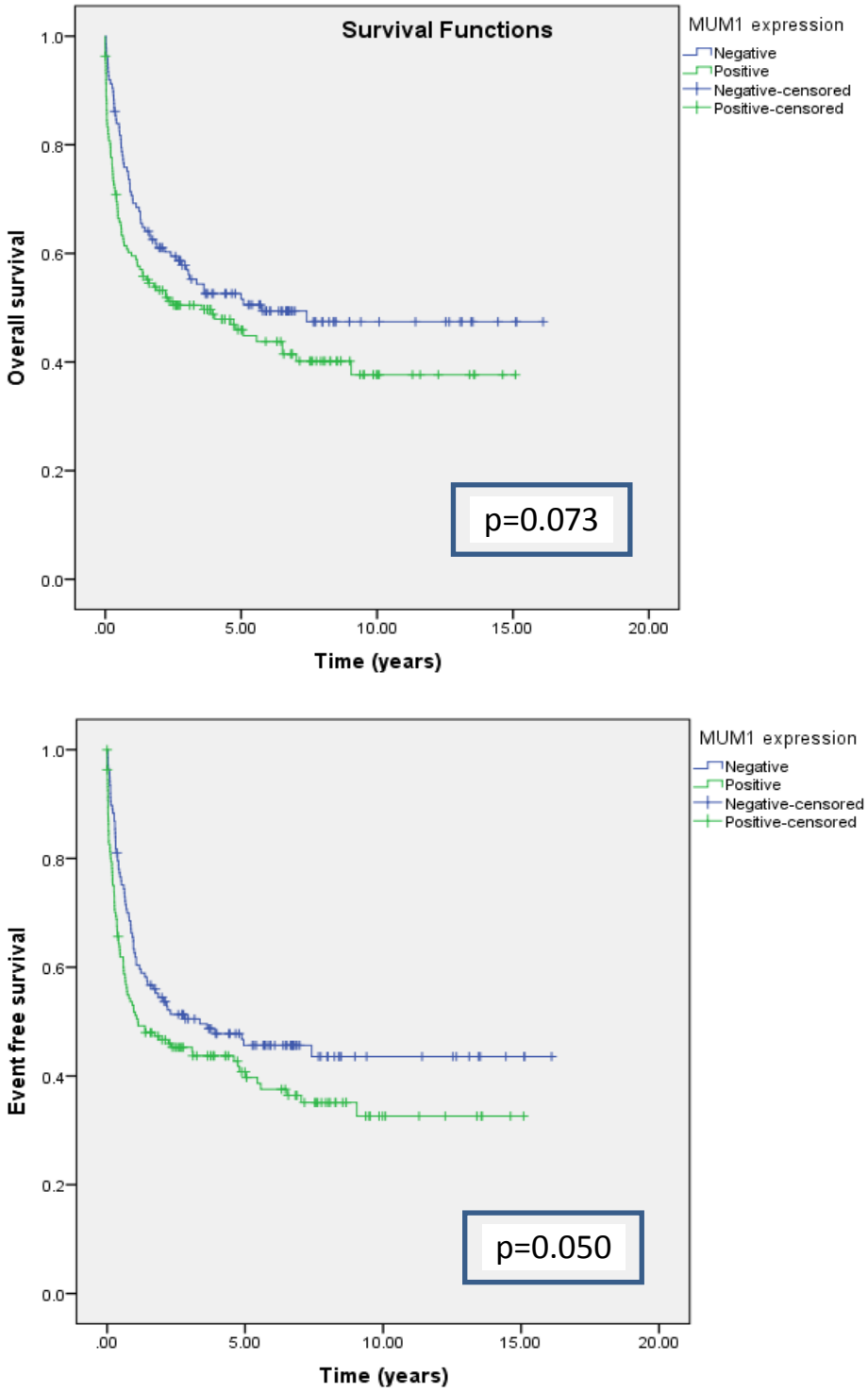

Figure 4.8: The Kaplan Meier overall and event free survival curves for DLBCL patients expressing MUM1.

4.7.3 Association of GCB and non-GCB subtypes with clinicopathological characteristics

Of the 300 tumours, 132 (44%) were categorized into GCB and 168 (56%) were non-GCB subtype. Table 4.5 illustrates the clinical characteristics of DLBCL patients separated into GCB and non-GCB subtypes. None of the clinical variables showed significant association with any of the subtypes. The median survival time for patients with the GCB subtype was 6.5 years and 3.4 years for the non-GCB subtype. Log rank test showed that there was no significant difference in the overall survival of patients with GCB and non-GCB subtypes (p =0.092), however the non GCB subtype showed a shorter event free survival (p-0.056)(Figure 4.12).

Table 4.5: Clinical characteristics of DLBCL patients by GCB and Non GCB subtypes.

Clinical characteristic	All patients (n=300)	GCB	Non-GCB	χ2 value	p value
Sex					
Male	171 (57.0)	75 (56.8%)	96 (57.1%)	0.003	0.955#
Female	129 (43.0)	57 (43.2%)	72 (42.9%)		
Age group					
< 60 years	99 (33.0%)	46 (34.8%)	53 (31.5%)	0.364	0.546#
≥ 60 years	201 (67.0%)	86 (65.2%)	115 (68.5%)		
ECOG PS (n=299)					
<2	66 (75.0%)	120 (91.6%)	156 (92.9%)	0.163	0.686#
≥2	22 (25.0%)	11 (8.4%)	12 (7.1%)		
B-symptoms					
Present	155 (51.7%)	63 (47.7%)	92 (54.8%)	1.465	0.226#
Absent	145 (48.3%)	69 (52.3%)	76 (45.2%)		
LDH level (n=297)					
Low (≤ 450 U/I)	153 (51.5%)	66 (50.8%)	87 (51.8%)	0.03	0.862#
High (> 450 U/I)	145 (48.5%)	64 (49.2%)	81 (48.2%)		
Ann Arbor stage					
1/II	164 (54.7%)	72 (54.5%)	92 (54.8%)	0.001	0.970#
III/IV	136 (45.3%)	60 (45.5%)	76 (45.2%)		
Site of involvement					
Nodal	171 (57.0%)	76 (57.6%)	95 (56.5%)	1.413	0.493#
Extranodal	123 (41.0%)	52 (39.4%)	71 (42.3%)		
Both	6 (2.0%)	4 (3.0%)	2 (1.2%)		
Extranodal involvement (n=299)					
≤ 1 site	270 (90.3%)	114 (87.0%)	155 (92.3%)	2.238	0.135#
> 1 site	29 (9.7%)	17 (13.0%)	13 (7.7%)		
Standard IPI (n=298)					
Low risk	127 (42.6%)	74 (44.0%)	53 (40.8%)	0.954	0.812#
Low to intermediate	92 (30.9%)	49 (29.2%)	43 (33.1%)		
Intermediate to high	63 (21.1%)	37 (22.0%)	26 (20.0%)		
High risk	16 (5.4%)	8 (4.8%)	8 (6.2%)		
Revised IPI (n=298)					
Very good	33 (11.1%)	15 (11.5%)	18 (10.7%)	0.056	0.972#
Good	186 (62.4%)	81(62.3%)	105(62.5%)		
Poor	79 (26.5%)	34 (26.2%)	45(26.8%)		
Outcome (n=298)					
Dead	157 (52.7%)	64 (49.2%)	93 (55.4%)	2.238	0.294#
Alive	141 (47.3%)	66 (50.8%)	75 (44.6%)		

chi square test, * Fisher's exact test

4.8 Characterization of EBV$^+$ DLBCL patients

14/300 (4.7%) of DLBCL patients were recorded as EBV positive. The mean age for the EBV$^+$ DLBCL patients was 57 years (median 63 years, range: 27-82 years) as compared to 65 years (median 66, range: 24-96 years) in EBV$^-$ DLBCL patients. Four EBV$^+$ patients (29%) were aged less than 50 years. The clinical characteristics of both groups of DLBCL are shown in Table 4.6. I found that a significantly higher proportion of EBV$^+$ DLBCL patients had B symptoms than did the EBV$^-$ patients (p=0.009). Furthermore,I found that all of the EBV$^+$ patients were of non-GCB subtype which was compared to 53.8% of EBV$^-$ patients (p=0.001)(Table 4.6).

2 (22.2%) of EBV$^+$ patients had an ECOG performance status of >1. LDH levels were elevated in 7 (50.0%) patients and eight (57.1%) patients had advanced stage of disease. IPI scores of > 2 were seen in 4 (29.5%) cases. Four (28.6%) patients showed extranodal presentation and nine (64.3%) patients presented with nodal disease, one (7.1%) had both nodal and extranodal disease (Table 4.6). The sites for extranodal involvement were skin, colon, brain and posterior pharyngeal wall.

Table 4.6: Clinical characteristics of DLBCL patients by EBV status

Clinical characteristic	All patients (n=300)	EBV+ DLBCL (n=14)	EBV- DLBCL (n=286)	p value
Sex				
Male	171 (57.0)	6 (42.8%)	164 (57.3%)	0.588#
Female	129 (43.0)	8 (57.1%)	122 (42.7%)	
Age				
Mean	64.7	57	65	-
Median	66	63	66	
Range	24-96	27-82	24-96	
Age group				
< 60 years	99 (33.0%)	6 (42.9%)	93 (32.5%)	0.402*
≥ 60 years	201 (67.0%)	8 (57.1%)	193 (67.5%)	
ECOG PS				
<2	66 (22.0%)	7 (77.8%)	59 (74.7%)	1.000*
≥2	22 (7.3%)	2 (22.2%)	20 (25.3%)	
B-symptoms				
Present	155 (51.7%)	12 (85.7%)	143 (50.0%)	**0.009#**
Absent	145 (48.3%)	2 (14.3%)	143 (50.0%)	
LDH level (n=297)				
Low (≤ 450 U/I)	153	7 (50.0%)	146 (51.6%)	0.907#
High (> 450 U/I)	144	7 (50.0%)	137 (48.4%)	
Ann Arbor stage				
1/II	164 (54.7%)	6 (42.9%)	158 (55.2%)	0.363#
III/IV	136 (45.3%)	8 (57.1%)	128 (44.8%)	
Subtype				
GCB	132 (44.0%)	0 (0.0%)	132 (46.2%)	**0.001***
Non GCB	168 (56.0%)	14 (100.0%)	154 (53.8%)	
Site of involvement				
Nodal	171 (57.0%)	9 (64.3%)	162 (56.6%)	0.268#
Extranodal	123 (41.0%)	4 (28.6%)	119 (41.6%)	
Both	6 (2.0%)	1 (7.1%)	5 (1.7%)	
Extranodal involvement (n=299)				
≤ 1 site	270 (90.6%)	12 (85.7%)	258 (90.5%)	0.553*
> 1 site	29 (9.4%)	2 (14.3%)	27 (9.5%)	
Standard IPI (n=298)				
Low	127 (42.6%)	5 (35.7%)	122 (42.3%)	1.000*
Low to intermediate	92 (30.9%)	5 (35.7%)	87 (30.8%)	
Intermediate to high	63 (21.1%)	3 (21.4%)	60 (21.3%)	
High	16 (5.4%)	1 (7.1%)	15 (5.3%)	
Revised IPI (n=298)				
Very good	31 (10.3%)	1 (7.1%)	30 (10.5%)	1.000*
Good	188 (62.7%)	9 (64.3%)	179 (62.6%)	
Poor	81 (27.0%)	4 (28.6%)	77 (26.9%)	

chi square test, * Fisher's exact test

4.8.1 Histological and phenotypic features of EBV+ DLBCL

In nine nodal EBV^+ DLBCL cases, the normal lymph node architecture was completely effaced by diffuse or polymorphic proliferation of malignant large pleomorphic lymphoid cells. The extranodal cases also showed diffuse permeation by malignant cells. Extensive necrosis was observed in 10/14 (71.4%) cases. The malignant cells were surrounded by reactive cells namely lymphocytes, plasma cells and histiocytes. The malignant cells exhibit strong CD20, CD79α and CD30 expression. CD15 was negative. HRS-like cells with distinct nucleoli were present in six (42.8%) cases. Three (21.4%) cases showed angioinvasion. Ten cases (71.4%) showed morphology of conventional DLBCL of either the centroblastic or the immunoblastic subtype. Three cases (21.4%) were classified as plasmablastic DLBCL, comprising a uniform population of large transformed cells. In one case (7.1%), the large B cells were widely scattered, resembling T-cell/histiocyte-rich B-cell lymphoma. The immunophenotypic characteristics of 14 EBV^+ DLBCL cases are shown in Table 5.7-5.8. All the EBV^+ DLBCL cases were reviewed by Dr Stefan Dojcinov, a consultant pathologist from the University Hospital of Wales, Cardiff, UK.

4.8.2 EBV latency pattern of EBV+ DLBCL

Eight (57.1%) patients showed EBV latency III pattern (EBER+,LMP1+, EBNA2+), 2 (14.3%) latency II (EBER+,LMP1+, EBNA2-) and 4 (28.6%) latency 1 (EBER+,LMP1-, EBNA2-) (Table 4.7).

Table 4.7: EBV latency pattern, protein expression and clinical outcome of EBV$^+$ DLBCL

No	Age	Sex	Site	Immuno-suppression	Latency	Eber	Lmp1	Ebna2	CD10	BCL6	MUM1	SPHK1	S1PR1	S1PR2	ABCC1	ATX	Treatment	Follow up (mo)	Outcome
1	**72**	**F**	**N**	**No**	**3**	+	+	+	-	-	+	+	+	-	+	**NA**	**NA**	**0**	**Dead**
2	77	F	N	Yes	3	+	+	+	-	-	+	+	+	+	-	+	NA	5	Dead
3	78	F	N	Yes	1	+	-	-	-	+	+	+	+	+	+	+	NA	NA	NA
4	32	M	N	Yes	3	+	+	+	-	+	+	-	-	+	+	NA	CHOP	5	Dead
5	**75**	**F**	**N**	**No**	**2**	**+**	**+**	**-**	-	+	+	**-**	**+**	**-**	**-**	**+**	NA	**2**	**Dead**
6	**82**	**F**	**N**	**No**	**3**	**+**	**+**	**+**	-	+	+	**-**	**-**	**+**	**-**	**+**	NA	**NA**	**NA**
7	49	F	N	No	2	+	+	-	-	+	+	-	-	+	-	-	NA	NA	NA
8	64	F	E	Yes	3	+	+	+	-	-	+	-	+	-	-	+	NA	1	Dead
9	36	M	N	Yes	1	+	-	-	-	-	+	-	+	-	-	+	RCHOP	9	Dead
10	27	M	N	Yes	1	+	-	-	-	-	+	+	+	+	-	NA	RCHOP	5	Dead
11	65	M	E	Yes	3	+	+	+	-	-	+	-	-	+	+	-	NA	NA	NA
12	29	M	N	Yes	3	+	+	+	-	-	+	-	-	-	-	+	NA	NA	NA
13	**54**	**M**	**E**	**No**	**1**	**+**	**-**	**-**	-	-	+	**+**	**-**	**+**	**-**	**-**	NA	**NA**	**NA**
14	61	F	E	Yes	3	+	+	+	-	+	+	-	+	-	+	+	surgery	16	Alive

**NA : not available, bold cases are the EBV+ DLBCL-E patients*

4.8.3 Immunosuppression

Of the 14 EBV$^+$ DLBCL cases, nine (64.3%) had a prior history of immunosuppression or of a haematological malignancy (Table 4.8). 3 patients were HIV positive, one had a bone marrow transplant for aplastic anaemia, one had a liver transplant, one had history of MALT lymphoma, two had a history of CLL and one had a history of low grade NHL. Nine patients were aged >50 years however, only four patients in this group had no prior evidence of immunosuppression or haematological malignancy and therefore met the criteria for a diagnosis of EBV$^+$ DLBCL of the elderly (EBV$^+$ DLBCL-E) which is described in further detail in section 4.8.8.

Table 4.8: Immune status of EBV$^+$ DLBCL cases

EBV$^+$ DLBCL patients (n=14)	**Non Immunosuppressed**	**Immunosuppressed/ History of haematological malignancy**
Age > 50 yrs	4 (28.6%)	5 (35.7%)
Age ≤ 50 yrs	1 (7.1%)	4 (28.6%)

4.8.4 Management and treatment response of EBV+ DLBCL

Seven (50.0%) of EBV^+ DLBCL patients were given chemotherapy, three (21.4%) had both chemotherapy and radiotherapy, one (7.1%) had surgery and three (21.4%) received palliative treatment. 71.2% of EBV^- DLBCL patients had complete remission compared to 35.7% in EBV^+ DLBCL (p=0.006)(Table 4.9).

Table 4.9: Management, treatment response and clinical outcome of DLBCL patients by EBV positivity

	All patients	**EBV+ DLBCL**	**EBV- DLBCL**	**χ2 value**	**p value**
Management (n=288)					
Chemotherapy	158 (54.9%)	7 (50.0%)	151 (55.1%)	0.854	0.931[#]
Radiotherapy	7 (2.4%)	0 (0.0%)	7 (2.6%)		
Chemotherapy & radiotherapy	63 (21.9%)	3 (21.4%)	60 (21.9%)		
Surgery	14 (4.9%)	1 (7.1%)	13 (4.7%)		
Palliative	46 (16.0%)	3 (21.4%)	43 (15.7%)		
Treatment response (n=288)					
Complete remission	200 (66.7%)	5 (35.7%)	195 (71.2%)	12.302	**0.006[#]**
Partial remission	27 (9.0%)	4 (28.6%)	23 (8.4%)		
Stable disease	14 (4.7%)	0 (0.0%)	14 (5.1%)		
Progressive disease	47(15.7%)	5 (35.7%)	42 (15.3%)		
Clinical outcome (n=124)					
Died of disease	57 (46.0%)	3 (25.0%)	54 (48.2%)	3.23	0.199[#]
Died of complications	4 (3.2%)	0 (0.0%)	4 (3.6%)		
Died of unrelated cause	63 (50.8%)	9 (75.0%)	54 (48.2%)		

[#] chi square test

4.8.5 Correlation between clinical characteristics and overall survival

In unadjusted univariate analysis, the presence of B symptoms correlated significantly with overall and event free survival (Figure 4.11). All patients who had B symptoms had significantly poorer OS and EFS than those without B symptoms ($p<0.001$). EBV^+ patients had significantly shorter EFS than their EBV^- counterparts ($p=0.033$)(Figure 4.9). However, EBV latency type did not correlate with OS ($p=0.886$) and EFS ($p=0.544$)(Figure 4.10). Other clinical variables such as gender and ethnicity did not show any significant correlation with OS and EFS (Figure 4.15-4.16). Patients with bulky tumours have significantly poorer OS ($p=0.004$) and shorter EFS ($p<0.001$)(Figure 4.14). All patients with higher IPI showed poorer OS and EFS ($p<0.001$)(Figure 4.17). Patients with poor R-IPI index showed shorter EFS)$p<0.001$)(Figure 4.18). Patients treated with R-CHOP had significantly longer OS ($p=0.006$) and EFS ($p=0.003$) than those treated with CHOP alone (Figure 4.13).

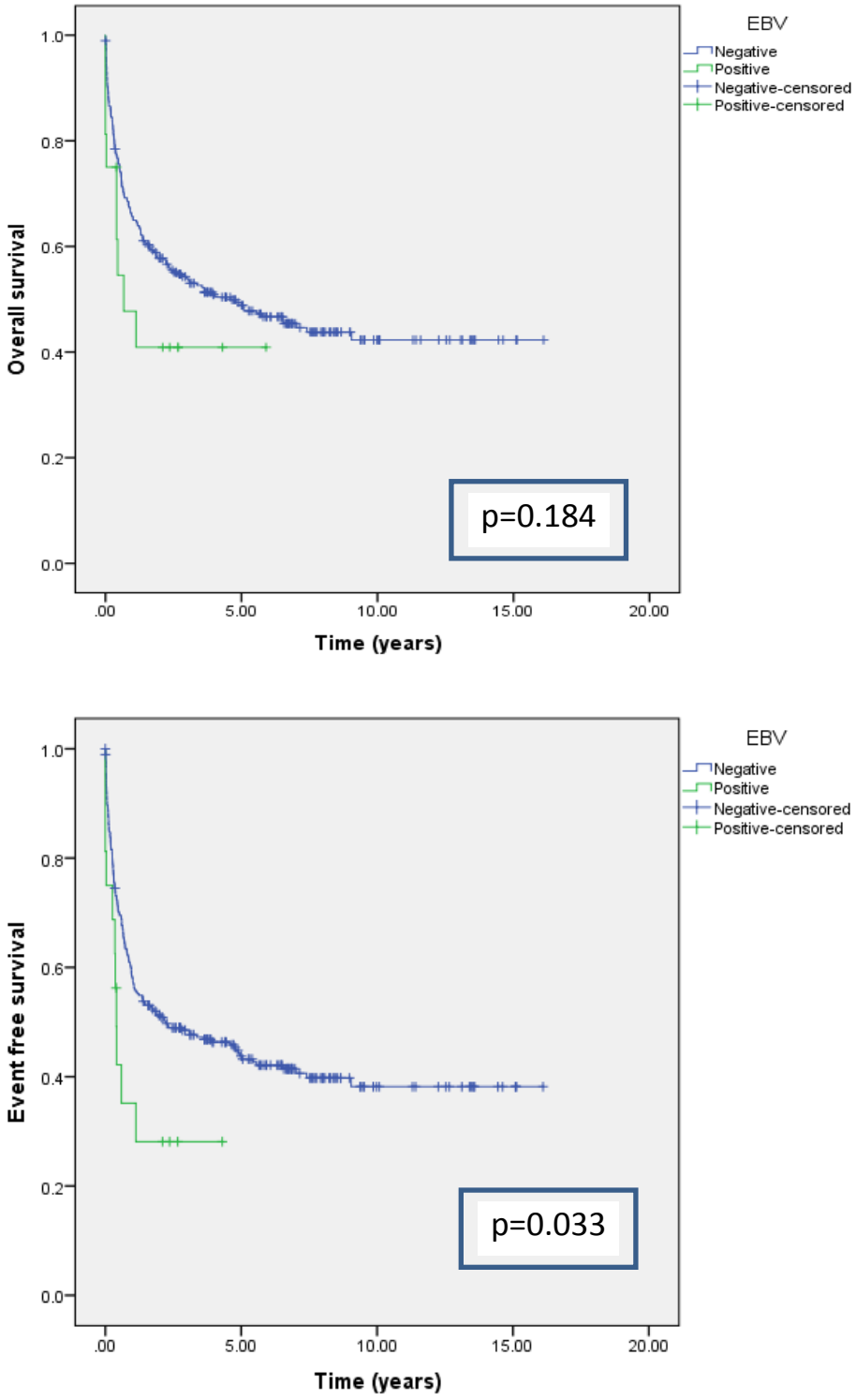

Figure 4.9: The Kaplan Meier overall and event free survival curves by EBV positivity of DLBCL patients.

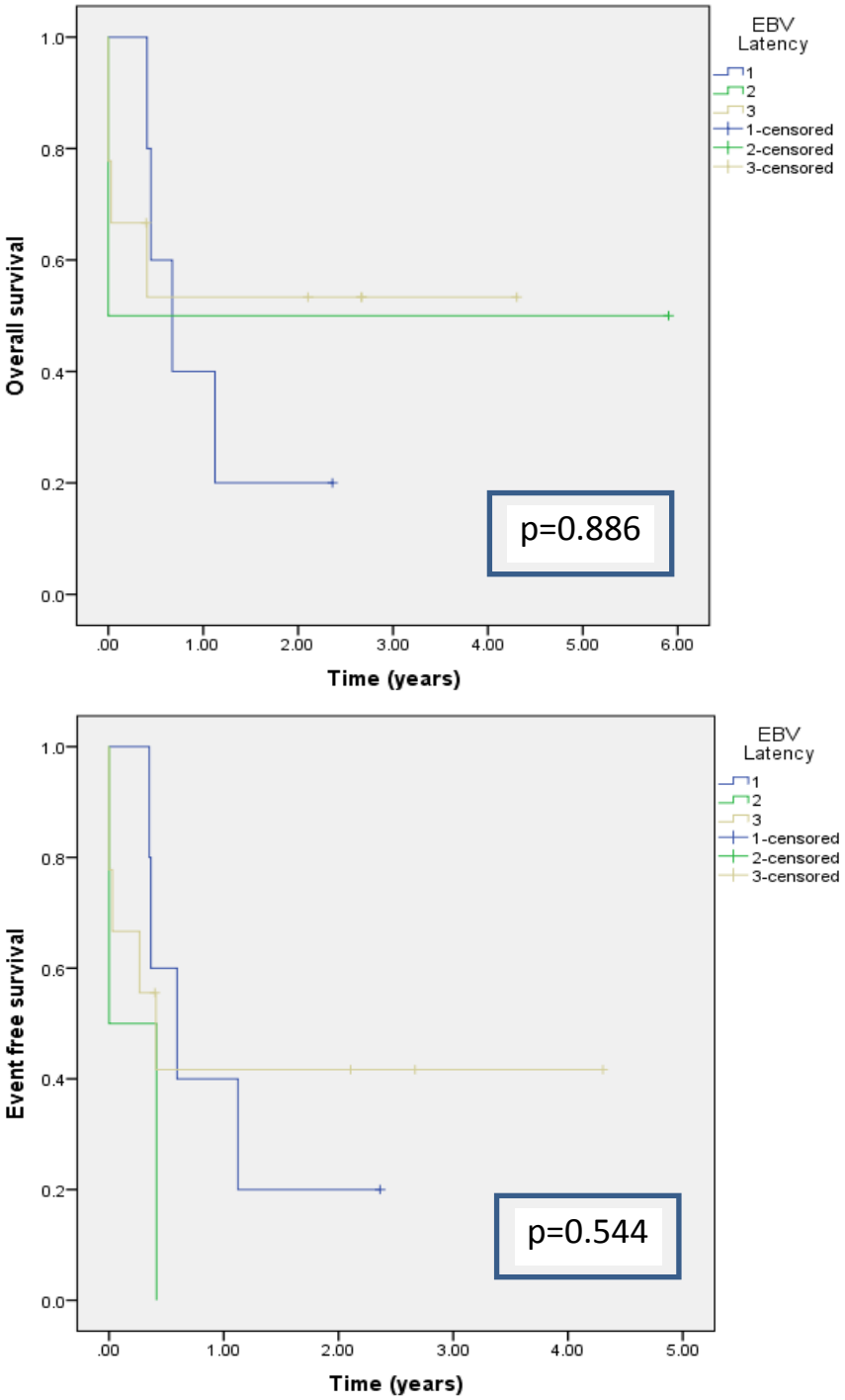

Figure 4.10: The Kaplan Meier overall and event free survival curves by EBV latency type of DLBCL patients.

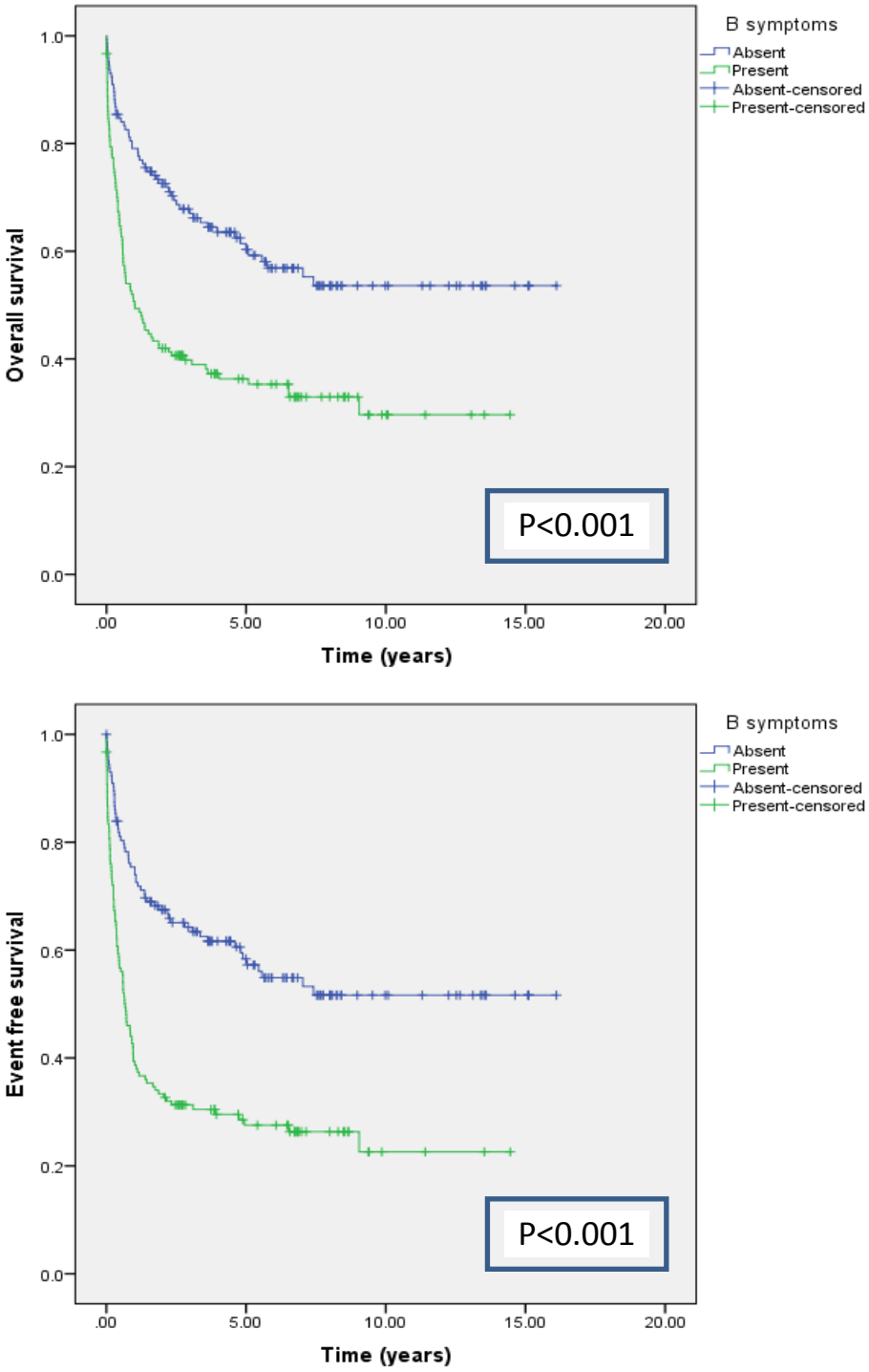

Figure 4.11: The Kaplan Meier overall and event free survival curves by the presence of B symptoms of DLBCL patients.

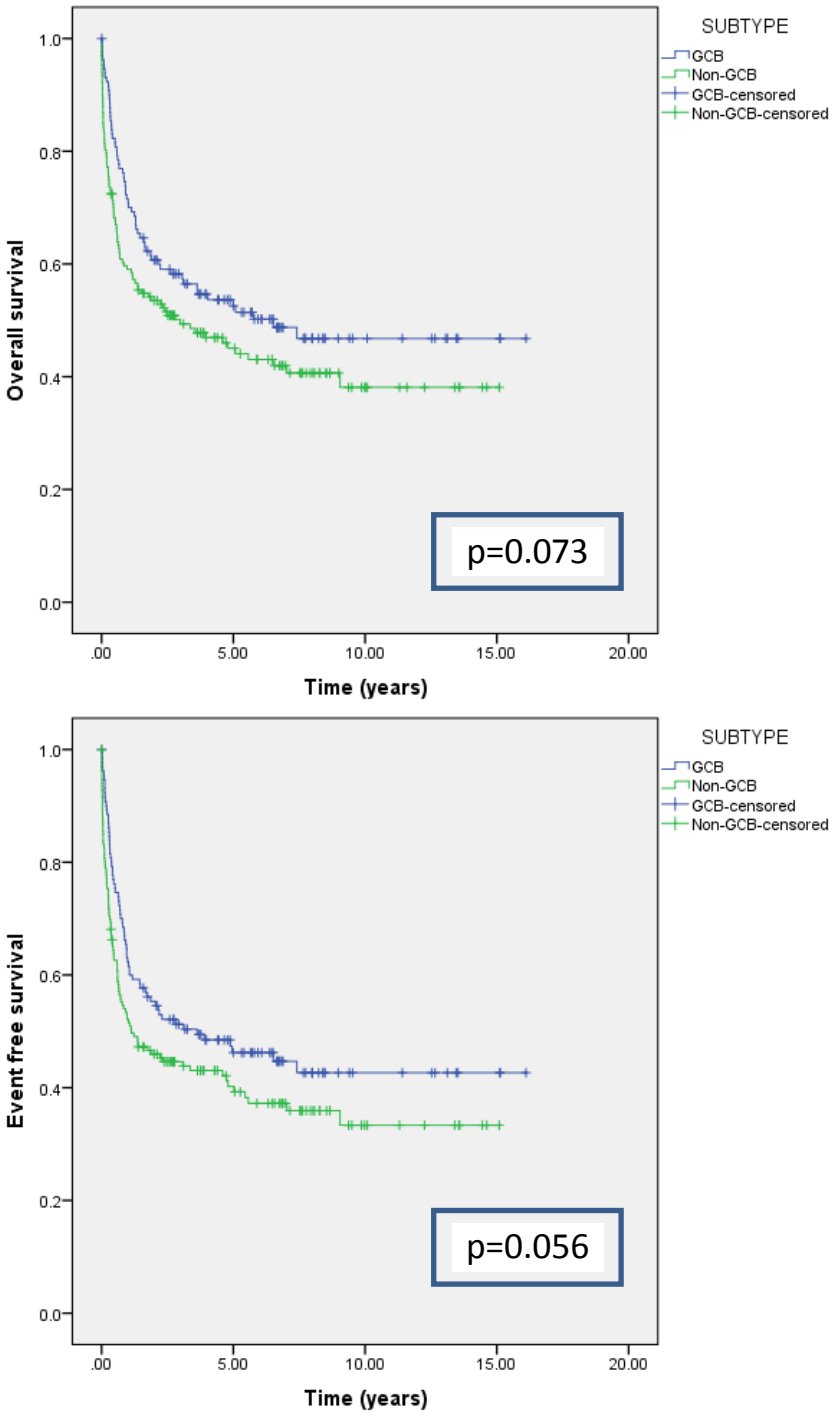

Figure 4.12: The Kaplan Meier overall and event free survival curves by disease subtype of DLBCL patients.

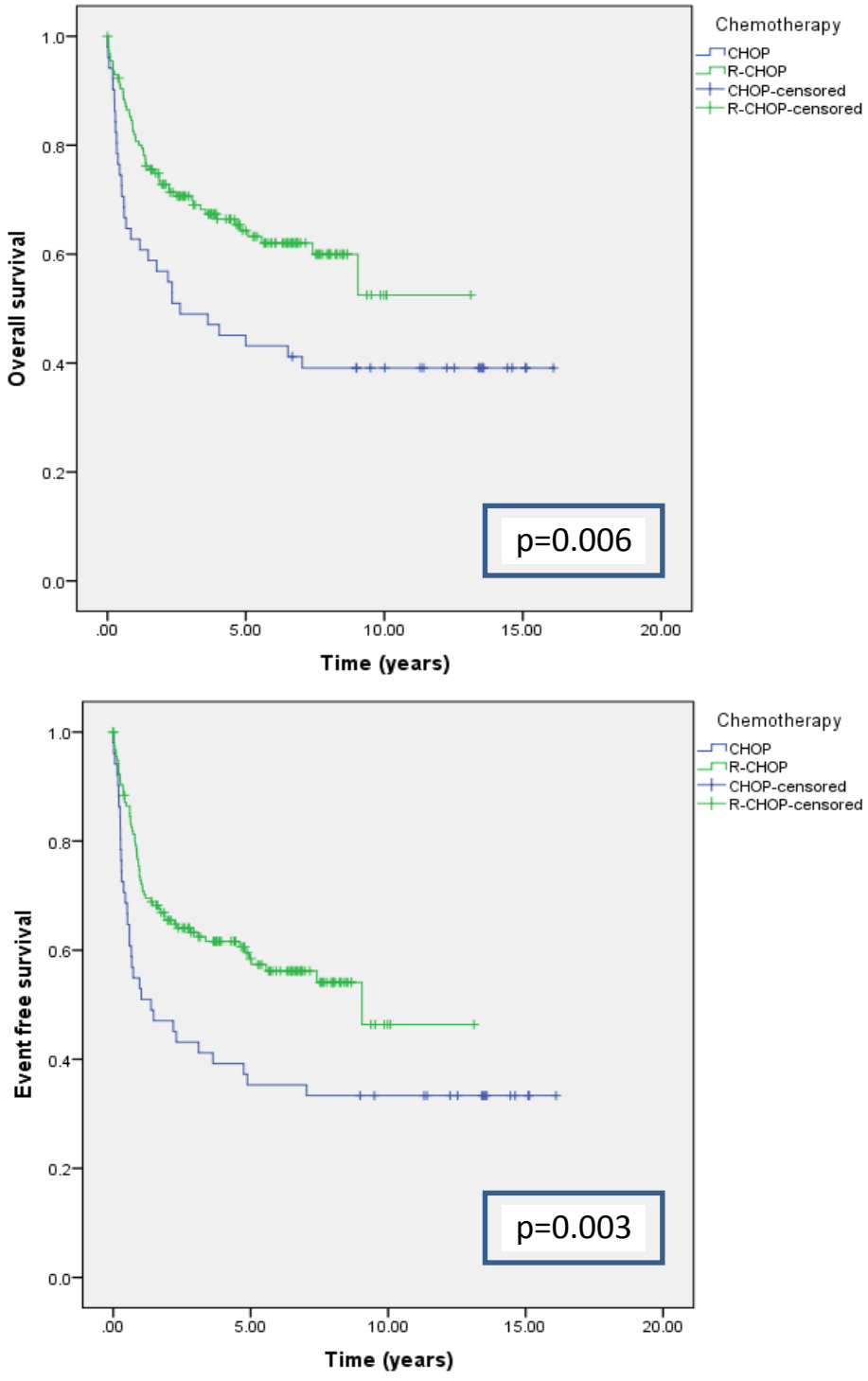

Figure 4.13: The Kaplan Meier overall and event free survival curves by chemotherapy regime of DLBCL patients

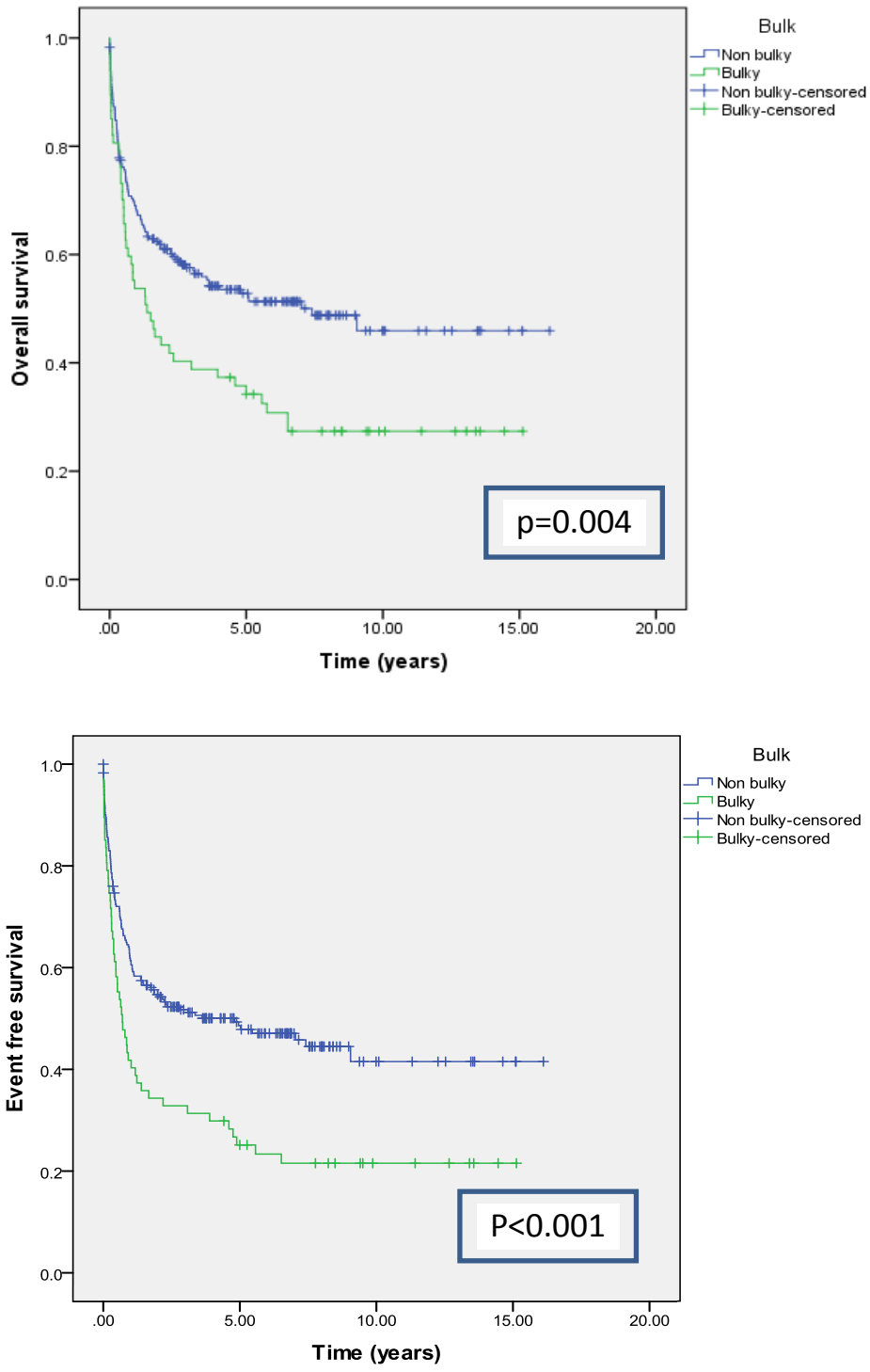

Figure 4.14: The Kaplan Meier overall and event free survival curves by bulkiness of disease of DLBCL patients

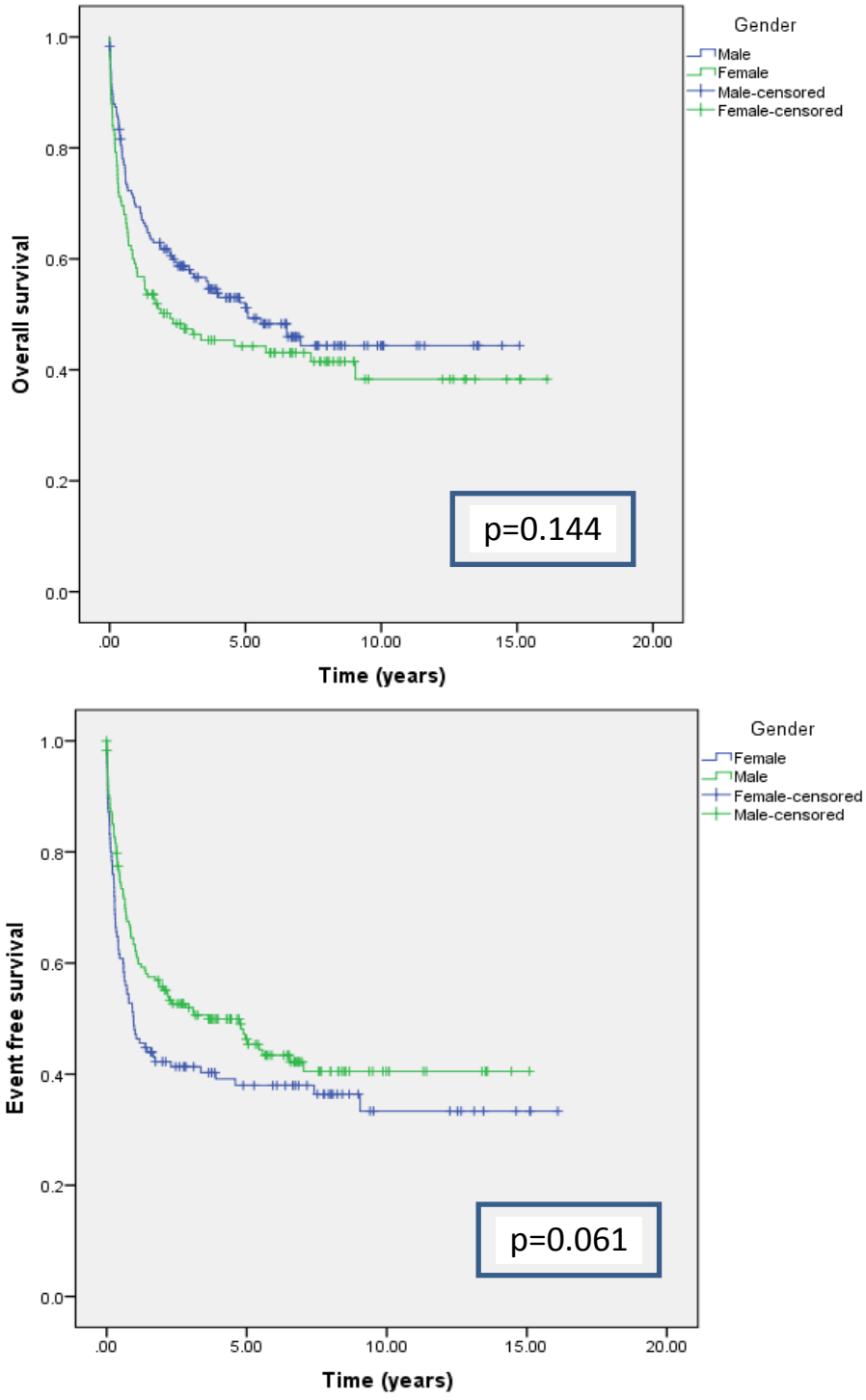

Figure 4.15: The Kaplan Meier overall and event free survival curves by gender of DLBCL patients

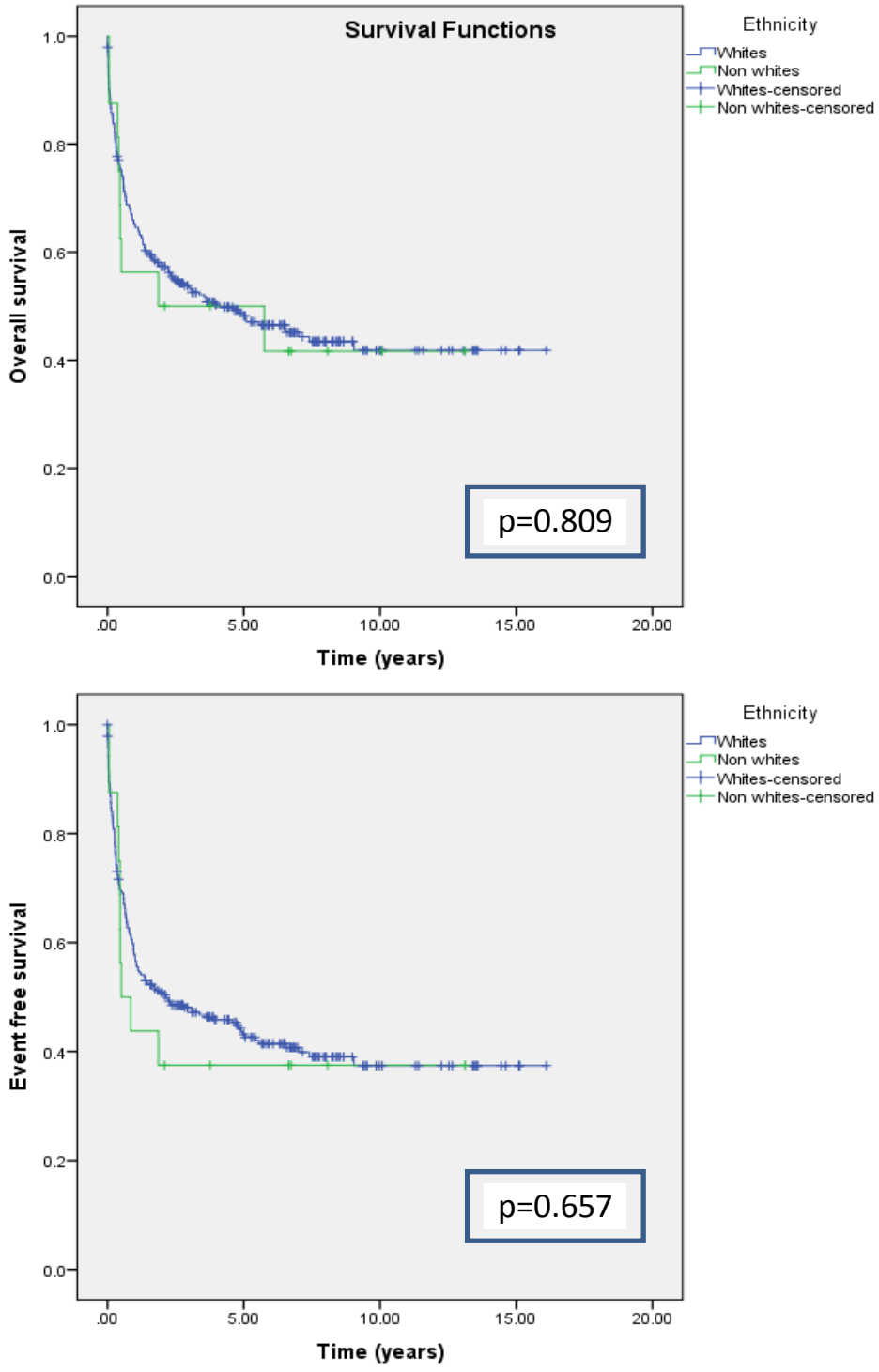

Figure 4.16: The Kaplan Meier overall and event free survival curves by ethnicity of DLBCL patients

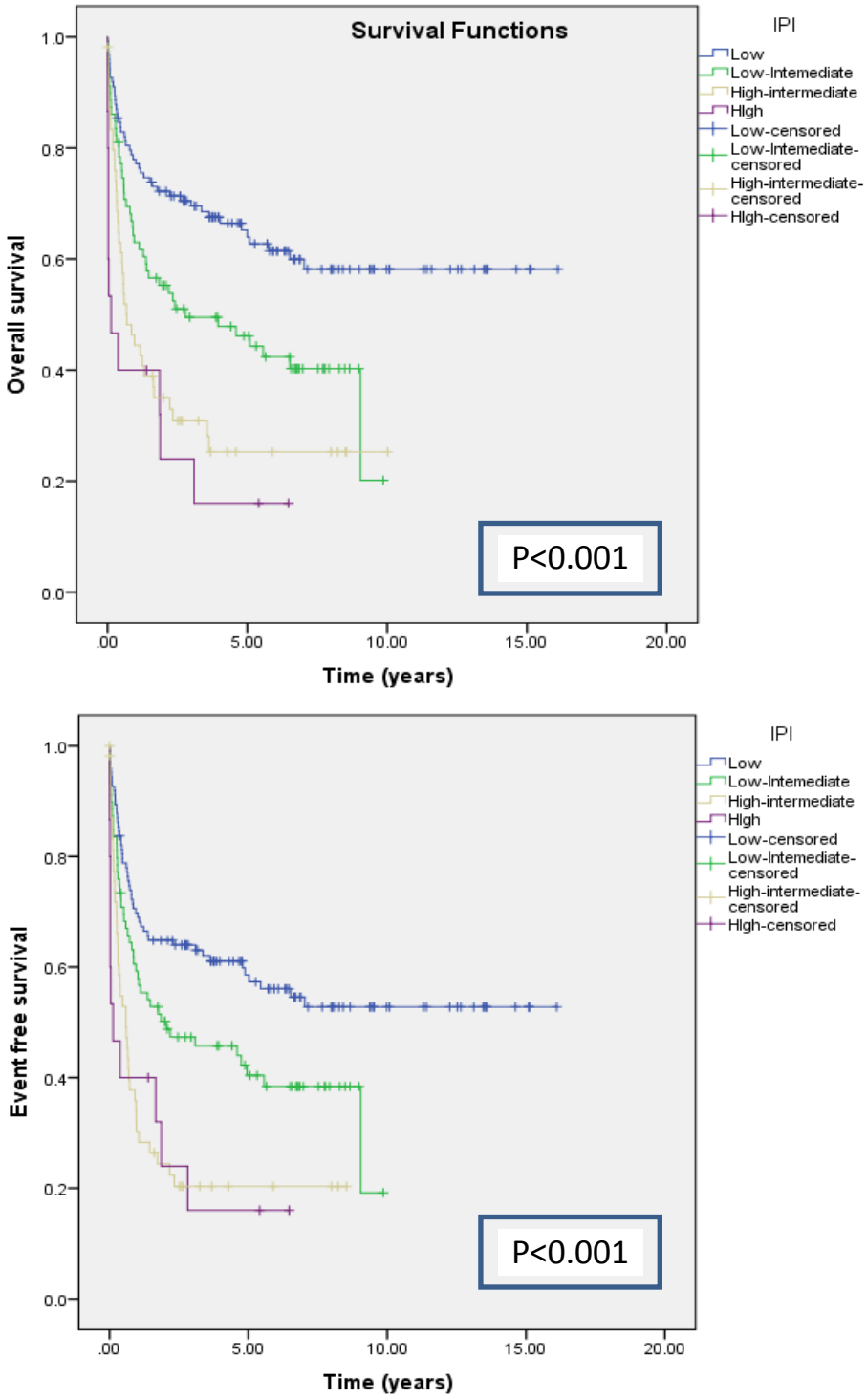

Figure 4.17: The Kaplan Meier overall and event free survival curves by IPI risk group of DLBCL patients

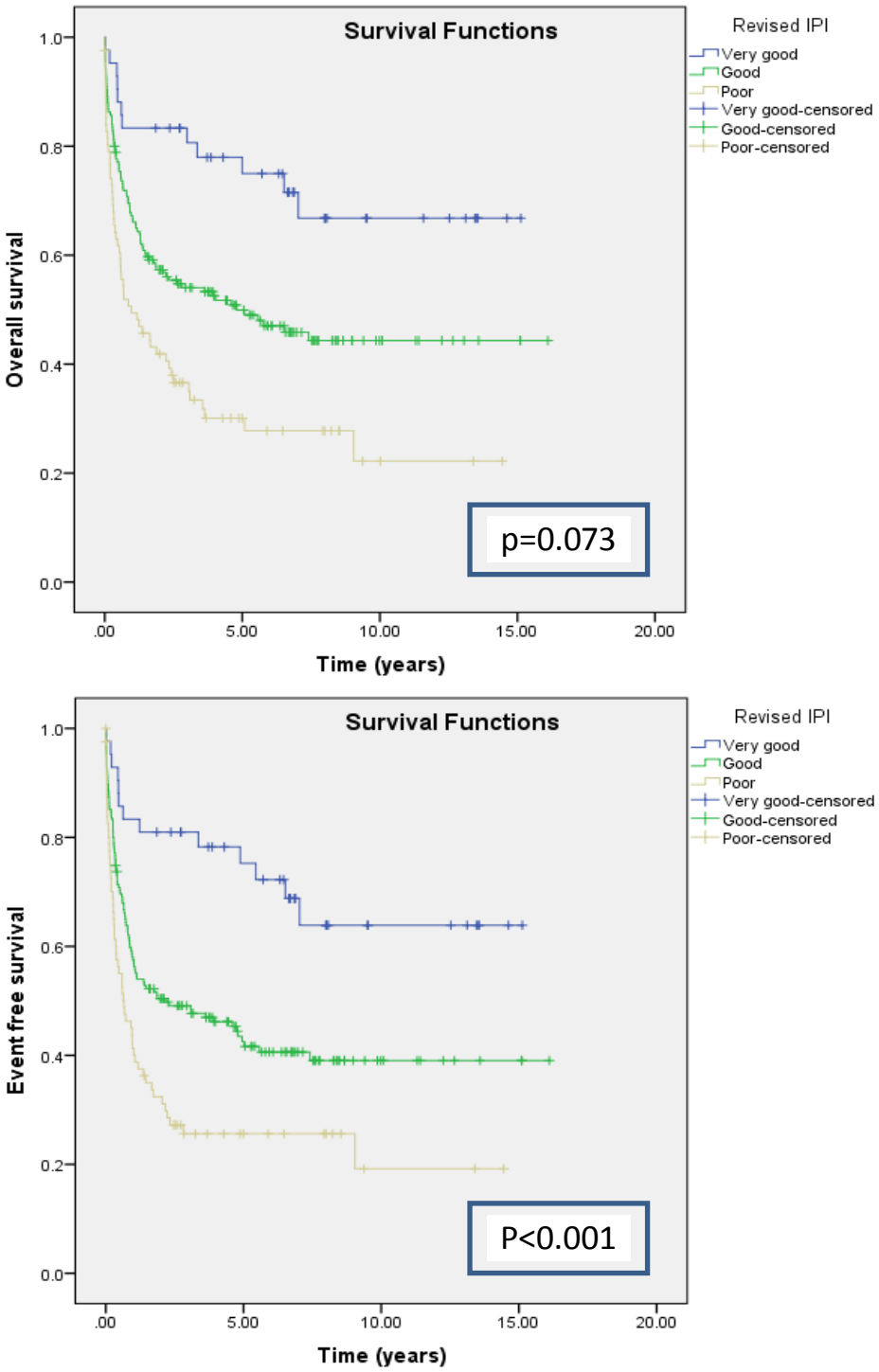

Figure 4.18: The Kaplan Meier overall and event free survival curves by revised IPI risk group of DLBCL patients

4.8.6 Prognostic factors for survival of DLBCL patients by simple Cox proportional hazards model

To determine if each variable is a prognostic factor for survival of DLBCL patients, I used the univariate simple Cox proportional hazards model. Crude hazard ratio indicates the increase or decrease in the risk of death incurred by each variable. Table 4.11 shows that age, ECOG PS, presence of B symptoms, LDH levels, involvement of ≥ 1 extranodal site, IPI, R-IPI and BCL6 positivity are prognostic factors for survival. A hazard ratio of > 1 shows a higher risk of death and a hazard ratio of <1 shows a lower risk of death.

4.8.7 Prognostic factors for survival of DLBCL patients by multiple Cox proportional hazards model

To exclude the confounders which may affect the significance of the analysis, I used the multiple Cox proportional hazards model. This analysis revealed that EBV positivity, presence of B symptoms, bulky disease, BCL6 and intermediate to high IPI were significantly associated with shorter time to death. The adjusted hazard ratio, 95% CI and p value are shown in Table 4.12.

Table 4.10: Prognostic factors of all DLBCL patients by Simple Cox proportional hazards model

Potential prognostic factors	Regression Coefficient	Crude HR (95% CI)	Wald Statistic	p value
Gender	0.233	1.263 (0.923, 1.728)	2.121	0.145
Age	0.025	1.027 (1.013,1.037)	16.533	< **0.001**
EBV positivity	0.453	1.573 (0.801, 3.089)	1.728	0.189
ECOG PS	0.797	2.218 (1.802, 2.731)	56.522	< **0.001**
B symptoms	0.777	2.174 (1.569, 3.011)	21.818	< **0.001**
LDH level	0.354	1.424 (1.027, 1.927)	4.490	**0.034**
Ann Arbor stage	0.314	1.370 (1.185, 1.582)	18.231	< **0.001**
Subtype	0.290	1.336 (0.972, 1.837)	3.181	0.074
Site of involvement	0.178	1.195 (0.894, 1.597)	1.441	0.230
No. of extranodal involvement	0.95	2.586 (1.667, 4.01)	17.999	< **0.001**
Low risk IPI			35.036	< **0.001**
Low to intermediate IPI	0.591	1.806 (1.196, 2.728)	7.893	**0.005**
Intermediate to high IPI	1.093	2.983 (1.937, 4.594)	24.476	< **0.001**
High risk IPI	1.512	4.535 (2.393, 8.595)	21.027	< **0.001**
Very good R-IPI			24.328	< **0.001**
Good R-IPI	0.839	2.279 (1.265, 4.234)	4.197	**0.006**
Poor R-IPI	1.385	3.924 (2.138, 7.465)	18.848	< **0.001**
CHOP chemotherapy	0.541	1.718 (1.035, 2.854)	4.375	0.036
CD10	-0.167	0.846 (0.61, 1.173)	1.004	0.316
BCL6	-0.659	0.517 (0.364, 0.736)	13.454	< **0.001**
MUM1	0.283	1.328 (0.958, 1.841)	2.893	0.089
SPHK1	0.133	1.142 (0.832, 1.566)	0.677	0.411
S1PR1	0.161	1.174 (0.818 , 1.686)	0.756	0.385
ABCC1	-0.119	0.888 (0.645, 1.222)	0.533	0.465

Table 4.11: Prognostic factors for survival of all DLBCL patients by multiple Cox proportional hazards model

Potential prognostic factors	Regression Coefficient	Adjusted HR (95% CI)	Wald Statistic	p value
EBV positivity	0.743	2.102 (1.056, 4.185)	4.472	**0.034**
B symptoms	0.422	1.525 (1.043, 2.230)	4.749	**0.029**
Bulky disease	0.526	1.693 (1.174, 2.441)	7.933	**0.005**
BCL6	-0.540	0.583 (0.402, 0.844)	8.154	**0.004**
Low risk IPI			18.876	**<0.001**
Low to intermediate IPI	0.479	1.615 (1.047,2.491)	4.694	0.335
Intermediate to high IPI	0.809	2.247 (1.391,3.629)	10.948	**<0.001**
High risk IPI	1.312	3.712 (1.905, 7.232)	14.851	**<0.001**

4.8.8 EBV$^+$ DLBCL of the elderly

4 out of 300 (1.3%) DLBCL patients fulfilled the 2008 WHO criteria of EBV$^+$ DLBCL-E ie they were more than 50 years old and had no prior evidence of immunosuppression. Table 4.7 showed the clinical characteristics of the EBV$^+$ DLBCL-E cases in bold. The age range was 54-82 with a median age of 74 years. Two patients were male and two were female. One case was excluded because the patient was < 50 years. Two patients had EBV latency 3 (EBER$^+$, LMP1$^+$, EBNA2$^+$), one patient had latency type 1 (EBER$^+$,LMP1$^-$, EBNA2$^-$) and the other had latency type 2 (EBER$^+$,LMP1$^+$, EBNA2$^-$). Three patients had nodal presentation and one had extranodal involvement presenting as a midline butterfly lesion in the brain. One patient received chemotherapy with R-CHOP, one had R-CHOP with radiotherapy while the other two patients were given palliative treatment. One patient with progressive disease relapsed while the other three did not relapse. Two patients with progressive disease died and the median survival of this group was less than 1 month.

4.9 Expression of lipid signaling molecules in DLBCL

SPHK1, S1PR1, ABCC1 and ATX were expressed in 51%, 73%, 43% and 21% of DLBCL patients, respectively (Figure 4.19). SPHK1, S1PR1, ABCC1 and ATX were expressed in the cytoplasm of malignant lymphoid cells.

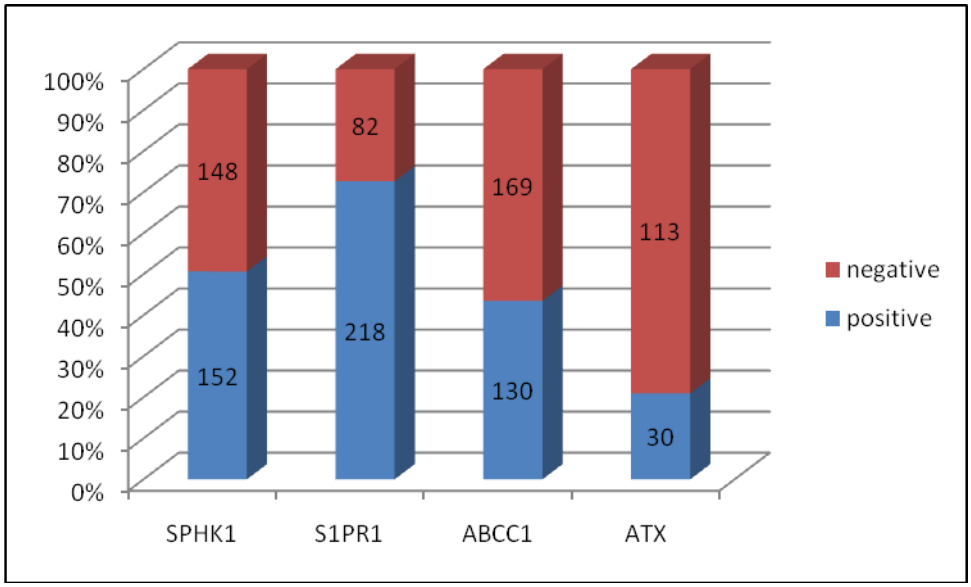

Figure 4.19: Expression of SPHK1, S1PR1, ABCC1 and ATX in DLBCL patients.

A

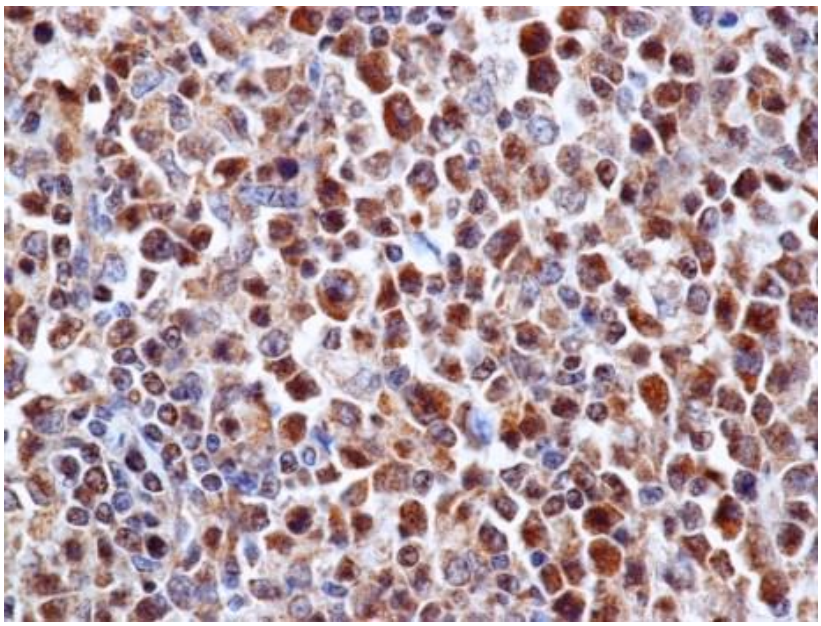

B

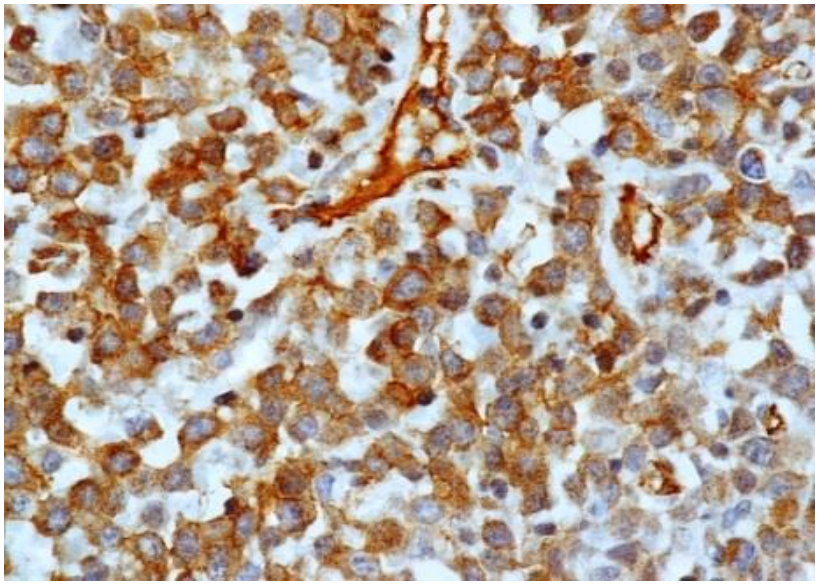

Figure 4.20: Expression of SPHK1 and S1PR1 in DLBCL. SPHK1 (A) and S1PR1 (B) were localised to the cytoplasm of malignant cells (x400).

A

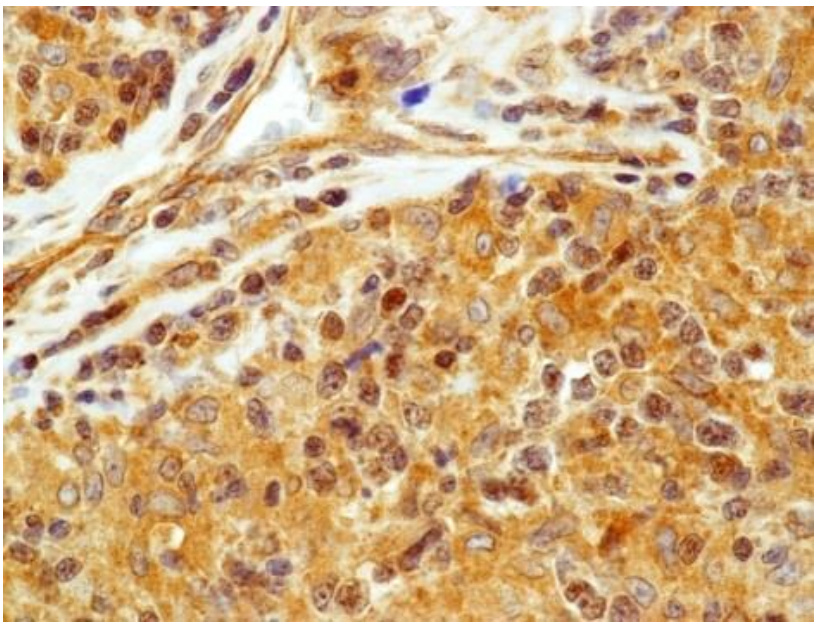

B

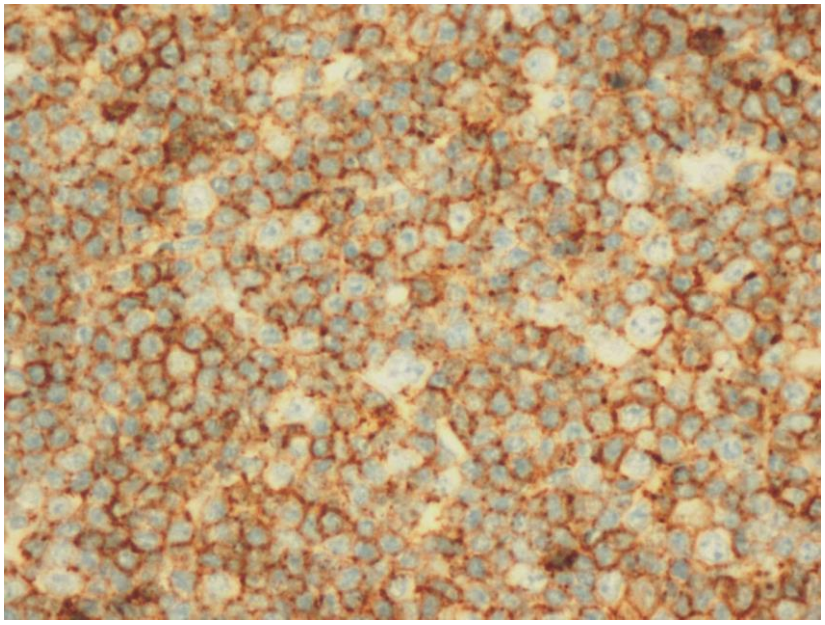

Figure 4.21: Expression of ABCC1 and ATX in DLBCL. ABCC1 (A) and ATX (B) were localised to the cytoplasm of malignant cells (x400).

4.9.1 Co-expression of lipid signaling molecules in DLBCL

None of the lipid signaling molecules showed significant co-expression (Table 4.12).

Table 4.12 Co-expression of lipid signaling molecules in DLBCL

S1P signalling molecule	Associated lipid molecule		χ^2 value	p value
	S1PR1+	S1PR1-		
SPHK1+	107 (49.1%)	45 (54.9%)	0.801	0.371#
SPHK1-	111 (50.9%)	37 (45.1%)		
	ABCC1+	ABCC1-		
SPHK1+	63 (48.5%)	88 (42.1%)	0.383	0.536#
SPHK1-	67 (51.5%)	81 (47.9%)		
	ATX+	ATX-		
SPHK1+	15 (50.0%)	56 (49.6%)	0.002	0.966#
SPHK1-	15 (50.0%)	57 (50.4%)		
	ABCC1+	ABCC1-		
S1PR1+	88 (67.7%)	129 (76.3%)	2.755	0.097#
S1PR-	42 (32.3%)	40 (23.7%)		
	ATX+	ATX-		
S1PR1+	21 (70.0%)	89 (78.8%)	1.025	0.311#
S1PR-	9 (30.0%)	24 (29.2%)		
	ATX+	ATX-		
ABCC1+	15 (50.0%)	39 (34.8%)	2.313	0.128#
ABCC1-	15 (50.0%)	73 (65.2%)		

chi square test, * Fisher's exact test

4.9.2 Relationship between lipid signaling molecules and clinical characteristics

Statistical analysis showed that SPHK1 expression was associated with lower ECOG performance status (p=0.042)(Table 4.13). There was no significant association between SPHK1 protein expression and any other clinical characteristics. Fewer patients with S1PR1 expression had B symptoms (p=0.048) and more patients expressing S1PR1 protein had >1 site of extranodal involvement (p=0.023). Significantly more S1PR1 positive patients were dead at last contact (p=0.049)(Table 4.14). ABBC1 expression was significantly less frequent in patients > 60 years (p=0.008) (Table 4.15). The expression of ATX was not significantly associated with any clinical characteristics (Table 4.16).

The expression of SPHK1, S1PR1, ABCC1 and ATX were not significantly associated with EBV positivity (Table 4.17).

Table 4.13: SPHK1 expression and clinicopathological parameters

Clinical characteristic	All patients (n=300)	SPHK1+ (n=152)	SPHK1- (n=148)	χ2 value	p value
Sex					
Male	171 (57.0)	83 (54.6%)	88 (59.5%)	0.721	0.396#
Female	129 (43.0)	69 (45.4%)	60 (40.5%)		
Age group					
< 60 years	99 (33.0%)	46 (30.3%)	47 (31.8%)	0.078	0.780#
≥ 60 years	201 (67.0%)	106 (69.7%)	101 (68.2%)		
ECOG PS (n=88)					
≤1	66 (75.0%)	145 (95.4%)	131 (89.1%)	4.149	**0.042#**
>1	22 (25.0%)	7 (4.6%)	16 (10.9%)		
B-symptoms					
Present	155 (51.7%)	73 (48.0%)	82 (55.4%)	1.635	0.201#
Absent	145 (48.3%)	79 (52.0%)	66 (44.6%)		
LDH level (n=297)					
Low (≤ 450 U/I)	153 (51.5%)	82 (53.9%)	72 (51.4%)	0.843	0.359#
High (> 450 U/I)	144 (48.5%)	70 (46.1%)	76 (48.6%)		
Ann Arbor stage					
1/II	164 (54.7%)	87 (57.2%)	77 (52.0%)	0.821	0.365#
III/IV	136 (45.3%)	65 (42.8%)	71 (48.0%)		
Subtype					
GCB	132 (44.0%)	60 (39.5%)	72 (48.6%)	2.562	0.109#
Non GCB	168 (56.0%)	92 (60.5%)	76 (51.4%)		
Site of involvement					
Nodal	171 (57.0%)	86 (56.6%)	85 (57.4%)	0.026	0.987*
Extranodal	123 (41.0%)	63 (41.4%)	60 (40.5%)		
Both	6 (2.0%)	3 (2.0%)	3 (2.0%)		
Extranodal involvement (n=299)					
≤ 1 site	270 (90.3%)	195 (89.9%)	75 (91.5%)	0.174	0.676#
> 1 site	29 (9.7%)	22 (10.5%)	7 (8.5%)		
Standard IPI					
Low/Low-intermediate	219 (73.0%)	100 (65.8%)	83 (57.2%)	2.293	0.130#
High-intermediate/ High	81 (27.0%)	52 (34.2%)	62 (42.8%)		
Revised IPI					
Very good/ Good	219 (73.0%)	126 (84.6%)	111 (84.1%)	0.012	0.913#
Poor	81 (27.0%)	23 (15.4%)	21 (15.9%)		
Outcome (n=298)					
Dead	157 (52.7%)	82 (54.7%)	75 (47.5%)	2.437	0.296#
alive	141 (47.3%)	68 (45.3%)	83 (52.5%)		

chi square test, * Fisher's exact test

Table 4.14: Relationship between S1PR1 expression and clinicopathological parameters

Clinical characteristic	All patients (n=300)	S1PR1+ (n=152)	S1PR1- (n=148)	$\chi 2$ value	p value
Sex					
Male	171 (57.0)	122 (56.0%)	49 (59.8%)	0.350	0.554#
Female	129 (43.0)	96 (44.0%)	33 (40.2%)		
Age group					
< 60 years	99 (33.0%)	66 (30.3%)	27 (32.9%)	0.196	0.658#
≥ 60 years	201 (67.0%)	152 (69.7%)	55 (67.1%)		
ECOG PS (n=88)					
≤1	66 (75.0%)	199 (91.7%)	77 (93.9%)	0.405	0.525#
>1	22 (25.0%)	18 (8.3%)	5 (6.1%)		
B-symptoms					
Present	155 (51.7%)	105 (48.2%)	50 (61.0%)	3.196	**0.048#**
Absent	145 (48.3%)	113 (51.8%)	32 (39.0%)		
LDH level (n=297)					
Low (≤ 450 U/I)	154 (51.5%)	114 (52.3%)	40 (48.8%)	0.294	0.587#
High (> 450 U/I)	145 (48.5%)	104 (47.7%)	42 (51.2%)		
Ann Arbor stage					
1/II	164 (54.7%)	120 (55.0%)	44 (53.7%)	0.046	0.830#
III/IV	136 (45.3%)	98 (45.0%)	38 (46.3%)		
Subtype					
GCB	132 (44.0%)	97 (44.5%)	35 (42.7%)	0.079	0.778#
Non GCB	168 (56.0%)	121 (55.5%)	47 (57.3%)		
Site of involvement					
Nodal	171 (57.0%)	122 (56.0%)	49 (59.8%)	0.602	0.740*
Extranodal	123 (41.0%)	91 (41.7%)	32 (39.0%)		
Both	6 (2.0%)	5 (2.3%)	1 (1.2%)		
Extranodal involvement (n=299)					
≤ 1 site	143 (48.0%)	95 (43.8%)	48 (58.5%)	5.194	**0.023#**
> 1 site	156 (52.0%)	122 (56.2%)	34 (41.5%)		
Standard IPI					
Low/Low-intermediate	183 (61.0%)	133 (61.9%)	50 (61.0%)	0.02	0.889#
High-intermediate/ High	114 (39.0%)	82 (38.1%)	32 (39.0%)		
Revised IPI					
Very good/ Good	237 (79.0%)	170 (83.3%)	67 (87.0%)	0.573	0.449#
Poor	44 (21.0%)	34 (16.7%)	10 (13.0%)		
Outcome (n=298)					
Dead	157 (52.3%)	118 (54.1%)	39 (48.7%)	6.024	**0.049#**
Alive	141 (47.7%)	100 (45.9%)	41 (51.3%)		

chi square test, * Fisher's exact test

Table 4.15: Relationship between ABCC1 expression and clinicopathological parameters

Clinical characteristic	All patients (n=300)	ABCC1+ (n=152)	ABCC1- (n=148)	χ^2 value	p value
Sex					
Male	170 (56.9%)	77 (59.2%)	93 (55.0%)	0.529	0.467#
Female	129 (43.1%)	53 (40.8%)	76 (45.0%)		
Age group					
< 60 years	93 (31.1%)	51 (39.2%)	42 (24.9%)	7.089	**0.008#**
≥ 60 years	206 (68.9%)	79 (60.8%)	127 (75.1%)		
ECOG PS (n=298)					
≤1	275 (92.3%)	123 (95.3%)	152 (89.9%)	3.004	0.083#
>1	23 (7.7%)	6 (4.7%)	17 (10.1%)		
B-symptoms					
Present	154 (51.5%)	69 (53.1%)	85 (50.3%)	0.228	0.633#
Absent	145 (48.5%)	61 (46.9%)	84 (49.7%)		
LDH level (n=297)					
Low (≤ 450 U/I)	154 (51.5%)	68 (52.3%)	86 (50.9%)	0.059	0.808#
High (> 450 U/I)	145 (48.5%)	62 (46.9%)	83 (49.7%)		
Ann Arbor stage					
1/II	164 (54.8%)	70 (53.8%)	94 (55.6%)	0.093	0.760#
III/IV	135 (45.2%)	60 (46.2%)	75 (44.4%)		
Subtype					
GCB	132 (44.1%)	58 (44.6%)	74 (43.8%)	0.02	0.886#
Non GCB	167 (55.9%)	72 (55.4%)	95 (56.2%)		
Site of involvement					
Nodal	170 (56.9%)	79 (60.8%)	91 (53.8%)	1.534	0.464*
Extranodal	123 (41.1%)	49 (37.7%)	74 (43.8%)		
Both	6 (2.0%)	2 (1.5%)	4 (2.4%)		
Extranodal involvement (n=299)					
≤ 1 site	143 (47.7%)	66 (51.2%)	76 (45.0%)	1.125	0.289#
> 1 site	156 (52.3%)	63 (48.8%)	93 (55.0%)		
Standard IPI					
Low/Low-intermediate	183 (61.8%)	83 (64.3%)	100 (59.9%)	0.614	0.433#
High-intermediate/ High	113 (38.2%)	46 (35.7%)	67 (40.1%)		
Revised IPI					
Very good/ Good	237 (84.3%)	105 (86.0%)	132 (83.0%)	0.446	0.504#
Poor	44 (15.7%)	17 (14.0%)	27 (17.0%)		
Outcome (n=298)					
Dead	157 (52.3%)	68 (52.3%)	89 (53.0%)	0.066	0.967#
Alive	141 (47.7%)	62 (47.7%)	79 (47.0%)		

chi square test, * Fisher's exact test

Table 4.16: Relationship between ATX expression and clinicopathological parameters

Clinical characteristic	All patients (n=143)	ATX+ (n=30)	ATX- (n=113)	χ2 value	p value
Gender					
Male	77 (53.8%)	15 (50.0%)	62 (54.9%)	0.226	0.635#
Female	66 (46.2%)	15 (50.0%)	51 (45.1%)		
Age group					
< 60 years	50 (35.0%)	7 (23.3%)	43 (38.1%)	2.259	0.133#
≥ 60 years	93 (65.0%)	23 76.7%)	70 (61.9%)		
ECOG PS (n=142)					
<2	130 (91.5%)	28 (93.3%)	102 (91.1%)	0.156	0.692#
≥2	12 (8.5%)	2 (6.7%)	10 (8.9%)		
B-symptoms					
Present	73 (51.0%)	18 (60.0%)	55 (48.7%)	1.217	0.270#
Absent	70 (49.0%)	12 (40.0%)	58 (51.3%)		
LDH level					
Low (≤ 450 U/I)	74 (52.5%)	14 (46.7%)	60 (54.1%)	0.517	0.472#
High (> 450 U/I)	67 (47.5%)	16 (53.3%)	51 (45.9%)		
Ann Arbor stage					
1/II	81 (56.6%)	15 (50.0%)	66 (58.4%)	0.682	0.409#
III/IV	62 (43.4%)	15 (50.0%)	47 (41.6%)		
Subtype					
GCB	63 (44.1%)	11 (36.7%)	52 (46.0%)	0.841	0.359#
Non GCB	80 (55.9%)	19 (63.3%)	61 (54.0%)		
Site of involvement					
Nodal	77 (53.8)	20 (66.7%)	57 (50.4%)	2.458	0.281*
Extranodal	62 (43.4%)	10 (33.3%)	52 (46.0%)		
Both	4 (2.8%)	0 (0.0%)	4 (3.5%)		
No. extranodal involvement					
≤ 1 site	125 (88.0%)	27 (90.0%)	98 (87.5%)		1.000*
> 1 site	17 (12.0%)	3 (10.0%)	14 (27.5%)		
Standard IPI					
Low	64 (45.54%)	10 (33.3%)	54 (48.6%)	2.581	0.461*
Low- intermediate	38 (27.0%)	10 (33.3%)	28 (25.2%)		
High- intermediate	33 (23.4%)	9 (30.0%)	24 (21.6)		
High	6 (4.3%)	1 (3.3%)	5 (4.5%)		
Revised IPI					
Very good	16 (11.3%)	3 (10.0%)	13 (11.7%)	0.621	0.733#
Good	86 (61.0%)	17 (56.7%)	69 (62.2%)		
Poor	39 (27.7%)	10 (33.3%)	29 (26.1%)		
Outcome					
Dead	91 (64.5%)	19 (66.3%)	72 (64.9%)	0.024	0.876#
Alive	50 (35.5%)	11 (33.7%)	39 (35.1%)		

Chi square, * Fisher's exact test

Table 4.17: Expression of lipid signaling molecules in DLBCL by EBV positivity

S1P signalling molecules	EBER$^+$	EBER$^-$	χ^2 value	p value
SPHK1$^+$	5 (35.7%)	147 (51.4%)	1.314	0.252$^{\#}$
SPHK1$^-$	9 (64.3%)	139 (48.6%)		
S1PR1$^+$	8 (57.1%)	210 (73.4%)	1.782	0.219*
S1PR1$^-$	6 (42.9%)	76 (26.6%)		
ABCC1$^+$	4 (28.6%)	126 (44.2%)	1.328	0.284$^{\#}$
ABCC1$^-$	10 (71.4%)	159 (55.8%)		
ATX$^+$	3 (25.0%)	27 (20.6%)	0.127	0.716*
ATX$^-$	9 (75.0%)	104 (79.4%)		

$^{\#}$ chi square test, * Fisher's exact test

4.9.3 Correlation of SPHK1, S1PR1, ABCC1 and ATX expression with overall and event free survival

Univariate analysis showed that none of the lipid signaling molecule expression correlated with significant OS and EFS (Figure 4.22-4.25).

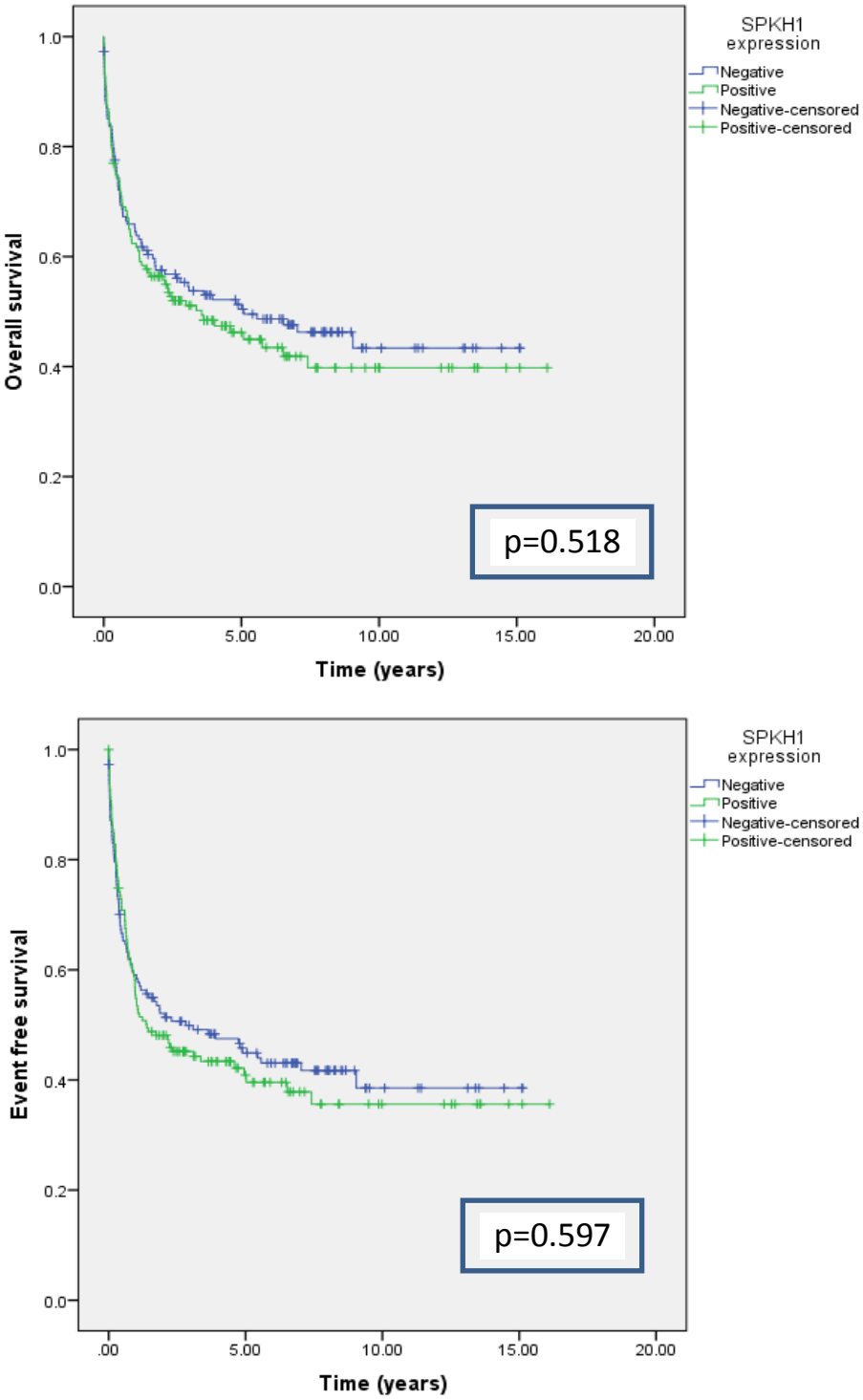

Figure 4.22: The Kaplan Meier overall and event free survival curves of DLBCL patients by SPHK1 positivity.

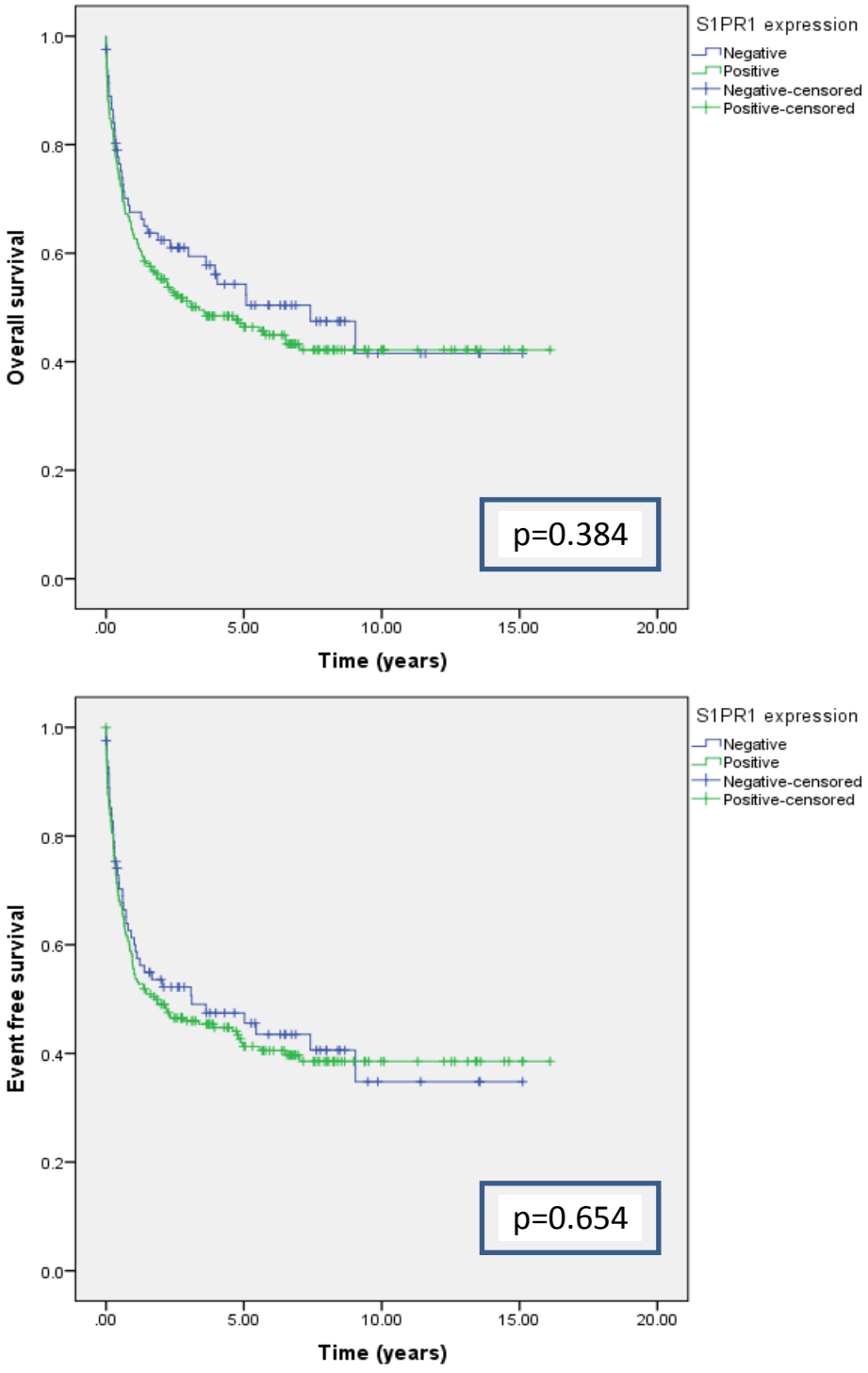

Figure 4.23: The Kaplan Meier overall and event free survival curves of DLBCL patients by S1PR1 positivity.

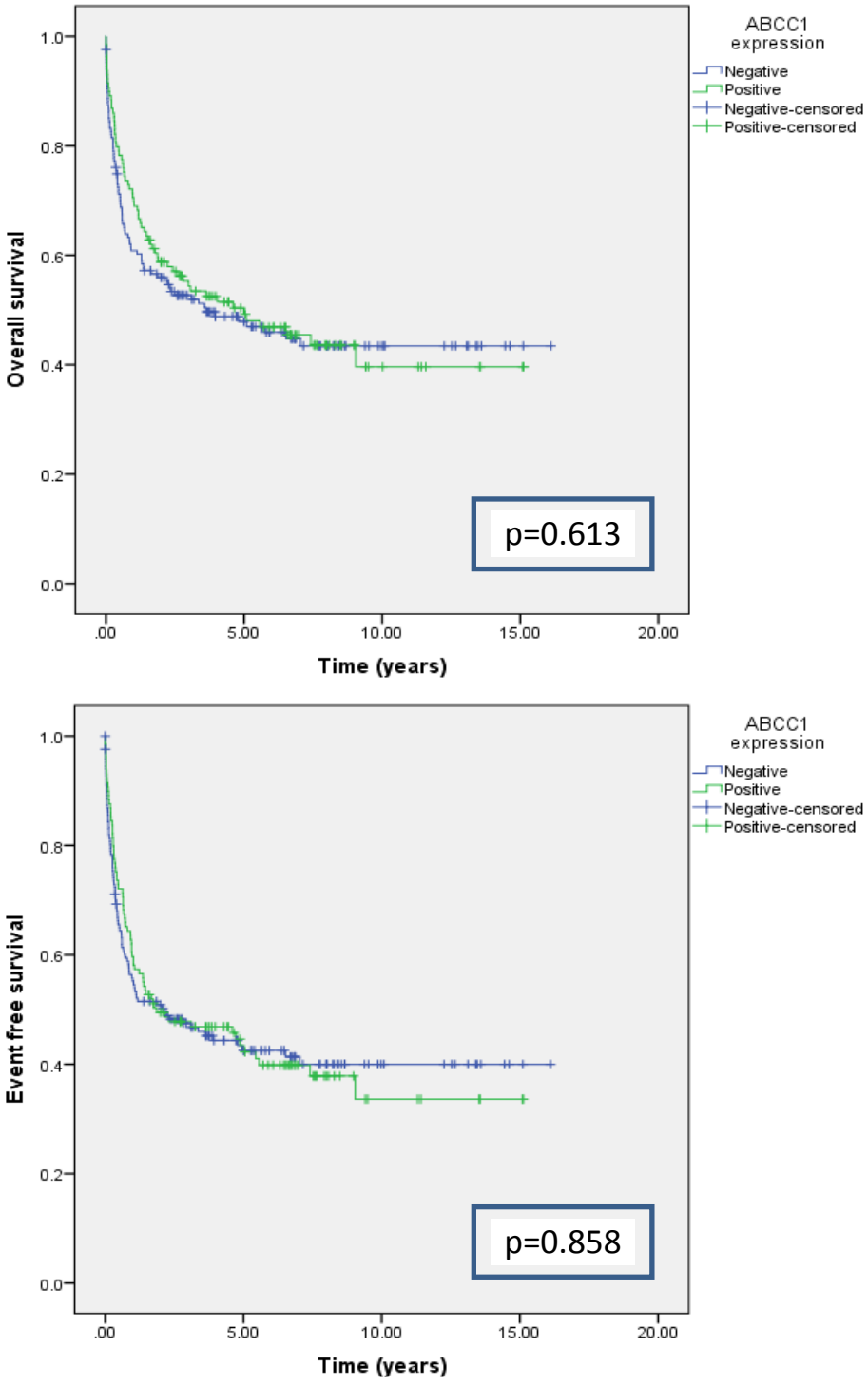

Figure 4.24: The Kaplan Meier overall and event free survival curves of DLBCL patients by ABCC1 positivity.

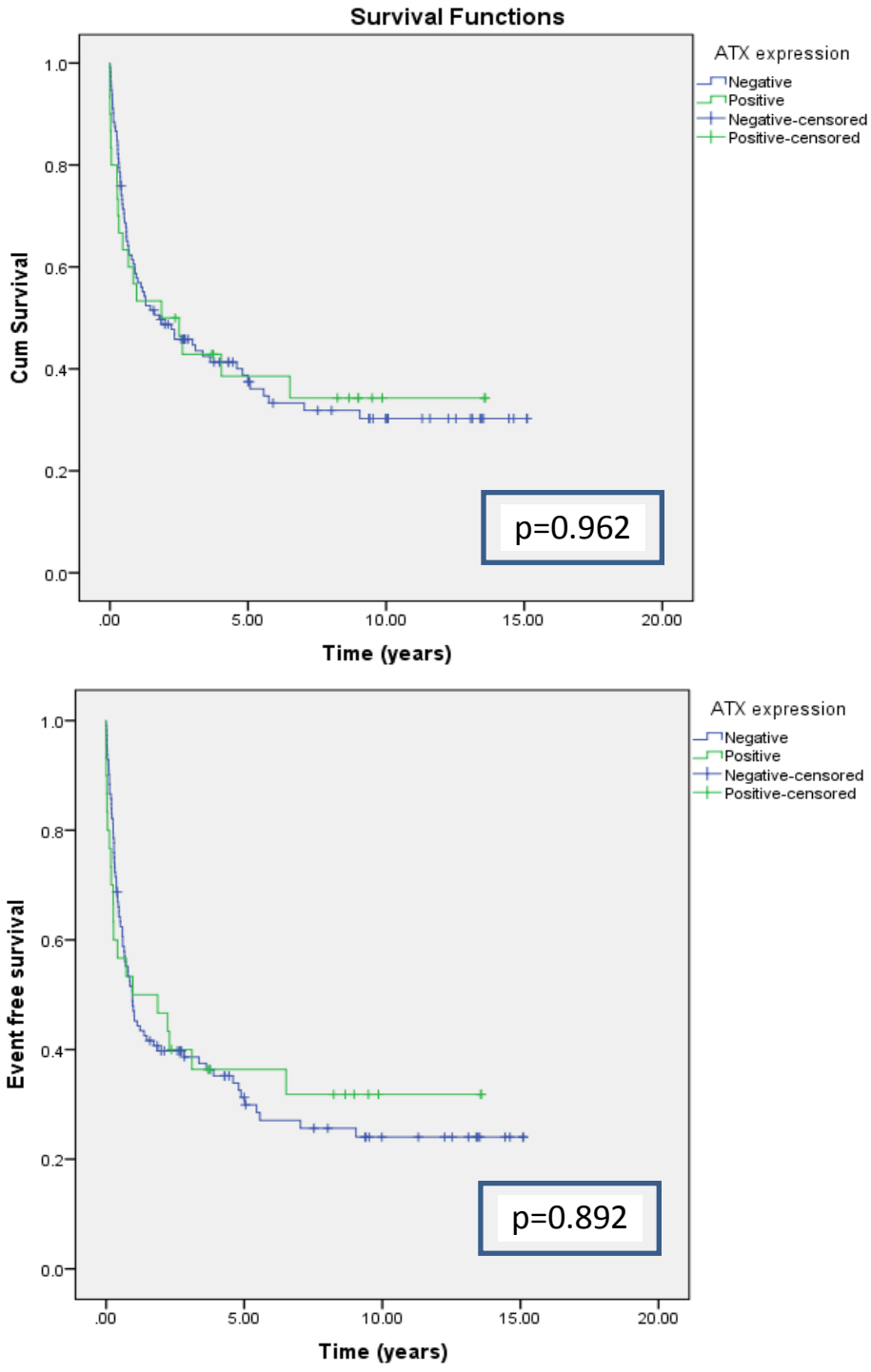

Figure 4.25: The Kaplan Meier overall and event free survival curves of DLBCL patients by ATX positivity.

4.10 Discussion

In the whole series of DLBCL, males were more commonly affected than females and majority of patients were aged ≥ 60 years. A higher proportion of DLBCL cases presented with nodal disease and less than 10% of cases had more than one site of extranodal involvement. I found that the frequency of non GCB subtype was higher than that of the GCB subtype (56% vs 44%) however this difference was not statistically significant. Analysis of subtypes in Western countries such as Norway, Sweden, Spain, Italy, France and the USA showed an incidence of the GCB subtype ranging from 42-58% which was in keeping with our study (Berglund et al., 2005; Chang et al., 2004; Hans et al., 2004). Shiozawa et al found that the non GCB subtype was more frequent in Asian countries (31-42%) compared to Western countries (Shiozawa et al., 2007). Shiozawa et al suggested that the difference between the Asian and Western distribution of DLBCL subtype may be due to different distribution of nodal and extranodal disease in these two populations.

The impact of EBV on DLBCL patients

In this series, 14/300 (4.7%) DLBCL patients were found to harbour EBV RNA by *in situ* hybridization, of these, 4 (1.3%) were defined as EBV^+ DLBCL-E. This low incidence corroborates with the findings of Hoeller et al who reported an incidence of EBV^+ DLBCL-E as 3.1%. in a European population (Hoeller et al., 2010). Gibson et al in the United States reported an incidence of less than 1% of DLBCL-E aged more than 60 from 2001 to 2007

(Gibson & Hsi 2009). A recent Turkish study reported an incidence of 5.3% of EBV^+ DLBCL and 3.5% of EBV^+ DLBCL-E among 340 patients (Uner et al. 2011).

There appears to be a striking difference in the incidence of EBV^+ DLBCL-E in the Asian compared to European countries. For example, the incidence of 9% reported by Park et al in Korea is seven fold higher than in our series (Park et al., 2007). Kuze et al reported an incidence of 11.4% of EBV^+ DLBCL-E in Japan (Kuze et al. 2000) and Oyama et al reported an incidence of 8.3% of EBV^+ B-cell LPDs (Oyama et al. 2007). Cho et al found that the incidence of EBV^+ DLBCL-E was 7.5% in Korea (Cho et al. 2008).

Our study showed that EBV positivity was significantly associated with disease subtype (p=0.001). All the EBV-positive cases were of non GCB subtype. This is in contrast with the findings of Hoeller et al which showed equal distribution of GCB and non GCB subtype in their series of EBV-positive cases (Hoeller et al., 2010). Our most intriguing finding is that EBV positivity showed inferior EFS compared to the EBV-negative counterpart (p=0.033). This corroborates with the findings of Oyama et al that EBV^+ DLBCL had poorer prognosis and behaved aggressively than the EBV^- DLBCL (Oyama et al. 2003). In a larger study, Oyama et al found that the EBV^+ B-cell LPDs had aggressive clinical features, higher performance status and higher LDH levels. This group also had significantly inferior overall survival (Oyama et al. 2007). To the best of my knowledge, our study constitute the first analysis on the impact of EBV on DLBCL patients with respect to age, gender, stage of disease, subtype, presence or absence of B symptoms, ECOG PS, site of involvement, number of extranodal site involvement, IPI, R-IPI and clinical outcome in a single centre in the UK.

I found that the presence of B symptoms was significantly associated with EBV positivity. 85.7% of EBV^+ DLBCL had B symptoms and those with B symptoms had inferior OS and EFS ($p<0.001$). The presence of B symptoms were found to be a negative prognostic factor (Gibson & Hsi 2009), and Oyama et al showed that patients with presence of B symptoms had higher risk of death by univariate and multivariate analyses (Oyama et al. 2007) which was in keeping with my findings.

In this study, EBV^+ DLBCL was found to have lower mean age compared to EBV- negative tumours. The median age for EBV^+ DLBCL was 63 which was close to that of the Turkish study (64 years)(Uner et al. 2011). The EBV^- DLBCL patients had a higher median age of 66 years. Age however showed no significant association with EBV positivity, which is in contrast with Asian studies; Oyama et al found that EBV^+ B- cell LPDs were more frequent in those aged > 60 years (Oyama et al. 2007) and Park et al also found that EBV^+ DLBCL was more frequent in those aged > 60 years (Park et al., 2007).

In the present series, the EBV positive cases showed EBER positivity in a majority of neoplastic cells. In this study I was able to evaluate the latency pattern of EBV using EBER, LMP1 and EBNA2 staining. EBV latency III was most frequently seen. This is in line with most reports which show that latency II and III are the most common forms of latency seen in EBV^+ DLBCLs (Oyama et al. 2003; Oyama et al. 2007). Hoeller et al observed a worse survival outcome for patients with latency type III compared to latency type II and I. However I found that EBV latency pattern did not have any prognostic impact or a worse survival rate. This could be due to the low number of EBV positive cases in our series.

Sehn et al found that re-distribution of the IPI factors into a R-IPI in the era of R-CHOP gave a better prediction of outcome as they found an overlapping survival curves for two low risk groups and two high risk groups in IPI but not for R-IPI groups (Sehn et al. 2007). In R-IPI, three prognostic groups were identified; very good (IPI score 0), good (IPI score 1,2) and poor group (IPI score 3,4,5) with OS of 94%, 79% and 55%, respectively. In line with most studies, I found that IPI was an important prognostic indicator in DLBCL by univariate and multivariate analyses. High risk IPI and poor R-IPI have high hazard ratios of 4.5 and 3.9, respectively. By log rank test, higher IPI correlated significantly with shorter OS and EFS ($p< 0.001$) while poor R-IPI correlated with shorter EFS ($p< 0.001$). Higher IPI and poor R-IPI were found to be significantly associated with the presence of B symptoms, relapse, age > 60 years, late stage of disease, LDH > 450 and ECOG ≥2. After considering only patients in the R-CHOP era, I found that IPI was still an important prognostic factor in determining survival of DLBCL patients which contradicts the finding of Sehn et al.

Pfreundschuh and colleagues have shown that bulky disease has adverse prognostic significance in young good-prognosis patients (Pfreundschuh et al. 2008). A cut off point of 10 cm has been able to distinguish two populations with EFS of significant difference in patients given R-CHOP chemotherapy. Looking at the entire DLBCL cases, I found that bulky disease has no impact on OS and EFS. Similarly, in patients aged < 60 years given R-CHOP, bulky disease showed insignificant contribution to prognosis. Hence the role of bulky disease in the era of Rituximab merits further investigation.

The significance of CD10, BCL6 and MUM1 in DLBCL

As microarray analysis is not yet feasible in daily routine diagnostic work, immunohistochemistry is useful in determining the subtype of DLBCL. In the pre-Rituximab era, the expression of CD10 (De Paepe et al. 2005) and BCL6 (Lossos et al. 2001) have been associated with good prognosis while MUM1 expression has been associated with adverse prognosis (Hans et al., 2004). Studies have shown that CD10 is expressed in the cytoplasm of tumour cells and is associated with improved survival and complete remission (Barrans, 2002).

BCL6 is a main regulator of germinal centre cell differentiation and is expressed in both centroblasts and centrocytes in the germinal centres. In DLBCL, BCL6 is overexpressed in the nucleus of 50-70% of cases, sparing the nucleolus. In this study, BCL6 protein was found to be expressed in 40% of DLBCL cases and its expression correlated significantly with superior OS ($p=0.001$) and EFS ($p=0.002$), hence is a good prognostic indicator.

MUM1 is a lymphoid specific member of the interferon regulatory factor family of transcription factors. It is expressed in the nucleus of lymphocytes and plasma cells. It is also expressed in a subset or germinal centre cells indicating the late stage of germinal center B-cell differentiation (Falini et al., 2011a; Tsuboi et al. 2000). Its critical role is regulating gene expression in response to signalling by interferons and other cytokines. MUM1 is also believed to play a role in plasma cell development. Most GCB and mantle cells are MUM1 negative, nevertheless it is expressed in 40–50% of DLBCL cases indicating a non GCB subtype (Chang et al. 2004; Hans et al., 2004; Falini et al., 2011b).

In this study, I have looked at groups of patients in both the pre-Rituximab and post-Rituximab era and found that DLBCL patients expressing BCL6 were associated with a favourable prognosis in both eras. In contrast to the findings of Hans et al, I found that MUM1 had no impact on survival. Differences in our results might be attributed to the study design; Han's study was a multi-centre study and my study was a single-centre study. Hans et al used MUM1 antibody from Falini et al while my MUM1 antibody was from Dako. Hans et al applied the antibody onto tissue microarray slides while my study used whole tissue section. In contrast to the findings of De Paepe et al, I found that CD10 was not associated with better OS and EFS. De Paepe et al used a different CD10 clone of antibody as compared to my study, although our cutoff levels of 30% were similar. Therefore, it is important to redefine the cutoff levels for different antibodies in order to validate the predictive value of immunohistochemical staining in DLBCL.

Lipid signalling molecules in DLBCL

The expression of S1P signalling molecules have never been looked into in DLBCL. I found that SPHK1 was expressed in half of DLBCL cases while S1PR1 was expressed in 73% of cases. The most intriguing finding was that S1PR1 expression was associated with the presence of B symptoms, higher number of extranodal involvement and poorer clinical outcome suggesting it as a poor prognostic marker. The role of S1PR1 in contributing to poorer clinical outcome warrants further investigation. As of today, there are very limited studies on the contribution of S1P signaling molecules in lymphoma. It would be interesting to explore whether S1PR1 would be a possible prognostic marker in DLBCL. The expression

of S1PR1 across different subtypes of malignant lymphoma would also be helpful to determine the diagnostic importance of S1PR1.

The need to use a a specific scoring system for S1P signaling molecules may have to be considered eg. using the semiquantitative Histo score which considers both percentage of positive tumour cells and the intensity of staining. For instance, a cut off value of 30% positivity is used in most studies with CD10,BCL6 and MUM1. A cut off value for positivity will have to be determined for expression of lipid signaling molecules in future studies. In this study I found that usage of polyclonal antibodies gave high background staining and nuclear positivity in some cases which made scoring difficult. Usage of monoclonal antibodies for all lipid signaling molecules needs to be considered. The higher rate of specificity of monoclonal antibodies might influence the significance in correlating protein expression with clinicopathological parameters of DLBCL. Taken together, this study has highlighted the possibility of future major studies in DLBCL.

CHAPTER 5

RESULTS

EXPRESSION IN EPITHELIAL MALIGNANCIES, OF LIPID SIGNALLING MOLECULES AND THEIR ASSOCIATION WITH CLINICOPATHOLOGICAL PARAMETERS

5.1 Introduction

S1P is a lysophospholipid mediator of diverse cellular processes important for cancer development and progression. The major enzyme that regulates the phosphorylation of sphingosine to S1P is SPHK1. French et al were the first group to demonstrate the expression of SPHK1 mRNA in human tissue samples of breast, lung, prostate, colon, gastric and head and neck cancer. A two to three fold increase in SPHK1 expression was observed in cancer tissue compared to adjacent normal tissue (French et al., 2003). For this reason, SPHK1 was suggested to be an oncogene. Increased SPHK1 expression was also found to be associated with decreased survival in breast cancer (Ruckhäberle et al. 2008), gastric cancer (Li et al., 2009) and glioblastoma multiforme patients (James R Van Brocklyn et al. 2005a). In prostate cancer, increased SPHK1 enzymatic activity was associated with higher prostate specific antigen (PSA) levels, higher tumour volumes and surgical failure (Malavaud et al. 2010). Strong SPHK1 expression was also observed in non small cell carcinoma of the lungs (K. R. Johnson et al. 2005) and in pancreatic adenocarcinoma (Guillermet-Guibert et al. 2009) compared to adjacent normal tissue. SPHK1 has also emerged as an important therapeutic target in cancer. (Van Brocklyn et al., 2005).

The aim of this study was to:

1) investigate the expression of lipid signalling molecules, including SPHK1, S1PR1, ABCC1 and ATX in breast, lung and bladder cancers.
2) explore the relationship of the expression of these lipid signaling molecules with clinical characteristics and survival of the different types of cancer.

3) determine if there is any possible co-expression of these lipid signaling molecules in the different types of cancer.

5.2 Expression of lipid signalling molecules in breast cancer

Immunohistochemistry was performed on 118 cases of primary breast cancer obtained from the Pathology Department of Queen Elizabeth Hospital, Birmingham. Each case was stained using antibodies to SPHK1, S1PR1, ABCC1 and ATX. Due to insufficient tissue sections, I was not able to perform S1PR2 staining. Immunohistochemical staining results were examined and scored according to the criteria set out in Section 2.2.4.4. Table 3.1 shows the clinical characteristics of breast cancer patients. 87/118 (73.7%) patients were histologically classified as infiltrating ductal carcinoma, not otherwise specified (NOS), 17/118 (14.4%) were infiltrating lobular carcinoma, 4/118 (3.4%) were mucinous carcinoma, 3/118 (2.5%) were medullary carcinoma, another 3/118 (2.5%) were ductal carcinoma in situ (DCIS) while 1/ 118 (1%) respectively were tubular carcinoma, atypical medullary carcinoma, lubular papillary and mixed NOS and lobular subtype (Figure 5.3).

A summary of the expression of lipid signalling molecules in breast cancer is shown in Figure 5.2. SPHK1 was expressed in the majority (81%) of breast cancer patients and was localised within the cytoplasm and occasionally in the nucleus of malignant cells (Figure 5.4). SPHK1 reactivity was not seen in the stroma. In eight cases, normal breast ducts were present in tumour samples and in 3 of these cases, normal breast epithelial cells also expressed SPHK1 but at levels lower than observed in malignant cells. In the remaining 5 cases, normal breast epithelial cells lacked SPHK1 expression. SPHK1 was also expressed in fibroblasts, macrophages, plasma cells and endothelial cells lining the blood vessels serving as internal positive controls (Figure 5.4).

Although S1PR1 was expressed in only 12% of breast cancer patients, it was not expressed in normal breast epithelial cells. When present, S1PR1 was found on the cell membrane and the cytoplasm or tumour cells (Figure 5.5). S1PR1 was also strongly expressed in the endothelial cells of blood vessels.

In 38 tumours expressing ABCC1, expression was generally higher than in normal mammary epithelium. When present, the expression of ABCC1 was observed on the cell membrane and in the cytoplasm of carcinoma cells as well as in the endothelial cells of blood vessels (Figure 5.6).

Autotaxin was expressed in in 76/118 (66.4%) cases. Staining intensity was stronger in breast cancer cells compared to normal breast epithelium (Figure 5.7). In 8 cases with normal breast ducts, 4 cases showed mild to moderate ATX expression in the ductal epithelium. ATX was 5localised to the cytoplasm of breast cancer cells and staining was clearly observed within the endothelial cells of blood vessels

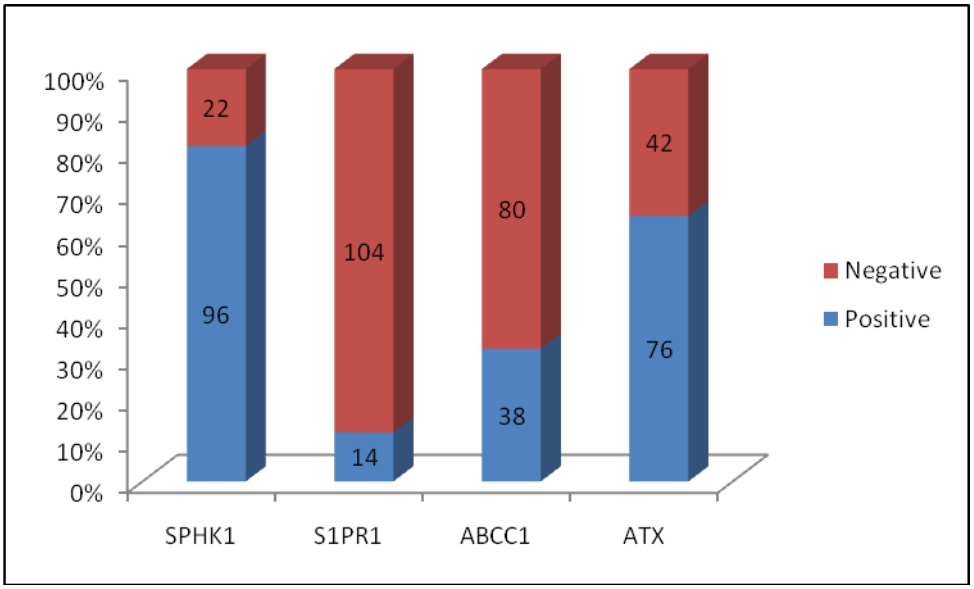

Figure 5.1: Summary of the expression of lipid signalling molecules in breast cancer

Table 5.1: Clinical characteristics of breast cancer patients

Characteristics	All patients (%)
Age	
< 50	22 (18.6)
≥ 50	96 (81.4)
Surgery type	
Mastectomy	73 (61.9)
Wire loop excision	45 (38.1)
Tumour size	
< 2 cm	49 (41.5)
≥ 2 cm	69 (58.5)
Nodal metastasis	
Positive	43 (39.1)
Negative	67 (60.1)
Tumour grade	
1	17 (14.4)
2	59 (50.0)
3	42 (35.6)
DCIS grade	
Low	4 (3.4)
Intermediate	19 (16.1)
High	52 (44.1)
Not seen	43 (36.4)
Tumour stage	
Limited, I-II	107 (90.7)
Advanced, III-IV	11 (9.3)
Side of tumour	
Left	53 (44.9)
Right	65 (55.1)
Vascular invasion	
Present	37 (31.4)
Absent	81 (68.6)
ER status	
Positive	86 (72.9)
Negative	32 (27.1)
PR status	
Positive	34 (61.7)
Negative	26 (38.3)
Nottingham Prognostic Index	
< 3.4	33 (28.0)
≥ 3.4	74 (62.7)

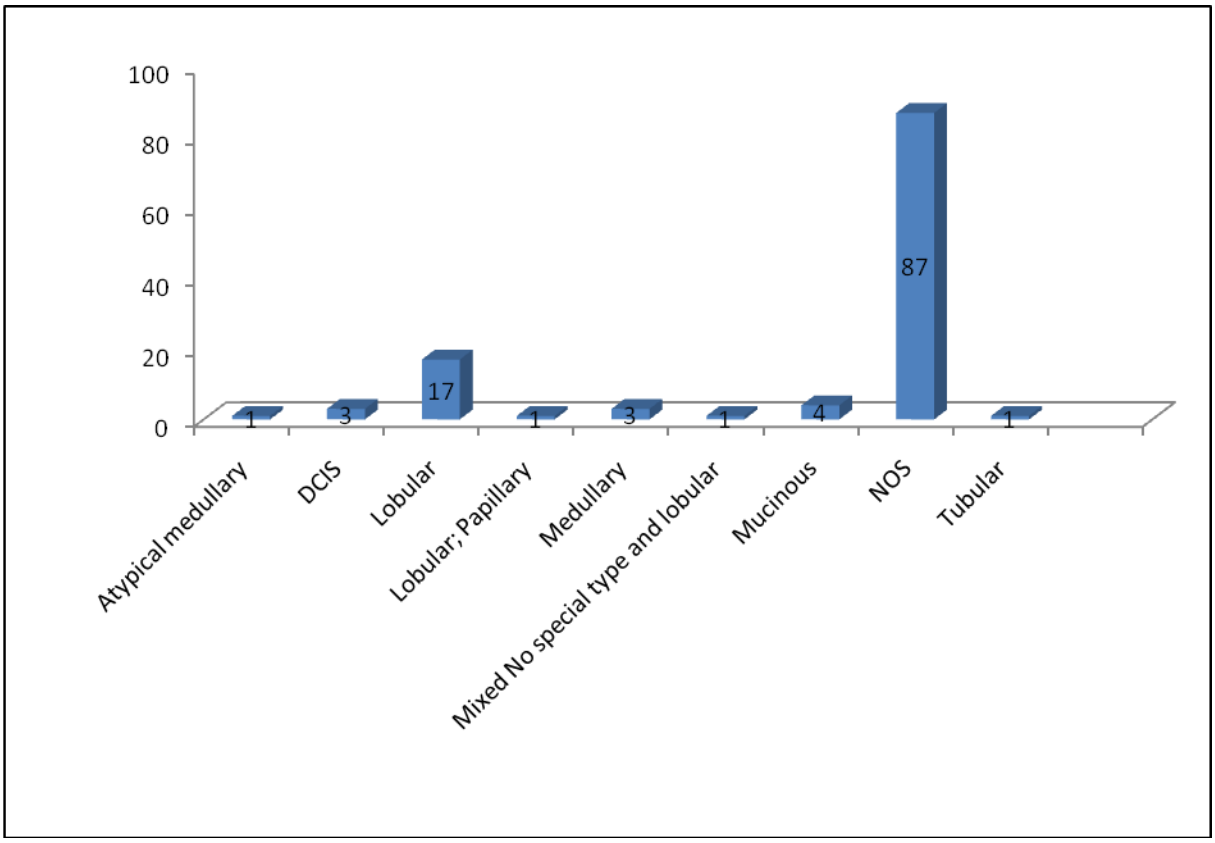

Figure 5.2: The histological subtypes of breast cancer patients

A

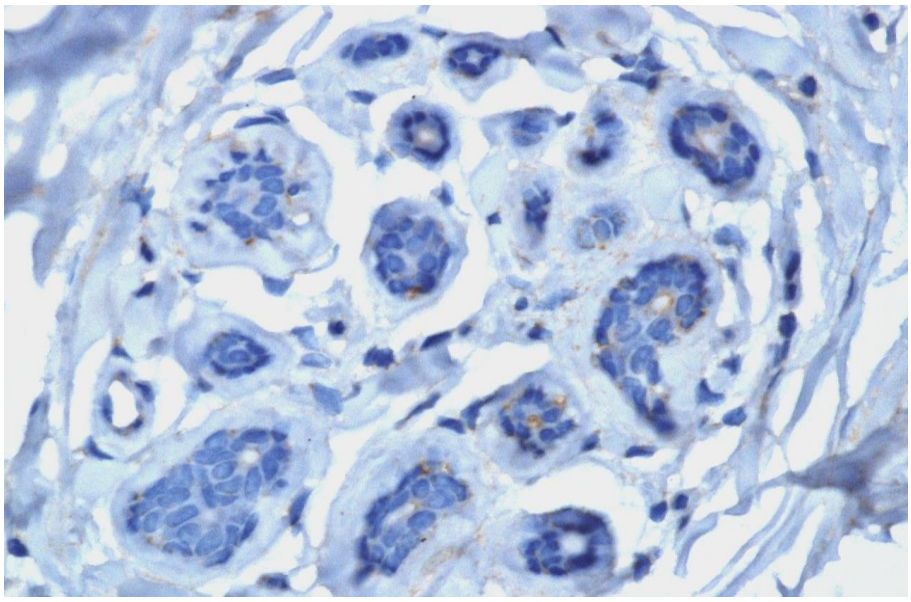

B

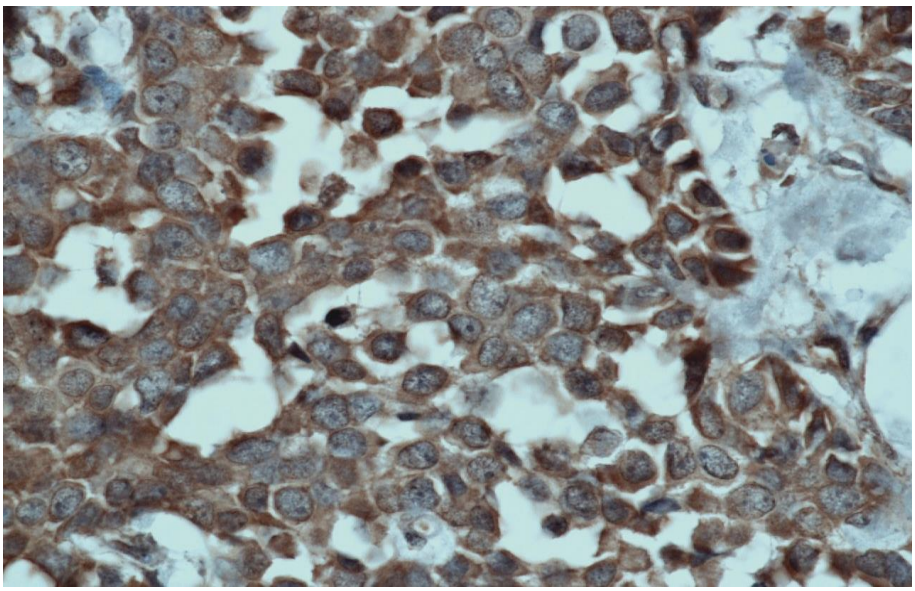

Figure 5.3: Expression of SPHK1 in normal breast tissue and breast cancer. A) Faint staining of SPHK1 in the cytoplasm of normal breast epithelium B) Strong SPHK1 expression in the cytoplasm of breast cancer cells

A

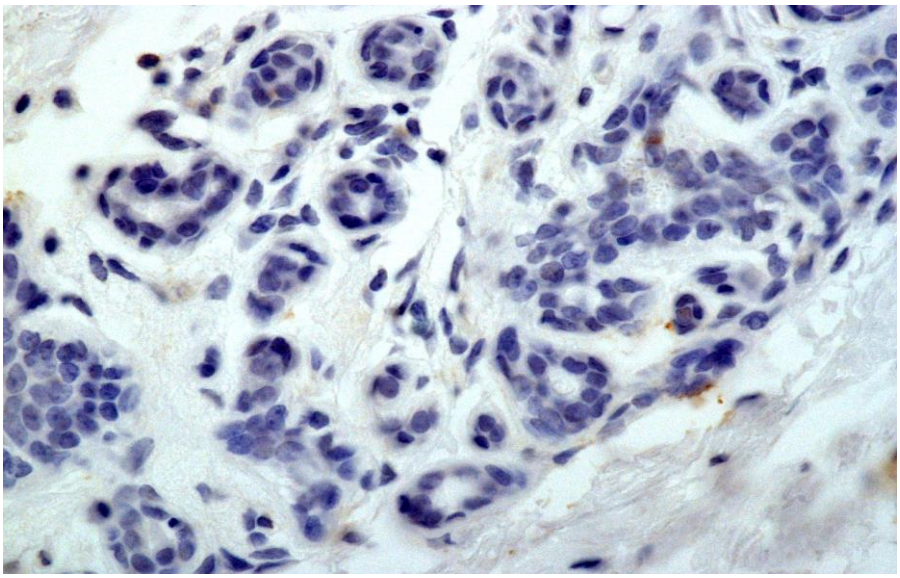

B

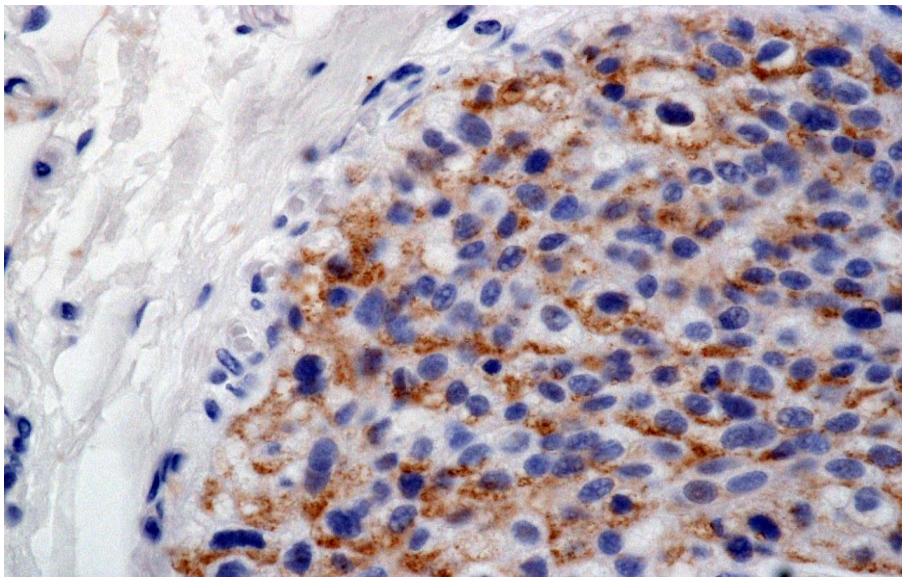

Figure 5.4:Expression of S1PR1 in normal breast tissue and breast cancer. A) Absent or faint expression of S1PR1 in the cytoplasm of normal breast ducts (x400) B) Strong S1PR1 expression in the cytoplasm and cytoplasmic membrane of breast cancer cells (x400).

A

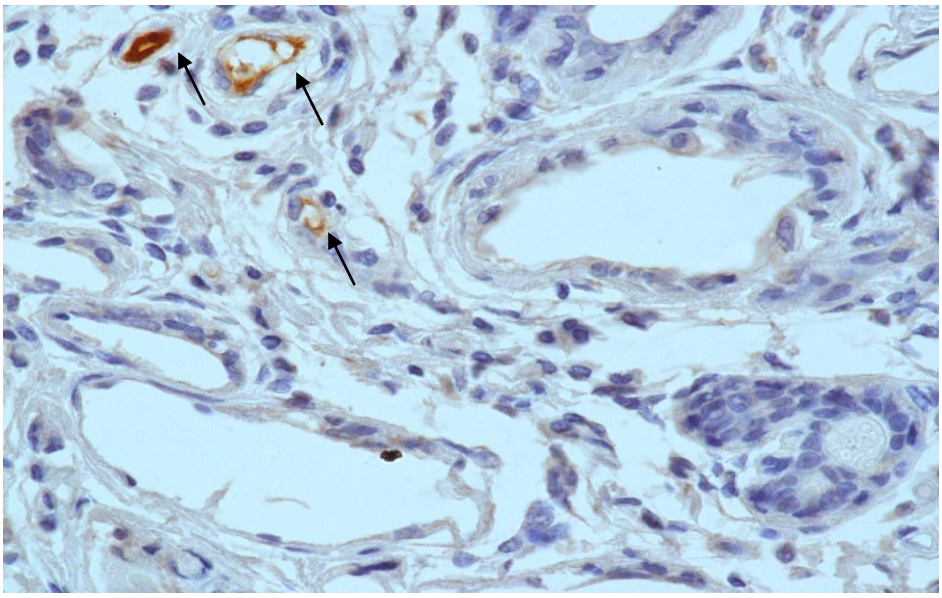

B

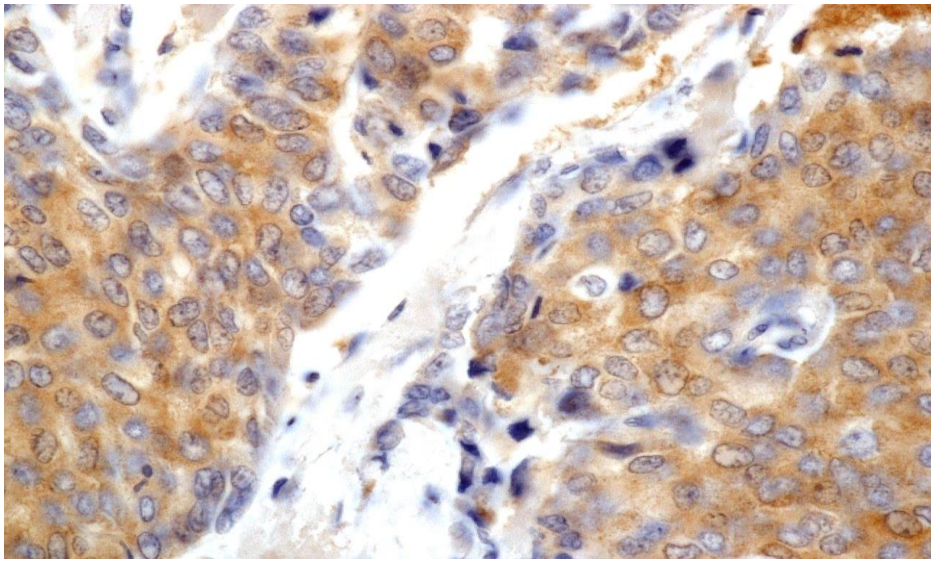

Figure 5.5: Expression of ABCC1 in normal breast tissue and in breast cancer. A) Absent ABCC1 expression in normal breast epithelial cells but strong positivity in the endothelial cells of blood vessels (arrowed; x400) B) Strong ABCC1 expression in the cytoplasm of breast cancer cells (x600).

A

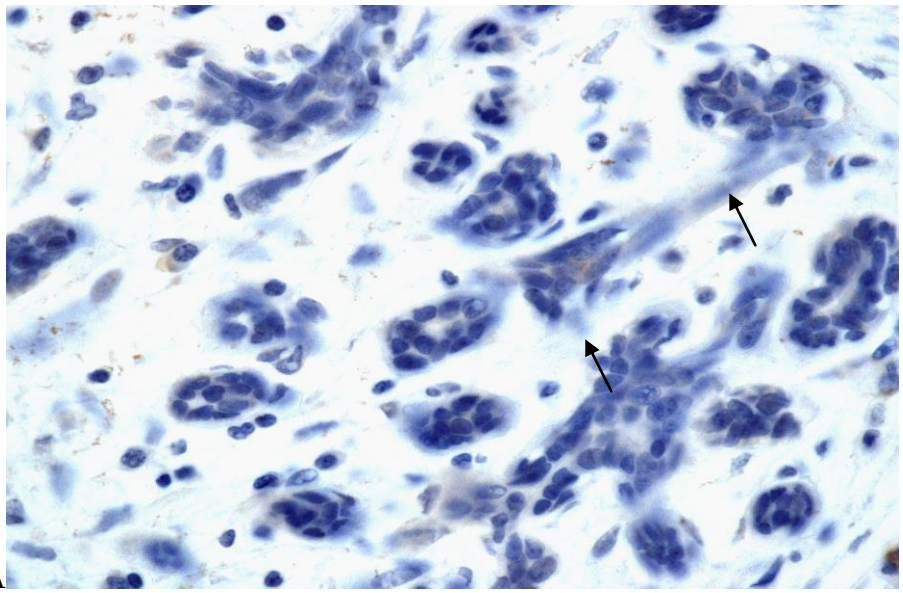

B

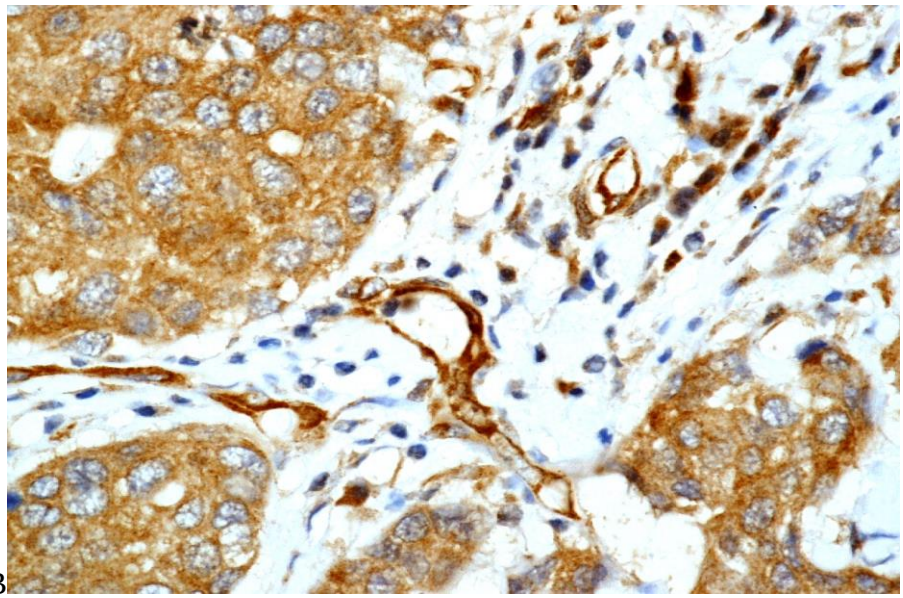

Figure 5.6: Expression of ATX in normal breast tissue and in breast cancer. A) A case lacking ATX expression in normal breast epithelial cells (x400) B) Strong ATX expression in the cytoplasm of breast cancer cells and in endothelial cells of blood vessels(fine arrows) (x600).

5.2.1 Relationship between the expression of each lipid signalling molecules in breast cancer

I next used chi square and Fisher's exact tests to determine if there was any relationship between the expression of each lipid signalling molecule. The expression of ABCC1 was significantly associated with ATX expression ($p = 0.007$). No other statistically significant associations were found (Table 5.2)

Table 5.2: Relationship between the expression of each lipid signalling molecules in breast cancer

Lipid signalling molecule	Associated lipid molecule		p value
	S1PR1+	S1PR1-	
SPHK1 +	11 (11.5)	85 (81.7)	0.776*
SPHK1 -	3 (13.6)	19 (8.64)	
	ABCC1+	ABCC1-	
SPHK1 +	32 (33.3)	64 (66.7)	0.583#
SPHK1 -	6 (27.3)	16 (72.7)	
	ATX+	ATX-	
SPHK1 +	65 (67.7)	31 (32.3)	0.118#
SPHK1 -	11 (50.0)	11 (50.0)	
	ABCC1+	ABCC1-	
S1PR1+	7 (50.0)	7 (50.0)	0.129*
S1PR1-	31 (29.8)	73 (70.2)	
	ATX+	ATX-	
S1PR1+	11 (78.0)	3 (21.4)	0.238
S1PR1-	65 (62.5)	39 (37.5)	
	ATX+	ATX-	
ABCC1+	31 (81.6)	7 (18.4)	0.007#
ABCC1-	45 (56.2)	35 (43.8)	

*Fisher's exact test, # chi square test

5.2.2 Correlation between the expression of lipid signalling molecules in breast cancer and clinical characteristics

Having established the prevalence of expression of the different lipid signalling proteins in breast cancer, I next studied the relationship of expression to various clinicopathological features, including age, surgery type, tumour size, nodal metastasis, tumour grade, ductal carcinoma in -situ (DCIS) grade, tumour grade, side of tumour, vascular invasion, ER and PR status and Nottingham Prognostic Index (NPI). I used chi-square and Fisher's exact test to

determine if the expression of each individual lipid signalling protein was significantly associated with any of these clinicopathological variables. The results of this analysis are summarised in Table 5.3 - 5.6. I found no significant association between the expression of SPHK1 and any clinicopathological variables (Table 5.3). S1PR1 was significantly more likely to be expressed in patients with larger tumour size (p= 0.028) in those tumours obtained by mastectomy (p= 0.011), and in those with a higher NPI (p= 0.016)(Figure 5.4). The expression of ABCC1 showed no significant association with any clinicopathological variables (Table 5.5). More patients who had mastectomy were ATX positive (p=0.049)(Table 5.6).

Table 5.3: Relationship between SPHK1 expression in breast cancer and clinicopathological parameters

Characteristics	All patients (%)	SPHK1 +	SPHK1 -	$\chi 2$ value	p value
Age					
< 50	22 (18.6)	18 (18.8)	4 (18.2)	0.004	0.951*
≥ 50	96 (81.4)	78 (81.2)	18 (81.8)		
Surgery type					
Mastectomy	73 (61.9)	61 (63.5)	12 (54.5)	0.614	0.433#
Wire loop excision	45 (38.1)	35 (36.5)	10 (45.5)		
Tumour size					
< 2 cm	49 (41.5)	41 (42.7)	8 (36.4)	0.297	0.586#
≥ 2 cm	69 (58.5)	55 (57.3)	14 (63.6)		
Nodal metastasis					
Positive	43 (39.1)	33 (36.3)	10 (52.6)	1.769	0.184#
Negative	67 (60.1)	58 (63.7)	9 (47.4)		
Tumour grade					
1	17 (14.4)	13 (13.5)	4 (18.2)	0.376	0.829#
2	59 (50.0)	48 (50.0)	11 (50.0)		
3	42 (35.6)	35 (36.5)	7 (31.8)		
DCIS grade					
Low	4 (3.4)	4 (4.2)	0 (0.0)	0.676	0.937*
Intermediate	19 (16.1)	16 (16.7)	3 (13.6)		
High	52 (44.1)	41 (42.7)	11 (50.0)		
Not seen	43 (36.4)	35 (36.5)	8 (36.4)		
Tumour stage					
Limited,I-II	107 (90.7)	88 (99.7)	19 (86.4)	0.590	0.428*
Advanced, III-IV	11 (9.3)	8 (8.3)	3 (13.6)		
Side of tumour					
Left	53 (44.9)	45 (46.9)	8 (36.4)	0.799	0.371#
Right	65 (55.1)	51 (53.1)	14 (63.6)		
Vascular invasion					
Present	37 (31.4)	27 (28.1)	10 (45.5)	2.497	0.114#
Absent	81 (68.6)	69 (71.9)	12 (54.5)		
ER status					
Positive	86 (72.9)	70 (72.9)	16 (72.7)	0.000	0.986#
Negative	32 (27.1)	26 (27.1)	6 (27.3)		
PR status					
Positive	34 (61.7)	26 (60.4)	22 (66.7)	0.159	0.752#
Negative	26 (38.3)	8(39.6)	4(33.3)		
Nottingham Prognostic Index					
< 3.4	33 (28.0)	27 (30.7)	6 (31.6)	0.006	0.939#
≥ 3.4	74 (62.7)	61 (69.3)	13 (68.4)		

*Fisher's exact test, # chi square test

Table 5.4: Relationship between S1PR1 expression in breast cancer and clinicopathological parameters

Characteristics	All patients (%)	S1PR1+	S1PR1-	$\chi 2$ value	p value
Age					
< 50	22 (18.6)	0 (0.0)	22 (21.2)	3.609	0.069*
≥ 50	96 (81.4)	14 (100.0)	82 (78.8)		
Surgery type					
Mastectomy	73 (61.9)	13 (92.9)	60 (57.7)	6.467	0.016#
Wire loop excision	45 (38.1)	1 (7.1)	44 (42.3)		
Tumour size					
< 2 cm	49 (41.5)	2 (14.3)	47 (45.2)	4.854	0.028#
≥ 2 cm	69 (58.5)	12 (85.7)	57 (54.8)		
Nodal metastasis					
Positive	43 (39.1)	7 (53.8)	36 (37.1)	1.348	0.246#
Negative	67 (60.1)	6 (46.2)	61 (62.9)		
Tumour grade					
1	17 (14.4)	0 (0.0)	17 (16.3)	3.215	0.200#
2	59 (50.0)	7 (50.0)	52 (50.0)		
3	42 (35.6)	7 (50.0)	35 (33.7)		
DCIS grade					
Low	4 (3.4)	0 (0.0)	4 (3.8)	1.258	0.733*
Intermediate	19 (16.1)	1 (7.1)	18 (17.3)		
High	52 (44.1)	8 (57.1)	44 (42.3)		
Not seen	43 (36.4)	5 (35.7)	38 (36.5)		
Tumour stage					
Limited,I-II	107 (90.7)	12 (85.7)	95 (91.3)	0.459	0.618*
Advanced, III-IV	11 (9.3)	2 (14.3)	9 (8.7)		
Side of tumour					
Left	53 (44.9)	6 (42.9)	47 (45.2)	0.027	0.869#
Right	65 (55.1)	8 (57.1)	57 (54.8)		
Vascular invasion					
Present	37 (31.4)	6 (42.9)	31 (29.8)	0.968	0.364*
Absent	81 (68.6)	8 (57.1)	73 (70.2)		
ER status					
Positive	86 (72.9)	10 (71.4)	76 (73.1)	0.017	1.000#
Negative	32 (27.1)	4 (28.6)	28 (26.9)		
PR status					
Positive	34 (61.7)	6 (54.5)	31 (63.3)	0.284	0.784*
Negative	26 (38.3)	5 (45.5)	18 (36.7)		
Nottingham Prognostic Index					
< 3.4	33 (28.0)	0 (0.0)	33 (35.1)	6.537	0.011*
≥ 3.4	74 (62.7)	13 (100.0)	61 (64.9)		

*Fisher's exact test, # chi square test

Table 5.5: Relationship between ABCC1 expression in breast cancer and clinicopathological variables

Characteristics	All patients (%)	ABCC1+	ABCC1-	χ2 value	p value
Age					
< 50	22 (18.6)	4 (10.5)	18 (22.5)	2.435	0.119#
≥ 50	96 (81.4)	34 (89.5)	62 (77.5)		
Surgery type					
Mastectomy	73 (61.9)	24 (63.2)	49 (61.2)	0.040	0.842#
Wire loop excision	45 (38.1)	14 (36.8)	31 (38.8)		
Tumour size					
< 2 cm	49 (41.5)	13 (34.2)	36 (45.0)	1.235	0.266#
≥ 2 cm	69 (58.5)	25 (65.8)	44 (55.0)		
Nodal metastasis					
Positive	43 (39.1)	14 (23.7)	29 (30.0)	0.037	0.458*
Negative	67 (60.1)	23 (65.8)	44 (61.2)		
Tumour grade					
1	17 (14.4)	3 (7.9)	14(17.5)	3.044	0.218#
2	59 (50.0)	18 (47.4)	41 (51.3)		
3	42 (35.6)	17 (44.7)	25 (31.2)		
DCIS grade					
Low	4 (3.4)	1 (2.6)	3 (3.8)	2.502	0.474*
Intermediate	19 (16.1)	9 (23.7)	10 (12.5)		
High	52 (44.1)	16 (42.1)	36 (45.0)		
Not seen	43 (36.4)	12 (31.6)	31 (38.8)		
Tumour stage					
Limited,I-II	107 (90.7)	35 (92.1)	72 (90.0)	0.134	1.000*
Advanced, III-IV	11 (9.3)	3 (7.9)	8 (10.0)		
Side of tumour					
Left	53 (44.9)	18 (47.4)	35 (43.8)	0.136	0.712#
Right	65 (55.1)	20 (52.6)	45 (55.0)		
Vascular invasion					
Present	37 (31.4)	10 (26.3)	27 (33.8)	0.662	0.416#
Absent	81 (68.6)	28 (73.7)	53 (66.2)		
ER status					
Positive	86 (72.9)	28 (73.7)	58 (72.5)	0.018	0.892#
Negative	32 (27.1)	10 (26.3)	22 (27.5)		
PR status					
Positive	34 (61.7)	13 (65.0)	24 (60.0)	0.141	0.707#
Negative	26 (38.3)	7 (35.0)	16 (40.0)		
Nottingham Prognostic Index					
< 3.4	33 (28.0)	9 (26.5)	24 (32.9)	0.441	0.504#
≥ 3.4	74 (62.7)	25 (73.5)	49 (67.1)		

*Fisher's exact test, # chi square test

Table 5.6: Relationship between ATX expression in breast cancer and clinicopathological variables

Characteristics	All patients (%)	ATX+	ATX-	χ2 value	p value
Age					
< 50	22 (18.6)	12 (15.8)	10 (23.8)	1.147	0.284#
≥ 50	96 (81.4)	64 (84.2)	32 (76.2)		
Surgery type					
Mastectomy	73 (61.9)	52 (68.4)	21 (50.0)	3.891	**0.049#**
Wire loop excision	45 (38.1)	24 (31.6)	21 (50.0)		
Tumour size					
< 2 cm	49 (41.5)	32 (42.1)	17 (40.5)	0.030	0.863#
≥ 2 cm	69 (58.5)	44 (57.9)	25 (59.5)		
Nodal metastasis					
Positive	43 (39.1)	26 (35.6)	17 (45.9)	1.100	0.294#
Negative	67 (60.1)	47 (64.4)	20 (54.1)		
Tumour grade					
1	17 (14.4)	10 (13.2)	7 (16.7)	0.700	0.705#
2	59 (50.0)	37 (48.7)	22 (52.4)		
3	42 (35.6)	29 (38.2)	13 (31.0)		
DCIS grade					
Low	4 (3.4)	4 (5.3)	0 (0.0)	2.182	0.584*
Intermediate	19 (16.1)	12 (15.8)	7 (16.7)		
High	52 (44.1)	34 (44.7)	18 (44.1)		
Not seen	43 (36.4)	26 (34.2)	17 (36.4)		
Tumour stage					
Limited,I-II	107 (90.7)	68 (89.5)	39 (92.9)	0.363	0.744*
Advanced, III-IV	11 (9.3)	8 (10.5)	3 (7.1)		
Side of tumour					
Left	53 (44.9)	34 (44.7)	19 (45.2)	0.003	0.958#
Right	65 (55.1)	42 (55.3)	23 (54.8)		
Vascular invasion					
Present	37 (31.4)	20 (26.3)	17 (40.5)	2.502	0.112#
Absent	81 (68.6)	56 (73.7)	25 (59.5)		
ER status					
Positive	86 (72.9)	53 (69.7)	33 (78.6)	1.068	0.301#
Negative	32 (27.1)	23 (30.3)	9 (21.4)		
PR status					
Positive	37 (61.7)	20 (54.1)	17 (73.9)	2.366	0.124#
Negative	23 (38.3)	17 (45.9)	6 (26.1)		
Nottingham Prognostic Index					
< 3.4	33 (30.8)	21 (30.0)	12 (32.4)	0.067	0.796#
≥ 3.4	74 (69.2)	49 (70.0)	25 (67.6)		

*Fisher's exact test, # chi square test

5.2.3 Relationship between the expression of each lipid signalling molecules and overall survival

All the breast cancer patients were followed up for 10 years. At the time of analysis, 41/118 (34.7%) patients had died. I explored the influence of various factors including the expression of lipid signalling molecules on overall survival (OS) in this cohort of breast cancer patients using the Kaplan Meier method and log-rank test. The Kaplan Meier curves for each clinical characteristics and lipid signalling molecules are shown in Figure. 5.8-5.11. The patients who had mastectomy had poorer overall survival compared to those who had wireloop excision (p=0.033). Patients with NPI of 3.4 or greater had significantly poorer OS (p=0.008). Other clinical characteristics including age group, stage and grade of tumour, lymph node status, side of tumour, ER and PR status showed no significant association with OS. Patients with presence of vascular invasion by tumour showed a borderline significant association with poorer OS (p= 0.058). A log rank test revealed that there was no significant association between the expression of SPHK1, S1PR1, ABCC1 and ATX with OS (Figure 5.11).

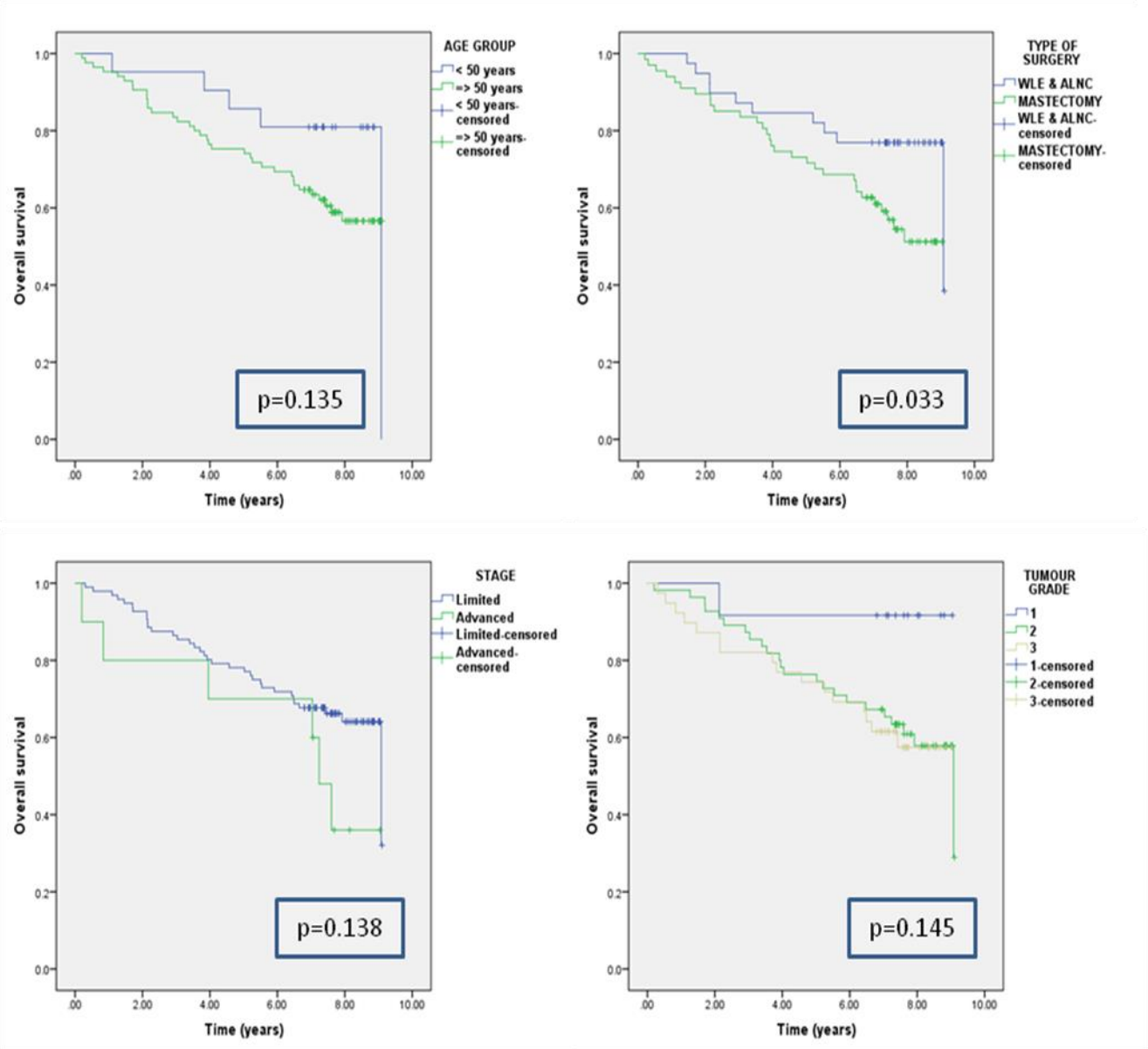

Figure 5.7 The Kaplan Meier overall survival curves by age group, type of surgery, tumour stage and grade of breast cancer patients.

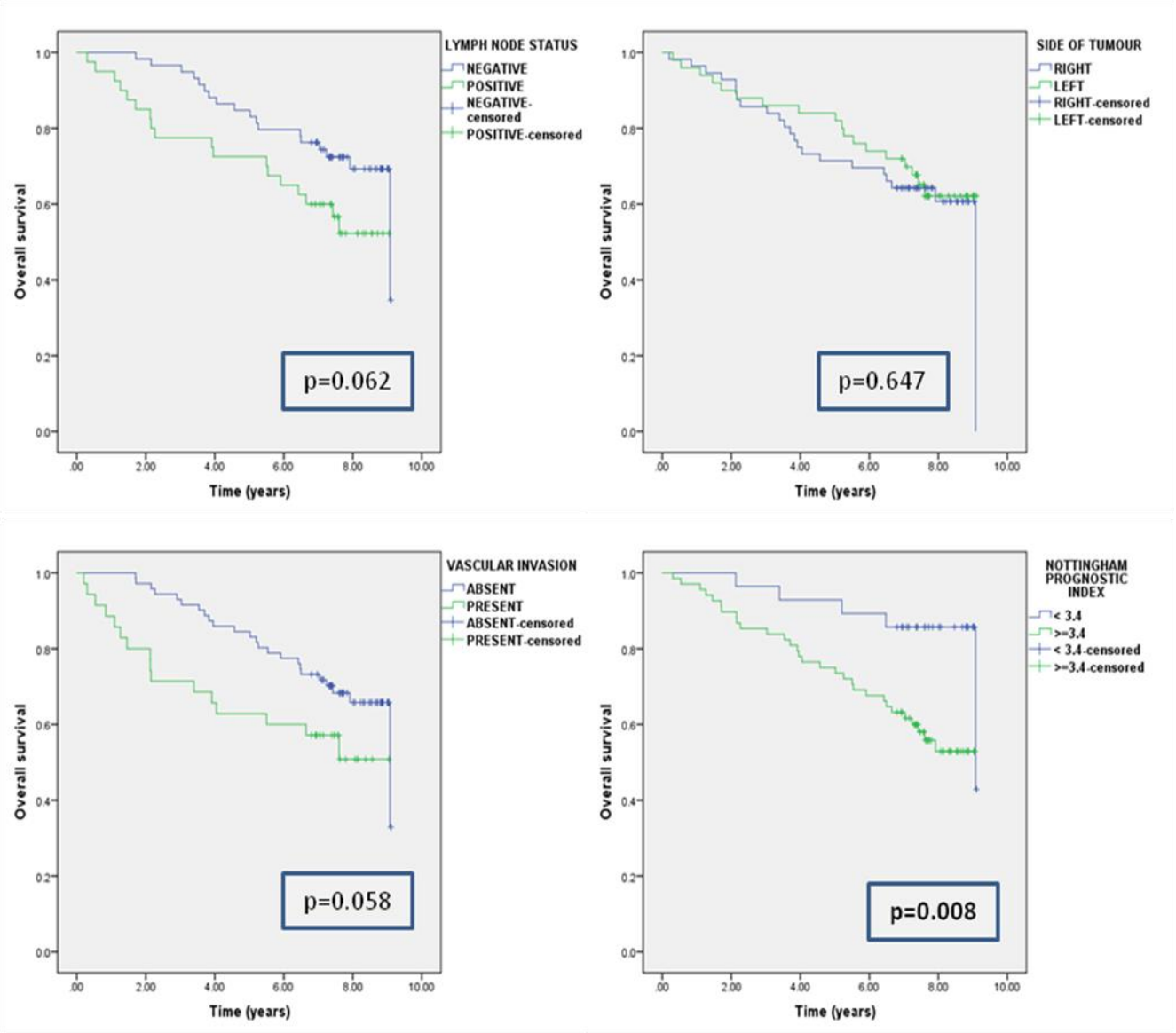

Figure 5.8: The Kaplan Meier overall survival curves by lymph node status, side of tumour, vascular invasion and NPI of breast cancer patients.

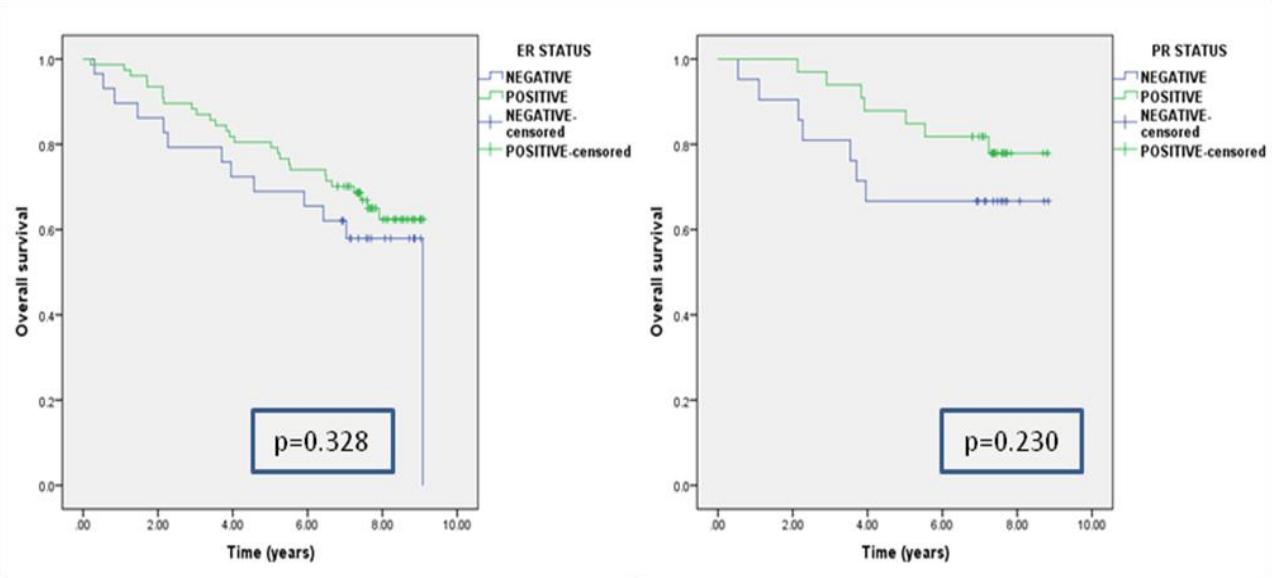

Figure 5.9: Kaplan Meier overall survival curves by ER and PR status of breast cancer patients.

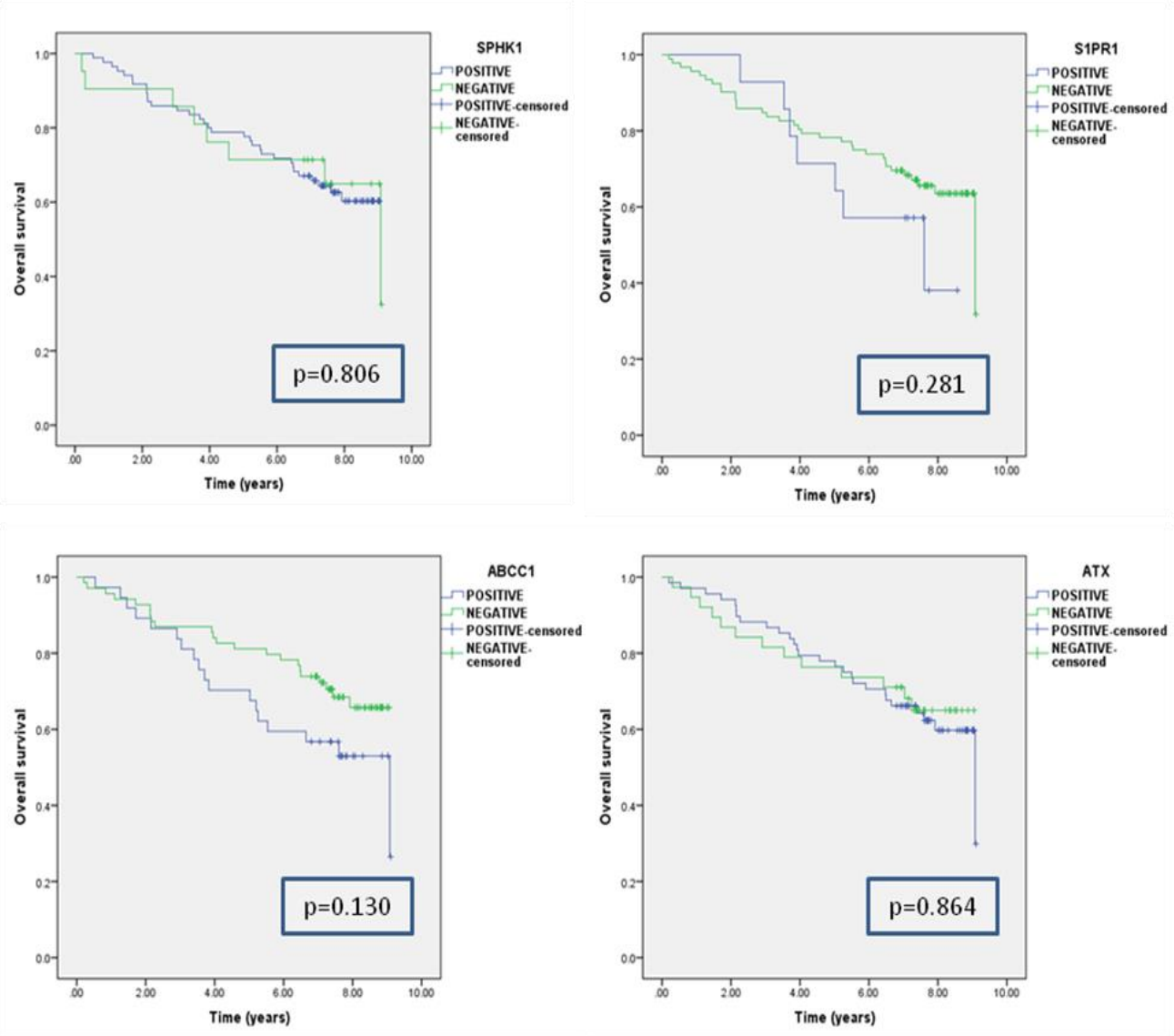

Figure 5.10: The Kaplan Meier overall survival curves by SPHK1, S1PR1 ABCC1 and ATX expression in breast cancer patients.

5.3 Expression of lipid signalling molecules in bladder cancer

I also had available to me 56 cases of primary transitional cell carcinoma of the urinary bladder obtained from the Pathology Department of the Queen Elizabeth Hospital. Each sample was stained for expression of SPHK1, S1PR1, ABCC1 and ATX. Patient demographics are shown in Table 5.7 and in Figure 5.12. Although 58.9% of tumours were smaller than 3 cm and 53.6% were in stage Ta, 62.5% were of high grade morphology. A summary of the expression of the lipid signalling molecules in bladder cancer is shown in Figure 5.13. 95% of cases expressed SPHK1 while 91% of cases were positive for S1PR1. ABCC1 was expressed in 45% of cases and ATX was expressed in 85% of cases.

SPHK1 expression was observed in the cytoplasm and nucleus of both normal urothelium and malignant cells. SPHK1 expression was also seen in fibroblasts, macrophages, plasma cells and endothelial cells lining the blood vessels which served as internal positive control (Figure 5.14). S1PR1 was expressed in both normal urothelium and malignant cells with localisation to the cytoplasm (Figure 5.15). Normal urothelium was either negative or showed only low levels of ABCC1, whereas in ABCC1 positive tumours, levels of expression in tumour cells were higher than in normal cells (Figure 5.16). ATX was weakly expressed in normal urothelium but was strongly expressed in malignant cells and endothelial lining of blood vessels (Figure 5.17).

Table 5.7: Clinical characteristics of 56 cases of transitional cell carcinoma of the bladder

Characteristic	All patients (%)
Tumour size	
Range (cm)	0.5-15
< 3 cm	33 (58.9)
≥ 3 cm	21 (37.5)
Unknown	2 (3.6)
Tumour grade	
Grade 1	14 (25.0)
Grade 2	7 (12.5)
Grade 3	35 (62.5)
Tumour stage	
Ta	30 (53.6)
T1	15 (26.8)
T2-T4	11 (19.6)

A

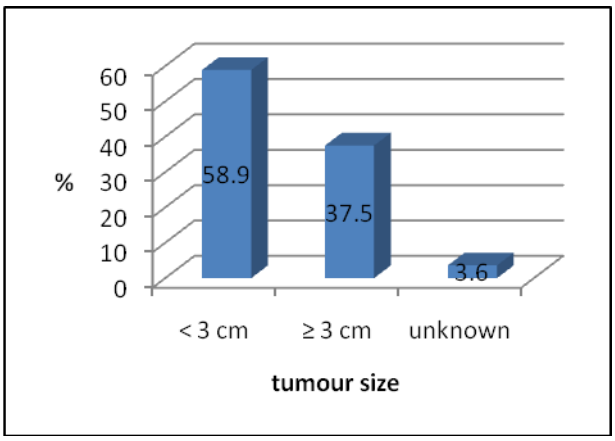

B

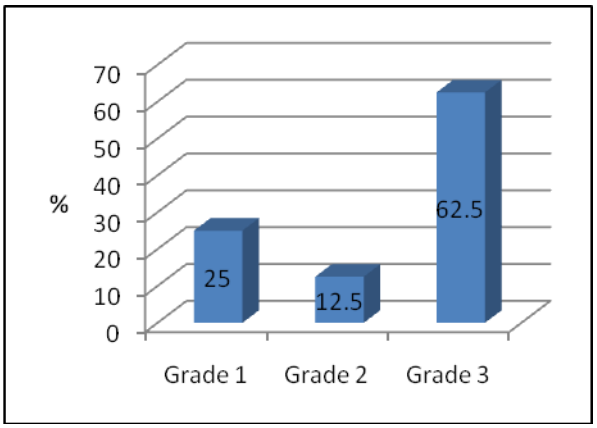

C

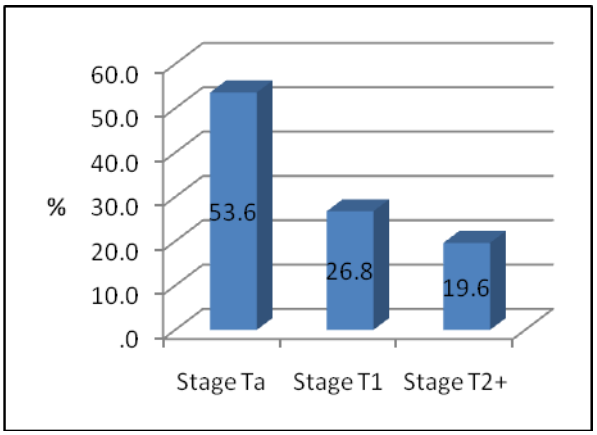

Figure 5.11: The clinicopathological characteristics of bladder cancer patients according to tumour A) size, B) grade and C) stage.

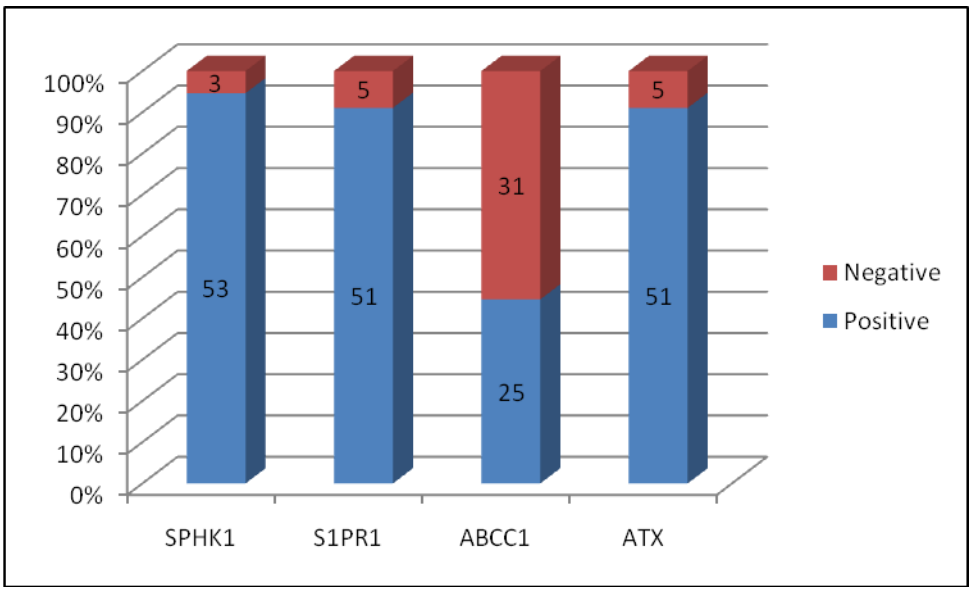

Figure 5.12: The summary of expression of lipid signalling molecules in bladder cancer.

A

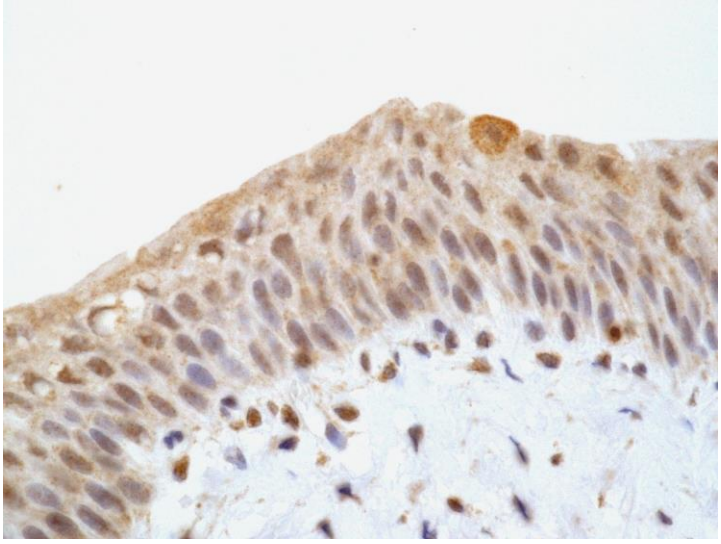

B

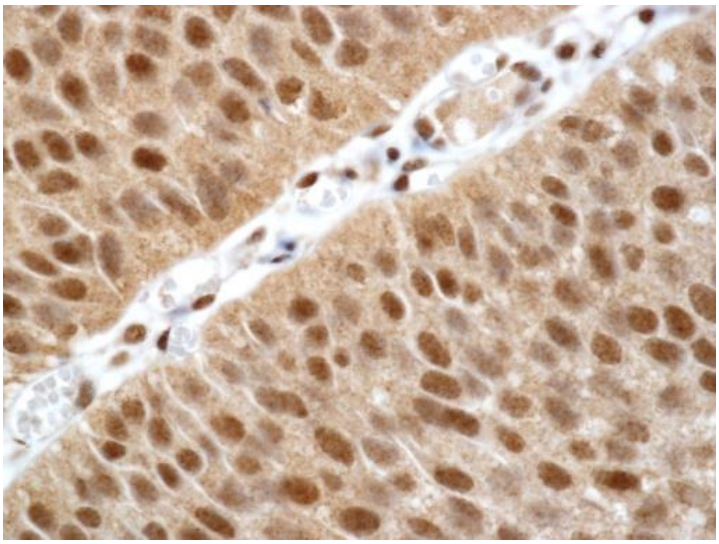

Figure 5.13: SPHK1 expression in normal urothelium and in bladder cancer. SPHK1 is expressed in both A) the normal urothelium (x400) B) and in the nucleus and cytoplasm of bladder cancer cells (x400).

A

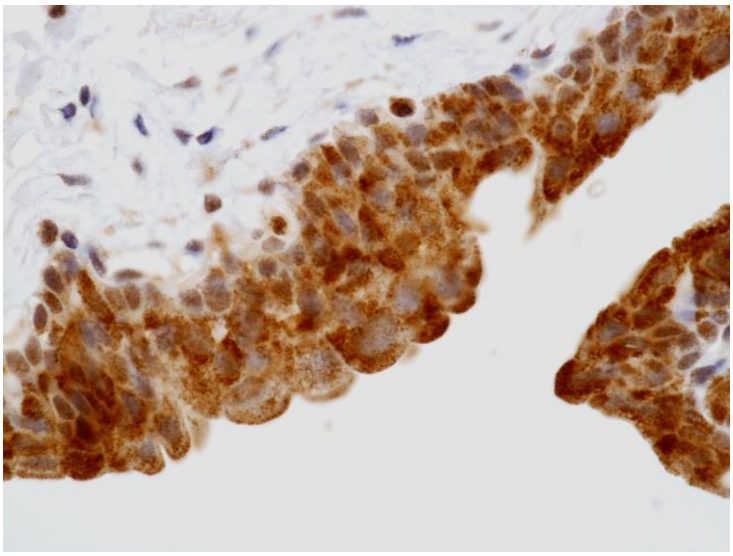

B

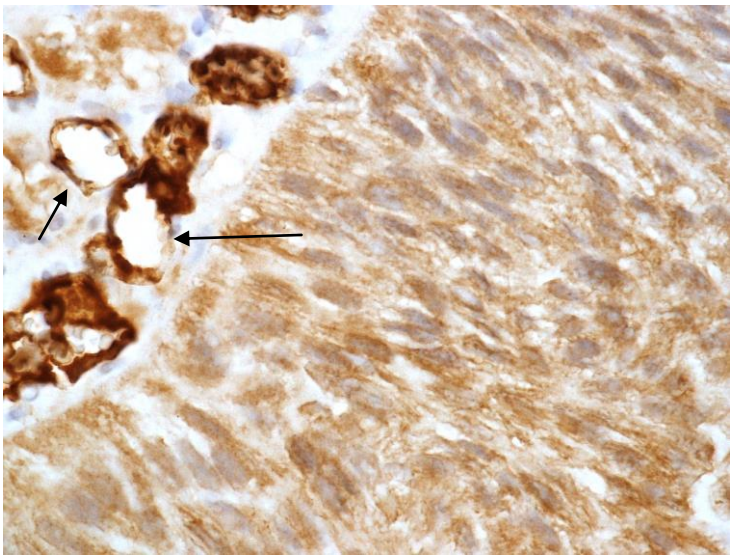

Figure 5.14: S1PR1 expression in normal urothelium and in bladder cancer A) Strong expression of S1PR1 in the cytoplasm and cytoplasmic membrane of normal urothelium (x400) B) Moderate S1PR1 expression in the cytoplasm and cytoplasmic membrane of bladder cancer cells. Note strong S1PR1 staining in the endothelial cells of blood vessels (arrowed) (x400).

A

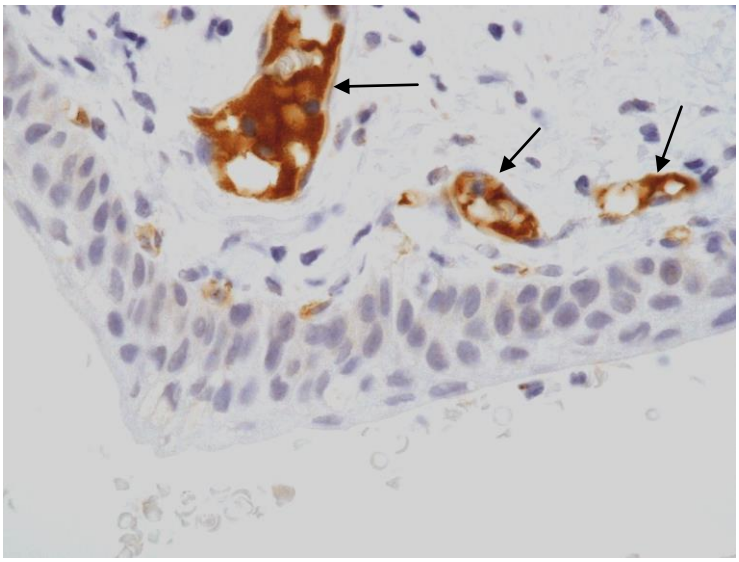

B

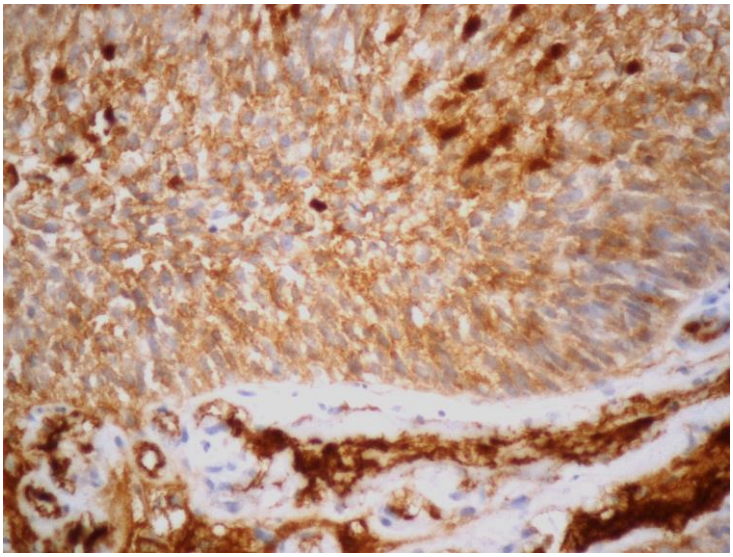

Figure 5.15: ABCC1 expression in normal urothelium and bladder cancer A) Absence of ABCC1 expression in normal urothelium but strong ABCC1 expression in the blood vessels (arrowed)(x400) B) Strong ABCC1 expression in the cytoplasm of bladder cancer cells (x400).

A

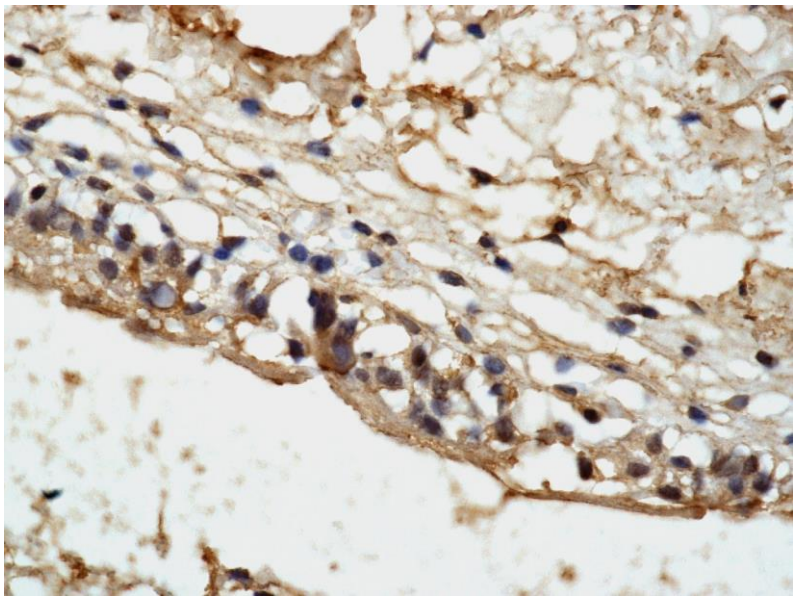

B …… .

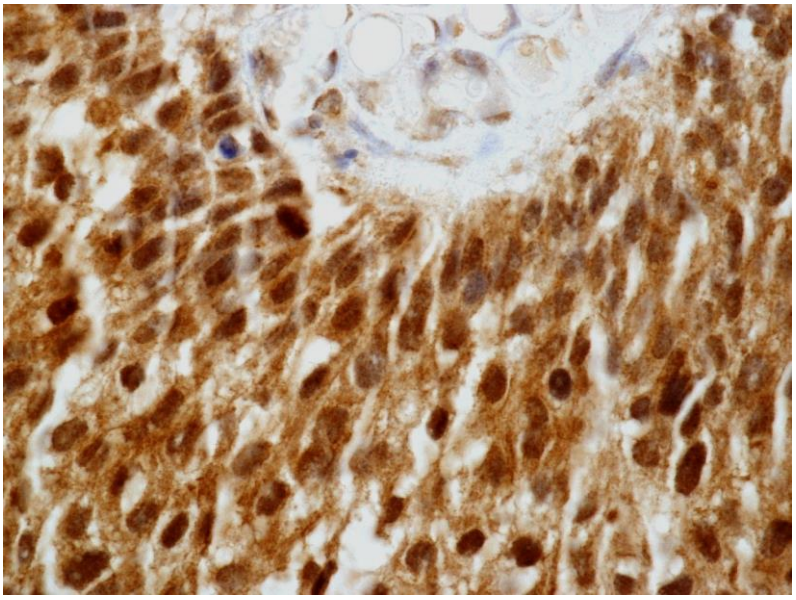

Figure 5.16: ATX expression in bladder cancer. A) Normal urothelium exhibited mild ATX expression (x 600). B) Strong ATX expression was observed in bladder cancer and the staining was localised to the cytoplasm of malignant cells. (x 600).

5.3.1 Relationship between the expression of lipid signalling molecules in bladder cancer and clinicopathological parameters

Having established the prevalence of expression of the different lipid signalling molecules in bladder cancer, I next studied the relationship between expression and clinicopathological features, including tumour size, tumour stage and tumour grade. I used Fisher's exact test to determine if the expression of each individual lipid signalling molecule was significantly associated with any of these clinicopathological features. No significant associations were found. The results of this analysis are summarised in Tables 5.8 - 5.11.

Table 5.8: SPHK1 expression in bladder cancer in relation to tumour size, grade and stage.

Characteristic	All patients (%)	SPHK1 +	SPHK1 -	p value
Tumour size				
< 3 cm	33 (58.9)	31 (58.5)	2 (66.7)	1.000*
≥ 3 cm	21 (37.5)	20 (37.7)	1 (33.3)	
Unknown	2 (3.6)	2 (3.8)	0 (0.0)	
Tumour grade				
Grade 1	14 (25.0)	13 (24.5)	1 (33.3)	1.000*
Grade 2	7 (12.5)	7 (13.2)	0 (0.0)	
Grade 3	35 (62.5)	33 (62.3)	2 (66.7)	
Tumour stage				
Ta	30 (53.6)	29 (54.7)	1 (33.3)	0.267*
T1	15 (26.8)	13 (24.5)	2 (66.7)	
T2-T4	11 (19.6)	11 (20.8)	0 (0.0)	

*Fisher's exact test

Table 5.9: S1PR1 expression in bladder cancer in relation to tumour size, grade and stage.

Characteristic	All patients (%)	S1PR1+	S1PR1-	p value
Tumour size				
< 3 cm	33 (58.9)	31 (60.8)	2 (40.0)	0.475*
≥ 3 cm	21 (37.5)	18 (35.3)	3 (60.0)	
Unknown	2 (3.6)	2 (3.9)	0 (0.0)	
Tumour grade				
Grade 1	14 (25.0)	13 (25.5)	1 (20.0)	0.808*
Grade 2	7 (12.5)	6 (11.8)	1 (20.0)	
Grade 3	35 (62.5)	32 (62.7)	3 (60.0)	
Tumour stage				
Ta	30 (53.6)	27 (52.9)	3 (60.0)	1.000*
T1	15 (26.8)	14 (27.5)	1 (20.0)	
T2-T4	11 (19.6)	10 (19.6)	1 (20.0)	

*Fisher's exact test

Table 5.10: ABCC1 expression in bladder cancer in relation to tumour size, grade and stage.

Characteristic	All patients (%)	ABCC1+	ABCC1-	p value
Tumour size				
< 3 cm	33 (58.9)	15 (60.0)	18 (58.1)	0.316*
≥ 3 cm	21 (37.5)	8 (32.0)	13 (41.9)	
Unknown	2 (3.6)	2 (8.0)	0 (0.0)	
Tumour grade				
G1	14 (25.0)	9 (36.0)	5 (16.1)	0.223*
G2	7 (12.5)	2 (8.0)	5 (16.1)	
G3	35 (62.5)	14 (56.0)	21 (67.7)	
Tumour stage				
Ta	30 (53.6)	15 (60.0)	15 (48.4)	0.424*
T1	15 (26.8)	7 (28.0)	8 (25.8)	
T2-T4	11 (19.6)	3 (12.0)	8 (25.8)	

*Fisher's exact test

Table 5.11: ATX expression in bladder cancer in relation to tumour size, grade and stage

Characteristic	All patients (%)	ATX+	ATX-	p value
Tumour size				
< 3 cm	33 (58.9)	29 (80.0)	4 (56.9)	0.700*
≥ 3 cm	21 (37.5)	20 (39.2)	1 (20.0)	
Unknown	2 (3.6)	2 (3.9)	0 (0.0)	
Tumour grade				
G1	14 (25.0)	11 (21.6)	3 (60.0)	0.204*
G2	7 (12.5)	7 (13.7)	0 (0.0)	
G3	35 (62.5)	33 (64.7)	2 (40.0)	
Tumour stage				
Ta	30 (53.6)	27 (52.9)	3 (60.0)	1.000*
T1	15 (26.8)	14 (27.5)	1 (20.0)	
T2-T4	11 (19.6)	10 (19.6)	1 (20.0)	

*Fisher's exact test

5.4 Expression of lipid signalling molecules in lung cancer

Finally I performed immunohistochemistry for SPHK1, S1PR1, ABCC1 and ATX on 68 cases of lung cancer obtained as a tissue microarray from the Department of Pathology and Laboratory of Molecular Pathology, Faculty of Medicine and Dentistry, Palacky University, Olomouc, Czech Republic. However due to tissue losses during sectioning and staining procedures, the number of cases analysed varied between each marker. The lung cancer patients comprised five histological subtypes; squamous cell carcinoma, adenocarcinoma, small cell, large cell and anaplastic carcinoma. The clinical characteristics of lung cancer patients are shown in Table 5.12.

Figure 5.18 provides a summary of the expression of each lipid signalling molecule. SPHK1 was expressed in 19/61 cases (31.1%). In all positive cases the expression was of moderate intensity compared to the positive control which was the endothelial lining of blood vessels. SPHK1 was localised to the nucleus and cytoplasm of malignant cells. SPHK1 was also seen in the cytoplasm of normal respiratory epithelium lining the bronchi. However in these cells, the cytoplasmic expression was of mild to moderate intensity. The apical surface of normal respiratory epithelium showed intense SPHK1 staining. Prominent SPHK1 staining was also observed within the alveolar macrophages and in nerve bundles. S1PR1 was weakly expressed in all cases. (S1PR1 downregulation in lung cancer wil be further discussed in the discussion section). Endothelial lining of blood vessels served as internal positive control for S1PR1 staining. Cytoplasmic expression of ABCC1 was weak in normal respiratory epithelium and arterioles but strong ABCC1 expression was observed in the cytoplasm of malignant cells in 85% of cases. ATX was expressed in 38% of lung cancer patients and

staining was localised in the cytoplasm of malignant cells. Moderate ATX staining was also seen in normal respiratory epithelium.

Table 5.12: Clinical characteristics of lung cancer patients

Characteristics	**All patients** **n=68 (%)**
Age	
< 70	60 (88.2)
≥ 70	8 (11.8)
Gender	
Male	55 (80.9)
Female	13 (19.1)
Histological subtype	
Squamous cell carcinoma	28 (41.2)
Adenocarcinoma	29 (42.6)
Small cell carcinoma	3 (4.4)
Large cell carcinoma	6 (8.8)
Anaplastic carcinoma	2 (2.9)
Tumour stage	
Limited,I-II	20 (35.7)
Advanced, III-IV	36 (64.3)
Nodal metastasis	
Positive	33 (58.9)
Negative	23 (41.1)
Distant metastasis	
Positive	6 (10.7)
Negative	50 (89.3)

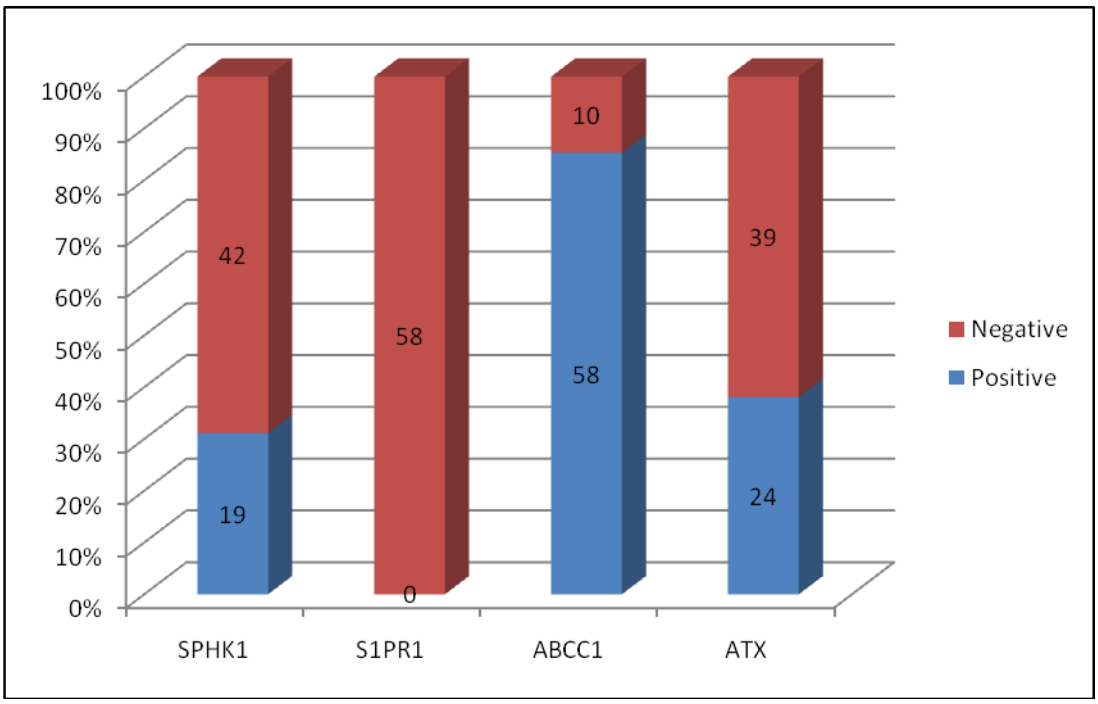

Figure 5.17: Summary of the expression of lipid signalling molecules in lung cancer.

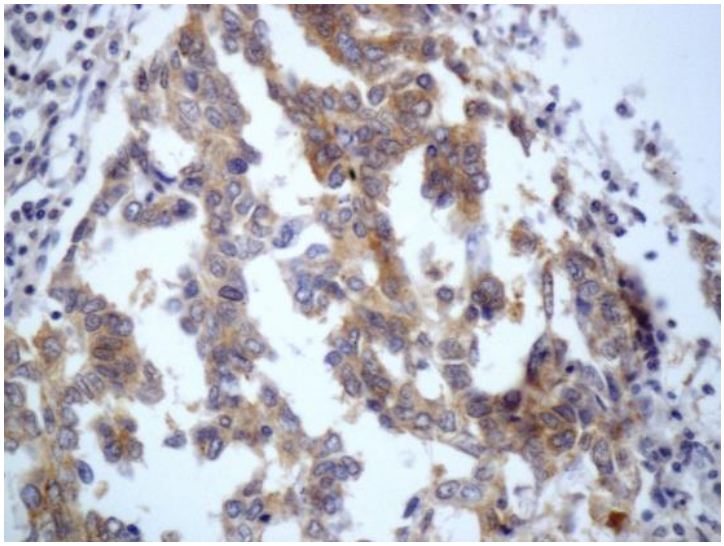

A

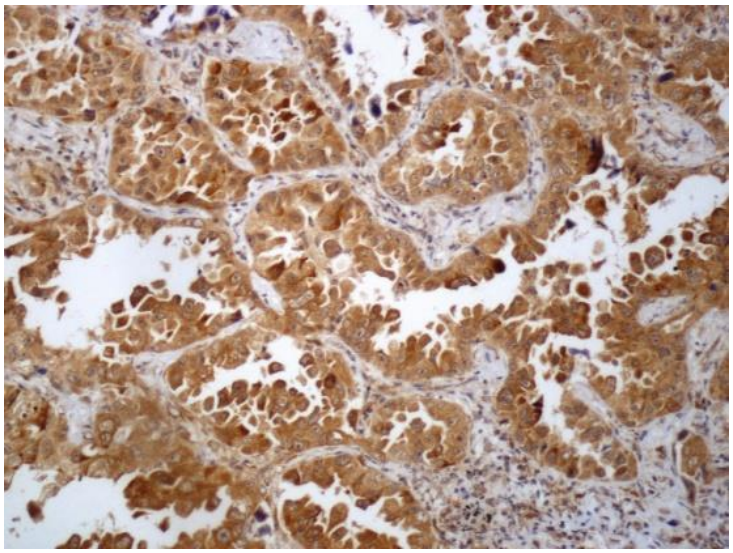

B

Figure 5.18: SPHK1 expression in normal lung and lung cancer A) Weak expression of SPHK1 in the cytoplasm of normal bronchial lining epithelium (x400) B) Strong SPHK1 expression in the cytoplasm of lung adenocarcinoma (x400)

A

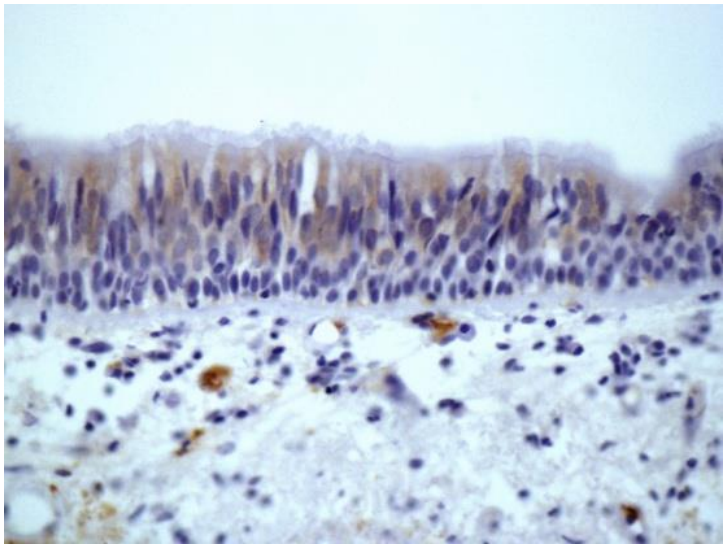

B

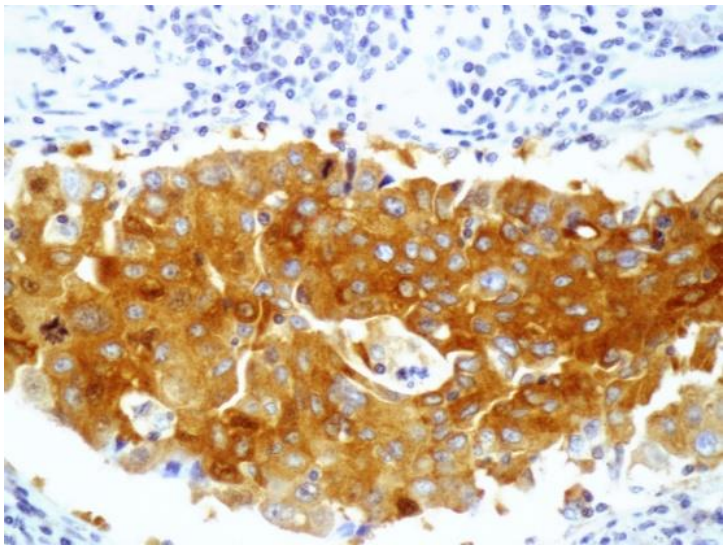

Figure 5.19: ABCC1 expression in normal lung tissue and lung cancer A) Weak ABCC1 expression in normal respiratory epithelium (x400) and B) Strong ABCC1 expression in malignant cells (x400).

A

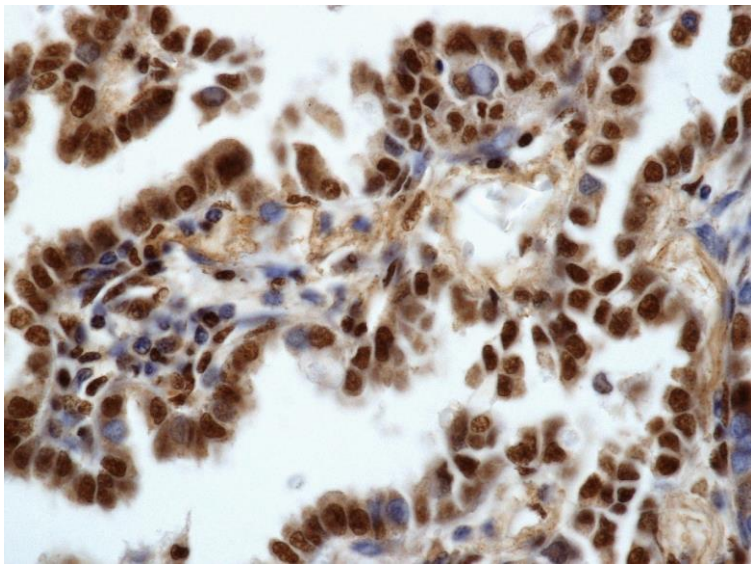

B

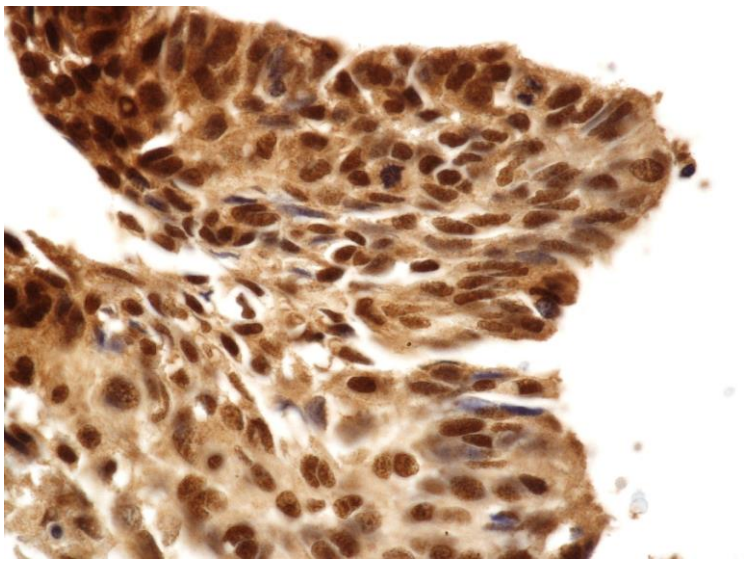

Figure 5.20: ATX expression in normal lung tissue and lung cancer A) Moderate to strong ATX expression was observed in the bronchiolar lining cells (x 600) B) Strong ATX expression was seen in lung cancer (x 600).

5.4.1 Expression of lipid signalling molecules in lung cancer and their relationship with clinicopathological parameters

Tables 5.13 to 5.15 summarise the expression of each lipid signalling molecule in lung cancer in relation to clinicopathological parameters. ABCC1 expression was commonly seen in adenocarcinoma subtype of lung cancer (Table 5.14, p= 0.015) and ATX positivity was more common in patients of advanced stage of disease (Table 5.15, p=0.015). No other significant associations were observed.

Table 5.13: Expression of SPHK1 in lung cancer in relation to clinicopathological parameters

Characteristics	All patients n=61 (%)	SPHK1 +	SPHK1 -	χ2 value	p value
Age					
< 70	51 (83.6)	16 (84.2)	35 (83.3)	0.007	0.624*
≥ 70	10 (16.4)	3 (15.8)	7 (16.7)		
Gender					
Male	48 (80.3)	17 (89.5)	32 (75.6)	1.461	0.309*
Female	12 (19.7)	2 (10.5)	10 (24.4)		
Histological subtype					
Squamous cell carcinoma	27 (44.3)	9 (47.4)	18 (42.9)	2.853	0.678*
Adenocarcinoma	26 (42.6)	8 (42.1)	18 (42.9)		
Small cell carcinoma	2 (3.3)	0 (0.0)	2 (4.8)		
Large cell carcinoma	5 (8.2)	1 (5.3)	4 (9.5)		
Anaplastic carcinoma	1 (1.6)	1 (5.3)	0 (0.0)		
Tumour stage					
Limited,I-II	16 (32.0)	3 (20.0)	13 (37.1)	1.418	0.328*
Advanced, III-IV	34 (68.0)	12 (80.0)	22 (62.9)		
Nodal metastasis					
Positive	30 (60.0)	10 (66.7)	20 (57.1)	0.397	0.529#
Negative	20 (40.0)	5 (33.3)	15 (42.9)		
Distant metastasis					
Positive	6 (12.0)	2 (13.3)	4 (11.4)	0.036	1.000*
Negative	43 (80.0)	13 (86.7)	31 (88.6)		

#chi square test, *Fisher's exact test

Table 5.14: Expression of ABCC1 in lung cancer in relation with clinicopathological parameters

Characteristics	All patients n=68 (%)	ABCC1+	ABCC1-	$\chi 2$ value	p value
Age					
< 70	60 (88.2)	52 (89.7)	8 (80.0)	0.766	0.381*
≥ 70	8 (11.8)	6 (10.3)	2 (20.0)		
Gender					
Male	55 (80.9)	46 (79.3)	9 (90.0)	0.630	0.427*
Female	13 (19.1)	12 (20.7)	1 (10.0)		
Histological subtype					
Squamous cell carcinoma	28 (41.2)	23 (39.7)	5 (50.0)	10.788	**0.015***
Adenocarcinoma	29 (42.6)	28 (48.3)	1 (10.0)		
Small cell carcinoma	3 (4.4)	1 (1.7)	2 (20.0)		
Large cell carcinoma	6 (8.8)	5 (8.6)	1 (10.0)		
Anaplastic carcinoma	2 (2.9)	1 (1.7)	1 (10.0)		
Tumour stage					
Limited,I-II	20 (35.7)	18 (38.3)	2 (22.2)	0.850	0.466*
Advanced, III-IV	36 (64.3)	29 (61.7)	7 (79.8)		
Nodal metastasis					
Positive	33 (58.9)	27 (57.4)	6 (66.7)	0.261	0.723*
Negative	23 (41.1)	20 (42.6)	3 (33.3)		
Distant metastasis					
Positive	6 (10.7)	5 (10.6)	1 (11.1)	0.002	0.669*
Negative	50 (89.3)	42 (89.4)	8 (88.9)		

*Fisher's exact test

Table 5.15: Expression of ATX in lung cancer in relation to clinicopathological parameters

Characteristics	All patients n=63 (%)	ATX+	ATX-	$\chi 2$ value	p value
Age					
< 70	52 (82.5)	20 (83.3)	32 (82.1)	0.017	1.000*
≥ 70	11 (17.5)	4 (16.7)	7 (17.9)		
Gender					
Male	50 (79.4)	17 (70.8)	33 (84.6)	1.723	0.214*
Female	13 (20.6)	7 (29.2)	6 (15.4)		
Histological subtype					
Squamous cell carcinoma	28 (44.4)	9 (37.5)	19 (48.7)	4.052	0.375*
Adenocarcinoma	25 (39.7)	13 (54.2)	12 (30.8)		
Small cell carcinoma	2 (3.2)	0 (0.0)	2 (5.1)		
Large cell carcinoma	7 (11.1)	2 (8.3)	5 (12.8)		
Anaplastic carcinoma	1 (1.6)	0 (0.0)	1 (2.6)		
Tumour stage					
Limited,I-II	19 (37.3)	3 (15.8)	16 (50.0)	5.969	**0.015**[#]
Advanced, III-IV	32 (62.7)	16 (84.2)	16 (50.0)		
Nodal metastasis					
Positive	30 (58.8)	12 (63.2)	18 (56.2)	0.235	0.628*
Negative	21 (41.2)	7 (36.8)	14 (35.9)		
Distant metastasis					
Positive	6 (11.8)	4 (21.1)	2 (6.2)	2.467	0.179*
Negative	45 (88.2)	15 (78.9)	30 (93.8)		

[#]Chi square test, *Fisher's exact test

A

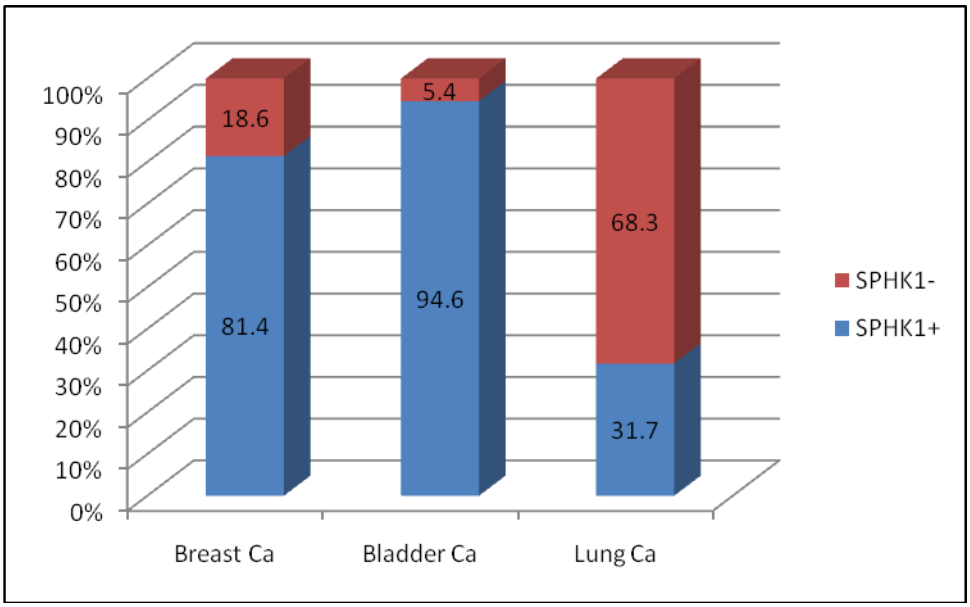

B

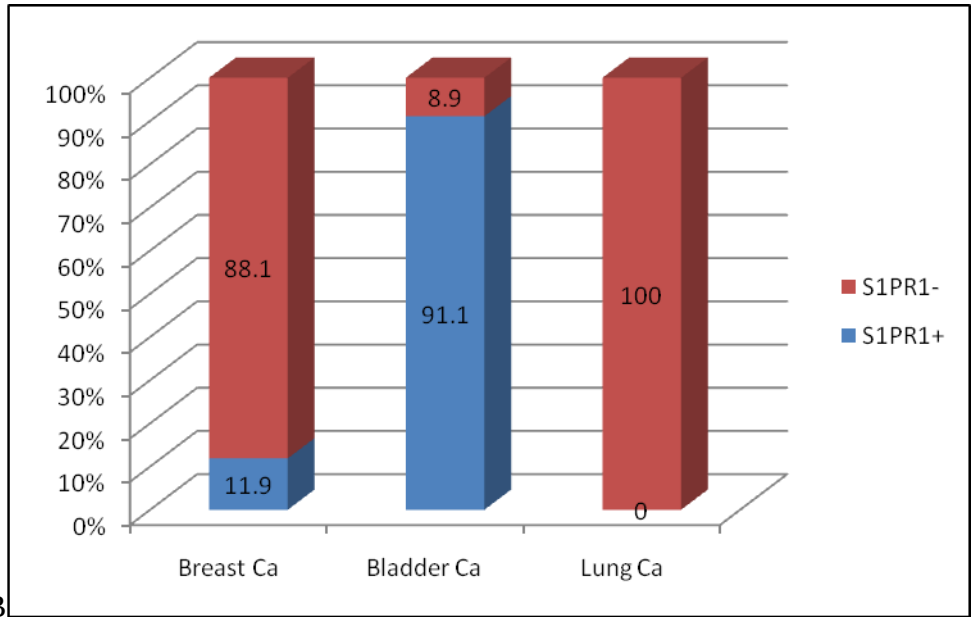

Figure 5.21: Expression of A) SPHK1 B) S1PR1 in breast, bladder and lung cancer

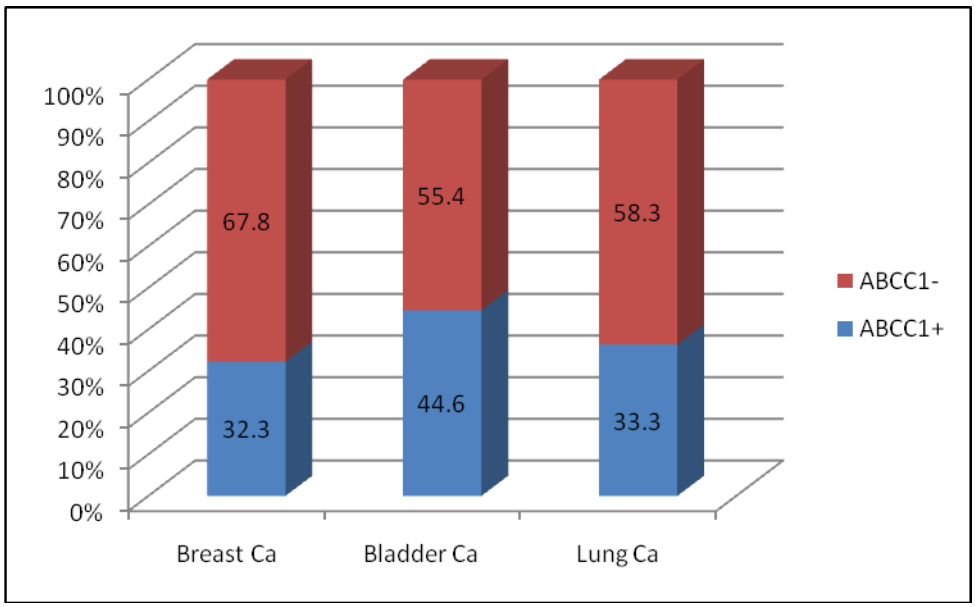

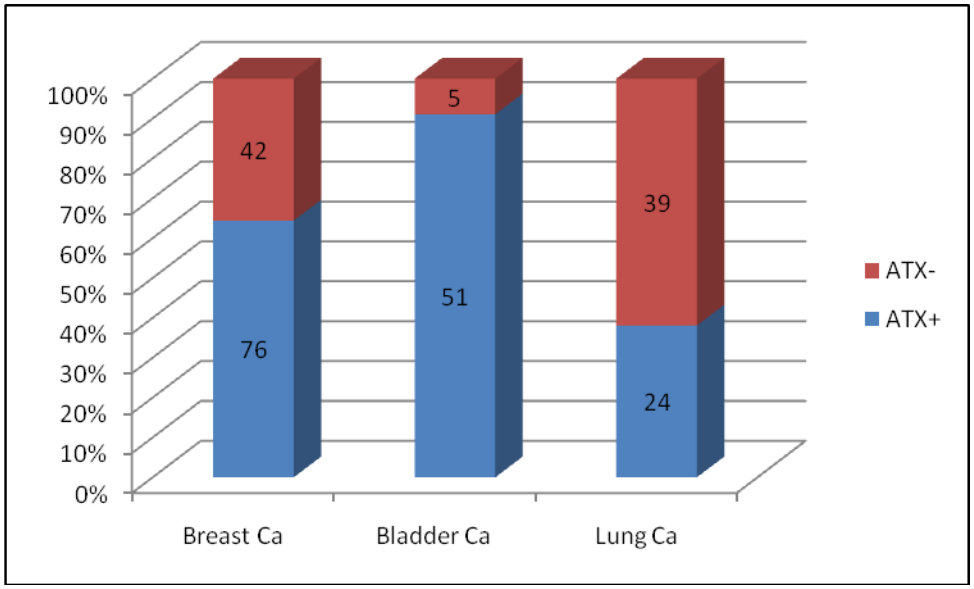

Figure 5.22: Expression of A) ABCC1 and B) ATX in breast, bladder and lung cancer

5.5 Discussion

Expression of lipid signaling molecules in breast cancer

In this study I have shown that SPHK1, which is the key regulator of S1P formation is overexpressed in the majority of breast cancer (81.4%). Breast cancer patients with tumours expressing high levels of cytoplasmic SPHK1 had significantly shorter recurrence times than those who expressed low levels of cytoplasmic SPHK1 with a difference in recurrence time of 10.5 years, suggesting that the overexpression of SPHK1 is a poor prognostic factor in breast cancer (Watson et al., 2010). Ling's group has found that SPHK1 mRNA levels increase with advanced stage breast cancer which suggest increased S1P levels during disease progression (Ling et al. 2011). In contrast to Ling's findings, I found that SPHK1 expression was not significantly associated with stage of breast cancer or with any other clinicopathological parameters. SPHK1 expression also did not show any significant association with survival which also contradicts the findings of Ruckhaberle et al who found that SPHK1 expression was associated with reduced patient survival (Ruckhäberle et al. 2008).

Export of S1P is mediated by ABCC1 and ABCG2 transporters. In this study, I found that ABCC1 was overexpressed in only 38% of cases; these data suggest that other S1P transporters are likely to be involved in transporting S1P in breast cancer cells.

Although I found that S1PR1 was expressed in only 14% of breast cancers, its expression showed a significant association with poor prognostic factors i.e. larger tumour size, and a higher Nottingham Prognostic Index. Strong membranous S1PR1 has been reported to be associated with shorter time to recurrence in breast cancer patients (Watson et al., 2010).

High cytoplasmic S1PR1 expression level was also associated with shorter disease-specific survival. The findings of Watson et al. suggest that there might be stimulation of a pathway including SPHK1, S1PR1 and ERK-1/2 which might drive the progression of breast cancer (Watson et al., 2010).

Yang's group has shown that ATX mRNA was overexpressed about 4.3 times more in cancerous as compared to normal breast tissues (Yang et al. 2002). ATX also affects motility dependent processes such as invasion and metastasis of breast cancer cells as well as angiogenesis (Nam et al. 2000). In this study I found that ATX positive breast cancer patients were more likely to undergo mastectomy than wire-loop excision (p= 0.049) however ATX was not associated with poorer OS. Previous work by Liu and others supports a role of LPA, ATX, LPA receptors and lipid phosphate phosphatases in cancer (Liu et al. 2009; Yu et al. 2008; Kitayama et al. 2004), therefore served as possible therapeutic targets for anti-cancer therapeutics. Among the therapeutics under development are monoclonal antibodies against LPA, ATX inhibitors and LPA receptor antagonists (M. Murph & Mills 2007). Lpathomab^{TM},, a monoclonal antibody targeting LPA has been developed and hopefully to enter clinical trials soon.

Expression of lipid signaling molecules in bladder cancer

I found that SPHK1 was expressed in 91.6% and S1PR1 was expressed in 91.1% of bladder cancer. J82 cells were shown to express S1PR1 and S1PR3 mRNA which regulate thrombin and LPA-stimulated motility. S1P caused enhancement of thrombin-stimulated migration in bladder cancer cells. Exogenous S1P and SPPC also caused a rapid and transient increase in intracellular Ca2+ in J82 cells but did not stimulate the growth of these cells (Rümenapp et

al. 2000). Stimulation of cell growth was however observed after treatment with LPA and thrombin.

ABCC1 expression was seen in 44.6% of bladder cancer cases and is also expressed in the endothelial lining cells of blood vessels. Scherman et al had shown that the expression of ABCC1 in endothelial cells of microvessels in the brain play a role in the blood brain barrier hence it has been a critical target for central nervous system (CNS) pharmaceuticals (Scherrmann 2005). Little is known about the role ABCC1 in bladder cancer.

ATX was expressed in 85% of bladder cancer and in the endothelial lining of blood vessels. ATX was found to be essential for angiogenesis (van Meeteren et al. 2006) and endothelial cell migration (Ptaszynska et al 2011). For bladder cancer, no clinical data was available to correlate the expression of these lipid molecules with overall survival.

Expression of lipid signaling molecules in lung cancer

SPHK1 mRNA levels were shown to be higher in lung cancer compared to their normal tissue counterparts (French et al.,2003a). The present study has shown that SPHK1 is overexpressed in 31% of lung cancers. SPHK1 over-expression was found in all histological subtypes of lung cancer except for small cell carcinoma. Johnson et al found that all 25 cases (100%) of non small cell lung cancer (NSCLC) stained with SPHK1 antibody showed overwhelmingly positive SPHK1 expression as compared to adjacent normal lung tissue (Johnson et al., 2005). The up-regulation of SPHK1 was confirmed at the mRNA level by cDNA profiling array. Nine out of 20 patients showed an elevation of more than two fold when tumour tissues were compared to adjacent normal tissues. In my study I have observed

the localization of SPHK1 staining in a variety of structures in lung tissue. The apical surface of normal respiratory epithelium displayed intense SPHK1 staining indicating a role for SPHK1 in the ciliary movement in aiding mucociliary clearance. SPHK1 was also seen in the serous glands but was absent in the mucous glands. This is not surprising as Boujaoude's group has found that the cystic fibrosis transmembrane conductance regulator was mainly localised to the serous cells and later it was discovered that this regulator protein could regulate the transport of S1P (which is produced by abundant SPHK1 in serous glands) across the plasma membrane of cells (Boujaoude et al. 2001). As serous cells produce abundant protein with antimicrobial, anti-inflammatory, antiprotease and antioxidant properties, it is possible that secreted S1P plays a role in these physiological and pathological functions. In this study, strong SPHK1 expression was also seen in the cytoplasm of alveolar macrophages which supports the findings of S1P as a physiological activator of alveolar macrophages (Hornuss et al., 2001).

S1PR1 was found to be strongly expressed in normal respiratory epithelium, however in this study I found that S1PR1 was weakly staining in lung cancer. It is plausible that S1PR1-mediated S1P signalling could negatively regulate tumour progression or growth. In support of this, it has been shown that S1PR1 signalling is downregulated in intestinal tumourigenesis (Sabino Zani et al., 2006). Furthermore, analysis of S1PR1 expression on ONCOMINE (www.oncomine.org) reveals the findings of Selamat's group that S1PR1 was downregulated in 47/117 (40.1%) of lung cancer patients via gene expression microarray. In another gene expression analysis study by Garber's group showed that S1PR1 was downregulated in 51 out of 73 (70%) lung cancer mRNA.(www.oncomine.org). Therefore, it can be speculated that S1PR1 signalling inhibits proliferation and survival in lung cancer. With this limited

study of mine, it is not known which signalling pathways might mediate the tumour suppressive role of S1PR1 in these malignancies, but this will be the subject of future investigastions in determining its potential for therapeutic intervention.

My finding showed that S1PR2 was expressed in 3% of lung cancer. The downregulation of S1PR2 has been shown to induce the formation of Diffuse large B cell lymphoma in transgenic mice (Cattoretti et al., 2010). ATX was overexpressed in 38% of lung cancer which is in keeping with the findings of Yang and co-workers who found ATX mRNA expression in eight out of 12 (58%) lung cancer cell lines. Strong ATX expression was observed mainly in poorly differentiated lung carcinomas. I found that lung cancer patients expressing ATX were more likely to present at advanced stage of disease. The impact of the overexpression of ATX in lung cancer warrants further investigation.

Taken together, my findings show that the levels of expression of lipid signalling proteins differ in different epithelial malignancies. Their expression pattern however provide clues as how these lipid signalling molecules may play a role in the pathogenesis of breast, bladder and lung cancer, for instance, S1PR1 and ATX may be a prognostic marker in breast cancer and lung cancer, respectively. The role of each signalling molecules in these malignancies warrants further investigation.

CHAPTER 6

FINAL CONCLUSION AND FUTURE WORK

Main findings

In this study I have profiled the expression of different lipid signalling molecules in two common haematological malignancies; HL and DLBCL and in three types of epithelial cancers. I found that S1PR1 was commonly expressed in both HL and DLBCL. I have also shown that in breast cancer, S1PR1 was associated with larger tumour size and higher NPI which suggest that S1PR1 is a poor prognostic marker in breast cancer. Given the availability of S1PR1 antagonists, my findings suggest that S1PR1 could be a therapeutic target in S1PR1 positive cancers. ATX is also an interesting lipid molecule to be studied further. ATX was commonly expressed in breast and bladder cancer and its expression was significantly associated with advanced stage of lung cancer.

Using gene expression I managed to show that anti-S1P, Sphingomab could restore the B cell receptor phenotype in HL L591 cell line and the downregulation of S1PR3 and S1PR5 by Sphingomab suggests that these two S1P signaling pathways are possible therapeutic targets for Sphingomab in cancer therapeutics.

I confirmed previous reports that EBV positivity was significantly associated with shorter time to death in DLBCL patients. Presence of more than one extranodal site of disease and intermediate to high IPI were also associated with poorer overall survival.

Future work

More detail analysis are required to determine the contribution of these lipid molecules in cancers. Using S1PR agonist/antagonists, we could explore their effects in the epithelial tumours, HL and DLBCL cell lines that over-express either one or more of the S1P receptors. The impact includes viability, proliferation, migration and apoptosis. Over-expression or knockdown experiments could be performed to see the cell signalling pathways regulated by these lipid molecules. Particularly in HL, we need to explore how SPHK1 mediates the oncogenicity of S1PR1 and in lung cancer, which signaling pathway mediates the downstream effects of S1PR1 downregulation. Alternatively, Sphingomab could also be used to explore in more detail how blockade of S1P influences the phenotypic changes induced by S1P. Measurement of S1P pre and post Sphingomab treatment would be useful in cell lines of different tumours.

It would be interesting to investigate if there are any differences in the morphology of the EBV^+ DLBCL vs the EBV^- DLBCL and also the GCB subtype of DLBCL vs the Non GCB subtype. Due to low number of EBV positive DLBCL cases, perhaps a multicenter study in the UK would be beneficial to investigate further if EBV positivity is a poor prognostic indicator in DLBCL. In view of the high positivity of S1PR1 in DLBCL, I would also like to investigate further if S1PR1 could be a diagnostic and prognostic marker in DLBCL. Perhaps S1PR1 expression across normal lymphoid tissues and different subtypes of lymphoma would be helpful to begin with.

APPENDIX

Table A1: List of genes downregulated after 2 hours of treatment with Sphingomab**.**

Transcript ID	Gene symbol	Gene description	p value	fold change
2472054	GDF7	growth differentiation factor 7	0.009862	1.260554
2351465	PROK1	prokineticin 1	0.011611	1.269725
3960042	SSTR3	somatostatin receptor 3	0.0122	1.218627
3514879	TPTE2P2	transmembrane phosphoinositide 3-phosphatase and tensin homolog 2 pseudogene 2	0.012462	1.244277
3335751	TSGA10IP	testis specific, 10 interacting protein	0.012702	1.213711
2948683	SFTA2	surfactant associated 2	0.012729	1.356907
3829398	CHST8	carbohydrate (N-acetylgalactosamine 4-0) sulfotransferase 8	0.013025	1.206956
4044363	CNR2	cannabinoid receptor 2 (macrophage)	0.013971	1.303814
3870824	LAIR1	leukocyte-associated immunoglobulin-like receptor 1	0.014486	1.208251
3886598	KCNK15	potassium channel, subfamily K, member 15	0.014953	1.210646
3721010	IGFBP4	insulin-like growth factor binding protein 4	0.015167	1.260658
2391005	C1orf159	chromosome 1 open reading frame 159	0.015732	1.211752
3882614	C20orf144	chromosome 20 open reading frame 144	0.015822	1.664164
3677103	PRSS27	protease, serine 27	0.016525	1.205747
3708597	SPEM1	spermatid maturation 1	0.017765	1.263845
3830306	HAMP	hepcidin antimicrobial peptide	0.018071	1.218567
3774906	SECTM1	secreted and transmembrane 1	0.018105	1.220535
3952762	CLDN5	claudin 5	0.018175	1.317094
3868681	KLK1	kallikrein 1	0.018794	1.227132
3415744	IGFBP6	insulin-like growth factor binding protein 6	0.018848	1.250835
3707127	MED11	mediator complex subunit 11	0.019065	1.279871

3273100	DUX4L4	double homeobox 4 like 4 | double homeobox 4 like 7	0.022343	1.420224
3850406	**S1PR5**	**sphingosine-1-phosphate receptor 5**	**0.023181**	**1.361607**
4035762	TTTY14	testis-specific transcript, Y-linked 14	0.024681	1.255197
3416353	HOXC8	homeobox C8	0.024789	1.247533
3273126	DUX4L4	double homeobox 4 like 4	0.024917	1.380069
3907210	MATN4	matrilin 4	0.026837	1.20311
3270840	MGMT	O-6-methylguanine-DNA methyltransferase	0.028647	1.247005
3923857	KRTAP10-9	keratin associated protein 10-9	0.028845	1.217307
2949993	BTNL2	butyrophilin-like 2 (MHC class II associated)	0.028901	1.219368
3356328	ADAMTS15	ADAM metallopeptidase with thrombospondin type 1 motif, 15	0.029037	1.202927
3762185	HILS1	histone linker H1 domain, spermatid-specific 1	0.029184	1.260129
3453513	WNT10B	wingless-type MMTV integration site family, member 10B	0.030785	1.365521
3838665	RCN3	reticulocalbin 3, EF-hand calcium binding domain	0.031084	1.216106
3662710	CCL17	chemokine (C-C motif) ligand 17	0.031084	1.234359
2502686	MARCO	macrophage receptor with collagenous structure	0.031093	1.220807
2505618	CFC1B	cripto, FRL-1, cryptic family 1B	0.032203	1.202504
3956984	ZMAT5|CABP7	zinc finger, matrin-type 5 | calcium binding protein 7	0.033461	1.226454
2435989	S100A8	S100 calcium binding protein A8	0.034439	1.245579
3709384	GUCY2D	guanylate cyclase 2D, membrane (retina-specific)	0.0355	1.250199
3841901	NLRP2	NLR family, pyrin domain containing 2	0.036825	1.202427
3557198	CEBPE	CCAAT/enhancer binding protein (C/EBP), epsilon	0.03805	1.219558
3849190	ACTL9	actin-like 9	0.03834	1.349617
3886576	WISP2	WNT1 inducible signaling pathway protein 2	0.039883	1.276118
3818446	CRB3	crumbs homolog 3 (Drosophila)	0.04086	1.251961
3377737	KCNK7	potassium channel, subfamily K, member 7	0.041239	1.2048
3851840	KLF1	Kruppel-like factor 1 (erythroid)	0.042253	1.253656

3629416	RASL12	RAS-like, family 12	0.042753	1.214962
3866106	GNG8	guanine nucleotide binding protein (G protein), gamma 8	0.043184	1.225943
2357961	BOLA1	bolA homolog 1 (E. coli)	0.04507	1.216382
3678316	ZNF500	zinc finger protein 500	0.045433	1.216138
3014227	BHLHA15	basic helix-loop-helix family, member a15	0.04549	1.246796
3837825	KCNJ14	potassium inwardly-rectifying channel, subfamily J, member 14	0.046201	1.239692
3815116	PALM	paralemmin	0.046403	1.233797
2536874	GAL3ST2	galactose-3-O-sulfotransferase 2	0.047326	1.234331
3656151	MYLPF	myosin light chain, phosphorylatable	0.047578	1.236727
3868033	TSKS	testis-specific serine kinase substrate	0.048042	1.204195
3015778	EPO	erythropoietin	0.04934	1.209653
2711604	CPN2	carboxypeptidase N, polypeptide 2	0.04948	1.303106

Table A2: List of genes downregulated after 12 hours of treatment with Sphingomab

Transcript ID	Gene symbol	Gene description	p value	fold change
3893642	LIME1	Lck interacting transmembrane adaptor 1	0.003311	1.217527
3551407	HHIPL1	HHIP-like 1	0.003581	1.285045
2900116	HIST1H2BO	histone cluster 1, H2bo	0.003746	1.425556
3842278	ZNF524	zinc finger protein 524	0.003747	1.271449
3031345	LRRC61	leucine rich repeat containing 61	0.003793	1.226793
3358241	SCT	secretin	0.003846	1.231226
3934614	KRTAP12-4	keratin associated protein 12-4	0.003891	1.25782
2381264	MOSC2	MOCO sulphurase C-terminal domain containing 2	0.004499	1.264808
3948528	UPK3A	uroplakin 3A	0.004565	1.220747
3871127	TNNI3	troponin I type 3 (cardiac)	0.004632	1.214861
3733590	SOX9	SRY (sex determining region Y)-box 9	0.004825	1.220222
3715460	PYY2	peptide YY, 2 (seminalplasmin)	0.005055	1.207429
2551189	SIX2	SIX homeobox 2	0.005447	1.24847
3740462	RILP	Rab interacting lysosomal protein	0.005509	1.200214
3472389	LHX5	LIM homeobox 5	0.005999	1.268392
3867326	MAMSTR	MEF2 activating motif and SAP domain containing transcriptional regulator	0.006184	1.237335
3817602	TNFAIP8L1	tumor necrosis factor, alpha-induced protein 8-like 1	0.006684	1.301432
3837081	NPAS1	neuronal PAS domain protein 1	0.007362	1.215552
3609098	LOC643797	AGVR6190	0.007457	1.328855
3685373	ERN2	endoplasmic reticulum to nucleus signaling 2	0.007756	1.204761
3285119	FZD8	frizzled homolog 8 (Drosophila)	0.007865	1.227744

3255938	OPN4	opsin 4	0.007882	1.409973
3762125	SAMD14|PDK2	sterile alpha motif domain containing 14 | pyruvate dehydrogenase kinase, isozyme 2	0.007905	1.2012
2326846	TRNP1	TMF1-regulated nuclear protein 1	0.007907	1.213377
2528159	WNT10A	wingless-type MMTV integration site family, member 10A	0.007953	1.237534
3868681	KLK1	kallikrein 1	0.008011	1.228527
2929699	RAB32		0.008168	1.234358
3178545	**C9orf47|S1PR3**	**chromosome 9 open reading frame 47 | sphingosine-1-phosphate receptor 3**	**0.008434**	**1.300196**
2323882	PLA2G2F	phospholipase A2, group IIF	0.008557	1.234817
3195059	LCNL1	lipocalin-like 1	0.008587	1.211874
3732721	LOC440461|LOC146880	SH3 domain containing 20 pseudogene | hypothetical LOC146880	0.008615	1.211667
3250726	KIAA1274		0.008933	1.265024
3303774	LBX1	ladybird homeobox 1	0.008945	1.32143
3815710	EFNA2	ephrin-A2	0.009018	1.241684
3950832	ADM2	adrenomedullin 2	0.009071	1.245749
3837536	CRX|TPRX1	cone-rod homeobox | tetra-peptide repeat homeobox 1	0.009716	1.200623
3962145	TNFRSF13C	tumor necrosis factor receptor superfamily, member 13C	0.00985	1.389514
3738306	NPB	neuropeptide B	0.010505	1.286477
3334125	COX8A	cytochrome c oxidase subunit VIIIA (ubiquitous)	0.010821	1.231539
3158377	ZNF251|SCRT1| C8ORFK29	zinc finger protein 251 | scratch homolog 1, zinc finger protein (Drosophila) | hypothetical LOC340393	0.010853	1.231619
3855320	MGC10814		0.010995	1.323741
2824144	FLJ11235		0.01107	1.255503
3913737	NKAIN4	Na+/K+ transporting ATPase interacting 4	0.011415	1.238623
3861905	IL28B|IL28A	interleukin 28B (interferon, lambda 3) | interleukin 28A	0.011464	1.308605

		(interferon, lambda 2)		
3756723	KRTAP2-4|KRTAP2-1| KRTAP2-2|LOC730755| KAP2.1B	keratin associated protein 2-4 | keratin associated protein 2-1 | keratin associated protein 2-2 | keratin associated protein 2-4-like | keratin associated protein 2.1B	0.011555	1.314308
3934344	LOC100129890	similar to hCG1750329	0.011582	1.201524
3893250	BIRC7	baculoviral IAP repeat-containing 7	0.012068	1.237511
3846390	RAX2	retina and anterior neural fold homeobox 2	0.012184	1.312011
3119792	MAPK15	mitogen-activated protein kinase 15	0.012503	1.261976
3954567	POM121L10P|POM121L1P | POM121L4P|POM121L8P| POM121L9P	POM121 membrane glycoprotein-like 10, pseudogene | POM121 membrane glycoprotein-like 1, pseudogene | POM121 membrane glycoprotein-like 4 pseudogene | POM121 membrane glycoprotein-like 8 pseudogene | POM121 membrane glycoprotein-like 9, pseudogene	0.012561	1.337372
3066613	ATXN7L1	ataxin 7-like 1	0.012572	1.366192
3720388	PNMT	phenylethanolamine N-methyltransferase	0.012576	1.201561
3671506	OSGIN1	oxidative stress induced growth inhibitor 1	0.012584	1.284828
2470805	MYCN	v-myc myelocytomatosis viral related oncogene, neuroblastoma derived (avian)	0.012615	1.452516
3118838	FLJ43860		0.013007	1.249176
3841102	PRKCG	protein kinase C, gamma	0.013405	1.216666
3328349	ACCS	1-aminocyclopropane-1-carboxylate synthase homolog (Arabidopsis)(non-functional)	0.013472	1.210305
3907210	MATN4	matrilin 4	0.013619	1.200984
3722039	RAMP2	receptor (G protein-coupled) activity modifying protein 2	0.013889	1.23828
2460422	FAM89A	family with sequence similarity 89, member A	0.014317	1.201617
2994981	PRR15	proline rich 15	0.014523	1.211084
3995088	FATE1	fetal and adult testis expressed 1	0.014788	1.210464

3414315	AQP5	aquaporin 5	0.015169	1.221794
3692280	IRX3|IRX1|IRX5	iroquois homeobox 3 | iroquois homeobox 1 | iroquois homeobox 5	0.015261	1.224307
3995765	DUSP9	dual specificity phosphatase 9	0.015427	1.203419
3415273	C12orf44	chromosome 12 open reading frame 44	0.015579	1.206711
2318242	LOC100130071	GSQS6193	0.015593	1.272391
3832865	NCCRP1	non-specific cytotoxic cell receptor protein 1 homolog (zebrafish)	0.015781	1.216984
3773426	NPTX1	neuronal pentraxin I	0.015963	1.216617
2820884	GPR150	G protein-coupled receptor 150	0.016136	1.210947
2904836	LHFPL5	lipoma HMGIC fusion partner-like 5	0.016209	1.22619
3602299	NEIL1|MAN2C1	nei endonuclease VIII-like 1 (E. coli) | mannosidase, alpha, class 2C, member 1	0.016295	1.261569
3870990	GP6	glycoprotein VI (platelet)	0.016467	1.223216
2359431	LCE1F	late cornified envelope 1F	0.01661	1.418236
2487963	ANKRD53	ankyrin repeat domain 53	0.016653	1.205573
4026624	PNCK	pregnancy up-regulated non-ubiquitously expressed CaM kinase	0.016701	1.202712
3098549	SOX17	SRY (sex determining region Y)-box 17	0.016875	1.219817
3378851	GPR152	G protein-coupled receptor 152	0.017317	1.356891
3951117	ACR	acrosin	0.017661	1.209925
3717775	CDK5R1	cyclin-dependent kinase 5, regulatory subunit 1 (p35)	0.018152	1.221159
3871389	FAM71E2	family with sequence similarity 71, member E2	0.018229	1.285293
3316057	DRD4	dopamine receptor D4	0.018604	1.292633
3851801	RTBDN	retbindin	0.018637	1.246632
3710406	SHISA6	shisa homolog 6 (Xenopus laevis)	0.018775	1.209048
3442249	C12orf53	chromosome 12 open reading frame 53	0.018827	1.35486
3194470	EGFL7|MIR126	EGF-like-domain, multiple 7 | microRNA 126	0.019038	1.205783

3704567	CBFA2T3|PABPN1L	core-binding factor, runt domain, alpha subunit 2; translocated to, 3 | poly(A) binding protein, nuclear 1-like (cytoplasmic)	0.019507	1.277086
2407359	EPHA10	EPH receptor A10	0.019562	1.286812
3384248	FAM181B	family with sequence similarity 181, member B	0.019808	1.22163
3475383	HPD	4-hydroxyphenylpyruvate dioxygenase	0.020065	1.25692
3580357	ANKRD9	ankyrin repeat domain 9	0.020122	1.202218
2697863	RBP1	retinol binding protein 1, cellular	0.020342	1.287323
3902552	FOXS1	forkhead box S1	0.020563	1.323761
3882823	ASIP	agouti signaling protein	0.020566	1.316178
3394315	C1QTNF5|MFRP	C1q and tumor necrosis factor related protein 5 | membrane frizzled-related protein	0.020683	1.23662
3756709	KRTAP2-2|KRTAP2-1| KRTAP2-4|LOC730755| KAP2.1B	keratin associated protein 2-2 | keratin associated protein 2-1 | keratin associated protein 2-4 | keratin associated protein 2-4-like | keratin associated protein 2.1B	0.020739	1.316847
3013894	DLX6	distal-less homeobox 6	0.020786	1.211607
2391425	DVL1	dishevelled, dsh homolog 1 (Drosophila)	0.020844	1.205483
2534509	RAMP1	receptor (G protein-coupled) activity modifying protein 1	0.021133	1.211694
3193942	OBP2A|OBP2B	odorant binding protein 2A | odorant binding protein 2B	0.021156	1.360897
3657552	TP53TG3|TP53TG3B	TP53 target 3 | TP53 target 3B	0.02174	1.315799
3338192	CCND1	cyclin D1	0.021794	1.234254
3639601	RGMA	RGM domain family, member A	0.021905	1.263049
3334633	SLC22A11	solute carrier family 22 (organic anion/urate transporter), member 11	0.021991	1.209618
2528774	SLC4A3	solute carrier family 4, anion exchanger, member 3	0.022069	1.201502
3892788	C20orf200	chromosome 20 open reading frame 200	0.022131	1.210422

2888304	CLTB	clathrin, light chain B	0.022425	1.233716
2887930	FLJ16171		0.022596	1.387873
3444593	PRB3|PRB4|PRB1 |PRB2	proline-rich protein BstNI subfamily 3 | proline-rich protein BstNI subfamily 4 | proline-rich protein BstNI subfamily 1 | proline-rich protein BstNI subfamily 2	0.022859	1.290559
3590239	DLL4	delta-like 4 (Drosophila)	0.02382	1.206722
3402444	LTBR	lymphotoxin beta receptor (TNFR superfamily, member 3)	0.024521	1.211369
2323172	IGSF21	immunoglobin superfamily, member 21	0.024764	1.25627
3015911	TRIP6	thyroid hormone receptor interactor 6	0.02486	1.202228
3336220	PELI3	pellino homolog 3 (Drosophila)	0.024892	1.220248
3655687	PRRT2	proline-rich transmembrane protein 2	0.026067	1.204707
3874168	GNRH2	gonadotropin-releasing hormone 2	0.026152	1.210199
3334919	MRPL49	mitochondrial ribosomal protein L49	0.026638	1.317266
2406662	C1orf113|FAM176B	chromosome 1 open reading frame 113 | family with sequence similarity 176, member B	0.027471	1.272064
3642946	SOLH	small optic lobes homolog (Drosophila)	0.027509	1.20925
3708223	BCL6B	B-cell CLL/lymphoma 6, member B	0.027617	1.230321
3208349	FOXD4L2|FOXD4L3| FOXD4L4|FOXD4L6| FOXD4L5|FOXD4L1	forkhead box D4-like 2 | forkhead box D4-like 3 | forkhead box D4-like 4 | forkhead box D4-like 6 | forkhead box D4-like 5 | forkhead box D4 | forkhead box D4-like 1	0.027665	1.308214
3643679	TPSD1	tryptase delta 1	0.027787	1.31544
3839171	FLJ26850		0.02788	1.252255
2600237	OBSL1	obscurin-like 1	0.027933	1.324396
3688270	PRSS36	protease, serine, 36	0.027938	1.212274
3642687	HBQ1	hemoglobin, theta 1	0.028009	1.300179

3944758	CDC42EP1	CDC42 effector protein (Rho GTPase binding) 1	0.028487	1.313417
3760552	RPRML	reprimo-like	0.028595	1.253123
3953196	DGCR6L	DiGeorge syndrome critical region gene 6-like | DiGeorge syndrome critical region gene 6	0.028787	1.21309
2487882	VAX2	ventral anterior homeobox 2	0.029701	1.217993
3847462	FUT6	fucosyltransferase 6 (alpha (1,3) fucosyltransferase)	0.030036	1.20603
3917582	KRTAP6-3	keratin associated protein 6-3	0.030772	1.213945
3886598	KCNK15	potassium channel, subfamily K, member 15	0.031553	1.24118
2984543	PRR18	proline rich 18	0.031723	1.218871
2408437	CITED4	Cbp/p300-interacting transactivator, with Glu/ Asp-rich carboxy-terminal domain, 4	0.032592	1.21
2961647	HTR1B	5-hydroxytryptamine (serotonin) receptor 1B	0.033109	1.220903
2898096	HDGFL1	hepatoma derived growth factor-like 1	0.03343	1.248323
3226208	PIP5KL1	phosphatidylinositol-4-phosphate 5-kinase-like 1	0.03359	1.326992
3726114	DLX4	distal-less homeobox 4	0.033732	1.260217
4003155	ARX	aristaless related homeobox	0.03413	1.223033
3839464	CLEC11A	C-type lectin domain family 11, member A	0.03445	1.202796
3923857	KRTAP10-9|KRTAP10-2| KRTAP10-11	keratin associated protein 10-9 | keratin associated protein 10-2 | keratin associated protein 10-11	0.034535	1.218608
3672609	FOXF1	forkhead box F1	0.034812	1.233776
2756630	CPLX1	complexin 1	0.035126	1.256843
3913335	C20orf166|MIR1-1| MIR133A2	chromosome 20 open reading frame 166 | microRNA 1-1 | microRNA 133a-2	0.035607	1.225886
2776305	NKX6-1	NK6 homeobox 1	0.036162	1.213078
3894545	SDCBP2	syndecan binding protein (syntenin) 2	0.036284	1.204013
3832906	IL29|IL28B	interleukin 29 (interferon, lambda 1) | interleukin 28B (interferon, lambda 3)	0.036921	1.223719

3867629	CGB5|CGB7|CGB8| NTF4	chorionic gonadotropin, beta polypeptide 5 | chorionic gonadotropin, beta polypeptide 7 | chorionic gonadotropin, beta polypeptide 8 | neurotrophin 4	0.037355	1.272945
3638699	C15orf38|AP3S2	chromosome 15 open reading frame 38 | adaptor-related protein complex 3, sigma 2 subunit	0.037422	1.236693
2357961	BOLA1	bolA homolog 1 (E. coli)	0.037485	1.279794
3902674	TSPY26P	testis specific protein, Y-linked 26, pseudogene	0.038466	1.514903
3652749	HS3ST2	heparan sulfate (glucosamine) 3-O-sulfotransferase 2	0.038743	1.242699
3554396	SIVA1		0.039938	1.201848
3817420	SHD	Src homology 2 domain containing transforming protein D	0.040109	1.207889
4027501	CTAG1A|CTAG1B| CTAG2	cancer/testis antigen 1A | cancer/testis antigen 1B | cancer/testis antigen 2	0.040506	1.201531
3755316	MLLT6|LOC100129395	myeloid/lymphoid or mixed-lineage leukemia (trithorax homolog, Drosophila); translocated to, 6 | NS5ATP13TP1	0.040588	1.551177
3459604	PPM1H	protein phosphatase, Mg2+/Mn2+ dependent, 1H	0.040599	1.293173
3687232	C16orf54	chromosome 16 open reading frame 54	0.040995	1.302866
3555675	RNASE1	ribonuclease, RNase A family, 1 (pancreatic)	0.041045	1.244802
3098454	MRPL15	mitochondrial ribosomal protein L15	0.042518	1.283998
3886576	WISP2	WNT1 inducible signaling pathway protein 2	0.042769	1.251165
2844461	LTC4S|MAML1	leukotriene C4 synthase | mastermind-like 1 (Drosophila)	0.043166	1.272022
3415193	GRASP|GRASPOS	GRP1 (general receptor for phosphoinositides 1)-associated scaffold protein | GRP1-associated scaffold protein opposite strand	0.043383	1.212265
2445876	NCRNA00083	non-protein coding RNA 83	0.043434	1.207612
2745712	LOC441046	glucuronidase, beta pseudogene	0.043753	1.241513
3834439	DMRTC2	DMRT-like family C2	0.043889	1.21691
2939232	TUBB2B	tubulin, beta 2B	0.044542	1.227506
2915133	TPBG	trophoblast glycoprotein	0.044752	1.281001

3677164	TCEB2	transcription elongation factor B (SIII), polypeptide 2 (18kDa, elongin B)	0.044821	1.218621
3663033	TEPP	testis, prostate and placenta expressed	0.045603	1.200095
3377886	CFL1	cofilin 1 (non-muscle)	0.045678	1.204996
3914050	STMN3	stathmin-like 3	0.045741	1.213972
3762185	HILS1	histone linker H1 domain, spermatid-specific 1	0.045748	1.214339
3119765	ZNF707	zinc finger protein 707	0.046298	1.24442
3672646	FOXC2	forkhead box C2 (MFH-1, mesenchyme forkhead 1)	0.047194	1.230515
3707141	ZMYND15	zinc finger, MYND-type containing 15	0.047294	1.22945
3279089	C10orf111	chromosome 10 open reading frame 111	0.047306	1.222135
3902871	C20orf203	chromosome 20 open reading frame 203	0.047619	1.220926
3852022	LYL1	lymphoblastic leukemia derived sequence 1	0.047664	1.343057
2648305	P2RY1	purinergic receptor P2Y, G-protein coupled, 1	0.047797	1.269203
3016316			0.04788	1.263108
3923896	KRTAP10-12|KRTAP10-4| KRTAP10-6|KRTAP10-7	keratin associated protein 10-12 | keratin associated protein 10-4 | keratin associated protein 10-6 | keratin associated protein 10-7	0.048039	1.226683
2451931	GOLT1A	golgi transport 1A	0.048085	1.218571
3584393	C15orf2	chromosome 15 open reading frame 2	0.048664	1.27735
3817072	GIPC3	GIPC PDZ domain containing family, member 3	0.049246	1.208209
3456840	PPP1R1A	protein phosphatase 1, regulatory (inhibitor) subunit 1A	0.049263	1.284999
3735089	LOC643008		0.049389	1.210745
3695315	CDH16	cadherin 16, KSP-cadherin	0.049445	1.2186
3554496	PLD4	phospholipase D family, member 4	0.049683	1.260256

References

Adam P, Bonzheim I, Fend F, et al. Epstein-Barr Virus-positive Diffuse Large B-cell Lymphomas of the Elderly. *Advances in Anatomic Pathology*. 2011;18(September):349–355.

Ader, I., Malavaud, B. & Cuvillier, Olivier, 2009. When the sphingosine kinase 1/sphingosine 1-phosphate pathway meets hypoxia signaling: new targets for cancer therapy. *Cancer research*, 69(9), pp.3723–6. Available at: http://www.ncbi.nlm.nih.gov/pubmed/19383898.

Albi, E., Lazzarini, R. & Viola Magni, M., 2008. Phosphatidylcholine/sphingomyelin metabolism crosstalk inside the nucleus. *The Biochemical journal*, 410(2), pp.381–9. Available at: http://www.ncbi.nlm.nih.gov/pubmed/18001268 [Accessed November 1, 2011].

Alizadeh, A. a et al., 2000. Distinct types of diffuse large B-cell lymphoma identified by gene expression profiling. *Nature*, 403(6769), pp.503–11. Available at: http://www.ncbi.nlm.nih.gov/pubmed/10676951.

Alvarez, S.E., Milstien, Sheldon & Spiegel, Sarah, 2007. Autocrine and paracrine roles of sphingosine-1-phosphate. *Trends in endocrinology and metabolism: TEM*, 18(8), pp.300–7. Available at: http://www.ncbi.nlm.nih.gov/pubmed/17904858.

Anagnostopoulos, I. et al., 1996. European Task Force on Lymphoma project on lymphocyte predominance Hodgkin disease : histologic and immunohistologic analysis of submitted cases reveals 2 types of Hodgkin disease with a nodular growth pattern and abundant lymphocytes European Task Force. *Blood*, pp.1889–1899.

Anelli, V. et al., 2010. Role of sphingosine kinase-1 in paracrine/transcellular angiogenesis and lymphangiogenesis in vitro. *The FASEB journal : official publication of the Federation of American Societies for Experimental Biology*, (1), pp.4 – 6. Available at: http://www.ncbi.nlm.nih.gov/pubmed/20335228 [Accessed July 3, 2010].

Anliker, B. & Chun, Jerold, 2004. Cell surface receptors in lysophospholipid signaling. *Seminars in cell & developmental biology*, 15(5), pp.457–65. Available at: http://www.ncbi.nlm.nih.gov/pubmed/15271291 [Accessed December 28, 2010].

Argraves, K.M. et al., 2004. Sphingosine-1-phosphate signaling promotes critical migratory events in vasculogenesis. *The Journal of biological chemistry*, 279(48), pp.50580–90. Available at: http://www.ncbi.nlm.nih.gov/pubmed/15377653 [Accessed July 21, 2011].

Armitage, James O & Weisenburger, Dennis D, 1998. New Approach to Classifying Non-Hodgkin ' s Lymphomas : Clinical Features of the Major Histologic Subtypes. *J Clin Oncology*, 16(8), pp.2780–2795.

Asano, N. et al., 2009. Age-related Epstein-Barr virus (EBV)-associated B-cell lymphoproliferative disorders: comparison with EBV-positive classic Hodgkin lymphoma in elderly patients. *Blood*, 113(12), pp.2629–36. Available at: http://www.ncbi.nlm.nih.gov/pubmed/19075188 [Accessed October 3, 2010].

Augé, N. et al., 1999. Role of sphingosine 1-phosphate in the mitogenesis induced by oxidized low density lipoprotein in smooth muscle cells via activation of sphingomyelinase, ceramidase, and sphingosine kinase. *The Journal of biological*

chemistry, 274(31), pp.21533–8. Available at: http://www.ncbi.nlm.nih.gov/pubmed/10419457.

Azarova, A.M. et al., 2007. Roles of DNA topoisomerase II isozymes in chemotherapy and secondary malignancies. *Proceedings of the National Academy of Sciences of the United States of America*, 104(26), pp.11014–9. Available at: http://www.pubmedcentral.nih.gov/articlerender.fcgi?artid=1904155&tool=pmcentrez&rendertype=abstract.

Babak Oskouian & Julie Saba, 2007. Sphingosine-1-Phosphate Metabolism and Intestinal Tumorigenesis. *Cell cycle*, 6(5), pp.522–527.

Baker, D.L. et al., 2006. Carba analogs of cyclic phosphatidic acid are selective inhibitors of autotaxin and cancer cell invasion and metastasis. *The Journal of biological chemistry*, 281(32), pp.22786–93. Available at: http://www.ncbi.nlm.nih.gov/pubmed/16782709 [Accessed November 18, 2012].

Barrans, S. L., 2002. Germinal center phenotype and bcl-2 expression combined with the International Prognostic Index improves patient risk stratification in diffuse large B-cell lymphoma. *Blood*, 99(4), pp.1136–1143. Available at: http://www.bloodjournal.org/cgi/doi/10.1182/blood.V99.4.1136 [Accessed September 6, 2011].

Barrans, Sharon L et al., 2003. The t (14 ; 18) Is Associated with Germinal Center-derived Diffuse Large B-Cell Lymphoma and Is a Strong Predictor of Outcome The t (14 ; 18)

Is Associated with Germinal Center-derived Diffuse Large B-Cell Lymphoma and Is a Strong Predictor of Outcome. *Clinical Cancer Research*, pp.2133–2139.

Bassi, R. et al., 2006. Sphingosine-1-Phosphate Is Released by Cerebellar Astrocytes in Response to bFGF and Induces Astrocyte Proliferation Through G i -Protein-Coupled Receptors. *Evaluation*, 630(December 2005), pp.621–630.

Baumforth, K.R.N. et al., 2008. Expression of the Epstein-Barr virus-encoded Epstein-Barr virus nuclear antigen 1 in Hodgkin's lymphoma cells mediates Up-regulation of CCL20 and the migration of regulatory T cells. *The American journal of pathology*, 173(1), pp.195–204. Available at: http://www.pubmedcentral.nih.gov/articlerender.fcgi?artid=2438297&tool=pmcentrez&rendertype=abstract [Accessed August 5, 2010].

Baumforth, K.R.N. et al., 2005. Induction of autotaxin by the Epstein-Barr virus promotes the growth and survival of Hodgkin lymphoma cells. *Blood*, 106(6), pp.2138–2146.

Baumruker, T. & Prieschl, E.E., 2002. Sphingolipids and the regulation of the immune response. *Seminars in immunology*, 14(1), pp.57–63. Available at: http://www.ncbi.nlm.nih.gov/pubmed/11884231 [Accessed August 22, 2011].

Bayerl, M.G. et al., 2008. Sphingosine kinase 1 protein and mRNA are overexpressed in non-Hodgkin lymphomas and are attractive targets for novel pharmacological interventions. *Leukemia & lymphoma*, 49(5), pp.948–54. Available at: http://www.ncbi.nlm.nih.gov/pubmed/18452097 [Accessed July 4, 2010].

Beltran, B.E. et al., 2011. EBV-positive diffuse large B-cell lymphoma of the elderly: a case series from Peru. *American journal of hematology*, 86(8), pp.663–7. Available at: http://www.ncbi.nlm.nih.gov/pubmed/21761432 [Accessed May 24, 2012].

Bergelin, N. et al., 2009. Sphingosine kinase as an oncogene: autocrine sphingosine 1-phosphate modulates ML-1 thyroid carcinoma cell migration by a mechanism dependent on protein kinase C-alpha and ERK1/2. *Endocrinology*, 150(5), pp.2055–63. Available at: http://www.ncbi.nlm.nih.gov/pubmed/19116345 [Accessed October 12, 2011].

Berglund, M. et al., 2005. Evaluation of immunophenotype in diffuse large B-cell lymphoma and its impact on prognosis. *Modern pathology : an official journal of the United States and Canadian Academy of Pathology, Inc*, 18(8), pp.1113–20. Available at: http://www.ncbi.nlm.nih.gov/pubmed/15920553 [Accessed September 11, 2010].

Bonhoure, E. et al., 2006. Overcoming MDR-associated chemoresistance in HL-60 acute myeloid leukemia cells by targeting sphingosine kinase-1. *Leukemia : official journal of the Leukemia Society of America, Leukemia Research Fund, U.K*, 20(1), pp.95–102. Available at: http://www.ncbi.nlm.nih.gov/pubmed/16281067 [Accessed July 4, 2010].

Boujaoude, L.C. et al., 2001. Cystic fibrosis transmembrane regulator regulates uptake of sphingoid base phosphates and lysophosphatidic acid: modulation of cellular activity of sphingosine 1-phosphate. *The Journal of biological chemistry*, 276(38), pp.35258–64. Available at: http://www.ncbi.nlm.nih.gov/pubmed/11443135 [Accessed June 5, 2011].

Van Brocklyn, J R et al., 1998. Dual actions of sphingosine-1-phosphate: extracellular through the Gi-coupled receptor Edg-1 and intracellular to regulate proliferation and

survival. *The Journal of cell biology*, 142(1), pp.229–40. Available at: http://www.pubmedcentral.nih.gov/articlerender.fcgi?artid=2133030&tool=pmcentrez&rendertype=abstract.

Van Brocklyn, James R et al., 2005a. Sphingosine kinase-1 expression correlates with poor survival of patients with glioblastoma multiforme: roles of sphingosine kinase isoforms in growth of glioblastoma cell lines. *Journal of neuropathology and experimental neurology*, 64(8), pp.695–705. Available at: http://www.ncbi.nlm.nih.gov/pubmed/16106218.

Van Brocklyn, James R et al., 2005b. Sphingosine kinase-1 expression correlates with poor survival of patients with glioblastoma multiforme: roles of sphingosine kinase isoforms in growth of glioblastoma cell lines. *Journal of neuropathology and experimental neurology*, 64(8), pp.695–705. Available at: http://www.ncbi.nlm.nih.gov/pubmed/16106218.

Brune, V. et al., 2008. Origin and pathogenesis of nodular lymphocyte-predominant Hodgkin lymphoma as revealed by global gene expression analysis. *The Journal of experimental medicine*, 205(10), pp.2251–2268. Available at: http://www.pubmedcentral.nih.gov/articlerender.fcgi?artid=2556780&tool=pmcentrez&rendertype=abstract [Accessed August 15, 2011].

Caldwell, R.G. et al., 1998. Epstein-Barr virus LMP2A drives B cell development and survival in the absence of normal B cell receptor signals. *Immunity*, 9(3), pp.405–11. Available at: http://www.ncbi.nlm.nih.gov/pubmed/9768760.

Carol M. Rivera-Lopez, A.L.T. & Lynch, Kevin R., 2008. Lysophosphatidic acid (LPA) and angiogenesis. *Angiogenesis*, 11(3), pp.301–310.

Cartwright, R. a & Watkins, G., 2004. Epidemiology of Hodgkin's disease: a review. *Hematological oncology*, 22(1), pp.11–26. Available at: http://www.ncbi.nlm.nih.gov/pubmed/15152367 [Accessed August 8, 2011].

Cattoretti, G. et al., 2010. Targeted disruption of the S1P2 sphingosine 1-phosphate receptor gene leads to diffuse large B-cell lymphoma formation. *Cancer*, 69(22), pp.8686–8692.

Chae, S. et al., 2004. Requirement for sphingosine 1 – phosphate receptor-1 in tumor angiogenesis demonstrated by in vivo RNA interference. *October*, 114(8).

Chang, C.-C. et al., 2004. Immunohistochemical expression patterns of germinal center and activation B-cell markers correlate with prognosis in diffuse large B-cell lymphoma. *The American journal of surgical pathology*, 28(4), pp.464–70. Available at: http://www.ncbi.nlm.nih.gov/pubmed/15087665.

Chang, C.-L. et al., 2009. S1P(5) is required for sphingosine 1-phosphate-induced autophagy in human prostate cancer PC-3 cells. *American journal of physiology. Cell physiology*, 297(2), pp.C451–8. Available at: http://www.ncbi.nlm.nih.gov/pubmed/19474291 [Accessed October 11, 2011].

Cheng, P. et al., 2001. Notch-1 regulates NF-kappaB activity in hemopoietic progenitor cells. *Journal of immunology*, 167(8), pp.4458–67. Available at: http://www.ncbi.nlm.nih.gov/pubmed/11591772.

Chi, H., 2011. Sphingosine-1-phosphate and immune regulation: trafficking and beyond. *Trends in pharmacological sciences*, 32(1), pp.16–24. Available at: http://www.pubmedcentral.nih.gov/articlerender.fcgi?artid=3017656&tool=pmcentrez&rendertype=abstract [Accessed September 7, 2011].

Chiba, K. et al., 2006. Role of sphingosine 1-phosphate receptor type 1 in lymphocyte egress from secondary lymphoid tissues and thymus. *Cellular & molecular immunology*, 3(1), pp.11–9. Available at: http://www.ncbi.nlm.nih.gov/pubmed/16549044.

Cho, E.-Y. et al., 2008. The spectrum of Epstein-Barr virus-associated lymphoproliferative disease in Korea: incidence of disease entities by age groups. *Journal of Korean medical science*, 23(2), pp.185–92. Available at: http://www.pubmedcentral.nih.gov/articlerender.fcgi?artid=2526432&tool=pmcentrez&rendertype=abstract [Accessed November 25, 2011].

Choi, J.W. & Chun, Jerold, 2013. Lysophospholipids and their receptors in the central nervous system. *Biochimica et biophysica acta*, 1831(1), pp.20–32. Available at: http://www.ncbi.nlm.nih.gov/pubmed/22884303 [Accessed December 12, 2012].

Choi, W.W.L. et al., 2009. A new immunostain algorithm classifies diffuse large B-cell lymphoma into molecular subtypes with high accuracy. *Clinical cancer research : an official journal of the American Association for Cancer Research*, 15(17), pp.5494–502. Available at: http://www.ncbi.nlm.nih.gov/pubmed/19706817 [Accessed August 8, 2011].

Chun, Jerold et al., 2002. International Union of Pharmacology . XXXIV . Lysophospholipid Receptor Nomenclature. *Pharmacological Reviews*, 54(2), pp.265–269.

Correa, P. & O'Conor, G.T., 1971. Epidemiologic patterns of Hodgkin's Disease. *International Journal of Cancer*, 8(2), pp.192–201. Available at: http://doi.wiley.com/10.1002/ijc.2910080203.

Dawson, P., 2003. Whatever happened to Dorothy Reed? *Annals of Diagnostic Pathology*, 7(3), pp.195–203. Available at: http://linkinghub.elsevier.com/retrieve/pii/S1092913403000200 [Accessed August 19, 2011].

Deutschman, D.H. et al., 2003. Predicting obstructive coronary artery disease with serum sphingosine-1-phosphate. *American heart journal*, 146(1), pp.62–8. Available at: http://www.ncbi.nlm.nih.gov/pubmed/12851609 [Accessed November 7, 2011].

Dojcinov, S.D. et al., 2011. Age-related EBV-associated lymphoproliferative disorders in the Western population: a spectrum of reactive lymphoid hyperplasia and lymphoma. *Blood*, 117(18), pp.4726–35. Available at: http://www.pubmedcentral.nih.gov/articlerender.fcgi?artid=3100685&tool=pmcentrez&rendertype=abstract [Accessed June 16, 2011].

Dolcetti, R. et al., 2001. Pathogenetic and histogenetic features of HIV-associated Hodgkin ' s disease. *European Journal of Cancer*, 37, pp.1276–1287.

Don, A.S. et al., 2007. Essential requirement for sphingosine kinase 2 in a sphingolipid apoptosis pathway activated by FTY720 analogues. *The Journal of biological chemistry*, 282(21), pp.15833–42. Available at: http://www.ncbi.nlm.nih.gov/pubmed/17400555 [Accessed August 30, 2011].

Donovan, E.E., Pelanda, R. & Torres, R.M., 2010. S1P3 confers differential S1P-induced migration by autoreactive and non-autoreactive immature B cells and is required for normal B-cell development. *European journal of immunology*, 40(3), pp.688–98. Available at: http://www.pubmedcentral.nih.gov/articlerender.fcgi?artid=2924669&tool=pmcentrez&rendertype=abstract [Accessed November 7, 2011].

Dudek, S.M. et al., 2004. Pulmonary endothelial cell barrier enhancement by sphingosine 1-phosphate: roles for cortactin and myosin light chain kinase. *The Journal of biological chemistry*, 279(23), pp.24692–700. Available at: http://www.ncbi.nlm.nih.gov/pubmed/15056655 [Accessed February 17, 2011].

Edsall, L.C., Pirianov, G.G. & Spiegel, S, 1997. Involvement of sphingosine 1-phosphate in nerve growth factor-mediated neuronal survival and differentiation. *The Journal of neuroscience : the official journal of the Society for Neuroscience*, 17(18), pp.6952–60. Available at: http://www.ncbi.nlm.nih.gov/pubmed/9278531.

Edsall, L.C. & Spiegel, S, 1999. Enzymatic measurement of sphingosine 1-phosphate. *Analytical biochemistry*, 272(1), pp.80–6. Available at: http://www.ncbi.nlm.nih.gov/pubmed/11070858.

Eichholtz, T. et al., 1993. The bioactive phospholipid lysophosphatidic acid is released from activated platelets. *The Biochemical journal*, 291 (Pt 3, pp.677–80. Available at: http://www.pubmedcentral.nih.gov/articlerender.fcgi?artid=1132420&tool=pmcentrez&rendertype=abstract.

Endo, K. et al., 1991. Cell Membrane Signaling as Target in Cancer Therapy : Inhibitory Effect of N , N -Dimethyl and N , N , N -Trimethyl Sphingosine Derivatives on in Vitro and in Vivo Growth of Human Tumor Cells in Nude Mice Cell Membrane Signaling as Target in Cancer Therap. *Cancer Res*, 51(March 15), pp.1613–1618.

Essler, M. et al., 1999. Mildly Oxidized Low Density of Human Endothelial Cells through Activation of Rho / Rho Kinase and Inhibition of Myosin. *Biochemistry*, pp.30361–30364.

Falini, B. et al., 2011a. A monoclonal antibody (MUM1p) detects expression of the MUM1 / IRF4 protein in a subset of germinal center B cells , plasma cells , and activated T cells A monoclonal antibody (MUM1p) detects expression of the MUM1 / IRF4 protein in a subset of germin. *Hematology*, pp.2084–2092.

Falini, B. et al., 2011b. A monoclonal antibody (MUM1p) detects expression of the MUM1 / IRF4 protein in a subset of germinal center B cells , plasma cells , and activated T cells A monoclonal antibody (MUM1p) detects expression of the MUM1 / IRF4 protein in a subset of germin. *Hematology*, pp.2084–2092.

Flavell, K.J. et al., 2001. South Asian ethnicity and material deprivation increase the risk of Epstein-Barr virus infection in childhood Hodgkin ' s disease. *British Journal of Cancer*, 85, pp.350–356.

French, K.J. et al., 2006. Antitumor Activity of Sphingosine Kinase Inhibitors. *Pharmacology*, 318(2), pp.596–603.

French, K.J. et al., 2003a. Discovery and Evaluation of Inhibitors of Human Sphingosine Kinase Discovery and Evaluation of Inhibitors of Human Sphingosine Kinase 1. *Cancer Research*, 63(September 15), pp.5962–5969.

French, K.J. et al., 2003b. Discovery and evaluation of inhibitors of human sphingosine kinase. *Cancer research*, 63(18), pp.5962–9. Available at: http://www.ncbi.nlm.nih.gov/pubmed/14522923.

Fuss, B. et al., 1997. Phosphodiesterase I, a novel adhesion molecule and/or cytokine involved in oligodendrocyte function. *The Journal of Neuroscience : the official journal of the Society for Neuroscience*, 17(23), pp.9095–103. Available at: http://www.ncbi.nlm.nih.gov/pubmed/9364056.

Gaetano, C.G. et al., 2009. Inhibition of autotaxin production or activity blocks lysophosphatidylcholine-induced migration of human breast cancer and melanoma cells. *Mol Carcinog.*, 48(9), pp.801–809.

Garcia, J.G.N. et al., 2001. Sphingosine 1-phosphate promotes endothelial cell barrier integrity by Edg-dependent cytoskeletal rearrangement. *Cell*, 108(5), pp.689–701.

Gatter, K. & Pezzella, F., 2010. Diffuse large B-cell lymphoma. *Diagnostic Histopathology*, 16(2), pp.69–81. Available at: http://linkinghub.elsevier.com/retrieve/pii/S1756231709002230 [Accessed May 20, 2011].

Ghofrani, M. et al., 2007. Richter transformation of chronic lymphocytic leukemia presenting as a dural-based non-hodgkin lymphoma mass. *AJNR. American journal of neuroradiology*, 28(2), pp.318–20. Available at: http://www.ncbi.nlm.nih.gov/pubmed/21504298.

Gibson, S.E. & Hsi, E.D., 2009. Epstein-Barr virus-positive B-cell lymphoma of the elderly at a United States tertiary medical center: an uncommon aggressive lymphoma with a nongerminal center B-cell phenotype. *Human pathology*, 40(5), pp.653–61. Available at: http://www.ncbi.nlm.nih.gov/pubmed/19144386.

Gierse, J. et al., 2010. A novel autotaxin inhibitor reduces lysophosphatidic acid levels in plasma and the site of inflammation. *The Journal of Pharmacology and Experimental Therapeutics*, 334(1), pp.310–317.

Glickman, M. et al., 1999. Molecular cloning, tissue-specific expression, and chromosomal localization of a novel nerve growth factor-regulated G-protein- coupled receptor, nrg-1. *Molecular and cellular neurosciences*, 14(2), pp.141–52. Available at: http://www.ncbi.nlm.nih.gov/pubmed/10532805.

Goetzl, E.J. & Tigyi, G., 2004. Lysophospholipids and their G protein-coupled receptors in biology and diseases. *Journal of cellular biochemistry*, 92(5), pp.867–8. Available at: http://www.ncbi.nlm.nih.gov/pubmed/15258911 [Accessed October 4, 2011].

Greaves, W. et al., 2012. Detection of ABCC1 expression in classical Hodgkin lymphoma is associated with increased risk of treatment failure using standard chemotherapy protocols. *Journal of hematology & oncology*, 5(1), p.47. Available at: http://www.pubmedcentral.nih.gov/articlerender.fcgi?artid=3470996&tool=pmcentrez&rendertype=abstract [Accessed December 9, 2012].

Green, J. a et al., 2011. The sphingosine 1-phosphate receptor S1P(2) maintains the homeostasis of germinal center B cells and promotes niche confinement. *Nature Immunology*, 12(7), pp.672–80. Available at: http://www.ncbi.nlm.nih.gov/pubmed/21642988 [Accessed July 19, 2011].

Gräler, M H, Bernhardt, G. & Lipp, M., 1998. EDG6, a novel G-protein-coupled receptor related to receptors for bioactive lysophospholipids, is specifically expressed in lymphoid tissue. *Genomics*, 53(2), pp.164–9. Available at: http://www.ncbi.nlm.nih.gov/pubmed/9790765.

Guillermet-Guibert, J. et al., 2009. Targeting the sphingolipid metabolism to defeat pancreatic cancer cell resistance to the chemotherapeutic gemcitabine drug. *Molecular cancer therapeutics*, 8(4), pp.809–20. Available at: http://www.ncbi.nlm.nih.gov/pubmed/19372554 [Accessed May 21, 2012].

Hait, N.C. et al., 2009. Regulation of histone acetylation in the nucleus by sphingosine-1-phosphate. *Nucleus*, 325(5945), pp.1254–1257.

Hans, C.P., Weisenburger, Dennis D, Greiner, Timothy C, Gascoyne, R.D., Delabie, J., Ott, G., Mu, H.K., et al., 2004. Confirmation of the molecular classification of diffuse large B-cell lymphoma by immunohistochemistry using a tissue microarray. , 103(1), pp.275–282.

Hans, C.P., Weisenburger, Dennis D, Greiner, Timothy C, Gascoyne, R.D., Delabie, J., Ott, G., Müller-Hermelink, H.K., et al., 2004. Confirmation of the molecular classification of diffuse large B-cell lymphoma by immunohistochemistry using a tissue microarray. *Blood*, 103(1), pp.275–82. Available at: http://www.ncbi.nlm.nih.gov/pubmed/14504078 [Accessed January 7, 2011].

Harada, J. et al., 2004. Sphingosine-1-phosphate induces proliferation and morphological changes of neural progenitor cells. *Journal of Neurochemistry*, 88(4), pp.1026–1039. Available at: http://doi.wiley.com/10.1046/j.1471-4159.2003.02219.x [Accessed February 23, 2011].

Hecht, J.H. et al., 1996. Ventricular zone gene-1 (vzg-1) encodes a lysophosphatidic acid receptor expressed in neurogenic regions of the developing cerebral cortex. *The Journal of cell biology*, 135(4), pp.1071–83. Available at: http://www.pubmedcentral.nih.gov/articlerender.fcgi?artid=2133395&tool=pmcentrez&rendertype=abstract.

Henle W, Diehl V, Kohn G, ZurHausen H, H.G., 1967. Herpes-type virus and chro mosome marker in normal leukocytes after growth with irradiated Burkitt cells. *Science 1967;157:1064–5*, 157, pp.1064–1065.

Hiroshi Okazaki, Nobukazu Ishizaka, Takeshi Sakurai, Kiyoshi Kurokawa, Katsutoshi Goto, Mamuro Kumada, Y.T., 1993. Molecular Cloning of A Novel Putative G Protein-Coupled Receptor Expressed in the Cardiovascular System. *Biochemical and Biophysical Research Communications*, 190(3), pp.1104–1109.

Hla, T & Maciag, T., 1990. An abundant transcript induced in differentiating human endothelial cells encodes a polypeptide with structural similarities to G-protein-coupled receptors. *The Journal of biological chemistry*, 265(16), pp.9308–13. Available at: http://www.ncbi.nlm.nih.gov/pubmed/2160972.

Ho, J.W.Y. et al., 2005. Effects of a novel immunomodulating agent, FTY720, on tumor growth and angiogenesis in hepatocellular carcinoma. *Molecular cancer therapeutics*, 4(9), pp.1430–8. Available at: http://www.ncbi.nlm.nih.gov/pubmed/16170036 [Accessed January 23, 2012].

Hobson, J.P. et al., 2001. Role of the sphingosine-1-phosphate receptor EDG-1 in PDGF-induced cell motility. *Science (New York, N.Y.)*, 291(5509), pp.1800–3. Available at: http://www.ncbi.nlm.nih.gov/pubmed/11230698 [Accessed July 3, 2010].

Hodgkin, T., 1832. On some morbid apperances of the absorbent glands and spleen. *Med. Chir. Trans*, 17, pp.68–114.

Hoeller, S. et al., 2010. Epstein-Barr virus-positive diffuse large B-cell lymphoma in elderly patients is rare in Western populations. *Human pathology*, 41(3), pp.352–7. Available at: http://www.ncbi.nlm.nih.gov/pubmed/19913281 [Accessed September 21, 2010].

Hofscheier, A. et al., 2011. Geographic variation in the prevalence of Epstein-Barr virus-positive diffuse large B-cell lymphoma of the elderly: a comparative analysis of a Mexican and a German population. *Modern pathology : an official journal of the United States and Canadian Academy of Pathology, Inc*, 24(8), pp.1046–54. Available at: http://www.ncbi.nlm.nih.gov/pubmed/21499229 [Accessed August 22, 2011].

Hornuss, C. et al., 2001. Human and rat alveolar macrophages express multiple EDG receptors. *European journal of pharmacology*, 429(1-3), pp.303–8. Available at: http://www.ncbi.nlm.nih.gov/pubmed/11698050.

Hsi, E.D. et al., 2006. MAL is expressed in a subset of Hodgkin Lymphoma and identifies a population of patients with poor prognosis. *Am J Clinical Path*, 125(5), pp.776–782. Available at: http://ajcp.ascpjournals.org/cgi/doi/10.1309/98KLHRDAM5CMDHE2 [Accessed January 3, 2013].

Huang, X. et al., 2007. Expression of HLA class I and HLA class II by tumor cells in Chinese classical Hodgkin lymphoma patients. *J Clin Onco*, (25), pp.3101–3108. Available at: http://www.pubmedcentral.nih.gov/articlerender.fcgi?artid=2878318&tool=pmcentrez&rendertype=abstract [Accessed January 3, 2013].

Hänel, P., Andréani, P. & Gräler, Markus H, 2007. Erythrocytes store and release sphingosine 1-phosphate in blood. *The FASEB journal : official publication of the*

Federation of American Societies for Experimental Biology, 21(4), pp.1202–9. Available at: http://www.ncbi.nlm.nih.gov/pubmed/17215483 [Accessed July 4, 2011].

Ibrahim MA et al., 2012. Discovery of a novel class of potent and orally bioavailable sphingosine 1-phosphate receptor 1 antagonists. J Med Chem 2012; 55: 1368-81.

Igarashi, N. et al., 2003. Sphingosine kinase 2 is a nuclear protein and inhibits DNA synthesis. *The Journal of Biological Chemistry*, 278(47), pp.46832–9. Available at: http://www.ncbi.nlm.nih.gov/pubmed/12954646 [Accessed August 23, 2011].

Im, D.S. et al., 2000. Characterization of a novel sphingosine 1-phosphate receptor, Edg-8. *The Journal of Biological Chemistry*, 275(19), pp.14281–6. Available at: http://www.ncbi.nlm.nih.gov/pubmed/10799507.

Inagaki, Y., 2003. Identification of functional nuclear export sequences in human sphingosine kinase 1. *Biochemical and Biophysical Research Communications*, 311(1), pp.168–173. Available at: http://linkinghub.elsevier.com/retrieve/pii/S0006291X03020242 [Accessed February 8, 2011].

Jaffe, E.S. et al., 2008. Classification of lymphoid neoplasms : the microscope as a tool for disease discovery. *Blood*, 112(12), pp.4384–4399.

Jardin, F. et al., 2006. Novel Ig V gene features of t(14;18) and t(3;14) de novo diffuse large B-cell lymphoma displaying germinal center-B cell like and non-germinal center-B cell like markers. *Leukemia : official journal of the Leukemia Society of America, Leukemia*

Research Fund, U.K, 20(11), pp.2070–4. Available at: http://www.ncbi.nlm.nih.gov/pubmed/16990787 [Accessed August 31, 2011].

Jelena Levitskaya, Michael Coram, Victor Levitsky, Stefan Imreh, Patty M. Steigerwald-Mullen, George Klein, M.G.K.& M.G.M., 1995. Inhibition of antigen processing by the internal repeat region of the Epstein–Barr virus nuclear antigen-1. *Nature*, 375, pp.685–688.

Jenne, C.N. et al., 2009. T-bet-dependent S1P5 expression in NK cells promotes egress from lymph nodes and bone marrow. *The Journal of Experimental Medicine*, 206(11), pp.2469–81. Available at: http://www.pubmedcentral.nih.gov/articlerender.fcgi?artid=2768857&tool=pmcentrez&rendertype=abstract [Accessed June 29, 2011].

Jing, W. et al., 2010. A new protein Girdin in tumor metastasis. *Chin Med J*, 123(2006), pp.1786–1788.

Johnson, K.R. et al., 2005. Immunohistochemical distribution of sphingosine kinase 1 in normal and tumor lung tissue. *The journal of histochemistry and cytochemistry : official journal of the Histochemistry Society*, 53(9), pp.1159–66. Available at: http://www.ncbi.nlm.nih.gov/pubmed/15923363.

Johnson, K.R. et al., 2002. PKC-dependent activation of sphingosine kinase 1 and translocation to the plasma membrane. Extracellular release of sphingosine-1-phosphate induced by phorbol 12-myristate 13-acetate (PMA). *The Journal of biological chemistry*,

277(38), pp.35257–62. Available at: http://www.ncbi.nlm.nih.gov/pubmed/12124383 [Accessed November 4, 2011].

Johnson, K.R. et al., 2003. Role of human sphingosine-1-phosphate phosphatase 1 in the regulation of intra- and extracellular sphingosine-1-phosphate levels and cell viability. *The Journal of biological chemistry*, 278(36), pp.34541–7. Available at: http://www.ncbi.nlm.nih.gov/pubmed/12815058 [Accessed October 1, 2011].

Kapitonov, D. et al., 2009. Targeting sphingosine kinase 1 inhibits Akt signaling, induces apoptosis, and suppresses growth of human glioblastoma cells and xenografts. *Cancer research*, 69(17), pp.6915–23. Available at: http://www.pubmedcentral.nih.gov/articlerender.fcgi?artid=2752891&tool=pmcentrez&rendertype=abstract [Accessed August 19, 2011].

Kehlen, A. et al., 2004. Expression, regulation and function of autotaxin in thyroid carcinomas. *International journal of cancer. Journal international du cancer*, 109(6), pp.833–8. Available at: http://www.ncbi.nlm.nih.gov/pubmed/15027116 [Accessed March 15, 2011].

Khabir, A. et al., 2005. EBV latent membrane protein 1 abundance correlates with patient age but not with metastatic behavior in north African nasopharyngeal carcinomas. *Virology journal*, 2, p.39. Available at: http://www.pubmedcentral.nih.gov/articlerender.fcgi?artid=1112617&tool=pmcentrez&rendertype=abstract [Accessed August 13, 2011].

Kita, M.O. et al., 1997. ELEVATED LEVELS AND ALTERED FATTY ACID COMPOSITION OF PLASMA LYSOPHOSPHATIDYLCHOLINE (LYSOPC) IN OVARIAN CANCER PATIENTS. *Human Biology*, 34(November 1996), pp.31–34.

Kitayama, J. et al., 2004. Over-expression of lysophosphatidic acid receptor-2 in human invasive ductal carcinoma. *Breast cancer research : BCR*, 6(6), pp.R640–6. Available at: http://www.pubmedcentral.nih.gov/articlerender.fcgi?artid=1064082&tool=pmcentrez&rendertype=abstract [Accessed February 17, 2011].

Kleuser, B. et al., 2001. Stimulation of nuclear sphingosine kinase activity by platelet-derived growth factor. *FEBS letters*, 503(1), pp.85–90. Available at: http://www.ncbi.nlm.nih.gov/pubmed/11513860.

Kohama, T. et al., 1998. Molecular cloning and functional characterization of murine sphingosine kinase. *The Journal of biological chemistry*, 273(37), pp.23722–8. Available at: http://www.ncbi.nlm.nih.gov/pubmed/9726979.

Koichi Gonda, Hiroyuki Okamoto, Noriko Takuwa, Yutaka Yatomis, Hiroshi Okazaki, Takeshi Sakurai, S.K. et al., 1999. The novel sphingosine 1-phosphate receptor AGR16 is coupled via pertussis toxin-sensitive and -insensitive G-proteins to multiple signalling pathways. *Biochemical Journal*, 337, pp.67–75.

Kono, M. et al., 2004. The sphingosine-1-phosphate receptors S1P1, S1P2, and S1P3 function coordinately during embryonic angiogenesis. *The Journal of biological*

chemistry, 279(28), pp.29367–73. Available at: http://www.ncbi.nlm.nih.gov/pubmed/15138255 [Accessed July 21, 2011].

Kulwichit, W. et al., 1998. Expression of the Epstein-Barr virus latent membrane protein 1 induces B cell lymphoma in transgenic mice. *Proceedings of the National Academy of Sciences of the United States of America*, 95(20), pp.11963–8. Available at: http://www.pubmedcentral.nih.gov/articlerender.fcgi?artid=21748&tool=pmcentrez&rendertype=abstract.

Kuppers, R. & Rajewsky, Klaus, 1998. THE ORIGIN OF HODGKIN AND REED / STERNBERG CELLS IN HODGKIN ' S DISEASE. *Annual review of immunology*, 16, pp.471–493.

Kutok, J.L. & Wang, F., 2006. Spectrum of Epstein-Barr virus-associated diseases. *Annual review of pathology*, 1, pp.375–404. Available at: http://www.ncbi.nlm.nih.gov/pubmed/18039120 [Accessed August 2, 2011].

Kuze, T. et al., 2000. The characteristics of Epstein-Barr virus (EBV)-positive diffuse large B-cell lymphoma: comparison between EBV(+) and EBV(-) cases in Japanese population. *Japanese journal of cancer research : Gann*, 91(12), pp.1233–40. Available at: http://www.ncbi.nlm.nih.gov/pubmed/11123421.

Küppers, R et al., 1994. Hodgkin disease: Hodgkin and Reed-Sternberg cells picked from histological sections show clonal immunoglobulin gene rearrangements and appear to be derived from B cells at various stages of development. *Proceedings of the National Academy of Sciences of the United States of America*, 91(23), pp.10962–6. Available at:

http://www.pubmedcentral.nih.gov/articlerender.fcgi?artid=45146&tool=pmcentrez&rendertype=abstract.

Küppers, Ralf, 2009a. Clonotypic B cells in classic Hodgkin lymphoma. *Blood*, 114(18), pp.3970–1; author reply 3971–2. Available at: http://www.ncbi.nlm.nih.gov/pubmed/19875526 [Accessed July 5, 2010].

Küppers, Ralf, 2009b. Molecular biology of Hodgkin lymphoma. *Hematology / the Education Program of the American Society of Hematology. American Society of Hematology. Education Program*, pp.491–6. Available at: http://www.ncbi.nlm.nih.gov/pubmed/20008234.

Küppers, Ralf, 2009c. The biology of Hodgkin's lymphoma. *Nature reviews. Cancer*, 9(1), pp.15–27. Available at: http://www.ncbi.nlm.nih.gov/pubmed/19078975 [Accessed July 31, 2011].

Lai, W. et al., 2008. The role of sphingosine kinase in a murine model of allergic asthma. *The Journal of Immunology*, (180), pp.4323–4329.

Lepley, D. et al., 2005. The G protein-coupled receptor S1P2 regulates Rho/Rho kinase pathway to inhibit tumor cell migration. *Cancer research*, 65(9), pp.3788–95. Available at: http://www.ncbi.nlm.nih.gov/pubmed/15867375 [Accessed July 6, 2011].

Levitskaya, J. et al., 1997. Inhibition of ubiquitin/proteasome-dependent protein degradation by the Gly-Ala repeat domain of the Epstein-Barr virus nuclear antigen 1. *Proceedings of the National Academy of Sciences of the United States of America*, 94(23), pp.12616–

21. Available at: http://www.pubmedcentral.nih.gov/articlerender.fcgi?artid=25057&tool=pmcentrez&rendertype=abstract.

Li, C. et al., 2009. Involvement of sphingosine 1-phosphate (SIP)/S1P3 signaling in cholestasis-induced liver fibrosis. *The American journal of pathology*, 175(4), pp.1464–72. Available at: http://www.pubmedcentral.nih.gov/articlerender.fcgi?artid=2751543&tool=pmcentrez&rendertype=abstract [Accessed March 14, 2011].

Li, Mei-hong et al., 2009. Induction of antiproliferative connective tissue growth factor expression in Wilms' tumor cells by sphingosine-1-phosphate receptor 2. *Molecular Cancer*, 6(10), pp.1649–1656.

Li, Wen et al., 2009. Sphingosine kinase 1 is associated with gastric cancer progression and poor survival of patients. *Clinical cancer research : an official journal of the American Association for Cancer Research*, 15(4), pp.1393–9. Available at: http://www.ncbi.nlm.nih.gov/pubmed/19228740 [Accessed April 8, 2012].

Licht, T. et al., 2003. Induction of pro-angiogenic signaling by a synthetic peptide derived from the second intracellular loop of S1P3 (EDG3). *Blood*, 102(6), pp.2099–107. Available at: http://www.ncbi.nlm.nih.gov/pubmed/12763936 [Accessed September 18, 2011].

Ling, B. et al., 2011. Sphingosine-1-phosphate: a potential therapeutic agent against human breast cancer. *Investigational new drugs*, 29, pp.396–399. Available at: http://www.ncbi.nlm.nih.gov/pubmed/20041340 [Accessed February 2, 2011].

Liu, H et al., 2000. Molecular cloning and functional characterization of a novel mammalian sphingosine kinase type 2 isoform. *The Journal of biological chemistry*, 275(26), pp.19513–20. Available at: http://www.ncbi.nlm.nih.gov/pubmed/10751414 [Accessed August 31, 2011].

Liu, Hong et al., 2003. Sphingosine kinase type 2 is a putative BH3-only protein that induces apoptosis. *The Journal of biological chemistry*, 278(41), pp.40330–6. Available at: http://www.ncbi.nlm.nih.gov/pubmed/12835323.

Liu, S. et al., 2009. Expression of autotaxin and lysophosphatidic acid receptors increases mammary tumorigenesis, invasion, and metastases. *Cancer cell*, 15(6), pp.539–50. Available at: http://www.ncbi.nlm.nih.gov/pubmed/19477432 [Accessed January 10, 2013].

Liu, Y et al., 2000. Edg-1, the G protein-coupled receptor for sphingosine-1-phosphate, is essential for vascular maturation. *The Journal of clinical investigation*, 106(8), pp.951–61. Available at: http://www.pubmedcentral.nih.gov/articlerender.fcgi?artid=314347&tool=pmcentrez&rendertype=abstract.

Lockman, K. et al., 2004. Sphingosine 1-phosphate stimulates smooth muscle cell differentiation and proliferation by activating separate serum response factor co-factors.

The Journal of biological chemistry, 279(41), pp.42422–30. Available at: http://www.ncbi.nlm.nih.gov/pubmed/15292266 [Accessed April 6, 2011].

Lossos, Izidore S. et al., 2001. Expression of a single gene, BCL-6, strongly predicts survival in patients with diffuse large B-cell lymphoma. *Blood*, 98(4), pp.945–951. Available at: http://www.bloodjournal.org/cgi/doi/10.1182/blood.V98.4.945 [Accessed October 22, 2012].

Lümmen, G. et al., 1997. Identification of G protein-coupled receptors potently stimulating migration of human transitional-cell carcinoma cells. *Naunyn-Schmiedeberg's archives of pharmacology*, 356(6), pp.769–76. Available at: http://www.ncbi.nlm.nih.gov/pubmed/9453463.

Maceyka, M, 2002. Sphingosine kinase, sphingosine-1- phosphate, and apoptosis. *Biochim. Biophys. Acta*, 1585, pp.193–201.

Maceyka, Michael et al., 2005. SphK1 and SphK2, sphingosine kinase isoenzymes with opposing functions in sphingolipid metabolism. *The Journal of biological chemistry*, 280(44), pp.37118–29. Available at: http://www.ncbi.nlm.nih.gov/pubmed/16118219.

Macmahon, B. & June, I., 1966. Epidemiology of Hodgkin ' s Disease. In *Cancer Research*. pp. 1189–1200.

Maghazachi, A.A., 2003. G protein-coupled receptors in natural killer cells. *Journal of Leukocyte Biology*, 74(July).

Malavaud, B. et al., 2010. Sphingosine kinase-1 activity and expression in human prostate cancer resection specimens. *European journal of cancer (Oxford, England : 1990)*, 46(18), pp.3417–24. Available at: http://www.ncbi.nlm.nih.gov/pubmed/20970322 [Accessed April 18, 2012].

Malek, R.L. et al., 2001. Nrg-1 belongs to the endothelial differentiation gene family of G protein-coupled sphingosine-1-phosphate receptors. *The Journal of biological chemistry*, 276(8), pp.5692–9. Available at: http://www.ncbi.nlm.nih.gov/pubmed/11069896 [Accessed September 18, 2011].

Malgorzata M. Ptaszynska, Michael L. Pendrak, Mary L. Stracke, and D.D.R., 2011. Autotaxin signaling via lysophosphatidic acid receptors contributes to vascular endothelial growth factor-induced endothelial cell migration. *Molecular Cancer*, 8(3), pp.309–321.

Mandala, Suzanne et al., 2002. Alteration of lymphocyte trafficking by sphingosine-1-phosphate receptor agonists. *Science (New York, N.Y.)*, 296(5566), pp.346–9. Available at: http://www.ncbi.nlm.nih.gov/pubmed/11923495 [Accessed August 2, 2011].

Martino, A., 2007. Sphingosine 1-phosphate as a novel immune regulator of dendritic cells. *Journal of biosciences*, 32(6), pp.1207–12. Available at: http://www.ncbi.nlm.nih.gov/pubmed/17954981.

McCormick, N.K., McCormick, K.J. & Trentin, J.J., 1976. Antinuclear antibodies and elevated anti-Epstein-Barr virus titers in cancer patients. *Infection and immunity*, 13(5), pp.1382–6. Available at:

http://www.pubmedcentral.nih.gov/articlerender.fcgi?artid=420769&tool=pmcentrez&rendertype=abstract.

van Meeteren, L. a et al., 2006. Autotaxin, a secreted lysophospholipase D, is essential for blood vessel formation during development. *Molecular and cellular biology*, 26(13), pp.5015–22. Available at: http://www.pubmedcentral.nih.gov/articlerender.fcgi?artid=1489177&tool=pmcentrez&rendertype=abstract [Accessed January 31, 2011].

Melendez, A.J., 2008. Sphingosine kinase signalling in immune cells: potential as novel therapeutic targets. *Biochimica et biophysica acta*, 1784(1), pp.66–75. Available at: http://www.ncbi.nlm.nih.gov/pubmed/17913601.

Melendez, A.J. & Khaw, A.K., 2002. Dichotomy of Ca2+ signals triggered by different phospholipid pathways in antigen stimulation of human mast cells. *The Journal of biological chemistry*, 277(19), pp.17255–62. Available at: http://www.ncbi.nlm.nih.gov/pubmed/11856736 [Accessed November 11, 2011].

Meyer zu Heringdorf, D. et al., 1998. Sphingosine kinase-mediated Ca2+ signalling by G-protein-coupled receptors. *The EMBO journal*, 17(10), pp.2830–7. Available at: http://www.pubmedcentral.nih.gov/articlerender.fcgi?artid=1170623&tool=pmcentrez&rendertype=abstract.

Michael C. Haffner, Martin J. Aryee, Antoun Toubaji, David M. Esopi, R., Albadine, Bora Gurel, William B. Isaacs, G. Steven Bova, Wennuan Liu, J.X. & Alan K. Meeker, George Netto, Angelo M. De Marzo1, William G. Nelson, Yegnasubramanian, S., 2011.

Androgen-induced TOP2B mediated double strand breaks and prostate cancer gene rearrangements. *Nat Genet*, 42(8), pp.668–675.

Mitra, P. et al., 2006. Role of ABCC1 in export of sphingosine-1-phosphate from mast cells. *Proceedings of the National Academy of Sciences of the United States of America*, 103(44), pp.16394–9. Available at: http://www.pubmedcentral.nih.gov/articlerender.fcgi?artid=1637593&tool=pmcentrez&rendertype=abstract.

Mizugishi, K. et al., 2005. Essential Role for Sphingosine Kinases in Neural and Vascular Development. *Society*, 25(24), pp.11113–11121.

Montanaro, L., Treré, D. & Derenzini, M., 2008. Nucleolus, ribosomes, and cancer. *The American journal of pathology*, 173(2), pp.301–10. Available at: http://www.pubmedcentral.nih.gov/articlerender.fcgi?artid=2475768&tool=pmcentrez&rendertype=abstract [Accessed March 28, 2012].

Moolenaar, Wouter H, 1995. Lysophosphatidic acid, a multifunctional phospholipid messenger. *The Journal of Biological Chemistry*, 270(June 2), pp.12949–12952.

Morente, M.M. et al., 1997. Adverse clinical outcome in Hodgkin's disease is associated with loss of retinoblastoma protein expression, high Ki67 proliferation index, and absence of Epstein-Barr Virus-Latent Membrane Protein 1 expression. *Blood*, 90, pp.2429–2436.

Murph, M. & Mills, G.B., 2007. Targeting the lipids LPA and S1P and their signalling pathways to inhibit tumour progression. *Expert reviews in molecular medicine*, 9(28),

pp.1–18. Available at: http://www.ncbi.nlm.nih.gov/pubmed/17935635 [Accessed December 28, 2010].

Murph, M.M. et al., 2009. Lysophosphatidic acid-induced transcriptional profile represents serous epithelial ovarian carcinoma and worsened prognosis. *PloS one*, 4(5), p.e5583. Available at: http://www.pubmedcentral.nih.gov/articlerender.fcgi?artid=2679144&tool=pmcentrez&rendertype=abstract [Accessed November 18, 2012].

N Young, J.R.V.B., 2007. Roles of Sphingosine-1-Phosphate (S1P) Receptors in Malignant Behavior of Glioma Cells. Differential Effects of S1P2 on Cell Migration and Invasiveness. *Exp Cell Res*, 313(8), pp.1615–1627.

Nakamura S, Jaffe E, S.S., 2008. WHO Classification of Tumours of Haematopoietic and Lymphoid Tissues. In *WHO Classification of Tumours of Haematopoietic and Lymphoid Tissues. Lyon, France: IARC*. pp. 243–244. Available at: http://www.ncbi.nlm.nih.gov/pubmed/19642739.

Nam, S.W. et al., 2000. Autotaxin (ATX), a potent tumor motogen, augments invasive and metastatic potential of ras-transformed cells. *Oncogene*, 19(2), pp.241–7. Available at: http://www.ncbi.nlm.nih.gov/pubmed/10645002.

Nava, V., 2002. Sphingosine Kinase Type 1 Promotes Estrogen-Dependent Tumorigenesis of Breast Cancer MCF-7 Cells. *Experimental Cell Research*, 281(1), pp.115–127. Available at: http://linkinghub.elsevier.com/retrieve/pii/S0014482702956582 [Accessed October 11, 2011].

Nishimura, H. et al., 2010. Expression of sphingosine-1-phosphate receptor 1 in mantle cell lymphoma. *Modern pathology*, 23(3), pp.439–49. Available at: http://www.ncbi.nlm.nih.gov/pubmed/20081804 [Accessed October 6, 2010].

Nishiuma, T. et al., 2008. Inhalation of sphingosine kinase inhibitor attenuates airway inflammation in asthmatic mouse model. *American journal of physiology- Lung cellular and molecular physiology*, 294(6), pp.L1085–93. Available at: http://www.ncbi.nlm.nih.gov/pubmed/18359884 [Accessed January 16, 2012].

Ogawa, C. et al., 2003. Identification and characterization of a novel human sphingosine-1-phosphate phosphohydrolase, hSPP2. *The Journal of biological chemistry*, 278(2), pp.1268–72. Available at: http://www.ncbi.nlm.nih.gov/pubmed/12411432 [Accessed September 30, 2011].

Ogretmen, Besim & Hannun, Yusuf a, 2004. Biologically active sphingolipids in cancer pathogenesis and treatment. *Nature reviews. Cancer*, 4(8), pp.604–16. Available at: http://www.ncbi.nlm.nih.gov/pubmed/15286740.

Okamoto, H. et al., 1998. EDG1 is a functional sphingosine-1-phosphate receptor that is linked via a Gi/o to multiple signaling pathways, including phospholipase C activation, Ca2+ mobilization, Ras-mitogen-activated protein kinase activation, and adenylate cyclase inhibition. *The Journal of biological chemistry*, 273(42), pp.27104–10. Available at: http://www.ncbi.nlm.nih.gov/pubmed/9765227.

Okoshi, H., Hakomori, Sen-itiroh & Nisar, M., 1991. Cell Membrane Signaling as Target in Cancer Therapy II : Inhibitory Effect of N , N , N -Trimethylsphingosine on Metastatic

Potential of Murine B16 Melanoma Cell Line through Blocking of Tumor Cell-dependent Platelet Aggregation Cell Membrane Signaling as. *Cancer Research*, 51, pp.6019–6024.

Olivera, A. et al., 2007. The sphingosine kinase-sphingosine-1-phosphate axis is a determinant of mast cell function and anaphylaxis. *Immunity*, 26(3), pp.287–97. Available at: http://www.ncbi.nlm.nih.gov/pubmed/17346996 [Accessed June 27, 2011].

Olivier Cuvillier, Grisha Pirianov, Burkhard Leuser, Philip G. Vanek, Omar A. Coso, J. Silvio Gutkind, S.S., 1996. Suppression of ceramide-mediated programmed cell death. , pp.800–803.

Oskouian, B. et al., 2006. Sphingosine-1-phosphate lyase potentiates apoptosis via p53- and p38-dependent pathways and is down-regulated in colon cancer. *Proceedings of the National Academy of Sciences of the United States of America*, 103(46), pp.17384–9. Available at: http://www.pubmedcentral.nih.gov/articlerender.fcgi?artid=1859938&tool=pmcentrez&rendertype=abstract.

Oyama, T. et al., 2007. Age-related EBV-associated B-cell lymphoproliferative disorders constitute a distinct clinicopathologic group: a study of 96 patients. *Clinical cancer research : an official journal of the American Association for Cancer Research*, 13(17), pp.5124–32. Available at: http://www.ncbi.nlm.nih.gov/pubmed/17785567.

Oyama, T. et al., 2003. Senile EBV+ B-cell lymphoproliferative disorders: a clinicopathologic study of 22 patients. *The American journal of surgical pathology*, 27(1), pp.16–26. Available at: http://www.ncbi.nlm.nih.gov/pubmed/12502924.

O'Brien, N. et al., 2009. Production and characterization of monoclonal anti-sphingosine-1-phosphate antibodies. *Journal of lipid research*, 50(11), pp.2245–57. Available at: http://www.pubmedcentral.nih.gov/articlerender.fcgi?artid=2759830&tool=pmcentrez&rendertype=abstract [Accessed October 11, 2011].

De Paepe, P. et al., 2005. Large cleaved and immunoblastic lymphoma may represent two distinct clinicopathologic entities within the group of diffuse large B-cell lymphomas. *Journal of clinical oncology*, 23(28), pp.7060–8. Available at: http://www.ncbi.nlm.nih.gov/pubmed/16129841 [Accessed November 21, 2012].

Paik, J.H. et al., 2001. Sphingosine 1-phosphate-induced endothelial cell migration requires the expression of EDG-1 and EDG-3 receptors and Rho-dependent activation of alpha vbeta3- and beta1-containing integrins. *The Journal of biological chemistry*, 276(15), pp.11830–7. Available at: http://www.ncbi.nlm.nih.gov/pubmed/11150298 [Accessed June 13, 2011].

Pappu, R. et al., 2007. Promotion of lymphocyte egress into blood and lymph by distinct sources of sphingosine-1-phosphate. *Science (New York, N.Y.)*, 316(5822), pp.295–8. Available at: http://www.ncbi.nlm.nih.gov/pubmed/17363629 [Accessed June 11, 2011].

Park, I.-K., 2002. Differential gene expression profiling of adult murine hematopoietic stem cells. *Blood*, 99(2), pp.488–498. Available at:

http://www.bloodjournal.org/cgi/doi/10.1182/blood.V99.2.488 [Accessed March 27, 2012].

Park, S. et al., 2007. The impact of Epstein-Barr virus status on clinical outcome in diffuse large B-cell lymphoma. *Blood*, 110(3), pp.972–8. Available at: http://www.ncbi.nlm.nih.gov/pubmed/17400912 [Accessed November 26, 2010].

Patrick Adam, Irina Bonzheim, Falko Fend, L.Q.-M., 2011. Epstein-Barr Virus-positive Diffuse Large B-cell Lymphomas of the Elderly. *AdvAnatomic Pathology*, 18(September), pp.349–355.

Paugh, S.W. et al., 2008. A selective sphingosine kinase 1 inhibitor integrates multiple molecular therapeutic targets in human leukemia. *Blood*, 112(4), pp.1382–91. Available at: http://www.pubmedcentral.nih.gov/articlerender.fcgi?artid=2515133&tool=pmcentrez&rendertype=abstract [Accessed February 24, 2012].

Pfreundschuh, M. et al., 2008. Prognostic significance of maximum tumour (bulk) diameter in young patients with good-prognosis diffuse large-B-cell lymphoma treated with CHOP-like chemotherapy with or without rituximab: an exploratory analysis of the MabThera International Trial Group . *The lancet oncology*, 9(5), pp.435–44. Available at: http://www.ncbi.nlm.nih.gov/pubmed/18400558 [Accessed October 22, 2012].

Pitson, Stuart M et al., 2003. Activation of sphingosine kinase 1 by ERK1/2-mediated phosphorylation. *The EMBO journal*, 22(20), pp.5491–500. Available at:

http://www.pubmedcentral.nih.gov/articlerender.fcgi?artid=213794&tool=pmcentrez&rendertype=abstract.

Pitson, Stuart M et al., 2005. Phosphorylation-dependent translocation of sphingosine kinase to the plasma membrane drives its oncogenic signalling. *The Journal of experimental medicine*, 201(1), pp.49–54. Available at: http://www.pubmedcentral.nih.gov/articlerender.fcgi?artid=2212769&tool=pmcentrez&rendertype=abstract.

Pogribny, I.P. et al., 2007. Methyl Deficiency , Alterations in Global Histone. *Journal of Nutrition*.

Ponnusamy, S. et al., 2012. Communication between host organism and cancer cells is transduced by systemic sphingosine kinase 1/sphingosine 1-phosphate signalling to regulate tumour metastasis. *EMBO molecular medicine*, 4(8), pp.761–75. Available at: http://www.pubmedcentral.nih.gov/articlerender.fcgi?artid=3494075&tool=pmcentrez&rendertype=abstract [Accessed December 31, 2012].

Portis, T., Dyck, P. & Longnecker, Richard, 2003. Epstein-Barr Virus (EBV) LMP2A induces alterations in gene transcription similar to those observed in Reed-Sternberg cells of Hodgkin lymphoma. *Gene*, 102(12), pp.4166–4178.

Pyne, N.J. & Pyne, S., 2010. Sphingosine 1-phosphate and cancer. *Nature reviews. Cancer*, 10(7), pp.489–503. Available at: http://www.ncbi.nlm.nih.gov/pubmed/20555359 [Accessed July 23, 2011].

Ramaswamy, S. et al., 2003. A molecular signature of metastasis in primary solid tumors. *Nature genetics*, 33(1), pp.49–54. Available at: http://www.ncbi.nlm.nih.gov/pubmed/12469122 [Accessed August 1, 2011].

Ramos-Vara, J. a, 2005. Technical aspects of immunohistochemistry. *Veterinary pathology*, 42(4), pp.405–26. Available at: http://www.ncbi.nlm.nih.gov/pubmed/16006601 [Accessed July 5, 2011].

Reed, D., 1902. On the pathological changes in Hodgkin's disease with special reference to its relation in tuberculosis. *John Hopkins Hosp. Rep*, 10, pp.133–193.

Rosen, H. & Goetzl, E.J., 2005. Sphingosine 1-phosphate and its receptors: an autocrine and paracrine network. *Nature reviews. Immunology*, 5(7), pp.560–70. Available at: http://www.ncbi.nlm.nih.gov/pubmed/15999095 [Accessed July 19, 2011].

Rosenwald, Andreas et al., 2002. The use of molecular profiling to predict survival after chemotherapy for diffuse large-B-cell lymphoma. *The New England journal of medicine*, 346(25), pp.1937–47. Available at: http://www.ncbi.nlm.nih.gov/pubmed/12075054.

Rowe, M. et al., 2009. Burkitt's lymphoma: the Rosetta Stone deciphering Epstein-Barr virus biology. *Seminars in cancer biology*, 19(6), pp.377–88. Available at: http://www.ncbi.nlm.nih.gov/pubmed/19619657.

Ruckhäberle, E. et al., 2008. Microarray analysis of altered sphingolipid metabolism reveals prognostic significance of sphingosine kinase 1 in breast cancer. *Breast cancer research*

and treatment, 112(1), pp.41–52. Available at: http://www.ncbi.nlm.nih.gov/pubmed/18058224 [Accessed January 14, 2011].

Rümenapp, U. et al., 2000. Sphingolipid receptor signaling and function in human bladder carcinoma cells: inhibition of LPA- but enhancement of thrombin-stimulated cell motility. *Naunyn-Schmiedeberg's archives of pharmacology*, 361(1), pp.1–11. Available at: http://www.ncbi.nlm.nih.gov/pubmed/10651140.

Sabbadini, R. a, 2011. Sphingosine-1-phosphate antibodies as potential agents in the treatment of cancer and age-related macular degeneration. *British journal of pharmacology*, 162(6), pp.1225–38. Available at: http://www.pubmedcentral.nih.gov/articlerender.fcgi?artid=3058156&tool=pmcentrez&rendertype=abstract [Accessed December 27, 2011].

Sachinidis, A. et al., 1999. Evidence That Lipoproteins Are Carriers of Bioactive Factors. *Arteriosclerosis, Thrombosis, and Vascular Biology*, 19(10), pp.2412–2421. Available at: http://atvb.ahajournals.org/cgi/doi/10.1161/01.ATV.19.10.2412 [Accessed February 16, 2012].

Sadahira, Y et al., 1992. Sphingosine 1-phosphate, a specific endogenous signaling molecule controlling cell motility and tumor cell invasiveness. *Proceedings of the National Academy of Sciences of the United States of America*, 89(20), pp.9686–90. Available at: http://www.pubmedcentral.nih.gov/articlerender.fcgi?artid=50197&tool=pmcentrez&rendertype=abstract.

Saini, K.S. et al., 2011. Rituximab in Hodgkin lymphoma: is the target always a hit? *Cancer treatment reviews*, 37(5), pp.385–90. Available at: http://www.ncbi.nlm.nih.gov/pubmed/21183282 [Accessed August 27, 2011].

Salinas, N.R. et al., 2009. Lung tumor development in the presence of sphingosine 1-phosphate agonist FTY720. *Pathology oncology research : POR*, 15(4), pp.549–54. Available at: http://www.ncbi.nlm.nih.gov/pubmed/19214784 [Accessed October 11, 2011].

Sato, K. et al., 2007. Critical role of ABCA1 transporter in sphingosine 1-phosphate release from astrocytes. *Journal of neurochemistry*, 103(6), pp.2610–9. Available at: http://www.ncbi.nlm.nih.gov/pubmed/17931360 [Accessed September 13, 2011].

Scherrmann, J.-M., 2005. Expression and function of multidrug resistance transporters at the blood-brain barriers. *Expert opinion on drug metabolism & toxicology*, 1(2), pp.233–46. Available at: http://www.ncbi.nlm.nih.gov/pubmed/16922639.

SchrecengostFrench, R.S. et al., 2003. Discovery and Evaluation of Inhibitors of Human Sphingosine Kinase Discovery and Evaluation of Inhibitors of Human Sphingosine Kinase 1. *Cancer Research*, 63, pp.5962–5969.

Schwab, S.R. et al., 2005. Lymphocyte sequestration through S1P lyase inhibition and disruption of S1P gradients. *Science (New York, N.Y.)*, 309(5741), pp.1735–9. Available at: http://www.ncbi.nlm.nih.gov/pubmed/16151014 [Accessed July 6, 2011].

Schwab, S.R. & Cyster, J.G., 2007. Finding a way out: lymphocyte egress from lymphoid organs. *Nature immunology*, 8(12), pp.1295–301. Available at: http://www.ncbi.nlm.nih.gov/pubmed/18026082 [Accessed July 17, 2011].

Sehn, L.H. et al., 2007. The revised International Prognostic Index (R-IPI) is a better predictor of outcome than the standard IPI for patients with diffuse large B-cell lymphoma treated with R-CHOP. *Blood*, 109(5), pp.1857–61. Available at: http://www.ncbi.nlm.nih.gov/pubmed/17105812 [Accessed October 10, 2012].

Seiden-Long, I.M. et al., 2006. Transcriptional targets of hepatocyte growth factor signaling and Ki-ras oncogene activation in colorectal cancer. *Oncogene*, 25(1), pp.91–102. Available at: http://www.ncbi.nlm.nih.gov/pubmed/16158056 [Accessed March 27, 2012].

Shida, K Takabe, D Kapitonov, S Milstien, S.S., 2008. Targeting SphK1 as a New Strategy against Cancer. *Curr Drug Targets*, 9(9), pp.662–673.

Shimoyama, Y. et al., 2008. Age-related Epstein-Barr virus-associated B-cell lymphoproliferative disorders: special references to lymphomas surrounding this newly recognized clinicopathologic disease. *Cancer science*, 99(6), pp.1085–91. Available at: http://www.ncbi.nlm.nih.gov/pubmed/18429953 [Accessed November 29, 2010].

Shiozawa, E. et al., 2007. The GCB subtype of diffuse large B-cell lymphoma is less frequent in Asian countries. *Leukemia research*, 31(11), pp.1579–83. Available at: http://www.ncbi.nlm.nih.gov/pubmed/17448534 [Accessed May 20, 2011].

Shipp, 1993. A predictive model for aggressive non-Hodgkin's lymphoma. The International Non-Hodgkin's Lymphoma Prognostic Factors Project. *N Engl J Med*, 329(14), pp.987–94.

Siehler, S. et al., 2001. Sphingosine 1-phosphate activates nuclear factor-kappa B through Edg receptors. Activation through Edg-3 and Edg-5, but not Edg-1, in human embryonic kidney 293 cells. *The Journal of biological chemistry*, 276(52), pp.48733–9. Available at: http://www.ncbi.nlm.nih.gov/pubmed/11673450 [Accessed February 23, 2012].

Spiegel, S, 1999. Sphingosine 1-phosphate: a prototype of a new class of second messengers. *Journal of leukocyte biology*, 65(3), pp.341–4. Available at: http://www.ncbi.nlm.nih.gov/pubmed/10080537.

Spiegel, Sarah & Milstien, Sheldon, 2002. Sphingosine 1-phosphate, a key cell signaling molecule. *The Journal of biological chemistry*, 277(29), pp.25851–4. Available at: http://www.ncbi.nlm.nih.gov/pubmed/12011102.

Spiegel, Sarah & Milstien, Sheldon, 2003. Sphingosine-1-phosphate: an enigmatic signalling lipid. *Nature reviews. Molecular cell biology*, 4(5), pp.397–407. Available at: http://www.ncbi.nlm.nih.gov/pubmed/12728273 [Accessed January 31, 2011].

Spiegel, Sarah & Milstien, Sheldon, 2011. The outs and the ins of sphingosine-1-phosphate in immunity. *Nature Reviews Immunology*, (May), pp.1–13. Available at: http://www.nature.com/doifinder/10.1038/nri2974 [Accessed May 6, 2011].

Stracke, M.L. et al., 1992. Identification, purification, and partial sequence analysis of autotaxin, a novel motility-stimulating protein. *The Journal of biological chemistry*, 267(4), pp.2524–9. Available at: http://www.ncbi.nlm.nih.gov/pubmed/1733949.

Sup, S.J. et al., 2005. Expression of bcl-2 in classical Hodgkin's lymphoma: an independent predictor of poor outcome. *J Clin Onco*, 23(16), pp.3773–9. Available at: http://www.ncbi.nlm.nih.gov/pubmed/15809450 [Accessed January 3, 2013].

Taha, T. a et al., 2006. Loss of sphingosine kinase-1 activates the intrinsic pathway of programmed cell death: modulation of sphingolipid levels and the induction of apoptosis. *The FASEB journal : official publication of the Federation of American Societies for Experimental Biology*, 20(3), pp.482–4. Available at: http://www.ncbi.nlm.nih.gov/pubmed/16507765.

Takabe, K. et al., 2008. " Inside-Out " Signaling of Sphingosine-1-Phosphate : *Pharmacological Reviews*, 60(2), pp.181–195.

Takabe, K. et al., 2010. Estradiol induces export of sphingosine 1-phosphate from breast cancer cells via ABCC1 and ABCG2. *The Journal of biological chemistry*, 285(14), pp.10477–86. Available at: http://www.ncbi.nlm.nih.gov/pubmed/20110355.

Takuwa, Yoh et al., 2008. Sphingosine-1-phosphate signaling and biological activities in the cardiovascular system. *Biochimica et biophysica acta*, 1781(9), pp.483–8.

Tay Hwee Kee, P.V. and A.J.M., 2005. SPHINGOSINE KINASE SIGNALLING IN IMMUNE CELLS. *Clinical and Experimental Pharmacology and Physiology*, pp.153–161.

Tilly, J.L. & Kolesnick, R.N., 2002. Sphingolipids, apoptosis, cancer treatments and the ovary: investigating a crime against female fertility. *Biochimica et biophysica acta*, 1585(2-3), pp.135–8. Available at: http://www.ncbi.nlm.nih.gov/pubmed/12531546.

Tsimberidou, A.-M. & Keating, M.J., 2005. Richter syndrome: biology, incidence, and therapeutic strategies. *Cancer*, 103(2), pp.216–28. Available at: http://www.ncbi.nlm.nih.gov/pubmed/15578683 [Accessed August 3, 2011].

Tsuboi, K. et al., 2000. MUM1/IRF4 expression as a frequent event in mature lymphoid malignancies. *Leukemia : official journal of the Leukemia Society of America, Leukemia Research Fund, U.K*, 14(3), pp.449–56. Available at: http://www.ncbi.nlm.nih.gov/pubmed/10720141.

Tzankov, A. et al., 2005. Rare expression of T-cell markers in classical Hodgkin's lymphoma. *Modern pathology : an official journal of the United States and Canadian Academy of Pathology, Inc*, 18(12), pp.1542–9. Available at: http://www.ncbi.nlm.nih.gov/pubmed/16056244 [Accessed January 22, 2012].

Uechi, T. et al., 2006. Ribosomal protein gene knockdown causes developmental defects in zebrafish. *PloS one*, 1(1), p.e37. Available at: http://www.pubmedcentral.nih.gov/articlerender.fcgi?artid=1762390&tool=pmcentrez&rendertype=abstract [Accessed March 28, 2012].

Umezu-Goto, M. et al., 2002. Autotaxin has lysophospholipase D activity leading to tumor cell growth and motility by lysophosphatidic acid production. *The Journal of cell biology*, 158(2), pp.227–33. Available at: http://www.pubmedcentral.nih.gov/articlerender.fcgi?artid=2173129&tool=pmcentrez&rendertype=abstract [Accessed November 14, 2012].

Uner, A. et al., 2011. The presence of Epstein-Barr virus (EBV) in diffuse large B-cell lymphomas (DLBCLs) in Turkey: special emphasis on "EBV-positive DLBCL of the elderly". *APMIS : acta pathologica, microbiologica, et immunologica Scandinavica*, 119(4-5), pp.309–16. Available at: http://www.ncbi.nlm.nih.gov/pubmed/21492232 [Accessed June 22, 2011].

Usui, S. et al., 2004. Blood lipid mediator sphingosine 1-phosphate potently stimulates platelet-derived growth factor-A and -B chain expression through S1P1-Gi-Ras-MAPK-dependent induction of Kruppel-like factor 5. *The Journal of biological chemistry*, 279(13), pp.12300–11. Available at: http://www.ncbi.nlm.nih.gov/pubmed/14711826 [Accessed July 29, 2011].

Venkataraman, K. et al., 2006. Extracellular export of sphingosine kinase-1a contributes to the vascular S1P gradient. *The Biochemical journal*, 397(3), pp.461–71. Available at: http://www.pubmedcentral.nih.gov/articlerender.fcgi?artid=1533315&tool=pmcentrez&rendertype=abstract [Accessed July 21, 2011].

Venkataraman, K. et al., 2008. Vascular endothelium as a contributor of plasma sphingosine 1-phosphate. *Circulation research*, 102(6), pp.669–76. Available at:

http://www.pubmedcentral.nih.gov/articlerender.fcgi?artid=2659392&tool=pmcentrez&rendertype=abstract [Accessed July 12, 2011].

Visentin, B. et al., 2006. Validation of an anti-sphingosine-1-phosphate antibody as a potential therapeutic in reducing growth, invasion, and angiogenesis in multiple tumor lineages. *Cancer cell*, 9(3), pp.225–38. Available at: http://www.ncbi.nlm.nih.gov/pubmed/16530706 [Accessed June 14, 2011].

Vockerodt, M. et al., 2008. The Epstein – Barr virus oncoprotein , latent membrane protein-1 , reprograms germinal centre B cells towards a Hodgkin ' s Reed – Sternberg-like phenotype. *Journal of Pathology, The*, 216, pp.83–92.

Wang, W., Graeler, M.H. & Goetzl, E.J., 2005. Type 4 sphingosine 1-phosphate G protein-coupled receptor (S1P4) transduces S1P effects on T cell proliferation and cytokine secretion without signaling migration. *The FASEB journal : official publication of the Federation of American Societies for Experimental Biology*, 19(12), pp.1731–3. Available at: http://www.ncbi.nlm.nih.gov/pubmed/16046470 [Accessed October 1, 2011].

Watson, C. et al., 2010. High expression of sphingosine 1-phosphate receptors, S1P1 and S1P3, sphingosine kinase 1, and extracellular signal-regulated kinase-1/2 is associated with development of tamoxifen resistance in estrogen receptor-positive breast cancer patients. *The American journal of pathology*, 177(5), pp.2205–15. Available at: http://www.pubmedcentral.nih.gov/articlerender.fcgi?artid=2966780&tool=pmcentrez&rendertype=abstract [Accessed March 2, 2011].

Weigert, A. et al., 2009. Sphingosine kinase 2 deficient tumor xenografts show impaired growth and fail to polarize macrophages towards an anti-inflammatory phenotype. *International journal of cancer. Journal international du cancer*, 125(9), pp.2114–21. Available at: http://www.ncbi.nlm.nih.gov/pubmed/19618460 [Accessed October 11, 2011].

Weiss, L.M. et al., 1991. Epstein-Barr Virus and Hodgkin ' s Disease. *American Journal of Pathology*, 139(6), pp.1259–1265.

Windh, R.T. et al., 1999. Differential coupling of the sphingosine 1-phosphate receptors Edg-1, Edg-3, and H218/Edg-5 to the G(i), G(q), and G(12) families of heterotrimeric G proteins. *The Journal of biological chemistry*, 274(39), pp.27351–8. Available at: http://www.ncbi.nlm.nih.gov/pubmed/10488065.

Withoff, S. et al., 1999. DNA topoisomerase IIalpha and -beta expression in human ovarian cancer. *British journal of cancer*, 79(5-6), pp.748–53. Available at: http://www.pubmedcentral.nih.gov/articlerender.fcgi?artid=2362692&tool=pmcentrez&rendertype=abstract.

Wright, G. et al., 2003. A gene expression-based method to diagnose clinically distinct subgroups of diffuse large B cell lymphoma. *Proceedings of the National Academy of Sciences of the United States of America*, 100(17), pp.9991–6. Available at: http://www.pubmedcentral.nih.gov/articlerender.fcgi?artid=187912&tool=pmcentrez&rendertype=abstract.

Wu, J.-M. et al., 2010. Autotaxin expression and its connection with the TNF-alpha-NF-kappaB axis in human hepatocellular carcinoma. *Molecular cancer*, 9, p.71. Available at: http://www.pubmedcentral.nih.gov/articlerender.fcgi?artid=2867819&tool=pmcentrez&rendertype=abstract.

Xia, P et al., 2000. An oncogenic role of sphingosine kinase. *Current biology : CB*, 10(23), pp.1527–30. Available at: http://www.ncbi.nlm.nih.gov/pubmed/11114522.

Xiaoyu Xu, Guanghui Yang, Honglu Zhang, and G.D.P., 2009. Evaluating dual activity LPA receptor pan-antagonist/ Autotaxin inhibitors as anti cancer agents in vivo using human engineered tumours. *Prostaglandins other lipid mediat.*, 89, pp.140–146.

Yamaguchi, F. et al., 1996. Molecular Cloning of the Novel Human G Protein-Coupled Receptor (GPCR) Gene Mapped on Chromosome 9. *Biochemical and Biophysical Research Communications*, 227(2), pp.608– 614.

Yamashita, H. et al., 2006. Sphingosine 1-phosphate receptor expression profile in human gastric cancer cells: differential regulation on the migration and proliferation. *The Journal of surgical research*, 130(1), pp.80–7. Available at: http://www.ncbi.nlm.nih.gov/pubmed/16183075 [Accessed October 29, 2011].

Yanagida, K. et al., 2013. Current progress in non-Edg family LPA receptor research. *Biochimica et biophysica acta*, 1831(1), pp.33–41. Available at: http://www.ncbi.nlm.nih.gov/pubmed/22902318 [Accessed December 21, 2012].

Yang, S.Y. et al., 2002. Expression of autotaxin (NPP-2) is closely linked to invasiveness of breast cancer cells. *Clinical & experimental metastasis*, 19(7), pp.603–8. Available at: http://www.ncbi.nlm.nih.gov/pubmed/12498389.

Yang, Y. et al., 1999. Autotaxin expression in non-small-cell lung cancer. *American journal of respiratory cell and molecular biology*, 21(2), pp.216–22. Available at: http://www.ncbi.nlm.nih.gov/pubmed/10423404.

Yasuyuki Igarashi, Y.Y., 1998. Sphingosine 1-phosphate is a blood constituent released from activated platelets, possibly playing a variety of physiological and pathophysiological roles. *Acta Biochimica Polonica*, 45(2), pp.299–309.

Young, Lawrence S & Murray, Paul G, 2003. Epstein-Barr virus and oncogenesis: from latent genes to tumours. *Oncogene*, 22(33), pp.5108–21. Available at: http://www.ncbi.nlm.nih.gov/pubmed/12910248.

Young, N. & Van Brocklyn, James R, 2006. Signal transduction of sphingosine-1-phosphate G protein-coupled receptors. *TheScientificWorldJournal*, 6, pp.946–66. Available at: http://www.ncbi.nlm.nih.gov/pubmed/16906327 [Accessed January 31, 2011].

Yu, S. et al., 2008. Lysophosphatidic acid receptors determine tumorigenicity and aggressiveness of ovarian cancer cells. *Journal of the National Cancer Institute*, 100(22), pp.1630–42. Available at: http://www.ncbi.nlm.nih.gov/pubmed/19001604.

Zhang, B. et al., 2009. Reduction of Akt2 inhibits migration and invasion of glioma cells. *International journal of cancer. Journal international du cancer*, 125(3), pp.585–95.

Available at: http://www.ncbi.nlm.nih.gov/pubmed/19330838 [Accessed March 26, 2012].

Zhang, N. et al., 2010. FTY720 induces necrotic cell death and autophagy in ovarian cancer cells: A protective role of autophagy. *Autophagy*, 6(8), pp.1157–1167. Available at: http://www.landesbioscience.com/journals/autophagy/article/13614/ [Accessed January 23, 2012].